

INFORMATION TO USERS

This manuscript has been reproduced from the microfilm master. UMI films the text directly from the original or copy submitted. Thus, some thesis and dissertation copies are in typewriter face, while others may be from any type of computer printer.

The quality of this reproduction is dependent upon the quality of the copy submitted. Broken or indistinct print, colored or poor quality illustrations and photographs, print bleedthrough, substandard margins, and improper alignment can adversely affect reproduction.

In the unlikely event that the author did not send UMI a complete manuscript and there are missing pages, these will be noted. Also, if unauthorized copyright material had to be removed, a note will indicate the deletion.

Oversize materials (e.g., maps, drawings, charts) are reproduced by sectioning the original, beginning at the upper left-hand corner and continuing from left to right in equal sections with small overlaps.

ProQuest Information and Learning
300 North Zeeb Road, Ann Arbor, MI 48106-1346 USA
800-521-0600

UMI[®]

University of Alberta

**High Throughput Wireless Downlink Packet Data Access with Multiple
Antennas and Multi User Diversity**

by

David Jean-Marie Mazzaresse



A thesis submitted to the Faculty of Graduate Studies and Research in partial
fulfillment of the requirements for the degree of Doctor of Philosophy

Department of Electrical and Computer Engineering

Edmonton, Alberta

Fall 2005



Library and
Archives Canada

Bibliothèque et
Archives Canada

Published Heritage
Branch

Direction du
Patrimoine de l'édition

0-494-08693-9

395 Wellington Street
Ottawa ON K1A 0N4
Canada

395, rue Wellington
Ottawa ON K1A 0N4
Canada

Your file *Votre référence*

ISBN:

Our file *Notre référence*

ISBN:

NOTICE:

The author has granted a non-exclusive license allowing Library and Archives Canada to reproduce, publish, archive, preserve, conserve, communicate to the public by telecommunication or on the Internet, loan, distribute and sell theses worldwide, for commercial or non-commercial purposes, in microform, paper, electronic and/or any other formats.

The author retains copyright ownership and moral rights in this thesis. Neither the thesis nor substantial extracts from it may be printed or otherwise reproduced without the author's permission.

In compliance with the Canadian Privacy Act some supporting forms may have been removed from this thesis.

While these forms may be included in the document page count, their removal does not represent any loss of content from the thesis.

AVIS:

L'auteur a accordé une licence non exclusive permettant à la Bibliothèque et Archives Canada de reproduire, publier, archiver, sauvegarder, conserver, transmettre au public par télécommunication ou par l'Internet, prêter, distribuer et vendre des thèses partout dans le monde, à des fins commerciales ou autres, sur support microforme, papier, électronique et/ou autres formats.

L'auteur conserve la propriété du droit d'auteur et des droits moraux qui protègent cette thèse. Ni la thèse ni des extraits substantiels de celle-ci ne doivent être imprimés ou autrement reproduits sans son autorisation.

Conformément à la loi canadienne sur la protection de la vie privée, quelques formulaires secondaires ont été enlevés de cette thèse.

Bien que ces formulaires aient inclus dans la pagination, il n'y aura aucun contenu manquant.


Canada

In memory of Dr. Vincent Cullen

Abstract

Wireless communication channels with multiple antennas at both the transmitter and the receiver, or multiple-input multiple-output (MIMO) systems, have been recognized as one of the most prominent enablers of future generation telecommunications systems. Recent advances in multiuser communications that exploit multiuser diversity with scheduling algorithms, adaptive coding and modulation, and automatic repeat request algorithms, have proven the high efficiency of multiuser single-input single-output systems. This thesis contributes to the knowledge of the capacity of multiuser multiple antenna systems, and more specifically of the MIMO broadcast channel, with scheduling algorithms and rate adaptation. A novel analysis is provided to study the optimal number of users that should be allocated power in order to achieve the sum-capacity of MIMO broadcast channels, as well as the optimal power allocation and the optimal transmitter covariance matrices in the asymptotically high power region. Cases where receivers are equipped with a single or with multiple antennas are considered, and the fundamental differences between these systems are discussed. It is shown that intuition can sometimes be deceptive and extensive examples are provided to illustrate our findings. This analysis is then applied to N -user scheduling algorithms for throughput maximization, with the additional goal of providing low-complexity solutions. Similarities and differences with receive antenna selection algorithms are discussed. N -user scheduling algorithms are also studied in the context of sub-optimal transmitter-based linear spatial multiplexing schemes with complete channel state information at the transmitter. A novel interference-avoidance scheme is proposed with only partial channel state information available at the transmitter. Both throughput maximization and proportionally fair scheduling are considered. We provide analytical results when possible. Simulations are used to illustrate our analysis, and to study the performance of transmission schemes and scheduling algorithms when analysis is too complex. Eventually future directions for possible research are given.

Acknowledgement

I would first like to thank my thesis supervisor Dr. Witold Krzymień for his guidance and support during the six years I was in Edmonton. I would also like to thank Dr. Ivan Fair and Dr. Christian Schlegel for their critical reviews of my work and for the very helpful discussions that allowed to improve the quality of this thesis. I would also like to thank Mr. Robert Elliot, Mr. Robert Novak, Dr. Bartosz Mielczarek and Dr. Gabriele Donà for the very stimulating discussions we had.

I also wish to thank my friends Dr. Matthieu Clouqueur and Caroline Clouqueur for their constant support in my endeavour. I thank all TRILabs students and staff for making these years such a wonderful experience. I thank my friends from the squash community of Edmonton, who also made this part of my life an unforgettable experience.

I wish to thank TRILabs, the University of Alberta, the Informatics Circle of Research Excellence (iCORE) and Dr. Witold Krzymień for their financial support.

Finally, I wish to thank my parents for their support and encouragements to pursue this thesis.

Table of Contents

1	Introduction	1
1.1	Presentation of the Problem and Research Goals	1
1.1.1	Problem	1
1.1.2	Research Goals	2
1.2	Thesis Organization	4
1.3	Definitions and Notation	6
2	Background on the Multiple Antenna Channel	8
2.1	Introduction	8
2.2	Diversity Antennas	8
2.3	The Single-User MIMO Channel	10
2.4	The Multiuser Single-Antenna Channel	14
2.5	The MIMO Broadcast Channel (BC)	17
2.5.1	Channel Model for the MIMO Broadcast Channel	17
2.5.2	Multiple Antennas and Multiuser Diversity	18
2.5.2.1	Channel state information	19
2.5.2.2	Single-user scheduling strategies	21
2.5.2.2.1	Partial CQI, no CSIT	21
	Single-user capacity scheduling, channel hardening and the effect of correlation ..	21
	Antenna selection scheduling	27
	Quantized feedback scheduling	27
	Opportunistic beamforming	27
2.5.2.2.2	Partial CQI, complete CSIT	28
2.5.2.2.3	Complete CQI and CSIT	28
2.5.2.3	Multiuser linear spatial multiplexing	29
2.5.3	Optimal Signalling	30
2.5.3.1	Dirty-Paper Coding	30
2.5.3.2	Duality between the MIMO BC and the MIMO MAC	31
2.5.3.3	Sum-Capacity	32
2.5.3.4	Capacity Region	33
3	Sum-Capacity of the MIMO BC and the Optimal Number of Active Users	36
3.1	Introduction	36
3.2	Channel Model	37
3.3	The $(2,1,K)$ MIMO BC	37
3.3.1	Mutual Information Maximization	37
3.3.2	Conditions for all Users to be Allocated Power at the Sum-Capacity	40
3.3.3	Optimal Number of Active Users at the Sum-Capacity	41
3.3.4	Geometric Interpretation on the $(2,1,3)$ MIMO BC	43
3.3.5	Numerical Examples	45
3.4	Asymptotically Optimal Power Allocation in the High Power Region	49
3.4.1	Introduction	49
3.4.2	The $(N,1,K)$ MIMO BC	51
3.4.3	The (N,N,K) MIMO BC	60
3.4.4	The (N,M_k,K) MIMO BC	63
3.5	Summary and Conclusions	69
4	Scheduling Algorithms and Linear Processing	71
4.1	Introduction	71
4.2	Channel Model	71
4.3	Throughput Maximization Scheduling Algorithms	71

4.3.1	Scheduling with Dirty-Paper Coding on the $(N,1,K)$ MIMO BC	71
4.3.1.1	Definition.....	71
4.3.1.2	Low-Complexity N -User Scheduling Algorithms.....	74
4.3.1.3	Relation to Receive Antenna Selection Algorithms on the Single-User MIMO Channel	77
4.3.1.4	Simulation Results.....	77
4.3.2	Scheduling with Linear Processing Schemes on the $(N,1,K)$ MIMO BC	81
4.3.2.1	Introduction	81
4.3.2.2	Scheduling with Complete CQI and CSIT	82
4.3.2.3	Scheduling with Partial CQI and no CSIT	84
4.3.2.4	Simulation Results.....	87
4.3.3	Scheduling with Linear Processing Schemes on the (N,M,K) MIMO BC.....	92
4.3.3.1	Introduction	92
4.3.3.2	Previously Proposed Schemes.....	92
4.3.3.2.1	Joint-Orthogonalization Schemes	92
4.3.3.2.2	Coordinated Beamforming.....	93
4.3.3.2.3	Receiver Processing Only.....	94
4.3.3.3	Joint-Linear Transmit and Receive Spatial Multiplexing.....	95
4.3.3.3.1	Two-User Channel.....	95
4.3.3.3.2	Asymptotic analysis of the sum-rate.....	97
4.3.3.4	Throughput Maximization and Spatial Multiplexing Gain	99
4.4	Proportionally-Fair Scheduling Algorithm.....	103
4.4.1	Introduction and Definition	103
4.4.2	Channel Model.....	104
4.4.3	Scheduling Algorithms for Linear Spatial Multiplexing Schemes	106
4.4.4	Simulation Results	110
4.5	Summary and Conclusions	115
5	Conclusion.....	117
5.1	Summary and Conclusions.....	117
5.2	Contributions and Future Work.....	121
2	Bibliography.....	125
	Appendix A: Classical Waterfilling.....	132
	Appendix B: Closed-Form Expression of the Sum-Capacity on the $(2,1,K_a)$ MIMO BC	134
	Appendix C: Geometric Interpretation of Power Allocation on the $(2,1,3)$ MIMO BC	135
	C.1 Definitions	135
	C.2 High Power Threshold Condition.....	136
	C.3 Non-Monotonicity Condition	137
	Appendix D: Asymptotically Optimal Power Allocation on the MIMO BC in the High Power Region.....	141
	D.1 Goal and Summary	141
	D.2 Definitions and Notation.....	142
	Background	142
	Definitions and Notation.....	143
	D.3 Proof for the $(N,1,K)$ MIMO BC	144
	Problem Statement	144
	Optimal BC Covariance Matrices	144
	Proof by Induction.....	146
	Induction Proof Part 1: Proof for User $j = 1$	148
	Induction Proof Part 2: Proof for User $j \leq K - N$	149
	Proof Part 3: Proof for User $j > K - N$	150
	Orthogonality Property.....	150

Asymptotic Sum-Capacity and Power Allocation.....	153
D.4 Proof for the (N,N,K) MIMO BC.....	155
Problem Statement	155
Proof.....	156
Proof Part 1: Asymptotically Optimal Covariance Matrix of User K	156
Proof Part 2: Initialization.....	157
Proof Part 3: Induction.....	159
Appendix E: N -user Scheduling Algorithm Optimization.....	161
Appendix F: Gorokhov's Receive Antenna Selection Algorithms.....	162
Appendix G: The Generalized Singular Value Decomposition.....	164

List of Tables

Table 3-1 Summary of high power threshold condition on the (2,1,3) MIMO BC	44
Table 3-2 Summary of non-monotonicity condition on the (2,1,3) MIMO BC.....	44
Table 4-1 Constraints on the number of transmit and receive antennas and on the number of simultaneously active users of several spatial multiplexing schemes.	93

List of Figures

Figure 2-1 The single-user MIMO channel.	11
Figure 2-2 Degraded broadcast channel model.....	15
Figure 2-3 Capacity region of the single-antenna broadcast channel.	16
Figure 2-4 The $(N,1,K)$ MIMO BC.....	18
Figure 2-5 CQI and CSIT model.	20
Figure 2-6 Channel hardening effect on multiuser diversity.	23
Figure 2-7 PDF of mutual information. Correlated and uncorrelated $(1,2,1)$ and $(1,2,8)$ channels	24
Figure 2-8 PDF of mutual information. Correlated and uncorrelated $(2,1,1)$ and $(2,1,8)$ channels without CSIT.....	26
Figure 2-9 Costa's channel model for dirty-paper coding.	30
Figure 2-10 Combined effects of multiple antennas and multiuser diversity on the ergodic sum- capacity in the Rayleigh fading broadcast channel with complete CSIT. $P = 20$ dB.....	33
Figure 2-11 Growth rate of the ergodic sum-capacity in the $(N,1,N)$ Rayleigh fading MIMO broadcast channel. $P = 10$ dB.....	35
Figure 2-12 Capacity region of the $(2,1,2)$ MIMO broadcast channel.....	35
Figure 3-1 Histograms of the optimal number of active users as a function of the total number of users and the total power in reference to the noise level. The horizontal axis represents the number of active users, the vertical axis the fraction of the number of channel realizations.	42
Figure 3-2 Channel vectors in Example 3.1.....	46
Figure 3-3 Fraction of power allocated to each user as a function of the total power in the channel of Example 3.1 with $K = 3$ and $N = 2$	47
Figure 3-4 Fraction of power allocated to each user as a function of the total power in the channel of Example 3.2 with $K = 3$ and $N = 2$	48
Figure 3-5 Fraction of power allocated to each user as a function of the total power in the channel of Example 3.3 with $K = 3$ and $N = 2$	49
Figure 3-6 $(2,1,3)$ MIMO BC optimal power allocation as a function of the total transmit power in reference to the noise level (a) on the MIMO MAC, (b) on the MIMO BC with encoding order $(1,2,3)$. (c) Users rates on the MIMO BC with encoding order $(1,2,3)$	57
Figure 3-7 $(2,1,3)$ MIMO BC optimal power allocation as a function of the total transmit power in reference to the noise level (a) on the MIMO MAC, (b) on the MIMO BC with encoding order $(3,2,1)$. (c) Users rates on the MIMO BC with encoding order $(3,2,1)$	58
Figure 3-8 $(3,1,8)$ MIMO BC optimal power allocation as a function of the total transmit power in reference to the noise level (a) on the MIMO MAC, (b) on the MIMO BC with encoding order 8 to 1. (c) Users rates on the MIMO BC with encoding order 8 to 1.....	59
Figure 3-9 $(4,4,4)$ MIMO BC optimal power allocation as a function of the total transmit power in reference to the noise level (a) on the MIMO MAC, (b) on the MIMO BC with encoding order 4 to 1. (c) Users rates on the MIMO BC with encoding order 4 to 1.....	61
Figure 3-10 Normalized eigenvalues of the optimal MAC covariance matrices as a function of the total power in reference to the noise level on the $(4,4,4)$ MIMO BC.....	62
Figure 3-11 Normalized eigenvalues of the optimal BC covariance matrices as a function of the total power in reference to the noise level on the $(4,4,4)$ MIMO BC.....	63
Figure 3-12 Normalized eigenvalues of the optimal MAC covariance matrices as a function of the total power in reference to the noise level on the $(3, \{2,1,1\}, 3)$ MIMO BC.....	64

Figure 3-13 $(3, \{2,1,1\}, 3)$ MIMO BC optimal power allocation as a function of the total transmit power in reference to the noise level (a) on the MIMO MAC, (b) on the MIMO BC with encoding order 1 to 3. (c) Users rates on the MIMO BC with encoding order 1 to 3.	65
Figure 3-14 Normalized eigenvalues of the optimal BC covariance matrices as a function of the total power in reference to the noise level on the $(3, \{2,1,1\}, 3)$ MIMO BC with the encoding order 1 to 3.	66
Figure 3-15 $(3, \{2,1,1\}, 3)$ MIMO BC optimal power allocation as a function of the total transmit power in reference to the noise level (a) on the MIMO MAC, (b) on the MIMO BC with encoding order 3 to 1. (c) Users rates on the MIMO BC with encoding order 3 to 1.	67
Figure 3-16 Normalized eigenvalues of the optimal BC covariance matrices as a function of the total power in reference to the noise level on the $(3, \{2,1,1\}, 3)$ MIMO BC with the encoding order 3 to 1.	68
Figure 4-1 Average spectral efficiency of the best L -user sub-channel as a function of the number of transmit antennas N . The total number of users is $K = 10$, each user is equipped with a single receive antenna. The total power in reference to the noise level is 10 dB.	73
Figure 4-2 Average spectral efficiency of the best L -user sub-channel as a function of the number of antennas N . The total number of users is $K = 10$, each user is equipped with N receive antennas. The total power in reference to the noise level is 10 dB.	74
Figure 4-3 Approximations of the sum-capacity as a function of the total power in reference to the noise level on the $(4,1,4)$ MIMO BC.	78
Figure 4-4 Spectral efficiency loss of N -user scheduling algorithms with respect to the sum-capacity on the $(2,1,6)$ MIMO BC.	79
Figure 4-5 Spectral efficiency loss of N -user scheduling algorithms with respect to the sum-capacity on the $(N,1,10)$ MIMO BC. The total power in reference to the noise level is 0 dB.	81
Figure 4-6 Ratio of spectral efficiency of N -user scheduling algorithms to the sum-capacity on the $(4,1,K)$ MIMO BC. The total power in reference to the noise level is 10 dB.	82
Figure 4-7 Cumulative bar plot of the number of active users for Scheme B. The total power in reference to the noise level is 10 dB. The number of transmit antennas is $N = 4$. 1000 channel realizations.	86
Figure 4-8 Cumulative bar plot of the number of active users for Scheme B. The total number of users is $K = 16$. The number of transmit antennas is $N = 4$. 1000 channel realizations.	87
Figure 4-9 Average spectral efficiency as a function of the total number of users K . The number of transmit antennas is $N = 2$. The total power in reference to the noise level is 10 dB.	88
Figure 4-10 Average spectral efficiency as a function of the total power in reference to the noise level. The total number of users is $K = 10$. The number of transmit antennas is $N = 2$	89
Figure 4-11 Average spectral efficiency as a function of the number of transmit antennas. The total number of users is $K = 10$. The total power in reference to the noise level is 10 dB.	89
Figure 4-12 Spectral efficiency loss of N -user scheduling algorithms with respect to the exhaustive search on the $(2,1,6)$ MIMO BC with zero-forcing beamforming at the transmitter.	91
Figure 4-13 Average spectral efficiency on the $(N,N,10)$ BC as a function of the number of antennas N . The total transmit power in reference to the noise level is 10 dB.	100
Figure 4-14 Average spectral efficiency on the $(N,N,2)$ BC as a function of the total transmit power in reference to the noise level.	101
Figure 4-15 Average spectral efficiency on the $(4,M,4)$ BC as a function of the number of receive antennas M per user. The total power in reference to the noise level is 10 dB.	102
Figure 4-16 Average spectral efficiency on the $(4,2,2)$ BC as a function of the total power in reference to the noise level.	103
Figure 4-17 CDF of average SNR with path loss and shadow fading.	105

Figure 4-18 Rate region of Coordinated Beamforming and JLTR-SM for one realization of the (4,4,2) MIMO BC.	108
Figure 4-19 Rate region of Coordinated Beamforming and JLTR-SM for one realization of the (2,2,2) MIMO BC.	109
Figure 4-20 CDF of sum-rate per slot on the (2,1,6) MIMO BC. The same legend is used for all simulations for the $(N,1,K)$ MIMO BC in the following three figures.	110
Figure 4-21 CDF of user delay on the (2,1,6) MIMO BC.	111
Figure 4-22 CDF of sum-rate per slot on the (2,1,16) MIMO BC.	112
Figure 4-23 CDF of user delay on the (2,1,16) MIMO BC.	112
Figure 4-24 CDF of sum-rate per slot on the (4,4,20) MIMO BC.	114
Figure 4-25 CDF of user delay on the (4,4,20) MIMO BC.	114
Figure 4-26 Legend of simulations for the (N,N,K) MIMO BC.	114

List of Abbreviations

AWGN	Additive white Gaussian noise
AMC	Adaptive modulation and coding
ARQ	Automatic repeat request
BC	Broadcast channel
CB	Coordinated Beamforming
CCDF	Complementary cumulative distribution function
CDF	Cumulative distribution function
CDI	Channel distribution information
CDMA	Code division multiple access
CQI	Channel quality indicator
CSI	Channel state information
CSIR	Channel state information at the receiver
CSIT	Channel state information at the transmitter
DPC	Dirty-paper coding
EP	Equipartition
FDMA	Frequency division multiple access
FSPF	Full-search proportionally-fair
GDPE	Generalized decision-feedback equalizer
GSM	Global system for mobile communications
GZFB	Group zero-forcing beamforming
HARQ	Hybrid ARQ
i.i.d.	Independent identically distributed
JLTR-SM	Joint linear transmit and receive spatial multiplexing
MAC	Multiple access channel
MIMO	Multiple input/multiple output
MISO	Multiple input/ single output
MMSE	Minimum mean squared error
MRC	Maximum ratio combining
OFDM	Orthogonal frequency division multiplexing
PDF	Probability density function
PF	Proportionally-fair

SDMA	Space division multiple access
SIMO	Single input/multiple output
SINR	Signal to interference and noise ratio
SNR	Signal to noise ratio
SU	Single-user
SUR	Single-user rates
SUWR	Single-user weighted rates
SVD	Singular value decomposition
TDMA	Time division multiple access
UMTS	Universal mobile telecommunication system
ZFB	Zero-forcing beamforming

1 Introduction

1.1 Presentation of the Problem and Research Goals

1.1.1 Problem

In our modern societies where economic growth is driven by technology, the success of a commercial product can be measured by it becoming a necessity. The most recent and successful ones are the mobile telephone and the Internet. They have only been commercially viable for about one or two decades, respectively, yet they already earned their place right next to the car, the television and the computer. In fact, their growth has even been faster. There are now over one billion GSM customers worldwide, which took twelve years to reach after commercial introduction in 1992 [1]. It took twenty-five years for the PC industry to reach that milestone [2]. Moreover, all of these necessity products are now expected to converge into a multitude of mobile communication capable devices. Voice communications and short text messages have made the success of mobile telephony. Future growth is foreseen to be driven by the convergence of high-speed Internet and transmission of images with mobile or fixed wireless communications. The preferred transmission medium is wireless. It is necessary for providing mobility, and it allows scalability of the network with a much smaller cost than wired media. Since regulatory bodies restrict bandwidth and radiated power, in order to meet the data rate requirements of future applications, more spectrally efficient systems than Second or Third Generation systems are required. Since the introduction of the first commercial wireless services there has been much progress in more efficient bandwidth utilization. Major advances such as the introduction of digital transmission, the development of cellular networks that allow spatial frequency reuse, the use of error control coding such as coded modulation and turbo coding, have allowed to improve the spectral efficiency.

One of the most promising enabling technologies for future wireless systems is multiple-input/multiple-output (MIMO) systems. These systems employ communication channels, in which multiple antennas are used to transmit a signal and multiple antennas are used to receive the signal. Theoretical and practical results have demonstrated that the information capacity of MIMO channels in a rich scattering environment is approximately a multiple of the information capacity of channels in which only one antenna is present at the transmitter or the receiver side. The multiplicative factor is equal to the minimum of the numbers of transmit and receive antennas. There has been a large amount of research devoted to point-to-point (single-user) MIMO systems in the past ten years since the first landmark papers have been published [3][4]. Numerous special issues of leading scientific journals have been devoted to space-time

communication systems, covering topics as diverse as space-time coding, space-time signal processing, space-time equalization, space-time modulation, spatial multiplexing schemes, information theory of MIMO channels, space-time CDMA, space-time OFDM, MIMO channel modeling, and measurements of MIMO channels. Future high-speed data services not only require a higher data rate, but they also impose different constraints than voice communications and low data-rate services. In particular they can tolerate higher latency in the delivery of the signal. This delay tolerance allows more freedom in the design of the communication system. Equivalently from the information theoretic view, it changes the nature of the transmission channel by imposing less stringent constraints. As a consequence, the capacity of the new channel is larger and novel strategies such as opportunistic scheduling take advantage of that capacity increase. Recently standardized single-antenna systems for the evolution of the third generation of cellular systems already use this technique. The study of multiuser MIMO systems has started much more recently with the broadcast channel [5]. The study of opportunistic scheduling algorithms in multiuser MIMO systems is still in its infancy. The goal of this thesis is to improve our knowledge and comprehension of multiuser MIMO channels beyond what is known at the time of writing, and to address some of the key issues that arise when MIMO systems and opportunistic scheduling are combined.

1.1.2 Research Goals

A complete study of a realistic cellular multiuser MIMO channel is beyond the scope of this thesis. Instead, we attempt to answer specific questions in the context of ideal channel models and packet-data access schemes. We are primarily interested in finding ways to increase throughput on the downlink of a cellular channel. This is where the highest data rates are expected to be required. Owing to the high speed of transmission and the delay tolerance of the application, the channel can be decomposed into time slots during which it is assumed to remain constant, with the exception of the additive noise process realization. The model for the channel within a time slot is a MIMO Gaussian broadcast channel with a transmit power constraint. The capacity region of that channel is the dirty-paper coding region. The sum-capacity of that channel has been shown to achieve the same multiplicative gain in spectral efficiency as MIMO channels over single-antenna channels, even though cooperation at the receivers is not possible. Our goal is to address questions that are central to the application of opportunistic scheduling algorithms. Based on the recent mathematical characterization of the sum-capacity of the MIMO Gaussian broadcast channel, we specifically aim at answering the following questions:

- What is the optimal number of active users?
- What is the optimal power allocation policy?

What makes these questions hard to answer is the fact that MIMO channels create self-interference. The underlying issue relates to the comparison with single-antenna multiuser channels that use opportunistic scheduling. On these channels (both uplink and downlink) throughput is maximized by transmitting with the maximum power to the user that experiences the best channel in any given time slot. Is this strategy still optimal on multiuser MIMO channels? We can still define the best user in terms of its maximum transmission rate, but can it reach the capacity of the multiuser MIMO channel alone? These questions will be answered in the next chapters after we have defined the assumptions of our work.

These questions have also been raised in recent publications, and they have only been partially addressed. Opportunistic scheduling algorithms for the quasi-static fading MIMO broadcast channel (BC) with dirty-paper coding or some sub-optimal transmission scheme have been proposed, with design guidelines mostly driven by intuition. However, intuition can be deceptive in the case of multiuser MIMO channels, and rigorous answers are still required. Furthermore the complexity of scheduling more than one user at a time in a given time slot can be very high. Optimal scheduling sometimes requires a combinatorial complexity in the number of users and the number of antennas. Dirty-paper coding will be described in the next chapter. It was first introduced as a theoretical coding scheme. Some simple implementations have been proposed, but the complexity of this coding scheme increases very quickly with the number of users. It is not yet practical to implement it. On the other hand, linear schemes for array processing are much better understood and less complex. It is therefore relevant to investigate their performance and their utilization with opportunistic scheduling on the MIMO BC. It is of interest to find such schemes that can accommodate any number of users, transmit and receive antennas, and perform close to the optimum, whether the design criterion is throughput maximization or proportionally-fair resource allocation.

Other important issues that must be addressed are the following:

- Is there a fundamental difference if the receivers are equipped with one or several antennas?
- What is the impact of not having complete channel knowledge at the transmitter? How is it possible to achieve a large throughput by spatial multiplexing in this case?
- What transmission strategy could be used if dirty-paper coding is not possible?

- What is the complexity of optimal scheduling algorithms?
- Are there near-optimal low-complexity scheduling algorithms and transmission schemes?
- How is the problem affected if we consider proportionally-fair scheduling instead of throughput maximization?

1.2 Thesis Organization

Chapter II contains background information on multiple antenna channels. We first briefly review fundamental concepts of single-user MIMO channels. The concepts of diversity and spatial multiplexing in fading channels are introduced. The information capacity of these channels is also reviewed with an emphasis on the maximum achievable spatial multiplexing gain with respect to the availability of channel state information. The multiuser single-antenna fading channel is then introduced in the context of packet-data access systems. We introduce the concepts of multiuser diversity, capacity region and sum-capacity. The first attempts at exploiting spatial and multiuser diversity simultaneously are reviewed. In particular we review the concept of channel hardening. We then present the state of the art in the knowledge of MIMO channels with multiuser diversity at the time of writing. Our channel model is then introduced, followed by an introduction to dirty-paper coding and the description of the capacity region. The important recent results on the MIMO Gaussian broadcast channel are then presented in detail, as they provide the mathematical foundation for Chapter III. We summarize the results on the duality between the MIMO broadcast channel and the MIMO multiple access channel (MAC) [6]. We defer to Appendix D the summary of the mathematical formulation of the sum-capacity optimization problem.

Chapter III starts with a presentation of our results on the optimal number of active users and the optimal power allocation policy on the sum-power MIMO MAC dual of the MIMO BC with two transmit antennas, and K users each equipped with a single receive antenna. The optimal number of active users is shown to depend on the channel matrix as well as on the total transmit power sometimes in a non-intuitive way. We show that it can be a non-monotonic function of the total transmit power for a given channel realization, and that it can be larger than the number of transmit antennas. The MIMO BC with two transmit antennas, and three users each equipped with a single receive antenna, is then completely characterized geometrically and we illustrate our result with numerical examples. We then prove that the asymptotically optimal number of active users that are allocated a non-vanishing fraction of the total transmit power in the high power region is equal to N (provided that $K \geq N$) on the MIMO BC with N transmit antennas, and K

users each equipped with a single receive antenna. The asymptotically optimal power allocation in this situation is shown to be uniform among the N users as a first order approximation. We deduce the asymptotically optimal transmission strategy in this case and give the asymptotic closed-form of the sum-capacity as a first order approximation. That result is finally extended to the MIMO BC with N transmit antennas, and K users each equipped with N receive antennas, where we show that asymptotically in the high power region only one user is allocated a non-vanishing fraction of the total transmitted power. Simulation results that help understand the intermediary power region are also provided. The respective roles of dirty-paper coding and spatial processing are discussed.

Chapter IV is concerned with scheduling algorithms for the MIMO BC. We first study throughput maximization N -user scheduling algorithms with dirty-paper coding transmission. We analyze the computational complexity of the optimal N -user scheduling algorithm, and then present a reduced-complexity near-optimal N -user scheduling algorithm. We also point out the similarities of this problem to receive antenna selection problems, and we study the performance of receive antenna selection algorithms for the purpose of throughput maximization N -user scheduling. We present simulation results to illustrate the spectral efficiency loss incurred by N -user scheduling for throughput maximization.

We then focus on the MIMO BC where users are equipped with single receive antennas. Our goal is to analyze systems where linear processing schemes are used instead of optimal dirty-paper coding. We first limit ourselves to throughput maximization scheduling algorithms. We study the joint design of throughput maximization scheduling algorithms with specific linear processing schemes. Simulation results are provided to illustrate the performance of such schemes in terms of throughput and spatial multiplexing gain. We study the case of complete channel state information at the transmitter (CSIT) and channel quality indicator (CQI), and the case of no CSIT and partial CQI. We apply the reduced-complexity scheduling algorithms proposed in Chapter IV to linear processing schemes with complete CSIT and CQI. We also propose a novel interference-avoidance transmission strategy in the case of partial CQI in the form of SINR feedback from each mobile user to the base station. CSIT and CQI will be defined in Chapter II.

Chapter IV also aims at proposing sub-optimal linear processing schemes and scheduling algorithms for throughput maximization when the users are equipped with multiple receive antennas. We first review previously proposed schemes and their limitations. We then propose a novel joint diagonalization scheme that addresses some of those limitations. We analytically

study the asymptotic behaviour of the maximum throughput achievable with this scheme, and we provide simulation results.

Chapter IV finally addresses proportionally-fair scheduling. We analyze the performance of the schemes proposed earlier in Chapter III along with previously proposed and novel reduced-complexity proportionally-fair scheduling algorithms. We study the trade-offs between throughput and delay, and the effect of using multiple antennas and the specific properties of the transmission schemes considered. We compare the performance of the optimal joint proportionally-fair scheduling algorithm with disjoint sub-optimal designs.

Chapter V concludes the thesis by summarizing our contributions and presenting some future directions of research that could complement the work presented in this thesis.

1.3 Definitions and Notation

All boldface letters indicate vectors (lower case) or matrices (upper case). The determinant of a matrix A will be denoted either by $\det(A)$ or $|A|$. Its trace will be denoted by $\text{tr}(A)$. Its transpose will be denoted by A^T . Its Hermitian transpose will be denoted by A^* . Its pseudo-inverse [7] will be denoted by A^\dagger . $\text{rank}(A)$ is the rank of the matrix A . $\text{diag}(a_1 \cdots a_N)$ represents the diagonal matrix whose diagonal elements are a_1, \dots, a_N . $E[X]$ is the expectation of the random variable X . $E_H[X]$ is the expectation of the random variable X over the random process H . The norm of a vector \mathbf{h} will be denoted by $\|\mathbf{h}\|$, while the norm of a complex scalar a will be denoted by $|a|$. The notation $A \geq 0$ specifies that the matrix A is positive semidefinite. The identity matrix of size $N \times N$ will be represented by I_N . The set of real numbers is denoted by \mathbb{R} , and the set of complex numbers is denoted by \mathbb{C} . By default we will represent the logarithm with base 2 of a real number a by $\log a$. The equivalence notation to express the limit of functions of x as x tends to x_0 is:

$$f(x) \underset{x \rightarrow x_0}{\sim} g(x) \text{ meaning that } \lim_{x \rightarrow x_0} \frac{f(x)}{g(x)} = 1.$$

The notation (N, M, K) MIMO BC will be used throughout the thesis to denote the MIMO Gaussian broadcast channel where the transmitter is equipped with N antennas and the K receivers are equipped with M antennas each. The reader is referred to Chapter II for the definition of the MIMO Gaussian broadcast channel. The notation (N, M_k, K) MIMO BC will be used when the K receivers could be equipped with different numbers of antennas, without explicitly specifying what these numbers are.

Knowledge of the channel at the transmitter or at the receiver will be described in this thesis in terms of channel state information (CSI). Complete CSI refers to the knowledge of the exact value of every channel gain (magnitude and phase), or equivalently exact knowledge of the channel matrix realization. Partial CSI will be explicitly described whenever used. For instance it could be some SINR value.

2 Background on the Multiple Antenna Channel

2.1 Introduction

This chapter presents background information on MIMO and multiuser mobile radio channels. More detailed information can be found in the relevant literature. Our aim in this section is to present the fundamental principles and the mathematical foundations that we will use in the remainder of this thesis. The body of work and tutorial papers on MIMO systems is such that it would be redundant and too ambitious to give an exhaustive overview of known facts on MIMO systems. In this chapter we will only emphasize the concepts that are pertinent to the goals of this thesis.

We begin by reviewing fundamental results on single-user MIMO channels. We present the concepts of spatial multiplexing gain and diversity order. Then we briefly review results on multiuser single-antenna fading channels with an emphasis on the model for packet-data access systems. We present the concepts of multiuser diversity and opportunistic scheduling. We next review early results on multiuser MIMO channels for packet-data access systems with opportunistic scheduling, and we emphasize the shortcomings of the proposed approaches. We finally summarize the important recent results on the capacity region and the sum-rate capacity of the MIMO BC. We summarize the duality between the MIMO BC and the MIMO MAC. We give the relevant mathematical description that will be used throughout this thesis.

2.2 Diversity Antennas

An antenna is a means to transform electrical currents from a transmission line into electromagnetic waves that propagate in free space, and to reverse the process at the receiving end of the communication channel. It can be made of a simple wire, or be a very complex system with active components. Traditionally the use of multiple collocated antennas was motivated by the need to extend the transmission range by increasing the antenna gain, therefore providing enhanced coverage with the same amount of transmitted power. This is performed by beamforming at the receiver side or at the transmitter side through the use of array processing. In both cases, the transmitter, or the receiver, acquires some amount of channel knowledge through channel estimation, and uses that knowledge to form beams in the direction of the receivers, if the channel knowledge is in the form of angles of departure or arrival, or in the direction of strong paths, if the channel knowledge is in the form of complex channel coefficients. The latter form of channel knowledge is of interest to us.

With an array of N antennas at the receiver and one antenna at the transmitter, the propagation channel, which is assumed to be constant for the time being, can be described by a vector of complex numbers:

$$\mathbf{h} = [h_1, \dots, h_N]^T. \quad (2.1)$$

The received signal vector is given by

$$\mathbf{y} = \mathbf{h}x + \mathbf{n}. \quad (2.2)$$

We assume that the AWGN processes at the receive antennas are independent and have the same power spectral density, and their samples are collected in the vector \mathbf{n} . We also assume that the transmitted scalar signal x is a signal with $|x|^2 = P$, such that all symbols in the constellation have equal energy. Then if the receiver has perfect knowledge of the vector \mathbf{h} , it can perform Maximal Ratio Combining (MRC) on the received vector \mathbf{y} , and obtain

$$\mathbf{h}^* \mathbf{y} = \|\mathbf{h}\|^2 x + \mathbf{h}^* \mathbf{n}. \quad (2.3)$$

MRC maximizes the signal-to-noise ratio after combining, which becomes equal to the sum of the SNR per branch. This operation can be thought of as beamforming in the direction of maximum SNR. The diversity gain achieved by MRC is large if the channel coefficients in \mathbf{h} are samples of independent processes. It can be shown that the pairwise probability of error between the transmitted symbol and the symbol detected at the receiver with maximum-likelihood detection decreases as the N -th power of the SNR for large values of the SNR [8].

Other forms of combining that achieve diversity gain can be used, although they do not achieve the maximum SNR achieved by MRC. However, depending on the amount of channel knowledge, other diversity combining strategies need to be adopted. Among them selection diversity offers the same order of diversity N as MRC, and its output SNR is equal to the maximum of the SNR per branch.

The same diversity techniques can be used at the transmitter, although in this case it is in general more difficult to obtain channel knowledge, since it requires either feedback of the channel estimated at the receiver, or that the channel be estimated at the transmitter when it is used in the receiver mode in a duplex communication system provided that the channels in both directions are the same. MRC beamforming at the transmitter is performed the same way as at the receiver, with the major difference that a transmitted power constraint is now applied. The transmitted vector is given by

$$\mathbf{x} = \mathbf{w}^* s, \quad (2.4)$$

where the beamforming vector is $\mathbf{w} = [w_1, \dots, w_N]$. The power constraint is

$$\|\mathbf{x}\|^2 = P. \quad (2.5)$$

The received symbol is

$$y = \mathbf{h}\mathbf{w}^*s + n, \quad (2.6)$$

where $\mathbf{h} = [h_1, \dots, h_N]$ is now a row-vector.

Having multiple antennas at the receiver provides array gain by allowing to collect more power as more samples of the energy carried by the electromagnetic waves can be captured, whereas at the transmitter the same amount of power as in the single transmit antenna system is required to be radiated.

Selection diversity at the transmitter can be performed with the knowledge of the SNR per branch for each of the transmit antennas. This knowledge can be acquired by feedback from the receiver. This type of channel state information requires less feedback than the complete knowledge of all the channel gains, and in time-varying channels it could possibly be updated less frequently. With transmit selection diversity only one of the N antennas is used for transmitting the signal using the total power P in each channel use.

The idea of using multiple antennas at the transmitter and at the receiver has only recently received considerable attention. These types of systems still offer diversity advantages [9][10][11], but more importantly they offer large advantages in terms of channel capacity. We will now summarize the recent results on MIMO channel capacity.

2.3 The Single-User MIMO Channel

The MIMO channel is the model for channels where the transmitter and the receiver are equipped with multiple collocated antennas. The transmitted signal vector is jointly processed by the transmitter signal processing block, and the received signal vector is jointly processed by the receiver signal processing block. N is the number of transmit antennas and M is the number of receive antennas. This is illustrated in Figure 2-1. The signal transmitted at a given time through all the transmit antennas simultaneously is represented by a column vector \mathbf{x} of complex symbols. The baseband complex channel model for frequency non-selective MIMO channels is described in the following. The signal received at a given time is given by the vector:

$$\mathbf{y} = \mathbf{H}\mathbf{x} + \mathbf{n}. \quad (2.7)$$

The channel between the transmitter and the receiver is modeled by a matrix \mathbf{H} of size $M \times N$ with elements h_{mn} . The AWGN \mathbf{n} is the $M \times 1$ white circularly symmetric complex Gaussian vector with covariance matrix \mathbf{Z} [4]. Without loss of generality, we assume that the noise covariance matrix is a scaled identity matrix [12]. The variance of the AWGN at each receive

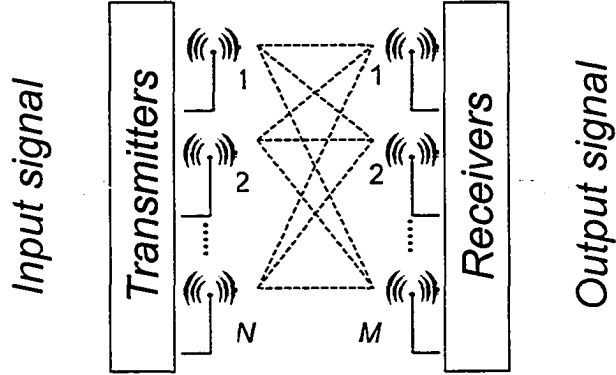


Figure 2-1 The single-user MIMO channel.

antenna is σ^2 . \mathbf{x} is the $N \times 1$ transmitted signal vector, and \mathbf{y} is the $M \times 1$ received signal vector. The transmitter has either a long term or a short-term transmit power constraint P such that $\text{tr}(E[\mathbf{x}\mathbf{x}^*]) \leq P$ or $\|\mathbf{x}\|^2 = P$.

Telatar in [4] considered a constant MIMO channel where \mathbf{H} is deterministic, and a fading channel where \mathbf{H} is random, for the cases of complete CSIR and complete or no CSIT. Foschini in [3] considered a quasi-static fading MIMO channel with CSIR. We will summarize the few fundamental results on MIMO channel capacity. For a more complete and detailed treatment the reader is referred to the original papers [3][4] and to tutorial papers, for example [12]. A good discussion of single-user and multiuser MIMO channels is provided in [12]. We will only summarize results on these channels in this chapter, and point out the main features that we will focus on in the next chapters.

It was shown in [3][4] that for a given channel realization, the mutual information between the transmitted Gaussian signal with covariance matrix $\mathbf{Q} = E[\mathbf{x}\mathbf{x}^*]$ and the received Gaussian signal is given by:

$$\mathcal{I}(\mathbf{x}; \mathbf{y}) = \log \det \left(\mathbf{I}_M + \frac{1}{\sigma^2} \mathbf{H}\mathbf{Q}\mathbf{H}^* \right). \quad (2.8)$$

The channel capacity of the deterministic MIMO channel is thus given by

$$C = \max_{\{\mathbf{Q} \geq 0, \text{tr}(\mathbf{Q}) \leq P\}} \log \det \left(\mathbf{I}_M + \frac{1}{\sigma^2} \mathbf{H}\mathbf{Q}\mathbf{H}^* \right). \quad (2.9)$$

The channel matrix can be expressed by its singular value decomposition (SVD) [7]:

$$\mathbf{H} = \mathbf{U}\mathbf{D}\mathbf{V}^*, \quad (2.10)$$

where \mathbf{U} and \mathbf{V} are unitary matrices and \mathbf{D} is a diagonal $M \times N$ matrix with nonnegative main

diagonal entries. These diagonal entries $d_1, \dots, d_{\min(M,N)}$ are the singular values of the matrix \mathbf{H} . After some simple manipulations, the capacity can be expressed as:

$$C = \max_{\{\mathcal{Q} \geq 0, \text{tr}(\mathcal{Q}) \leq P\}} \log \det \left(\mathbf{I}_M + \frac{1}{\sigma^2} \mathbf{D} \mathbf{V}^* \mathcal{Q} \mathbf{V} \mathbf{D}^* \right). \quad (2.11)$$

The matrix $\mathbf{V}^* \mathcal{Q} \mathbf{V}$ must be diagonal to maximize the determinant as a consequence of Hadamard's inequality [13]. Thus Telatar [4] proved that the deterministic MIMO channel is decomposed into $\min(M, N)$ parallel (non-interfering) single-input/single-output Gaussian channels. The gains of these channels are given by the squared singular values of the channel matrix. The solution to the maximization is obtained by waterfilling the total transmit power across the parallel Gaussian channels:

$$C = \max_{\{a_k, k=1, \dots, \min(M, N)\}} \sum_{k=1}^{\min(M, N)} \log \left(1 + \frac{P}{\sigma^2} d_k^2 a_k \right) \quad (2.12)$$

$$\text{Subject to } \sum_{k=1}^{\min(M, N)} a_k \leq 1 \text{ and } a_k \geq 0, k = 1, \dots, \min(M, N). \quad (2.13)$$

The solution to the waterfilling problem is summarized in Appendix A. If the matrix \mathbf{H} has full rank equal to $\min(M, N)$, then the capacity of the constant MIMO channel grows $\min(M, N)$ times faster than the capacity of the single-input/single-output link in the high power region as the transmit power increases. Moreover spatial multiplexing on the $\min(M, N)$ parallel Gaussian channels only requires matrix multiplication at the transmitter and at the receiver, thus only linear processing. As the power P goes to infinity, the capacity grows as $\min(M, N) \log P$. Hence it is more advantageous to increase N and M than P in order to increase the capacity of the channel, which is why MIMO systems have become so popular.

When the channel matrix \mathbf{H} is random and time-varying such that the fading process is ergodic, and the transmitter and the receiver have complete CSI, the capacity achieved by coding across all fading states with capacity-achieving codes is obtained by averaging the constant MIMO channel capacity over all fading states:

$$C = E_{\mathbf{H}} \left[\max_{\{\mathcal{Q} \geq 0, \text{tr}(\mathcal{Q}) \leq 1\}} \log \det \left(\mathbf{I}_M + \frac{P}{\sigma^2} \mathbf{H} \mathcal{Q} \mathbf{H}^* \right) \right]. \quad (2.14)$$

In fading channels within a rich scattering environment and sufficiently spaced antenna elements, the fading processes affecting each pair of transmit and receive antennas can be considered independent. In the popular case of Rayleigh fading the elements of the matrix \mathbf{H} are modeled as i.i.d. complex Gaussian random variables with zero mean and unit variance. In this case the

channel matrix \mathbf{H} will be full rank almost surely in each fading state, and the growth rate as a function of the total transmit power will be given by $\min(M, N)$. Multipath propagation in a rich scattering environment is thus beneficial to the capacity of MIMO channels. If a line-of-sight component is dominant in the propagation environment then the channel matrix will be of rank one and the growth rate will only be equal to one as for a single-input/single-output channel.

In fading channels with CSIR and only knowledge of the channel matrix distribution at the transmitter, when the channel matrix is zero-mean spatially white, the ergodic capacity still has a growth rate equal to $\min(M, N)$ as shown in [3][4]. In this case, the optimal transmit covariance matrix is a scaled identity matrix, and the transmit power is uniformly distributed across the transmit antennas. The resulting ergodic capacity can be expressed with Laguerre polynomials and the growth rate is equal to $\min(M, N)$. We will subsequently refer to this capacity as *open-loop capacity*, as opposed to the *closed-loop capacity* given by (2.14). The *open-loop capacity* is given by:

$$C = E_H \left[\log \det \left(\mathbf{I}_M + \frac{P}{N\sigma^2} \mathbf{H}\mathbf{H}^* \right) \right]. \quad (2.15)$$

In fading channels with channel distribution information at the transmitter and at the receiver, when the channel matrix is zero-mean spatially white, it was shown in [14] that it is not useful to increase the number of transmit or receive antennas beyond T , where T is the coherence time of the block-fading channel model measured in space-time modulation symbol intervals. Thus the spatial multiplexing gain reaches a maximum that cannot be exceeded by adding more antennas when T is fixed. Under models where the transmitter has partial channel knowledge in the form of the mean channel matrix or the channel covariance matrix, and the receiver has complete CSIR, it is still useful to increase the number of antennas beyond T in order to achieve increasing spatial multiplexing gains, as long as transmit antenna fading gains are correlated [12]. A good tutorial on several such scenarios of channel knowledge and types of channels can be found in [12].

Viewing the mutual information in random channels as a random variable brings insights into the properties of MIMO channels. It is sometimes required to adopt such a view if the fading channel is not ergodic. In quasi-static fading channels, where coding is allowed for the maximum length of the coherence time of the fading channel during which the channel matrix remains constant, the maximum of the mutual information is equal to zero, thus the capacity in the ergodic sense is zero [15]. Under the quasi-static fading assumption, one cannot guarantee to transmit at a

non-zero rate over every interval, in which the channel matrix is constant. Instead one must consider the outage capacity.

In the case of CSIR and channel distribution information at the transmitter, the mutual information is a random variable and it is defined as

$$I_{RV} = \log \det \left(\mathbf{I}_M + \frac{P}{M\sigma^2} \mathbf{H}\mathbf{H}^* \right). \quad (2.16)$$

One is interested in the capacity with outage probability p , where a rate at most equal to the outage capacity can be ensured with probability p over all fading states. A Gaussian approximation of the random variable I_{RV} for large numbers of antennas was proposed in [16]. [3] also provided the CCDF of I_{RV} obtained from Monte-Carlo simulations.

In summary, we have seen that, as summarized in [12], increasing the number of antennas to arbitrarily increase the spatial multiplexing gain can only be achieved with complete CSIR. Thus in the rest of this thesis, we will only be interested in systems where CSIR is available, since our goal is to achieve high throughput by spatial multiplexing on multiuser channels. Note that the cooperative multiuser MIMO channel, where the antennas of all users belong to a single array, can be seen as a single-user MIMO channel, thus it always provides an upper bound on the capacity of the multiuser MIMO channel. Hence without CSIR it is also not possible to keep increasing the spatial multiplexing gain arbitrarily by adding antennas on the multiuser MIMO channel. The maximum spatial multiplexing gain $\min(N, M)$ can only be achieved with complete CSIR.

2.4 The Multiuser Single-Antenna Channel

In cellular systems, a base station must communicate with K mobile users. A multiple access strategy must be adopted in order to serve all users. Commonly used strategies are TDMA, FDMA and CDMA. CDMA is the only strategy that introduces interference among the users, and it is inspired by the optimal access strategy, namely superposition coding [13]. On the downlink of cellular systems, orthogonal CDMA codes can be used since the orthogonality will be preserved (at least on a flat-fading channel) at each receiver due to the synchronous transmission of the users' signals from the base station. In this case, each CDMA code represents a dimension, in which a signal can be transmitted without interfering with the signals sent using other CDMA codes. Since our interest is primarily on the downlink, we assume that the radio channel can be partitioned into a number of orthogonal sub-channels, and we focus on only one of these sub-channels. Similarly, we can also assume that orthogonal dimensions can be created in frequency-selective channels using OFDM with cyclic prefix. Thus we also restrict our attention to flat

fading channels. Since we are interested in packet-data access systems, we assume that the channel fading gains remain constant for the duration of several consecutive transmission time slots. We adopt a short term transmit power constraint.

With the goal of maximizing the throughput of the cellular system, we consider the sum-rate as the criterion to be maximized. The sum-rate is the sum of the rates simultaneously achievable by all K users in a given time slot. The capacity of multiuser channels is now described in terms of achievable rate vectors. A rate vector (R_1, \dots, R_K) is simultaneously achievable by all users. The capacity of the multiuser channel is described by a capacity region, for any given time slot where the channel multiplicative gains remain constant. The sum-capacity is defined as the maximum sum-rate over all achievable rate vectors. The goal in throughput maximization is to achieve or approach the sum-capacity.

The deterministic single-antenna broadcast channel with a transmitted power constraint is an instance of a physically degraded broadcast channel [13]. Let P be total transmit power constraint. Let the two users experience AWGN at the receivers with variances respectively equal to N_1 and N_2 . Assume that $N_1 < N_2$ without loss of generality. Then the signals received by users 1 and 2 are:

$$Y_1 = X + Z_1 \quad (2.17)$$

$$Y_2 = X + Z_2, \quad (2.18)$$

where X is the transmitted signal, and Z_1 and Z_2 represent the AWGN signals at the receivers.

The sender wishes to transmit to receiver 1 with rate R_1 and to receiver 2 with rate R_2 . Using the fact that the channel is degraded, thus that the channels can be represented as a succession of two channels as shown in Figure 2-2, the capacity region is shown to be achievable by superposition coding and successive decoding [13], and the achievable rates are given by:

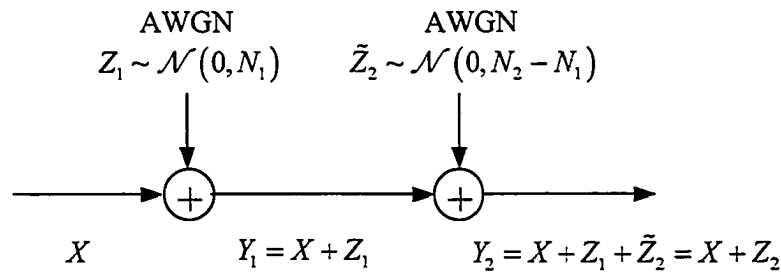


Figure 2-2 Degraded broadcast channel model.

$$R_1 < \log\left(1 + \frac{\alpha P}{N_1}\right) \quad (2.19)$$

$$R_2 < \log\left(1 + \frac{(1-\alpha)P}{\alpha P + N_2}\right), \quad (2.20)$$

where $0 \leq \alpha \leq 1$ is arbitrary. The capacity region is illustrated in Figure 2-3. The sum-rate can thus be expressed and maximized in a straightforward way, so we omit the proof here. Transmitting with all the power to the user with the smallest AWGN variance maximizes the sum-rate, and thus it achieves the sum-capacity, which is then given by:

$$C_{sum} = \log\left(1 + \frac{P}{N_1}\right). \quad (2.21)$$

We note that transmitting to only one user in order to achieve the sum-capacity is only applicable when the transmitter has knowledge of the SNR of each user, and it does not require superposition coding and successive decoding

This result has been extended to fading channels. If no constraint is put on the minimum rate to be achieved by any user or on the delay experienced by any user, throughput maximization on the single-antenna fading broadcast channel is obtained by transmitting to the user that

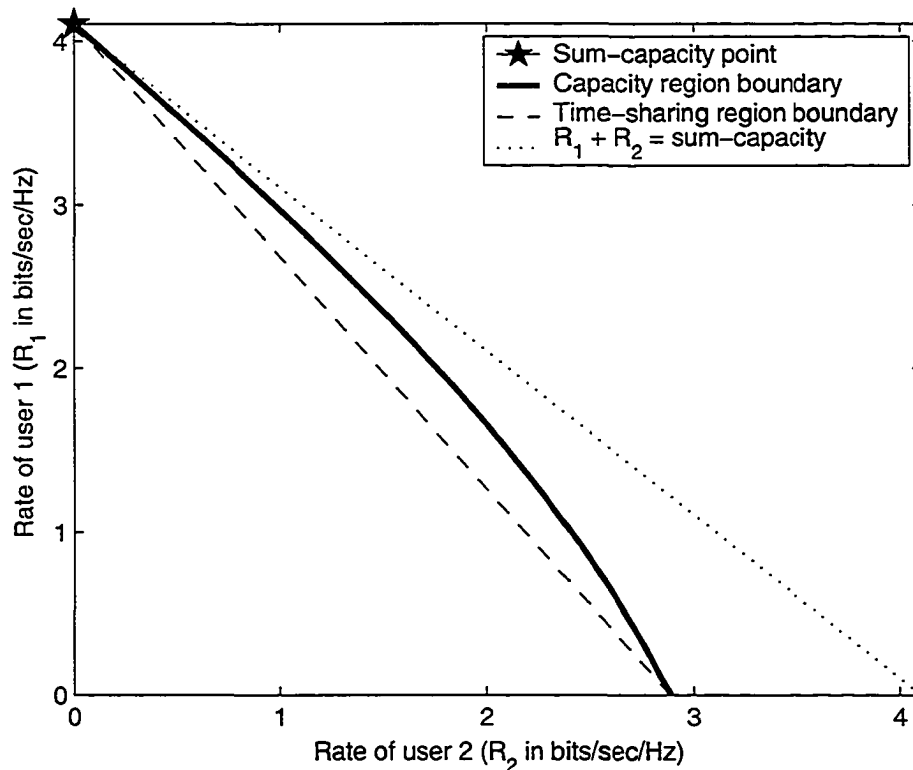


Figure 2-3 Capacity region of the single-antenna broadcast channel.

experiences the largest SNR in any given fading state [17]. The same result was shown for the multiple access channel [18]. In the context of packet-data access, where the channel is assumed to remain constant during a time slot, it is therefore optimal in the sense of throughput maximization to transmit with all the available transmit power to the user with the largest SNR in any given time slot. Obviously the transmitter must have access to that knowledge, which is in practice provided through a feedback channel by the mobile users after they estimate their respective SNR. It was also showed in [17] that if several users share such parallel (non-interfering) broadcast channels with a global transmit power constraint, it is optimal to transmit to the user with the largest SNR on each of the broadcast channels, and to allocate the transmit power with a waterfilling solution.

In practice, a high throughput can be achieved when the mobile users experience independent fading. The base station can schedule the user that experiences a peak of its fading process for transmission in a given time slot. The system thus takes advantage of the inherent multiuser diversity present in the channel. A throughput larger than the one achievable on the Gaussian channel with the same average SNR per user can be achieved. As mentioned previously, this strategy is made possible thanks to the relaxed constraints on the transmission delays allowed by packet-data access systems. Cellular systems that exploit multiuser diversity in single-antenna channels use scheduling algorithms with adaptive coding and modulation, and have already been standardized [19][20].

2.5 The MIMO Broadcast Channel (BC)

2.5.1 Channel Model for the MIMO Broadcast Channel

We adopt the channel model of [6] for the MIMO BC. We consider a channel where the transmitter is equipped with N antennas. There are K receivers. Receiver k is equipped with M_k antennas. The channel between the transmitter and receiver k is modeled by a matrix \mathbf{H}_k of size $M_k \times N$ with fixed complex elements. The AWGN variance at the receiver of each user is assumed to be equal to one. The transmitter is subject to a total power constraint P . We will thus equivalently refer to P as the total power in reference to the noise level. We assume that the receivers have complete channel state information. Thus they perfectly know the channel complex fading gains. The channel state information available at the transmitter depends on the amount of feedback from the receivers.

The complex baseband model for the signal received by the user k is:

$$\mathbf{y}_k = \mathbf{H}_k \mathbf{x} + \mathbf{n}_k. \quad (2.22)$$

The main feature of this channel is that the receivers cannot jointly process the received signals as if they were received by a single antenna array. Thus traditional array processing techniques are not applicable. Moreover in general this channel is a non-degraded broadcast channel. When complete CSIT is available, the channel is non-degraded. The spatial dimensions do not allow to represent the channel of one user as a degraded version of the channel of another user, even though it is still possible to rank the users in the order of their individual capacities.

2.5.2 Multiple Antennas and Multiuser Diversity

There have been numerous recent attempts at exploiting multiuser diversity in multiple-antenna systems. Some approaches aim at achieving spatial multiplexing gain or diversity gain by adopting a single-user transmission strategy where the active user is chosen among the users in a cell according to some criterion. Other approaches aim at creating multiple spatial channels to multiplex signals to several users simultaneously. Eventually, information-theoretic studies provided the optimal strategy that achieves the capacity region of the MIMO BC. We will review these approaches briefly and especially emphasize the information-theoretic results that we will use in subsequent sections in this thesis.

We mainly distinguish between two categories of MIMO BCs. The receivers can be equipped with one or many antennas. The former case is of relevance mainly due to the difficulty of placing multiple antennas on a small device. It is also of relevance to consider that mobile communication service providers can easily upgrade the network by adding antennas to the base station, whereas it is much more difficult to change the devices used by every customer in a short period of time. The $(N,1,K)$ MIMO BC is represented in Figure 2-4. The difference with the

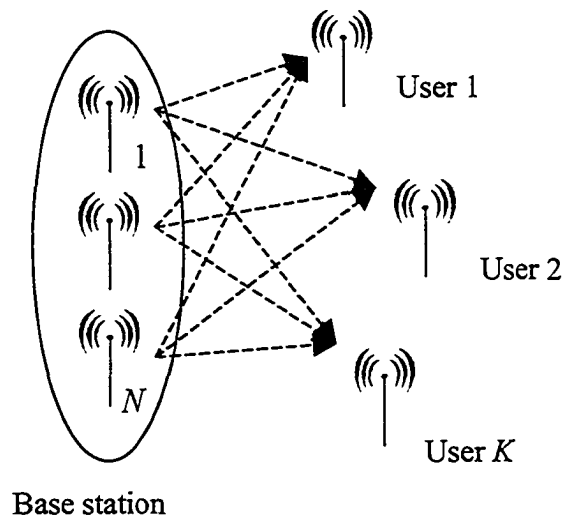


Figure 2-4 The $(N,1,K)$ MIMO BC.

single-user MIMO channel is that the receive antennas are not collocated and thus they cannot jointly process the received signal vector. However the sum-capacity of the $(N,1,K)$ MIMO BC still enjoys the linear growth in the minimum of N and K in the high power region with complete CSIT and CSIR [45]. Thus the spatial multiplexing gain of MIMO systems can be achieved when only the transmitter is equipped with multiple antennas in a multiuser channel. However it cannot be achieved by transmitting to a single user at a time since the channel is not MIMO in this case in any given time slot.

The (N,N,K) MIMO BC where the users are equipped with as many antennas as the base station represents a differently challenging situation. The channel between the base station and any user is already a MIMO channel with a maximum achievable spatial multiplexing gain of N . The cooperative MIMO BC, where the receive antennas of all users are assumed to be collocated, is a $(N,1,NK)$ MIMO channel, with the same maximum spatial multiplexing gain of N . Thus single-user MIMO techniques can be used to achieve a large throughput. However, one is interested in achieving the maximum rates over the channel at hand. Thus it is still relevant to study the optimal transmission strategy and its properties. In particular, it is still not obvious whether transmitting to one user at a time is optimal in some or all situations, even though it is sufficient to achieve the maximum spatial multiplexing gain.

2.5.2.1 Channel state information

In packet-data access systems, the base station transmitter adapts its transmission strategy to the channel conditions of the users it serves. We assume that receivers can estimate the channel coefficients perfectly and thus have perfect and complete CSIR. Transmission adaptation is made possible by feedback information made available by each user to the base station. A scheduler, which is aware of the transmitter architecture, then uses that information to choose when to transmit to certain users and how to adapt the modulation and channel coding to meet transmission quality targets. Then the transmitter sends the data according to the choice made by the scheduler. The transmitter uses some specific architecture that may also require channel state information, possibly different from the channel state information required by the scheduler. We will then consider these two types of CSI. We use the UMTS term of Channel Quality Indicator (CQI) to refer to the type of CSI required by the scheduler to make informed decisions. We denote as CSIT the type of information required by the specific transmitter architecture to filter the signals to be transmitted, where the filter coefficients directly depend on the CSI. This is illustrated in Figure 2-5. We always assume that feedback information is sent to the transmitter through an errorless channel. The CQI feedback channel is required for all users at all times. The

CSIT feedback channel needs only be used once the scheduler has chosen the users that the base station will transmit to in a subsequent time slot. Hence only these users need to feedback CSIT to the transmitter. Obviously these users need to be informed by the base station that they have been scheduled and that they need to feedback the information that will be the CSIT at the base station. For example, in a single-user transmission setting, users could feedback the value of their respective SNRs as CQI for scheduling, and only the scheduled user would later feedback the exact value of its fading gains as CSIT to the transmitter, that will then compute a beamforming vector.

It is also possible that CQI and CSIT use the same feedback channel to convey the same information. A trade-off between the amount of information and the feedback delay (or the complexity of the protocol) is apparent in this model. In some scenarios, the amount of information carried by the CQI could be less than the amount of information carried by the CSIT. In this case we would like to reduce the amount of feedback channels used for CSIT, thus only requiring scheduled users to feedback their CSIT to the base station. In this thesis, we also assume that perfect unquantized CQI and CSIT are available whenever considered. From now on we do not worry about the amount of information needed to transmit such feedback CSI. However it is an important area of research and the effects of imperfect CSI and of limited feedback on the performance of MIMO systems can have a large impact on system design [21][22].

Note that if CSI is provided to the scheduler and to the transmitter by the same feedback channel, then both entities should be able to use the same CSI. However, to cope with complexity or robustness issues for instance, the transmitter architecture could be chosen to be simple so that it does not use CSIT and the system relies only on the scheduler and the modulation and coding adaptation to cope with the varying channel conditions. This is another reason why we consider CQI and CSIT separately. Moreover, CQI could be as bandwidth demanding as complete CSIT.

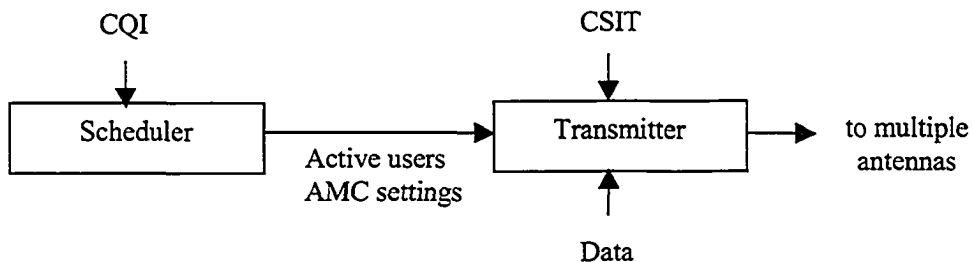


Figure 2-5 CQI and CSIT model.

The best decision the scheduler could make could only be based on complete CSI if the transmission strategy was such that the rate achieved by one user depends on the rate simultaneously achieved by another user. Since users cannot feedback their expected rate as CQI to the transmitter because they have no knowledge of the channels of the other users, they must feedback complete CSI.

In this thesis we only consider adaptation such that a capacity-achieving code is chosen for the given channel realization. This would require an infinite-length time slot. However there exist modern error-control codes that provide near-capacity performance with relatively short sequences. In practice error detection codes are also used in conjunction with ARQ strategies, but this is beyond the scope of this thesis, although it is of foremost importance.

2.5.2.2 Single-user scheduling strategies

Some of the first attempts to take advantage of multiuser diversity and spatial diversity used a direct approach inspired from single-antenna multiuser channels, where a single user is selected for transmission in any given time slot. These approaches were not motivated by information-theoretic results on MIMO multiuser channels, but aimed at achieving large gains using a single-user MIMO channel strategy. The active user is chosen from the CQI available at the transmitter.

2.5.2.2.1 Partial CQI, no CSIT

Single-user capacity scheduling, channel hardening and the effect of correlation

It was pointed out quite early [23] that the single-user scheduling strategies can have serious drawbacks depending on the type of CQI when CSIT is not available. Several authors later also showed the same effects in more mathematical terms [16]. The underlying phenomenon is a consequence of an effect called channel hardening [16]. Channel hardening refers to the reduction of random variations of the channel due to the presence of multiple antennas. In other words, the mutual information of a random channel realization will be close to the mutual information of the average channel realization as the number of antennas increases. The best illustration comes from transmit diversity, which transforms the fading channel into a Gaussian channel in the limit of an infinite number of transmit antennas [4]. As shown in [16] the distribution of the mutual information of the single-user uncorrelated MISO channel with uniform power allocation across the transmit antennas can be closely approached by a Gaussian distribution as the number of antennas becomes large. It is shown that the mean converges to a non-zero constant while the variance decreases to zero.

On the single-user MISO channel, channel hardening was in fact observed directly in [3], where it can be seen from the outage open-loop capacity CCDF curves that the mean of the mutual information increases, while at the same time the variance decreases, as the number of transmit antennas increases from 1 to 2. Thus the tail of the PDF of the mutual information decreases, which means that the mutual information will experience fewer realizations with large values. The diversity offered by multiple transmit antennas reduces the amount of fading thus high peaks occur less frequently.

On the $(N,1,K)$ MIMO BC, observations first made in [23] on the use of spatial diversity with multiuser diversity are summarized as follows. Let us consider the following scheduling strategy, inspired from the maximum-throughput scheduling strategy on the single-antenna multiuser fading channel. Based on the channel matrix estimated at the receiver, each user estimates its instantaneous open-loop channel capacity as if the transmitter was to transmit to that user alone with uniform power allocation across the transmit antennas. Each user then sends this CQI value back to the transmitter. On the $(1,1,K)$ BC, this is equivalent to sending back the value of the instantaneous SNR. However on the MISO channel the definition of SNR is more complex than on the single-antenna channel, and the adoption of the capacity as the measure of the quality of the channel makes sense. Then the base station scheduler chooses the user with the largest reported capacity for transmission using uniform power allocation. Thus transmit diversity and multiuser diversity are exploited. As a consequence of channel hardening, with a fixed number of users and as the transmitter is equipped with more transmit antennas, the average rate achieved by the users decreases. This specific use of transmit diversity reduces the amount of fading, and thus impairs the advantage of using multiuser diversity. Numerical results illustrate this phenomenon in Figure 2-6. The other curves in Figure 2-6 will be explained later.

On the (N,N,K) MIMO BC however, [16] showed that the mean of the mutual information with uniform power allocation increases with N , and although it increases faster than the variance, multiplexing gain allows to exploit spatial diversity without impairing multiuser diversity.

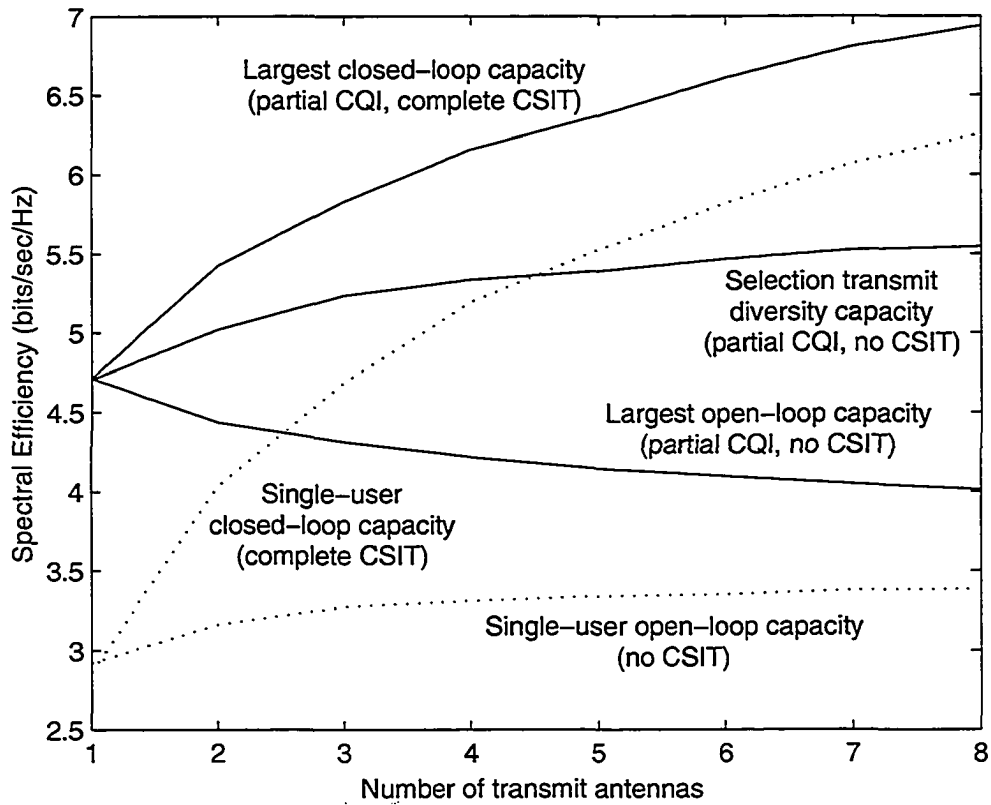


Figure 2-6 Channel hardening effect on multiuser diversity.
 $(N,1,K)$ MIMO BC with $K = 8$ users, and $P = 10$ dB.

The $(1,N,K)$ BC might not be envisioned to play an important role in future communication systems because it is in general more difficult to place multiple antennas at the user equipment than at the base station transmitter due to the small size of the user terminal, and because it is easier for a company to install new antennas at the base station than to replace every user's device. Nevertheless, one can think of applications that would require users to purchase advanced equipment using multiple antennas in order to obtain higher quality of service in a network equipped with single-antenna base stations. Moreover interesting observations can be made on the effect of receive correlations and its implications on multiuser diversity gain.

The cooperative $(1,N,K)$ BC is not a MIMO channel since the transmitter still only has one transmit antenna. Therefore it is not possible to exploit spatial multiplexing gain, and a single-user transmission strategy makes sense. The scheduler thus only needs to receive CQI on the individual channel conditions and choose the user with the largest achievable throughput. We consider then single-user channel capacity as CQI. The transmitter does not need any CSIT. However we still assume that the receivers have perfect CSIR, thus they can perform MRC and coherently combine the signals received at the multiple antennas. Figure 2-7a shows the PDF of

the mutual information of the single-user channel with one transmit antenna and two receive antennas with no receiver correlations and with receiver correlations with correlation coefficient $\rho = 0.7$. We assume the exponential correlation model such that the receiver correlation matrix is given by:

$$\mathbf{H}_R = \begin{pmatrix} 1 & \rho \\ \rho & 1 \end{pmatrix}. \quad (2.23)$$

Thus the channel vector of user k is given by:

$$\mathbf{h}_k = \mathbf{H}_R \mathbf{h}_w, \quad (2.24)$$

where \mathbf{h}_w is of size 2×1 and its elements are independent with a zero-mean unit-variance complex Gaussian distribution. The AWGN at each receive antenna is taken to be equal to one, and the total transmit power is taken to be equal to 10. The PDF of the mutual information of the single-user single-antenna Rayleigh fading channel is also shown for comparison. As is well known, we see that the mean of the mutual information, or ergodic capacity, increases by adding receive antennas. This increase is smaller with receiver correlations. However we also notice that the tail of the PDF towards high spectral efficiencies is larger in the correlated case. We thus expect that multiuser diversity offers greater gains in the correlated case than in the uncorrelated

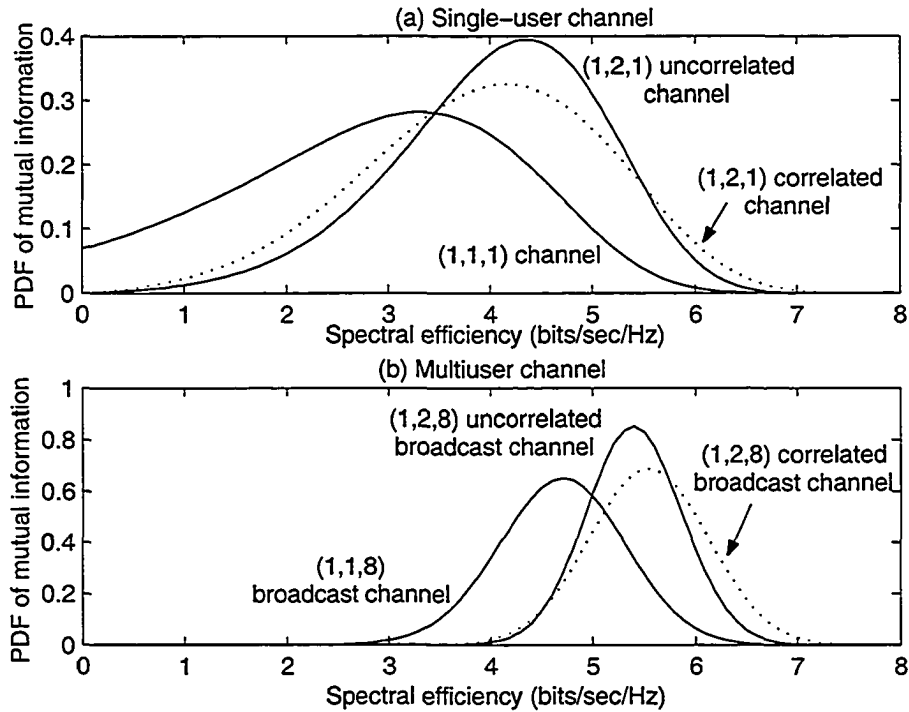


Figure 2-7 PDF of mutual information. Correlated and uncorrelated (1,2,1) and (1,2,8) channels

case, and that receiver spatial diversity increases the throughput in the multiuser channel with the proposed strategy. This is illustrated in Figure 2-7b where the PDF of the mutual information of the user with the largest mutual information in each fading state is shown. There are 8 users with independent fading processes in the channel. We see that in the three cases multiuser diversity is exploited to increase the ergodic capacity. However now it is the correlated channel that offers the largest ergodic capacity with multiuser diversity. The average rate of the scheduled user is thus higher in the correlated case, and the variance of the rate of the scheduled user is also larger in the correlated case. We also noticed that the Gaussian approximation of the capacity [16] provided highly inaccurate results because the number of antennas is small.

For comparison we also consider the case of transmit correlations on the (2,1,8) MIMO BC. We first consider the case where the base station is informed by CQI of the users individual capacities with uniform power allocation, but it does not have any CSIT. The two transmit antennas experience either uncorrelated fading processes or correlated processes with correlation coefficient equal to 0.7 and the transmitter correlation matrix is of the same form as the previously considered receiver correlation matrix (2.23). The PDF of the mutual information in single-user channels is shown in Figure 2-8a, and the PDF in the multiuser case is shown in Figure 2-8b. We still see that antenna correlations enhance multiuser diversity. However we note again the effect of channel hardening that causes spatial diversity to act destructively on multiuser diversity since adding a transmit antenna decreases the average rate of the scheduled user, both in the correlated and uncorrelated cases.

If the transmitter is additionally assumed to have complete CQI and CSIT and to transmit to the user with the largest closed-loop capacity, then the same performance as in the previous case of multiple receive antennas with MRC can be achieved as shown in Figure 2-6. Channel hardening does not impair the effect of multiuser diversity and transmit correlations are beneficial. However in this case the cooperative channel is a MIMO channel, and better strategies can be devised in order to achieve spatial multiplexing and make better use of multiuser diversity than transmitting to a single-user at a time, as will be discussed later. If only partial CQI and no CSIT is available at the transmitter, then strategies such as opportunistic beamforming [24] can be used to still take advantage of multiuser diversity without being impaired by channel hardening. Opportunistic beamforming in fact artificially creates correlations among antennas at the transmitter. In this case, transmit correlations have also been found beneficial in terms of throughput [24].

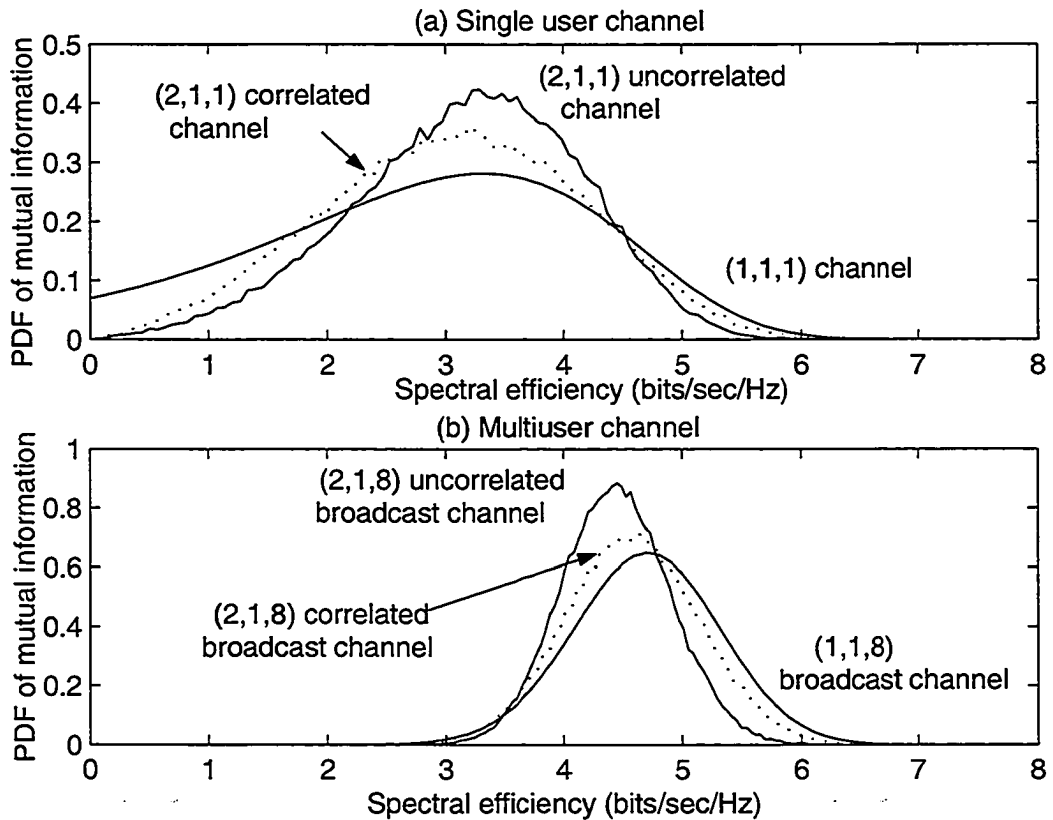


Figure 2-8 PDF of mutual information.
Correlated and uncorrelated (2,1,1) and (2,1,8) channels without CSIT.

The effects of antenna correlations have been studied in systems that exploit multiuser diversity when the users are equipped with as many antennas as the transmitter [25]. The fading gains between the transmitter and each user are correlated, but the fading gains among different users are independent. In this case, it was shown that the rank-deficiency in each single user MIMO channel can be compensated by multiuser diversity in order to still achieve the maximum spatial multiplexing gain. The independence of the fading processes among different users allows to still find N independent spatial dimensions as long as the base station transmits to several users simultaneously. The authors studied the downlink and the uplink with complete CSIT and CSIR. Nevertheless, even though the maximum spatial multiplexing gain can be achieved in the correlated case like in the uncorrelated case, their results showed a degradation of the throughput from the uncorrelated to the correlated case.

Antenna selection scheduling

While still considering partial CQI, transmit spatial diversity could be exploited along with multiuser diversity without requiring a lot of feedback from the users on the $(N,1,K)$ MIMO BC. Each user could feedback the index of the transmit antenna that offers the highest received SNR, along with the value of that SNR. The base station scheduling algorithm now selects the user and the transmit antenna that offer the highest SNR, and use a single-antenna transmission strategy by allocating all the transmit power to that antenna. The order of diversity achieved is the same as if the transmitter had a single antenna and there were NK users experiencing independent fading. Thus the aggregate throughput increases as the number of transmit antennas increases, so spatial diversity and multiuser diversity are exploited jointly. This is illustrated in Figure 2-6.

Quantized feedback scheduling

Application of vector-quantization techniques for MIMO channel state information low-rate feedback to the transmitter has been considered in [21][22], with the goal of maximizing capacity or minimizing error rates. A linear precoding matrix is applied at the transmitter to multiplex signals to a single user at a time. It is chosen from the CQI feedback by a mapping to a codebook of precoding matrices. This strategy is currently one of the closest to being applicable in a real system since it only requires low-rate feedback similar to a rate request in current standards.

Opportunistic beamforming

With partial CQI, other strategies that efficiently exploit spatial and multiuser diversity have been proposed. In particular, opportunistic beamforming allows to achieve the coherent beamforming gains of closed-loop capacity scheduling without the need for complete CQI and complete CSIT, provided that a large number of users is available. A time-varying random beamforming vector is applied at the base station with the hope that one user's channel vector will be close to being in the same beamforming configuration. The advantage of that strategy is that it could be directly applicable for the evolution of third generation packet-data access systems with the addition of transmit antennas at the base station and without any change in the mobile handsets that still perceive the base station as having only one transmit antenna. It allows to achieve array gain and multiuser diversity simultaneously without the need for CSIT. Another advantage of that strategy is that it can create the illusion of fast fading in a slow fading channel, thus increasing the efficiency of multiuser diversity in slow fading channels. Opportunistic scheduling is in a way already being exploited by sectorization, or fixed-beams systems, along with handover among cell sectors.

2.5.2.2.2 Partial CQI, complete CSIT

A simple instance of partial CQI and complete CSIT strategy would be to consider transmitter waterfilling power and rate adaptation in the case of single-user transmission. The CQI for each user is the closed-loop mutual information achievable with waterfilling power allocation given by (2.12), where each user assumes that the base station transmits to no other user at the same time. Each user is able to compute that quantity because it has complete CSIR. The scheduler chooses the user with the largest reported CQI. The transmitter then informs that user that it has been scheduled. In order to achieve the closed-loop capacity for that user, the user is then required to feedback the values of its fading gains as complete CSIT. In order to keep the amount of feedback information small, only the scheduled user would be required to feedback its complete channel matrix to the transmitter. This strategy is able to exploit transmit or receive diversity without impairing the effect of multiuser diversity due to the coherent combining of fading processes. This is illustrated as previously mentioned in Figure 2-6 for the $(N,1,K)$ MIMO BC. If the receivers are equipped with multiple antennas this strategy takes advantage of both spatial multiplexing and multiuser diversity. However this type of CQI does not allow more elaborate strategies such as spatial multiplexing to several users simultaneously.

2.5.2.2.3 Complete CQI and CSIT

One could use coherent transmission at the base station with complete CSI feedback for both CQI and CSIT from each user. The amount of feedback required is larger than in the previous case, but in this case only one feedback channel can be used instead of two since both CQI and CSIT carry the same information. The transmitter can exploit the knowledge of spatial channels and perform transmit spatial multiplexing with optimal power allocation across the transmit antennas. Thus the closed-loop capacity can be achieved by the user with the largest closed-loop capacity, as in the case described in the previous paragraph, but with a different feedback strategy. In this case, feedback is required only once, and the computation of the closed-loop capacity for each user is performed by the scheduler at the transmitter. This strategy allows to increase the aggregate throughput as the number of transmit antennas increases on the $(N,1,K)$ MIMO BC. It is not surprising as the open-loop $(N,1,1)$ MIMO channel capacity asymptotically loses $\log N$ bits/sec/Hz in the high power region compared to the closed-loop $(N,1,1)$ MIMO channel capacity due to non-coherent combining of the fading processes.

However, one can use complete CSI as CQI and CSIT to perform space-division multiple access (SDMA) in order to transmit to several users simultaneously. The advantages of such a strategy are multiple. It can allow to achieve spatial multiplexing gain in cases where it is not

achievable by transmitting to a single user at a time on the $(N,1,K)$ MIMO BC. It allows to reduce the delay between consecutive transmissions to the same user and possibly to make better use of multiuser diversity. It also allows to increase the aggregate throughput as demonstrated theoretically [6][26][27][28]. Before we present the optimal signalling strategy in Section 2.5.3, we focus on linear spatial multiplexing schemes. They offer the advantage of being better understood and realizable in practice with a lower complexity than optimal signalling.

2.5.2.3 Multiuser linear spatial multiplexing

The goal is to perform spatial multiplexing of signals to several users simultaneously by the action of matrix multiplication at the transmitter or at the receiver or at both ends of the communication link. Typically interference-avoidance or joint-orthogonalization is sought.

On the $(N,1,N)$ MIMO BC, Joint-Transmission was proposed in [29] for spatial multiplexing. There the channel matrix is pseudo-inverted at the transmitter so the channels seen by the different users are orthogonal. The same strategy, called zero-forcing beamforming (ZFB), was also considered in [5] with the goal of maximizing the sum of rates simultaneously achievable by all N users. This strategy incurs a power penalty when the channel matrix is close to singular. No scheduling algorithm was proposed since in this case $K = N$.

On the (N,M_k,K) MIMO BC, joint-orthogonalization is implemented by transmit and receive beamforming in [30] with the goal of maximizing an approximation of the product of the signal-to-interference and noise ratios. This scheme constrains the total number of receive antennas to be less than or equal to the number of transmit antennas. Thus if one or more users has multiple receive antennas then transmission can only occur to less than N users at a time. Variations of this scheme are proposed in [31][32]. An extension of ZFB to multiple antenna receivers by group zero-forcing beamforming (GZFB) with the goal of maximizing the sum of rates was proposed in [33]. There the total number of receive antennas must be less than or equal to the number of transmit antennas. The authors also considered scheduling algorithms for the ZFB strategy. The exploitation of multiuser diversity on the (N,N,K) MIMO BC was studied in [34]. The authors proposed a spatial multiplexing strategy where each user performs pseudo-inversion of its own channel matrix at its own receiver, which is only possible if each user is equipped with a least as many antennas as the base station. The resulting channel can be seen as K parallel (non-interfering) single-antenna broadcast channels. The authors called the scheduling algorithm the *independent stream scheduler*, where antennas are allocated independently to users by the maximum SNR criterion. No optimization of power allocation is performed at the transmitter. This strategy still suffers from noise enhancement at the receivers due to the pseudo-

inversion of the channel matrix. This effect increases as the number of antennas increases. Coordinated Beamforming was proposed in [35], where the receivers are all equipped with multiple antennas, with the goal of maximizing the users' rates. A coordinated transmitter-receiver scheme using a generalized zero-forcing algorithm is applied to find the transmit and receive filters for each user. An iterative solution is proposed that converges in general. This scheme is still applicable with single-antenna receivers and becomes equivalent to zero-forcing beamforming. It does not have any constraint on the number of transmit or receive antennas, and achieves spatial multiplexing to a maximum of N users simultaneously. The number of independent streams sent to each user is a design parameter. No scheduling algorithm is considered. Coordinated beamforming will be presented in more detail in Chapter IV.

2.5.3 Optimal Signalling

The problem, especially on the $(N,1,K)$ MIMO BC, is to achieve spatial multiplexing gain. It is obviously not possible to achieve it by transmitting to one user at a time. Thus the solution must be geared towards transmitting to several users at a time in any given time slot. Intuition tells us that the number of active users should be at least N in the high power region in order to achieve the maximum spatial multiplexing gain of N . More precise questions relevant to this problem were presented in Chapter 1. We now summarize the information-theoretic results obtained in [5][6][26][27][28][36] for the (N,M,K) MIMO BC. The direct consequence of the presence of multiple antennas is that the broadcast channel is in general non-degraded when complete CSIT is available [5].

2.5.3.1 Dirty-Paper Coding

Dirty-paper coding is a channel coding scheme applicable for channels with non-causal knowledge of the interference at the transmitter. It was first introduced by Costa [37] for the Gaussian channel with one Gaussian interferer whose realization is known at the transmitter but not at the receiver. Costa proved that a random binning strategy [13] can be used for encoding the

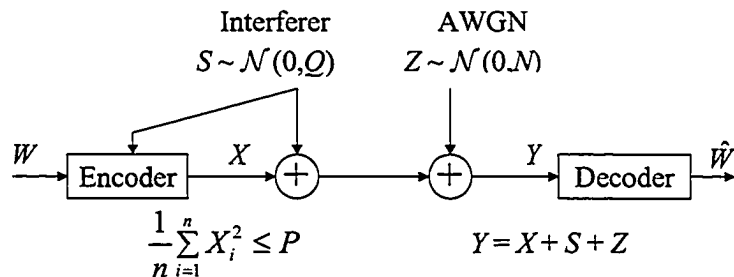


Figure 2-9 Costa's channel model for dirty-paper coding.

desired user's signal so that the maximum mutual information is equal to the capacity of the channel where the interferer would not exist. Thus the capacity of the channel where the transmitter has non-causal knowledge of the interferer is the same as the capacity of the channel without the interferer. The channel model is shown in Figure 2-9. If the transmitter does not have knowledge of the interferer's signal, then the capacity of the channel is:

$$C = \frac{1}{2} \log \left(1 + \frac{P}{N+Q} \right). \quad (2.25)$$

However if the transmitter has non-causal knowledge of the interferer's signal, then the capacity of the channel is:

$$C^* = \frac{1}{2} \log \left(1 + \frac{P}{N} \right). \quad (2.26)$$

This result was later extended to the non-Gaussian case [38], and to the vector case applicable for MIMO channels [39].

The implementation of dirty-paper coding is hard, even for small-sized problems. Precoding techniques such as Tomlinson-Harashima precoding [40][41] handle the case of real constellations with a limited amount of non-causal knowledge. Modulo precoding with nested lattices [38] is in theory able to achieve Costa's capacity, but its complexity becomes very large when the codewords become long and the lattices have large dimensions. Only a few attempts have been made to perform dirty-paper coding with practical coding schemes [42]. However, dirty-paper coding is the tool that allowed to characterize the capacity region of the MIMO BC [36]. Costa's result and its extensions can be directly used to express the achievable rate vectors and perform the maximization of the mutual information on the MIMO BC.

2.5.3.2 Duality between the MIMO BC and the MIMO MAC

A general duality property between the BC and MAC channels was obtained for single antenna channels [43]. In this section we only focus on the duality between the MIMO MAC and the MIMO BC, as first presented in [6]. This duality emerges from the similarity between the successive encoding and decoding processes.

On the MIMO BC, the transmitter knows non-causally the information sequences to be transmitted to each user. A successive encoding strategy using dirty-paper coding can thus be used. The user whose sequence is encoded at stage k will be encoded such that the codewords of users previously encoded will be treated as non-causally known interference. From the dirty-paper coding result, this user will be able to achieve a maximum rate as large as if the users encoded before it did not exist. However it will still suffer from the interference created by the

signals of the users that are encoded after it is encoded. This situation is alike the one for successive decoding where the signal decoded at stage k will not suffer from the interference caused by the signals that have been decoded at previous stages since they have been successfully decoded and subtracted from the received signal.

The dual sum-power MIMO MAC is defined as the channel where the receivers become the transmitters, the transmitter becomes the receiver, and the channel matrices are conjugated and transposed. The transmitter power constraint of the MIMO BC becomes a sum-power constraint shared by all the transmitters of the dual MIMO MAC. The duality result states that given any achievable rate vector in the MIMO BC capacity region, the same rate vector is *achievable in the dual sum-power MIMO MAC capacity region, and vice-versa*. The optimal transmit covariance matrices are related by the MAC to BC and the BC to MAC transformations [6] that are summarized in Appendix D. The rate vectors are achieved by dirty-paper coding on the MIMO BC, and by superposition coding and successive decoding on the dual sum-power MIMO MAC. In particular, the sum-capacity is the same for both channels.

2.5.3.3 Sum-Capacity

The sum-capacity of the MIMO BC has been proved to be achievable by dirty-paper coding [6][26][27][28]. Efficient computation of the sum-capacity of the MIMO BC is carried out on the dual sum-power MIMO MAC:

$$C_{sum} = \max_{\{P_1, \dots, P_K\}} \log \det \left(I_N + \sum_{k=1}^K H_k^* P_k H_k \right) \quad (2.27)$$

$$\text{Subject to } \sum_{k=1}^K \text{tr}(P_k) \leq P.$$

P_k is the transmit covariance matrix of user k on the dual MIMO MAC.

Efficient numerical algorithms have been proposed, and we used the sum-power iterative waterfilling algorithm proposed in [44] to obtain numerical results. These results allowed to demonstrate that the benefits of increased capacity due to the use of multiple antennas and due to the presence of multiple users can be achieved simultaneously as illustrated in Figure 2-10. Monte-Carlo simulations were used to obtain the average sum-capacity over all fading states. The total power in reference to the noise level is 20 dB.

Even when the users are equipped with a single receive antenna, the growth rate of the capacity typical of MIMO systems can be achieved. It was shown mathematically in [45][46] and it is illustrated in Figure 2-11. We let the number of transmit antennas and the number of users grow simultaneously such that $N = K$. We plot the ergodic sum-capacity of the $(N, 1, K)$ MIMO

BC and the ergodic capacity of the $(N,K,1)$ MIMO channel with and without CSIT (respectively the closed-loop capacity and open-loop capacity).

The growth rate of the sum-capacity of the MIMO BC has been studied by several authors. In [45] it was proved that on the $(N,1,K)$ MIMO BC with complete CSIT and CSIR, when both K and N become large with a fixed ratio such that $K \leq N$, the sum-capacity scales linearly with K . In [46] it was proved that with complete CSIT and CSIR, when N and K increase, a lower bound on the sum-capacity scales as $N \log \log K$. This lower bound is given by the maximum sum-rate achievable with a generalization of opportunistic beamforming that provides spatial multiplexing gain, and which is applicable with little feedback from the users to the base station in the form of SINR values and beam index. This result also shows that this capacity scaling is achievable without complete CSIT.

2.5.3.4 Capacity Region

The capacity region of the MIMO BC has been proved to be equal to the dirty-paper coding region in [36]. An example of the capacity region of the MIMO BC is given in Figure 2-12 for a given realization of the $(2,1,2)$ MIMO BC. The sum-capacity is achieved along a

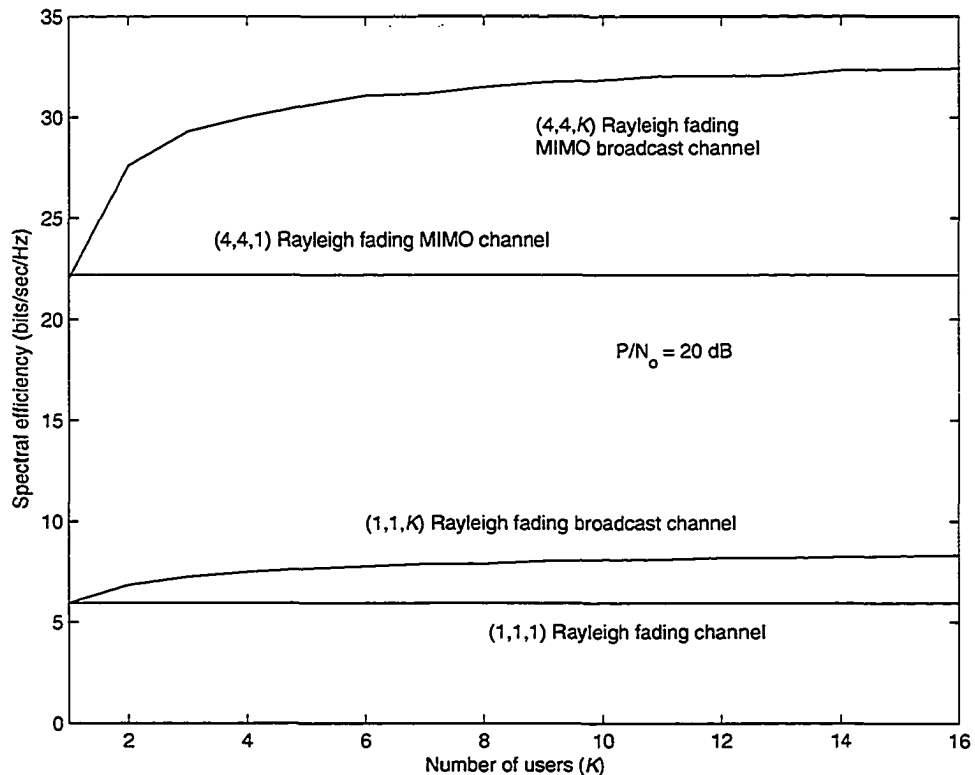


Figure 2-10 Combined effects of multiple antennas and multiuser diversity on the ergodic sum-capacity in the Rayleigh fading broadcast channel with complete CSIT. $P = 20$ dB

segment (in the two-user channel) whose end points correspond to the two possible dirty-paper encoding orders and along which $R_1 + R_2$ is constant. The sum-capacity is achieved by transmitting to more than one user at a time. Single-user transmission strategies as well as time-sharing between single-user transmissions do not allow to achieve the sum-capacity in general.

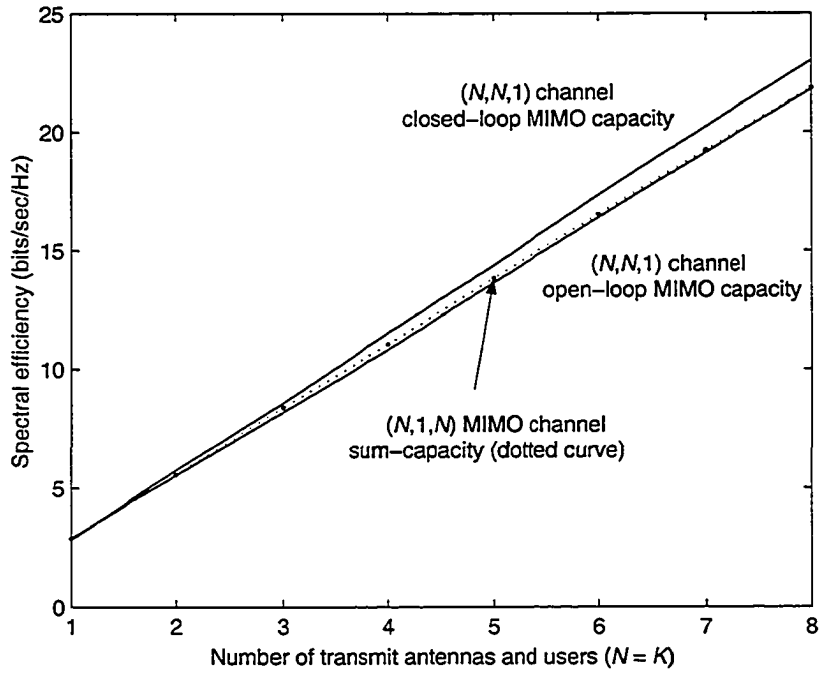


Figure 2-11 Growth rate of the ergodic sum-capacity in the $(N,1,N)$ Rayleigh fading MIMO broadcast channel. $P = 10$ dB.

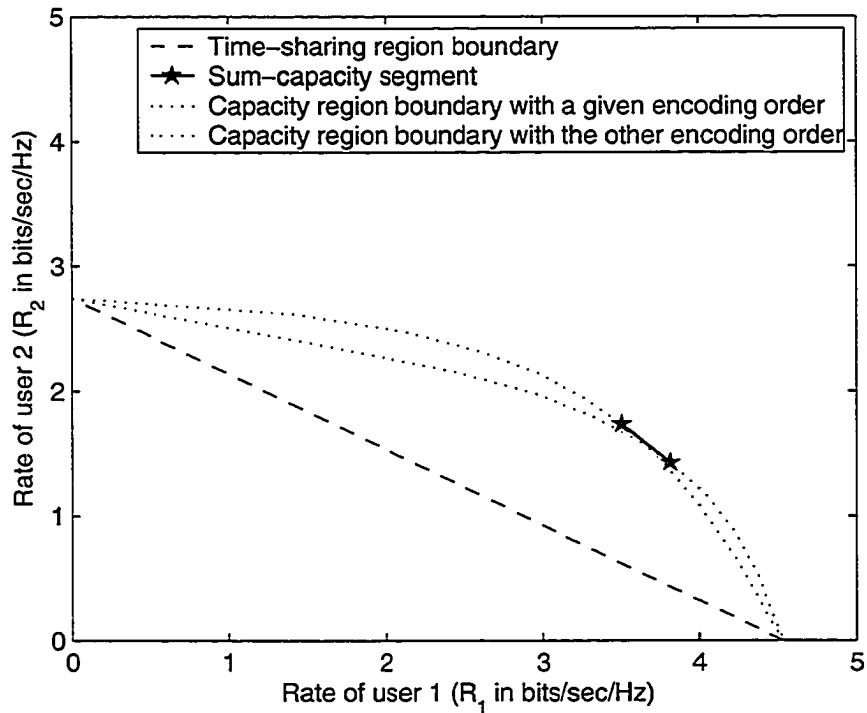


Figure 2-12 Capacity region of the $(2,1,2)$ MIMO broadcast channel.

3 Sum-Capacity of the MIMO BC and the Optimal Number of Active Users

3.1 Introduction

This chapter presents an analysis of the sum-capacity of the Gaussian MIMO broadcast channel, i.e., when all channel matrices or vectors are deterministic. The focus is on understanding the optimal power allocation and on determining the optimal number of active users, i.e. the number of users that are allocated non-zero power. In particular, we study the asymptotically optimal power allocation in the limit where the total transmit power goes to infinity. The study of the number of active users allows us to draw some conclusions on the impact of using multiple antennas at the base station only, or at the base station and at the mobile stations, on scheduling algorithms for throughput maximization applicable to packet-data access transmission.

We first study the sum-power MIMO MAC dual to the $(2,1,K)$ MIMO BC, which allows us to completely characterize the optimal number of active users and the optimal power allocation strategy that achieves the sum-capacity of the sum-power MAC. In particular, we give a geometrical interpretation of our analysis for the $(2,1,3)$ MIMO BC. We then study the optimal power allocation on the MIMO BC after MAC to BC transformations have been applied on the optimal covariance matrices of the dual MIMO MAC. We treat the $(N,1,K)$ MIMO BC and the (N,N,K) MIMO BC separately. We focus on the high power region, and show that only a limited number of one-dimensional channels are allocated a non-vanishing fraction of the total transmit power as it goes to infinity. That number is equal to the number of transmit antennas, provided that these many one-dimensional channels are available. Our main conclusions are the following:

- On the $(N,1,K)$ MIMO BC only N users are allocated a non-vanishing fraction of the total transmit power in the high power region. The asymptotically optimal power allocation is uniform among these users, and the joint action of dirty-paper coding and optimal covariance matrices completely diagonalizes the channels among these N users.

- On the (N, N, K) MIMO BC, only one user is allocated a non-vanishing fraction of the total transmit power in the high power region, as long as the channel matrix of that user is of full rank N .

Our findings are summarized in more detail in Section 3.5. The longest proofs can be found in Appendix D. Next we present the channel model, followed by the mathematical analysis illustrated with numerical examples.

3.2 Channel Model

We consider a channel where one base station is equipped with N transmit antennas. There are K users (receivers) in the sector served by the base station. User k is equipped with M_k antennas. The complex channel gains are assumed to be constant, as they represent a snapshot of the time-varying channel in a time slot during which they are assumed to change slowly enough so they can be considered constant. The underlying random process is such that the complex channel gains can be assumed to be samples of i.i.d. complex Gaussian random variables with zero mean and unit variance, which are assumed to be independent among users and among antenna elements. Thus the channel matrix is random, but it is fixed once it is chosen.

The channel between the transmitter and user k is modeled by a matrix \mathbf{H}_k of size $M_k \times N$. When the users are equipped with a single receive antenna, this matrix becomes a row-vector \mathbf{h}_k . The aggregate channel matrix can then be written in the form $\mathbf{H} = [\mathbf{h}_1^T \ \cdots \ \mathbf{h}_K^T]^T$. The AWGN variance at each antenna of the receiver of each user is assumed to be equal to one. The transmitter is subject to a total power constraint P . If \mathbf{x} is the transmitted vector of symbols at a given time then $\|\mathbf{x}\|^2 \leq P$. We assume that the transmitter and the mobile users have complete channel state information. Thus they perfectly know the channel complex fading gains.

3.3 The $(2,1,K)$ MIMO BC

3.3.1 Mutual Information Maximization

The maximum mutual information between the random variables that represent the transmitted signals and the random variables that represent the received signals is in general difficult to obtain directly for a MIMO BC. Therefore we can consider the maximization problem on the dual sum-power MIMO MAC, where it is a convex optimization problem. Moreover, when the users have a single antenna, the optimization on the sum-power MIMO MAC reduces to power allocation, whereas on the MIMO BC the optimization is over covariance matrices. We propose to reformulate this convex problem in the special case where the base station has $N = 2$

transmit antennas. It allows us to find a closed-form expression for the sum-capacity and to understand the nature of the power allocation solution.

Let p_1, \dots, p_K be the powers allocated to users 1 to K . The sum-capacity of the dual sum-power MAC is given by [6]:

$$C = \max_{\mathbf{p}: \sum_{i=1}^K p_i = P, p_i \geq 0} \log \det \left(\mathbf{I}_N + \sum_{i=1}^K p_i \mathbf{h}_i^* \mathbf{h}_i \right). \quad (3.1)$$

We define $\mathbf{p} = [p_1 \ \dots \ p_K]^T$. Let \mathbf{M} be a matrix with elements $M_{mn} = \|\mathbf{h}_m\|^2 \|\mathbf{h}_n\|^2 - \langle \mathbf{h}_m, \mathbf{h}_n \rangle^2$.

When $N = 2$ we can easily develop the determinant and we write the sum-capacity as:

$$C = \max_{\mathbf{p}: \sum_{i=1}^K p_i = P, p_i \geq 0} \log \left(1 + \sum_{i=1}^K p_i \|\mathbf{h}_i\|^2 + \sum_{i=1}^K \sum_{j>i}^K p_i p_j \left(\|\mathbf{h}_i\|^2 \|\mathbf{h}_j\|^2 - \langle \mathbf{h}_i, \mathbf{h}_j \rangle^2 \right) \right). \quad (3.2)$$

We next express the equivalent minimization problem:

$$\min_{\mathbf{p}} - \left(1 + \sum_{i=1}^K p_i \|\mathbf{h}_i\|^2 + \frac{1}{2} \mathbf{p}^T \mathbf{M} \mathbf{p} \right)$$

$$\text{Subject to } \sum_{i=1}^K p_i = P \text{ and } p_i \geq 0, i = 1, \dots, K. \quad (3.3)$$

We then express the Lagrange dual problem [47] with the Lagrange multiplier ν and the dual vector $\boldsymbol{\lambda} = [\lambda_1 \ \dots \ \lambda_K]^T$. The Lagrange dual function is:

$$L(\mathbf{p}, \boldsymbol{\lambda}, \nu) = -1 - \sum_{i=1}^K p_i \|\mathbf{h}_i\|^2 - \frac{1}{2} \mathbf{p}^T \mathbf{M} \mathbf{p} - \boldsymbol{\lambda}^T \mathbf{p} + \nu \left(\sum_{i=1}^K p_i - P \right). \quad (3.4)$$

Let $\mathbf{u} = [\|\mathbf{h}_1\|^2 \ \dots \ \|\mathbf{h}_K\|^2]^T$ and let \mathbf{I}_K be the column vector composed of K ones. Then the gradient of L at \mathbf{p} is [47]:

$$\nabla L = -\mathbf{u} - \mathbf{M} \mathbf{p} - \boldsymbol{\lambda} + \nu \mathbf{I}_K. \quad (3.5)$$

The Karush-Kuhn-Tucker optimality conditions [47] are:

$$\begin{cases} \sum_{i=1}^K p_i - P = 0, p_i \geq 0, i = 1, \dots, K \\ \lambda_i \geq 0, i = 1, \dots, K \\ \nabla L = 0 \\ \lambda_i p_i = 0, i = 1, \dots, K \end{cases} \quad (3.6)$$

Equivalently:

$$\begin{cases} \sum_{i=1}^K p_i - P = 0, p_i \geq 0, i = 1, \dots, K \\ \lambda_i \geq 0, i = 1, \dots, K \\ -\|\mathbf{h}_i\|^2 - \sum_{j=1}^K p_j M_{ij} - \lambda_i + \nu = 0, i = 1, \dots, K \\ \lambda_i p_i = 0, i = 1, \dots, K \end{cases} \quad (3.7)$$

The dual variables λ_i can be substituted to give:

$$\begin{cases} \sum_{i=1}^K p_i - P = 0, p_i \geq 0, i = 1, \dots, K \\ v - \|\mathbf{h}_i\|^2 - \sum_{j=1}^K p_j M_{ij} \geq 0, i = 1, \dots, K \\ \left(v - \|\mathbf{h}_i\|^2 - \sum_{j=1}^K p_j M_{ij} \right) p_i = 0, i = 1, \dots, K \end{cases} \quad (3.8)$$

Solving this problem directly for p_1, \dots, p_K, v is not easy, but we can solve it recursively assuming that all the users are allocated non-zero power at the optimum. In this case, (3.8) reduces to solving a linear system of $K+1$ equations with $K+1$ unknowns p_1, \dots, p_K, v :

$$\begin{cases} -\sum_{j=1}^K p_j M_{ij} + v = \|\mathbf{h}_i\|^2, i = 1, \dots, K \\ \sum_{i=1}^K p_i = P \end{cases} \quad (3.9)$$

If this system has a solution such that $p_i \geq 0, i = 1, \dots, K$ then the power allocation is optimal. In particular if $p_i > 0, i = 1, \dots, K$ then all users are allocated power. If this system does not have a solution such that $p_i \geq 0, i = 1, \dots, K$ then the solution has to be found by removing users one after the other and solving the mutual information maximization for each of the channels with $K-1$ users. If a solution is still not found, then two users are removed and the same procedure is repeated until a solution is found.

Define the symmetric matrix:

$$\Phi = \begin{bmatrix} 0 & \dots & M_{1i} & \dots & M_{1K} & -1 \\ \vdots & \ddots & & & & \vdots \\ M_{1i} & & 0 & & M_{iK} & -1 \\ \vdots & & & \ddots & & \vdots \\ M_{1K} & & M_{iK} & & 0 & -1 \\ -1 & \dots & -1 & \dots & -1 & 0 \end{bmatrix} \quad (3.10)$$

The system (3.9) can be written as:

$$\Phi \begin{bmatrix} \mathbf{p} \\ v \end{bmatrix} = - \begin{bmatrix} \mathbf{u} \\ P \end{bmatrix}. \quad (3.11)$$

Let $\Phi \leftarrow_i \mathbf{b}$ be the matrix whose i -th column is \mathbf{b} and whose remaining columns coincide with those of Φ . Assuming that Φ is non-singular, the solutions of the system (3.11) can be expressed using Cramer's rule [7]:

$$p_i = \frac{\det \left(\Phi \leftarrow_i \begin{bmatrix} -\mathbf{u} \\ -P \end{bmatrix} \right)}{\det \Phi}. \quad (3.12)$$

Let $\Phi_{k,i}$ be the matrix obtained by deleting row k and column i from Φ . Then using the Laplace expansion by minors along column i [7]:

$$\det(\Phi \leftarrow \mathbf{b}) = \sum_{k=1}^{K+1} (-1)^{k+i} b_k \det \Phi_{k,i}. \quad (3.13)$$

Thus the solution to the system (3.11) is given by:

$$P_i = \frac{(-1)^{K+i} \det \Phi_{K+1,i} P + \sum_{k=1}^K (-1)^{k+i+1} \|h_k\|^2 \det \Phi_{k,i}}{\det \Phi}, \quad i = 1, \dots, K. \quad (3.14)$$

3.3.2 Conditions for all Users to be Allocated Power at the Sum-Capacity

We now express conditions to identify channels where all users are allocated power in order to achieve the sum-capacity. We distinguish between two types of conditions. We establish a general condition for a given total power P . Then we deduce a high power region condition such that all users are allocated power when the total power P is larger than some threshold.

The necessary and sufficient condition for all users to be allocated non-zero power is for $i = 1, \dots, K$:

$$P_i = \frac{(-1)^{K+i} \det \Phi_{K+1,i} P + \sum_{k=1}^K (-1)^{k+i+1} \|h_k\|^2 \det \Phi_{k,i}}{\det \Phi} > 0. \quad (3.15)$$

Assuming that $\det \Phi < 0$ (for example), we can rewrite (3.15) as inequalities on the total transmit power. This way we obtain a system of inequalities on the total transmit power P . If this system is consistent then all users are active for some values of P . Then for each $i = 1, \dots, K$, assuming $\det \Phi_{K+1,i} \neq 0$:

$$P < \frac{-\sum_{k=1}^K (-1)^{k+i+1} \|h_k\|^2 \det \Phi_{k,i}}{(-1)^{K+i} \det \Phi_{K+1,i}} \text{ if } (-1)^{K+i} \det \Phi_{K+1,i} > 0. \quad (3.16)$$

$$P > \frac{-\sum_{k=1}^K (-1)^{k+i+1} \|h_k\|^2 \det \Phi_{k,i}}{(-1)^{K+i} \det \Phi_{K+1,i}} \text{ if } (-1)^{K+i} \det \Phi_{K+1,i} < 0. \quad (3.17)$$

$$P > 0 \quad (3.18)$$

There are three possibilities for the solution of the system $\{(3.16), (3.17), (3.18)\}$:

- There is no value of P that satisfies the system.
- The solution is $P \in [P_1 \ P_2]$ where $0 < P_1 < P_2 < +\infty$.
- The solution is $P \geq P_{th}$. This occurs if and only if the inequality on the total power P is of the type (3.17) for each i . Then there exists a power threshold P_{th} such that all users are allocated power above that threshold. In the general case

where $\det \Phi \neq 0$, using (3.15), the necessary and sufficient condition for the existence of a power threshold such that all users are allocated non-zero power when the total power is larger than that threshold is:

$$i=1, \dots, K: (-1)^{K+i} \det \Phi_{K+1,i} \det \Phi > 0. \quad (3.19)$$

We immediately notice the difference of this system with a waterfilling solution [48]. As the total power available at the base station for transmission is increased, the number of active users could vary non-monotonically. For instance with channel realizations such that the system of inequalities $\{(3.16), (3.17), (3.18)\}$ is consistent when $P \in [P_1 \ P_2]$, some user is allocated power for a certain value of $P \in [P_1 \ P_2]$, but it would not be allocated power for a value of $P > P_2$. We prove in Appendix A that there are channels where this situation occurs, and we give numerical examples of this fact later.

When all users are allocated power at the sum-capacity we can express the sum-capacity in a more compact form. Let $\mathbf{b} = [\|h_1\|^2 \ \dots \ \|h_K\|^2 \ P]^T$. If Φ is non-singular and the power allocation vector \mathbf{p} given by $[\mathbf{p}^T \ v]^T = -\Phi^{-1} \mathbf{b}$ is component-wise positive, then the sum-capacity is given in closed-form as (see Appendix B):

$$C = \log(1 - 1/2 \mathbf{b}^T \Phi^{-1} \mathbf{b}). \quad (3.20)$$

3.3.3 Optimal Number of Active Users at the Sum-Capacity

We have noticed that the matrix Φ is ill-conditioned when $K \geq 6$. We have not been able to prove it, but simulations using numerical algorithms to compute the sum-capacity of the MIMO broadcast channel [44] also show that a component-wise positive solution is not produced if $K > 5$ when the base station is equipped with two transmit antennas. Figure 3-1 shows the histogram of the number of active users as a function of the total number of users K and the power level P in reference to the receiver noise level for 10000 channel realizations for each value of K and P . We observed that no more than five users are allocated power simultaneously even as K and P increase. Similar results have been reported in [49] in the case of real channels. The author of [49] proved that the maximum number of active users equipped with one receive antenna when the base station has N transmit antennas is $N(N+1)/2$. In the complex channel considered in this paper with $N=2$ transmit antennas, there are four real dimensions available for transmission. According to the result in [49] the maximum number of users using only one

real dimension is ten, which is intuitively consistent with our observation of a maximum number of five active users where each user uses two real dimensions.

In the low power region it is straightforward to recognize that only one user is allocated power. As P increases to the high power region at least two users will be allocated power. This is intuitively satisfying since the two degrees of freedom present in the MIMO channel can only be exploited by at least two users since one user alone can only exploit one spatial dimension. A closed-form expression of the sum-capacity of the MIMO BC with N transmit antennas and two users equipped with a single receive antenna was derived in [5] where it was shown that both users are active in the high power region unless their channel vectors are collinear. Moreover, the previous analysis also proves that there could be more than two active users in the high power region when the number of users in the channel is larger than two. The reason is that the best two users cannot always exploit the two degrees of freedom of the MIMO channel in the best possible way, whereas more users together can on some channels. Thus the sum-capacity averaged over all possible channel realizations cannot be attained at all values of signal-to-noise ratio by any

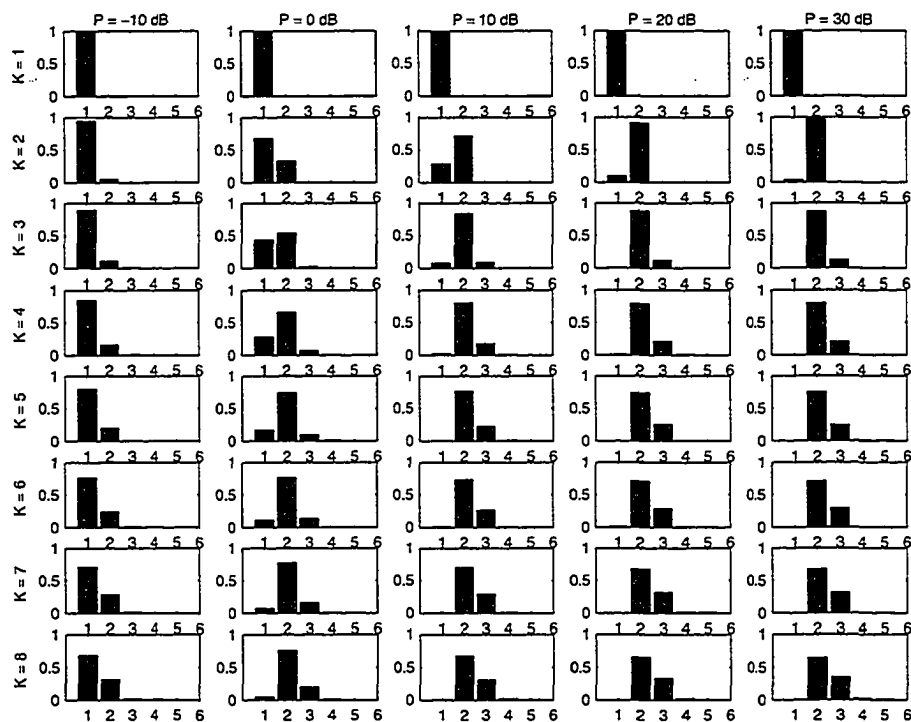


Figure 3-1 Histograms of the optimal number of active users as a function of the total number of users and the total power in reference to the noise level. The horizontal axis represents the number of active users, the vertical axis the fraction of the number of channel realizations.

scheme that transmits to two users at a time, which was the case with the schemes proposed in [5].

3.3.4 Geometric Interpretation on the (2,1,3) MIMO BC

The system {(3.16), (3.17), (3.18)} is not guaranteed to have a solution a-priori. In this section we summarize the results proved in Appendix C. We proved that this system has a solution for some channel realizations, and we completely characterize these realizations on the (2,1,3) MIMO BC. In the case of real channel vectors, this result can be interpreted in the Euclidean plane with respect to the norms of the channel vectors and the angles between the channel vectors of the three users. We first need some definitions.

We can define unambiguously the angle θ between two non-zero vectors x and y in \mathbb{C}^n by [7]:

$$\cos \theta = \frac{|\langle y, x \rangle|}{\langle x, x \rangle^{1/2} \langle y, y \rangle^{1/2}}, \quad 0 \leq \theta \leq \frac{\pi}{2}. \quad (3.21)$$

Thus we define the angle θ_{mn} for $1 \leq m, n \leq 3$ such that

$$M_{mn} = \|\mathbf{h}_m\|^2 \|\mathbf{h}_n\|^2 (1 - \cos^2 \theta_{mn}) = \|\mathbf{h}_m\|^2 \|\mathbf{h}_n\|^2 \sin^2 \theta_{mn}. \quad (3.22)$$

Without loss of generality (see Appendix C), we assume that

$$\begin{aligned} 0 < \|\mathbf{h}_1\| &\leq \|\mathbf{h}_2\| \\ 0 < \|\mathbf{h}_1\| &\leq \|\mathbf{h}_3\| \end{aligned} \quad (3.23)$$

Thus we can define the angles $\tilde{\theta}_{12}$ and $\tilde{\theta}_{13}$ unambiguously on $[0 \ \pi/2]$ such that

$$\sin(\tilde{\theta}_{12}) = \sqrt{\frac{\|\mathbf{h}_1\|^2}{\|\mathbf{h}_3\|^2}} \sin(\theta_{12}). \quad (3.24)$$

$$\sin(\tilde{\theta}_{13}) = \sqrt{\frac{\|\mathbf{h}_1\|^2}{\|\mathbf{h}_2\|^2}} \sin(\theta_{13}). \quad (3.25)$$

The results for the high power threshold condition are summarized in Table 3.1. The results for the non-monotonicity condition are summarized in Table 3.2.

	Complex channel	Real channel
$\det(\Phi) > 0$	Impossible	Impossible
$\det(\Phi) < 0$	<p>If $\ h_1\ \leq \ h_2\ , \ h_1\ \leq \ h_3\$</p> <p>Requires that:</p> $\begin{cases} \sin^2 \tilde{\theta}_{23} < \sin^2 \tilde{\theta}_{12} + \sin^2 \tilde{\theta}_{13} \\ \sin^2 \tilde{\theta}_{13} < \sin^2 \tilde{\theta}_{12} + \sin^2 \tilde{\theta}_{23} \\ \sin^2 \tilde{\theta}_{12} < \sin^2 \tilde{\theta}_{13} + \sin^2 \tilde{\theta}_{23} \end{cases}$	<p>If $\ h_1\ = \ h_2\ = \ h_3\$ requires that:</p> $\theta_{12} + \theta_{13} + \theta_{23} = \pi$ <p>If $\ h_1\ = \ h_2\ < \ h_3\$ requires that:</p> $\frac{ \sin^2 \theta_{13} - \sin^2 \theta_{23} }{\sin^2 \theta_{12}} < \frac{\ h_1\ ^2}{\ h_3\ ^2} < \frac{\sin^2 \theta_{13} + \sin^2 \theta_{23}}{\sin^2 \theta_{12}}$

Table 3-1 Summary of high power threshold condition on the (2,1,3) MIMO BC

	Complex channel	Real channel
$\det(\Phi) > 0$	Impossible	Impossible
$\det(\Phi) < 0$	<p>If $\ h_1\ \leq \ h_2\ , \ h_1\ \leq \ h_3\$ and</p> <p>$\ h_1\ \neq \ h_2\$ or $\ h_2\ \neq \ h_3\$</p> <p>Requires that:</p> $\begin{cases} \sin^2 \tilde{\theta}_{13} + \sin^2 \theta_{23} < \sin^2 \tilde{\theta}_{12} < (\sin \tilde{\theta}_{13} + \sin \theta_{23})^2 \\ (\ h_2\ ^2 - \ h_3\ ^2) \sin^2 \tilde{\theta}_{12} < (\ h_2\ ^2 - \ h_1\ ^2) \sin^2 \theta_{23} \\ (\ h_1\ ^2 - \ h_3\ ^2) \sin^2 \tilde{\theta}_{12} < (\ h_1\ ^2 - \ h_2\ ^2) \sin^2 \tilde{\theta}_{13} \end{cases}$ <p>And implicitly $\tilde{\theta}_{13} + \theta_{23} < \pi/2$.</p> <p>If $\ h_3\ \leq \ h_1\$ and $\ h_3\ \leq \ h_2\$: impossible.</p>	<p>If $\ h_1\ = \ h_2\ < \ h_3\$</p> <p>Requires that:</p> $\theta_{12} = \theta_{13} + \theta_{23}$ <p>and</p> $\begin{cases} \frac{\sin^2 \theta_{13} + \sin^2 \theta_{23}}{\sin^2 \theta_{12}} < \frac{\ h_1\ ^2}{\ h_3\ ^2} \\ \frac{\ h_1\ ^2}{\ h_3\ ^2} < \left(\frac{\sin \theta_{13} + \sin \theta_{23}}{\sin \theta_{12}} \right)^2 \\ 0 \leq \theta_{13} + \theta_{23} < \pi/2 \end{cases}$

Table 3-2 Summary of non-monotonicity condition on the (2,1,3) MIMO BC (the users are ordered such that user 3 is not active in the high power region)

3.3.5 Numerical Examples

We illustrate our analysis with three simple examples where $K = 3$ users have real channel vectors. We assume without loss of generality that $0 < \|h_1\| \leq \|h_2\|$ and $0 < \|h_1\| \leq \|h_3\|$. We use the results shown in Appendix C:

- All 3 users are active in the high power region, i.e. above some certain threshold, if:

$$\left\{ \begin{array}{l} 0 < \|h_1\| = \|h_2\| \leq \|h_3\| \\ \frac{|\sin^2 \theta_{23} - \sin^2 \theta_{13}|}{\sin^2 \theta_{12}} < \frac{\|h_1\|^2}{\|h_3\|^2} < \frac{\sin^2 \theta_{13} + \sin^2 \theta_{23}}{\sin^2 \theta_{12}} \end{array} \right. \quad (3.26)$$

- All 3 users are active in some interval of power values, but only users 1 and 2 are allocated power in the high power region if:

$$\left\{ \begin{array}{l} 0 < \|h_1\| = \|h_2\| < \|h_3\| \\ \theta_{12} = \theta_{13} + \theta_{23} < \pi/2 \\ \frac{\sin^2 \theta_{13} + \sin^2 \theta_{23}}{\sin^2 \theta_{12}} < \frac{\|h_1\|^2}{\|h_3\|^2} < \left(\frac{\sin \theta_{13} + \sin \theta_{23}}{\sin \theta_{12}} \right)^2 \end{array} \right. \quad (3.27)$$

(3.26) and (3.27) are special cases that lend themselves to a graphical representation as shown in the examples below. We consider the case where $0 < \|h_1\| = \|h_2\| < \|h_3\|$.

We let $\theta_{12} = \frac{\pi}{4}$, $\theta_{13} = \frac{\pi}{12}$ and $\theta_{23} = \frac{\pi}{6}$ thus $\theta_{12} = \theta_{13} + \theta_{23} < \pi/2$.

With the assumed values of θ_{12} , θ_{13} and θ_{23} we get:

$$\begin{aligned} \frac{|\sin^2 \theta_{23} - \sin^2 \theta_{13}|}{\sin^2 \theta_{12}} &= 0.3660 \\ \frac{\sin^2 \theta_{13} + \sin^2 \theta_{23}}{\sin^2 \theta_{12}} &= 0.6340 \\ \left(\frac{\sin \theta_{13} + \sin \theta_{23}}{\sin \theta_{12}} \right)^2 &= 1.1516 \end{aligned}$$

Example 3.1: A channel realization where at most 2 users are active.

Let $\|h_1\|^2 = \|h_2\|^2 = \frac{1}{3}$, $\|h_3\|^2 = 1$.

$$\text{Thus } H = \begin{bmatrix} h_1 \\ h_2 \\ h_3 \end{bmatrix} = \begin{bmatrix} \frac{1}{\sqrt{3}} & 0 \\ \frac{1}{\sqrt{3}} \cos\left(\frac{\pi}{4}\right) & \frac{1}{\sqrt{3}} \sin\left(\frac{\pi}{4}\right) \\ \cos\left(\frac{\pi}{12}\right) & \sin\left(\frac{\pi}{12}\right) \end{bmatrix} = \begin{bmatrix} \frac{1}{\sqrt{3}} & 0 \\ \frac{\sqrt{2}}{2\sqrt{3}} & \frac{\sqrt{2}}{2\sqrt{3}} \\ \frac{\sqrt{6} + \sqrt{2}}{4} & \frac{\sqrt{6} - \sqrt{2}}{4} \end{bmatrix}.$$

The system of inequalities $\{(3.16), (3.17), (3.18)\}$ is:

$$\begin{cases} P < -171.138 \\ P > -1.395 \\ P < -26.609 \\ P > 0 \end{cases}$$

There is no value of the power such that all three users are active. Figure 3-2 shows the channel vectors of the users. Figure 3-3 shows the fraction of the total power

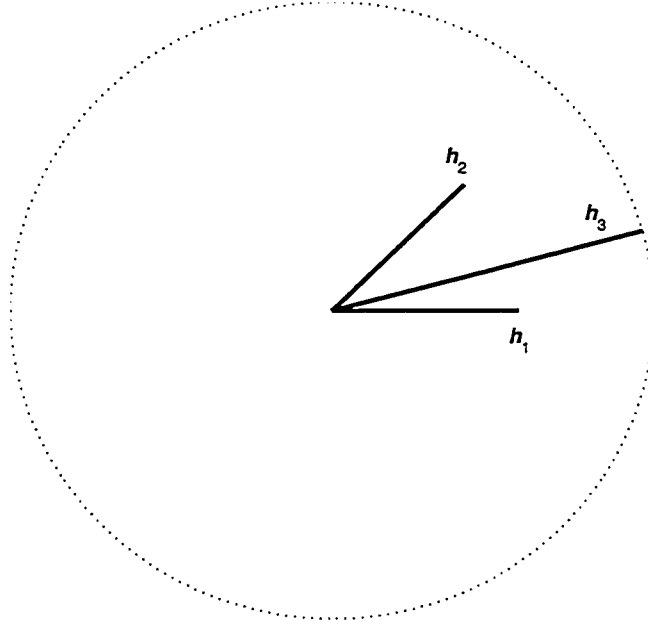


Figure 3-2 Channel vectors in Example 3.1

allocated to each user as a function of the total power in reference to the noise level.

Example 3.2: A channel realization where all 3 users are active in the high power region.

Let $\|h_1\|^2 = \|h_2\|^2 = \frac{1}{2}$, $\|h_3\|^2 = 1$.

$$\text{Thus } H = \begin{bmatrix} h_1 \\ h_2 \\ h_3 \end{bmatrix} = \begin{bmatrix} \frac{1}{\sqrt{2}} & 0 \\ \frac{1}{\sqrt{2}} \cos\left(\frac{\pi}{4}\right) & \frac{1}{\sqrt{2}} \sin\left(\frac{\pi}{4}\right) \\ \cos\left(\frac{\pi}{12}\right) & \sin\left(\frac{\pi}{12}\right) \end{bmatrix} = \begin{bmatrix} \frac{1}{\sqrt{2}} & 0 \\ \frac{1}{2} & \frac{1}{2} \\ \frac{\sqrt{6}+\sqrt{2}}{4} & \frac{\sqrt{6}-\sqrt{2}}{4} \end{bmatrix}.$$

The system of inequalities {(3.16), (3.17), (3.18)} is:

$$\begin{cases} P > 25.856 \\ P > 2.309 \\ P > -29.856 \\ P > 0 \end{cases}$$

A solution exists when $P > 25.856$. Figure 3-4 shows the fraction of the total power allocated to each user as a function of the total power in reference to the noise level.

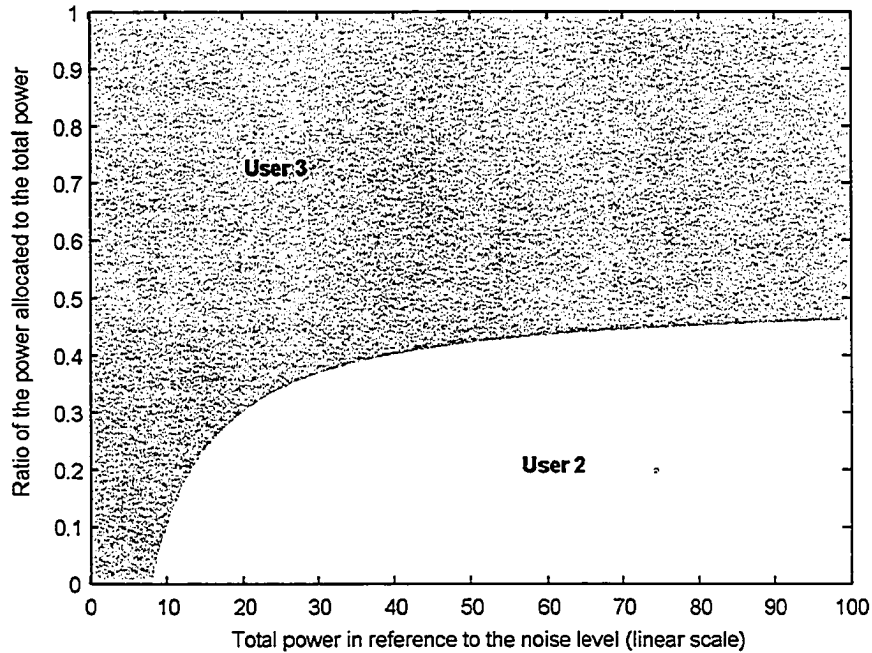


Figure 3-3 Fraction of power allocated to each user as a function of the total power in the channel of Example 3.1 with $K = 3$ and $N = 2$.

Example 3.3: A channel realization with non-monotonic behaviour of the number of active users as a function of the total transmit power.

Let $\|h_1\|^2 = \|h_2\|^2 = \frac{3}{4}$, $\|h_3\|^2 = 1$.

$$\text{Thus } H = \begin{bmatrix} h_1 \\ h_2 \\ h_3 \end{bmatrix} = \begin{bmatrix} \sqrt{\frac{3}{4}} & 0 \\ \sqrt{\frac{3}{4}} \cos\left(\frac{\pi}{4}\right) & \sqrt{\frac{3}{4}} \sin\left(\frac{\pi}{4}\right) \\ \cos\left(\frac{\pi}{12}\right) & \sin\left(\frac{\pi}{12}\right) \end{bmatrix} = \begin{bmatrix} \frac{\sqrt{3}}{2} & 0 \\ \frac{\sqrt{6}}{4} & \frac{\sqrt{6}}{4} \\ \frac{\sqrt{6} + \sqrt{2}}{4} & \frac{\sqrt{6} - \sqrt{2}}{4} \end{bmatrix}.$$

The system of inequalities {(3.16), (3.17), (3.18)} is:

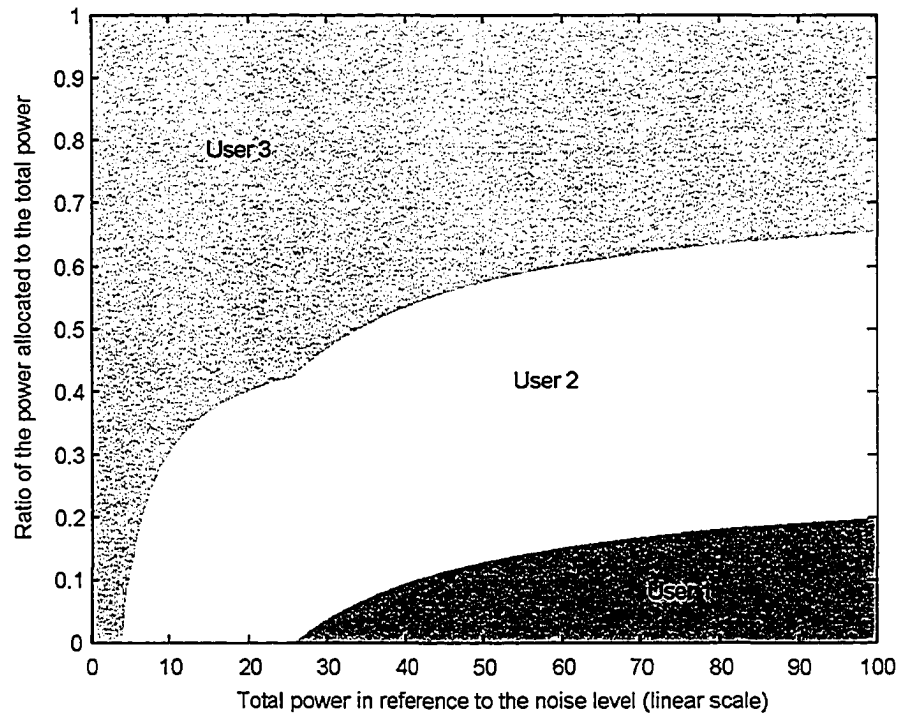


Figure 3-4 Fraction of power allocated to each user as a function of the total power in the channel of Example 3.2 with $K = 3$ and $N = 2$.

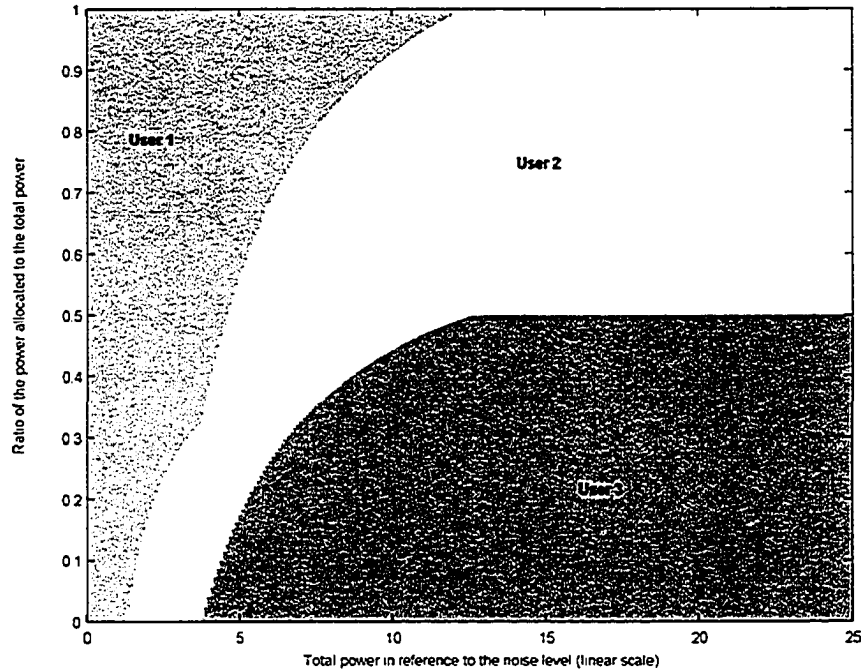


Figure 3-5 Fraction of power allocated to each user as a function of the total power in the channel of Example 3.3 with $K = 3$ and $N = 2$.

$$\begin{cases} P > 3.875 \\ P > 1.712 \\ P < 11.491 \\ P > 0 \end{cases}$$

A solution exists when $3.875 < P < 11.491$. Figure 3-5 shows the fraction of the total power allocated to each user as a function of the total power in reference to the noise level.

3.4 Asymptotically Optimal Power Allocation in the High Power Region

3.4.1 Introduction

In this section we study the optimal power allocation required to achieve the sum-capacity as the total transmit power becomes large. The optimality we consider is to achieve the sum-capacity. Other optimality criteria could be used. The goodness of a power allocation policy could be judged by the ratio of the sum of rates achievable with this power allocation policy to the sum-capacity. A power allocation policy would then be declared to be optimal if the ratio goes to 1 as the power goes to infinity. This criterion is in general easier to analyse. For instance,

on the (N,N,K) MIMO BC, we can directly see from single-user MIMO channel capacity results that the growth rate of the capacity of the cooperative $(N,NK,1)$ MIMO channel and the growth rate of the capacity of any of the users' $(N,N,1)$ channels are the same, namely $N \log P$ in the high power region. Thus the ratio of any of the users' $(N,N,1)$ channel capacity to the sum-rate capacity of the (N,N,K) MIMO BC goes to 1 as the power becomes large. However, we can prove a stronger result, and gain more knowledge about the optimal transmission strategy. We can prove that asymptotically in the high power region, the optimal dirty-paper coding strategy and power allocation policy is such that only one user will be allocated a non-vanishing fraction of the total transmit power, and other active users are allocated a vanishing fraction of the total transmit power, while some users might be allocated no power at all. The user in question depends on a design choice, namely choosing which user is encoded first in the dirty-paper coding process, as long as that user's channel matrix is full rank.

On the other hand, on the $(N,1,K)$ MIMO BC with $K \geq N$, it is not straightforward to conclude even on the optimality in the ratio sense for any power allocation policy since the absence of receiver cooperation makes the analysis difficult and one cannot use single-user MIMO channel results to conclude on the optimality of any power allocation policy in the ratio sense. One can only conclude that the ratio of any of the users' $(N,1,1)$ channel capacity to the cooperative $(N,N,1)$ MIMO channel capacity goes to 0 as the power becomes large. Other transmission strategies with linear spatial multiplexing and waterfilling power allocation to N users can be shown to be optimal in the ratio sense in the high power region [5]. Thus one can prove that transmitting to N users is sufficient to achieve the same growth rate as the growth rate of the sum-capacity. However here again we can prove a stronger result, namely that it is asymptotically optimal to allocate a non-vanishing fraction of the total transmit power to only N users, while other active users are allocated a vanishing fraction of the total transmit power, while some users might be allocated no power at all. Other properties of the optimal transmission strategy are obtained simultaneously.

We will now present these results in the next sections. The details of the proofs are left to Appendix D.

3.4.2 The $(N,1,K)$ MIMO BC

This section is devoted to studying the asymptotically optimal power allocation required to achieve the sum-capacity of the $(N,1,K)$ MIMO BC in the limit where the total transmit power becomes large. The power allocated to user i is equal to the trace of its transmit covariance matrix. This covariance matrix can be obtained by transforming the dual sum-power MIMO MAC covariance matrix of users i as shown in [6]. On the MIMO MAC dual to the $(N,1,K)$ MIMO BC the covariance matrix of users i is a scalar p_i . In order to prove our results, we make the following assumptions:

- There are at least as many users as transmit antennas: $K \geq N$.
- At least N users are allocated a non-vanishing fraction of the total transmit power on the dual sum-power MIMO MAC.

These assumptions are reasonable. As long as there are at least as many users as transmit antennas, it is only possible to exploit the N dimensions available in the MIMO channels by allocating power to at least N users. We saw on the $(2,1,K)$ MIMO BC that it is even possible that more than N users be allocated a non-vanishing fraction of the total transmit power on the dual sum-power MIMO MAC. If we consider the sub-channel composed of the $K_a \geq 2$ active users in the high power region, we saw that the power allocated to user i in the high power region is given by (3.14) as:

$$p_i = \frac{(-1)^{K+i} \det \Phi_{K+1,i} P + \sum_{k=1}^K (-1)^{k+i+1} \|h_k\|^2 \det \Phi_{k,i}}{\det \Phi} \quad (3.28)$$

So

$$\alpha_i^{MAC} = \lim_{P \rightarrow \infty} \frac{p_i}{P} = \frac{(-1)^{K+i} \det \Phi_{K+1,i}}{\det \Phi}. \quad (3.29)$$

The fraction α_i^{MAC} of the total transmit power allocated to user i on the sum-power MIMO MAC in the high power region is a constant.

After MAC to BC transformation of the MIMO MAC power allocation we obtain the optimal MIMO BC transmit covariance matrices $\Sigma_1, \dots, \Sigma_K$. We consider the following arbitrary encoding order used for dirty-paper coding on the MIMO BC. User K is encoded first, then user $K-1$, and so on until user 1 is encoded last. We prove in Appendix D that asymptotically in the high power region:

$$\lim_{P \rightarrow \infty} \frac{\text{tr}(\Sigma_i)}{P} = 0 \text{ if } i \leq K - N \quad (3.30)$$

$$\lim_{P \rightarrow \infty} \frac{\text{tr}(\Sigma_i)}{P} > \alpha_i^{MAC} \text{ if } i > K - N \quad (3.31)$$

α_i^{MAC} is the limit of the power allocated to user i on the dual sum-power MIMO MAC divided by the total transmit power as the total transmit power goes to infinity.

Therefore only N users are allocated a non-vanishing fraction of the total transmit power at the sum-capacity in the high power region on the MIMO BC. In other words, with K users and possibly more than N active users being allocated a non-vanishing fraction of the total transmit power at the sum-capacity of the dual sum-power MIMO MAC, only N of these users will still be allocated a non-vanishing fraction of the total transmit power on the MIMO BC in the high power region. Moreover this fraction is at least as large as the fraction they are allocated on the dual sum-power MIMO MAC in the high power region.

Furthermore we also prove the following property of the optimal BC covariance matrices of these N users. Let the optimal covariance matrix of user i , which has rank one, be:

$$\Sigma_i = \text{tr}(\Sigma_i) \mathbf{v}_i \mathbf{v}_i^*, \quad (3.32)$$

where \mathbf{v}_i is the beamforming vector used to transmit to user i . We prove that for a given $j > K - N$:

$$\lim_{P \rightarrow \infty} \mathbf{h}_j \mathbf{v}_i^* = 0 \text{ for all } i \text{ such that } K - N < i < j. \quad (3.33)$$

This result tells us that asymptotically in the high power region on the $(N,1,K)$ MIMO BC, the optimal beamforming vector for user $i > K - N$ on the BC becomes orthogonal to the channel matrix of user j for all $j > i$. In other words, the optimal transmit beamforming vector of user $i > K - N$ becomes asymptotically orthogonal to the channel matrices of all other users that are allocated an asymptotically non-vanishing fraction of the total transmit power and that are encoded with dirty-paper coding prior to user i .

As a consequence on the $(N,1,N)$ MIMO BC, all N users are allocated a non-vanishing fraction of the total transmit power P asymptotically in the high power region on the MIMO BC. Using the above property of the asymptotically optimal covariance matrices we can express the asymptotic rates achieved by the N users in the high power region as a first order approximation:

$$\lim_{P \rightarrow \infty} R_j^{BC} \approx \log \left| \mathbf{I}_{M_j} + \mathbf{h}_j \Sigma_j \mathbf{h}_j^* \right|. \quad (3.34)$$

The channel is completely orthogonalized by the joint action of dirty-paper coding and the optimal transmit covariance matrices in order to achieve the sum-capacity of the $(N,1,N)$ MIMO

BC. The first order asymptotic approximation of the sum-capacity can thus be obtained:

$$\lim_{P \rightarrow \infty} C_{sum}^{BC} \approx N \log \left(P + \sum_{n=1}^N \frac{1}{\|h_n \mathbf{W}_{1:n}\|^2} \right) - N \log N + \sum_{j=1}^N \log \left(\|h_j \mathbf{W}_{1:j}\|^2 \right). \quad (3.35)$$

$\mathbf{W}_{1:j}$ is an $N \times j$ matrix composed of orthonormal columns, as defined in Appendix D. The asymptotically optimal power allocation is also obtained as:

$$\lim_{P \rightarrow \infty} tr(\Sigma_j) = \frac{P}{N} + \frac{1}{N} \sum_{n=1}^N \left(\frac{1}{\|h_n \mathbf{W}_{1:n}\|^2} - \frac{1}{\|h_j \mathbf{W}_{1:j}\|^2} \right). \quad (3.36)$$

Also as a first order approximation, the asymptotically optimal power allocation on the MIMO BC, given an arbitrary encoding order, is uniform among the N users that are allocated a non-vanishing fraction of the total transmit power in the high power region. Our proof is valid for any value of N .

The asymptotic optimality of uniform power allocation in the high power region was known for $N=2$ in [5] where the authors characterized the optimal power allocation on the (2,1,2) MIMO BC. When

$$P \geq \frac{\|h_1\|^2 - \|h_2\|^2}{\det(\mathbf{H}\mathbf{H}^*)}. \quad (3.37)$$

The sum-capacity is given by

$$C = \log \left[1 + \frac{\left(P \det(\mathbf{H}\mathbf{H}^*) + tr(\mathbf{H}\mathbf{H}^*) \right)^2}{4 \det(\mathbf{H}\mathbf{H}^*)} - \frac{\|h_1\|^2 \|h_2\|^2}{\det(\mathbf{H}\mathbf{H}^*)} \right]. \quad (3.38)$$

Or equivalently by

$$C = \log \left[\frac{P^2}{4} \det(\mathbf{H}\mathbf{H}^*) + \frac{P}{2} tr(\mathbf{H}\mathbf{H}^*) + \frac{\left(tr(\mathbf{H}\mathbf{H}^*) \right)^2}{4 \det(\mathbf{H}\mathbf{H}^*)} - \frac{\|h_1\|^2 \|h_2\|^2}{\det(\mathbf{H}\mathbf{H}^*)} + 1 \right]. \quad (3.39)$$

The users are allocated powers:

$$\frac{P}{2} \pm \frac{1}{2} \frac{\|h_1\|^2 - \|h_2\|^2}{\det(\mathbf{H}\mathbf{H}^*)}. \quad (3.40)$$

In [45], the authors proved that in the sum-power MIMO MAC dual to the $(N,1,K)$ MIMO BC, it is optimal to allocate equal power to each user as the numbers of users and antennas tend to infinity such that $N/K \geq 1$. Therefore we can apply this result to the $(N,1,N)$

MIMO BC in the case of large N . Using (3.31) it is straightforward to show that the optimal power allocation on the MIMO BC is also uniform in this case. The fraction of power allocated to any of the N users after transformation from MAC to BC is greater than or equal to the fraction of power allocated to the same user on the dual MIMO MAC, thus these two quantities must be equal in order to meet the total power constraint. We can then directly deduce from [45] that uniform power allocation is asymptotically optimal on the $(N,1,N)$ MIMO BC for the N users that are allocated a non-vanishing fraction of the total transmit power in the high power region in the case of large N . However, our result from Appendix D is stronger since we proved that it is true for any value of N in the high power region.

Moreover, we also proved that the first-order asymptotic optimization of the BC covariance matrices is an instance of a QR decomposition of the $N \times N$ channel matrix. The first-order asymptotic optimality of QR decomposition with dirty-paper coding on the $(N,1,N)$ MIMO BC was first proved by Caire and Shamai [5]. Here we prove that not only QR decomposition with dirty-paper coding is asymptotically optimal, but it is the first-order asymptotically optimal procedure to achieve the sum-capacity of the $(N,1,N)$ MIMO BC in the high power region.

As a consequence of the orthogonality property we deduced that uniform power allocation is optimal on the $(N,1,N)$ MIMO BC in the high power region as a first-order approximation. Following this line of thought, we can prove that the asymptotically optimal power allocation on the dual sum-power MIMO MAC is also uniform for any N . Starting from (3.31) and since there are only N users in the channel, it is necessary that:

$$\lim_{P \rightarrow \infty} \frac{\text{tr}(\boldsymbol{\Sigma}_i)}{P} = \alpha_i^{\text{MAC}}. \quad (3.41)$$

Otherwise the total power constraint would not be met. Thus as a first-order approximation $\alpha_i^{\text{MAC}} \approx 1/N$ in the high power region, thus the asymptotically optimal power allocation is also uniform on the dual sum-power MIMO MAC. As a direct consequence we can conclude that the sum-capacity of the sum-power MIMO MAC is equal to the sum-capacity of the MIMO MAC with individual transmit power constraints of P/N for each user in the high power region. As noted by [50] this sum-capacity is equal to the $(N,N,1)$ open-loop single-user MIMO capacity. Thus the $(N,N,1)$ open-loop MIMO capacity is also an accurate first-order approximation of the high power region sum-capacity of the $(N,1,N)$ MIMO BC.

The (2,1,2) MIMO BC provides an effective example for observing the accuracy of the first-order approximation of the sum-capacity since a closed-form expression is available in (3.38). It can be easily shown that the open-loop (2,2,1) MIMO capacity is given by

$$C_{OL} = \log \left(1 + \frac{P}{2} \text{tr}(\mathbf{H}\mathbf{H}^*) + \frac{P^2}{4} \det(\mathbf{H}\mathbf{H}^*) \right). \quad (3.42)$$

The expression (3.35) can also be easily manipulated. Let the (i,i) diagonal element of the triangular matrix in the QR decomposition of the channel matrix be r_{ii} . Then

$$\lim_{P \rightarrow \infty} C_{sum}^{BC} \approx N \log \left(P + \sum_{n=1}^N \frac{1}{r_{nn}^2} \right) - N \log N + \sum_{j=1}^N \log(r_{jj}^2). \quad (3.43)$$

On the (2,1,2) MIMO BC this expression specializes to

$$\lim_{P \rightarrow \infty} C_{sum}^{BC} \approx N \log \left[\left(\frac{P}{2} r_{11}^2 + \frac{1}{2} \left(1 + \frac{r_{11}^2}{r_{22}^2} \right) \right) \left(\frac{P}{2} r_{22}^2 + \frac{1}{2} \left(1 + \frac{r_{22}^2}{r_{11}^2} \right) \right) \right]. \quad (3.44)$$

$$\lim_{P \rightarrow \infty} C_{sum}^{BC} \approx N \log \left[\frac{\left(P r_{11}^2 r_{22}^2 + r_{11}^2 + r_{22}^2 \right)^2}{4 r_{11}^2 r_{22}^2} \right]. \quad (3.45)$$

Finally

$$\lim_{P \rightarrow \infty} C_{sum}^{BC} \approx N \log \left[\frac{\left(P \det(\mathbf{H}\mathbf{H}^*) + \text{tr}(\mathbf{H}\mathbf{H}^*) \right)^2}{4 \det(\mathbf{H}\mathbf{H}^*)} \right]. \quad (3.46)$$

Thus the sum-capacity (3.38) and the open-loop capacity (3.42) differ in the log by the term:

$$\frac{\left(\text{tr}(\mathbf{H}\mathbf{H}^*) \right)^2}{4 \det(\mathbf{H}\mathbf{H}^*)} - \frac{\|h_1\|^2 \|h_2\|^2}{\det(\mathbf{H}\mathbf{H}^*)}. \quad (3.47)$$

And the sum-capacity (3.38) and the QR-based approximation (3.46) differ in the log by the term:

$$1 - \frac{\|h_1\|^2 \|h_2\|^2}{\det(\mathbf{H}\mathbf{H}^*)}. \quad (3.48)$$

Using the well-known inequality for an $N \times N$ matrix A ,

$$\det(A) \leq \left(\frac{\text{tr}(A)}{N} \right)^N, \quad (3.49)$$

we can directly conclude that the open-loop capacity approximation is tighter than the QR-based approximation in the high power region.

In general, on the $(N,N,1)$ MIMO channel it is well known that the open-loop capacity is closely approached both in ratio and in difference by a sequential MIMO equalizer that performs successive interference cancellation with a QR decomposition filter at the receiver [51]. However the open-loop capacity is in fact achieved with an MMSE GDFE filter [52][53]. Therefore the fact that the open-loop capacity is a better approximation of the sum-capacity than the one based on the QR decomposition is not surprising in the light of the results of [28]. The authors of [28] proved that the sum-capacity of the MIMO BC is in fact achieved with an MMSE GDFE structure where the decision-feedback part is moved to the transmitter in the form of successive encoding by dirty-paper coding, and the matched-filter is diagonal at the sum-capacity thus removing the need for receiver cooperation on the broadcast channel. However as we saw, the asymptotic sum-capacity is not equal to the open-loop capacity but only closely approximated by it.

It is important to note that dirty-paper coding alone would not allow to achieve the maximum spatial multiplexing gain on the $(N,1,K)$ MIMO BC. N users need to be allocated power such that this power keeps increasing with the total transmit power in order to achieve the maximum spatial multiplexing gain of N . Dirty-paper coding would only allow one user to cancel the interference from all other users. That user would be able to achieve a rate that scales logarithmically with the total transmit power. However other users would only be able to achieve at best a constant rate in the high power region, since the power of their intended signals to the power of the interference are both linearly proportional to the total transmit power.

We now show some numerical results to illustrate our findings. In the following examples, we considered fixed channel realizations and we let the total transmit power increase to very large values. We observe the fraction of power allocated to each user, and the rates achieved by these users, both on the dual MIMO MAC, and on the MIMO BC with several encoding orders.

Example 3.4: Let us consider the channel matrix of Example 3.2 on the (2,1,3) MIMO BC. We apply the MAC to BC transformations to the optimal covariance matrices obtained for the MIMO MAC by the optimization of the sum-capacity for the two encoding orders (1,2,3) and (3,2,1). Figure 3-6 illustrates the results obtained with the encoding order (1,2,3). Figure 3-6a shows the optimal power allocation on the MIMO MAC as a function of the total transmit power in reference to the noise level. The power allocation is independent of the encoding order. The power allocated to each user is normalized to the total transmit power. As seen previously all three users are allocated a non-vanishing fraction of the total transmit power as it goes to infinity. However since users 1 and 2 are encoded first, only they are allocated a non-vanishing fraction of the total transmit power on the MIMO BC in the high power region as shown in Figure 3-6b. User 3 is still allocated some power, so it achieves a seemingly constant rate, whereas the rates of users 1 and 2 keep increasing with the total transmit power as shown in Figure 3-6c. The rate of user 3 could be proved to stay constant.

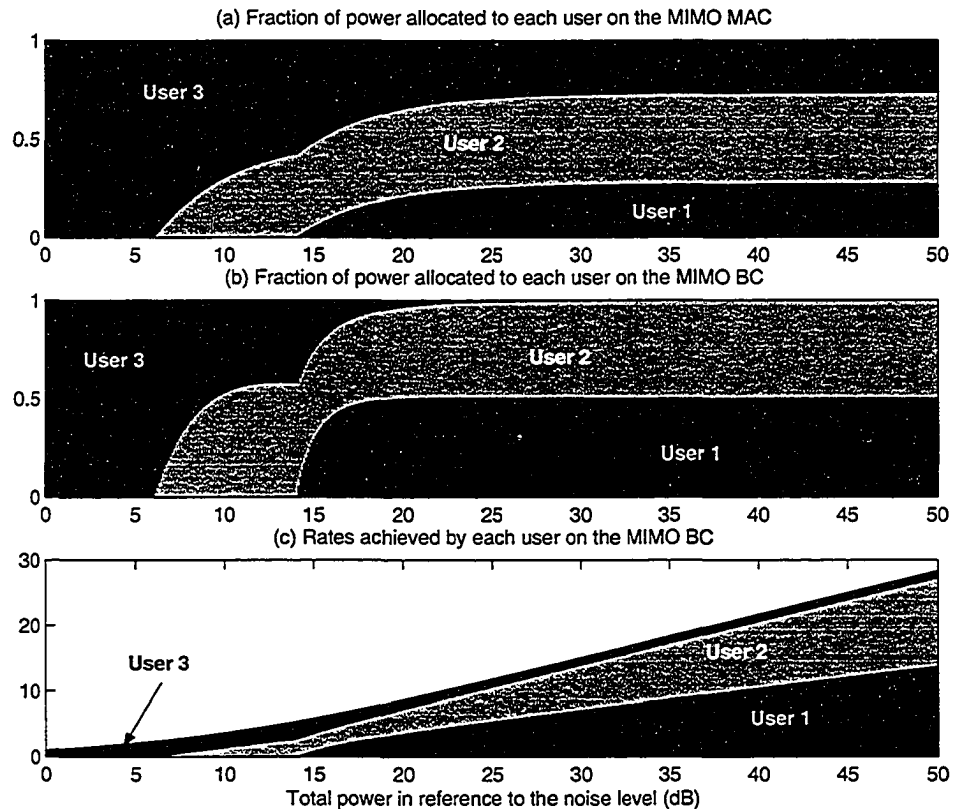


Figure 3-6 (2,1,3) MIMO BC optimal power allocation as a function of the total transmit power in reference to the noise level (a) on the MIMO MAC, (b) on the MIMO BC with encoding order (1,2,3). (c) Users rates on the MIMO BC with encoding order (1,2,3).

Since only linear operations are involved in the MAC to BC transformations, the power allocated to user 3 could only be polynomial in the total transmit power if it was not constant. With the encoding order (3,2,1), we see in Figure 3-7 that users 2 and 3 are allocated a non-vanishing fraction of the total transmit power in the high power region on the MIMO BC, and user 1 only achieves a constant rate asymptotically.

We note that on the $(N,1,K)$ MIMO BC scheduling N users at a time is asymptotically optimal in the high power region, provided that these users are chosen among the active users that are allocated a non-vanishing fraction of the total transmit power at the sum-capacity of the dual sum-power MIMO MAC. This also shows that the choice of the N users is not very critical in the sense that several sets of N users are asymptotically optimal in the high power region when more than N users are allocated a non-vanishing fraction of the total transmit power on the MIMO MAC. The choice of the N users only depends on the chosen encoding order. Thus we expect that

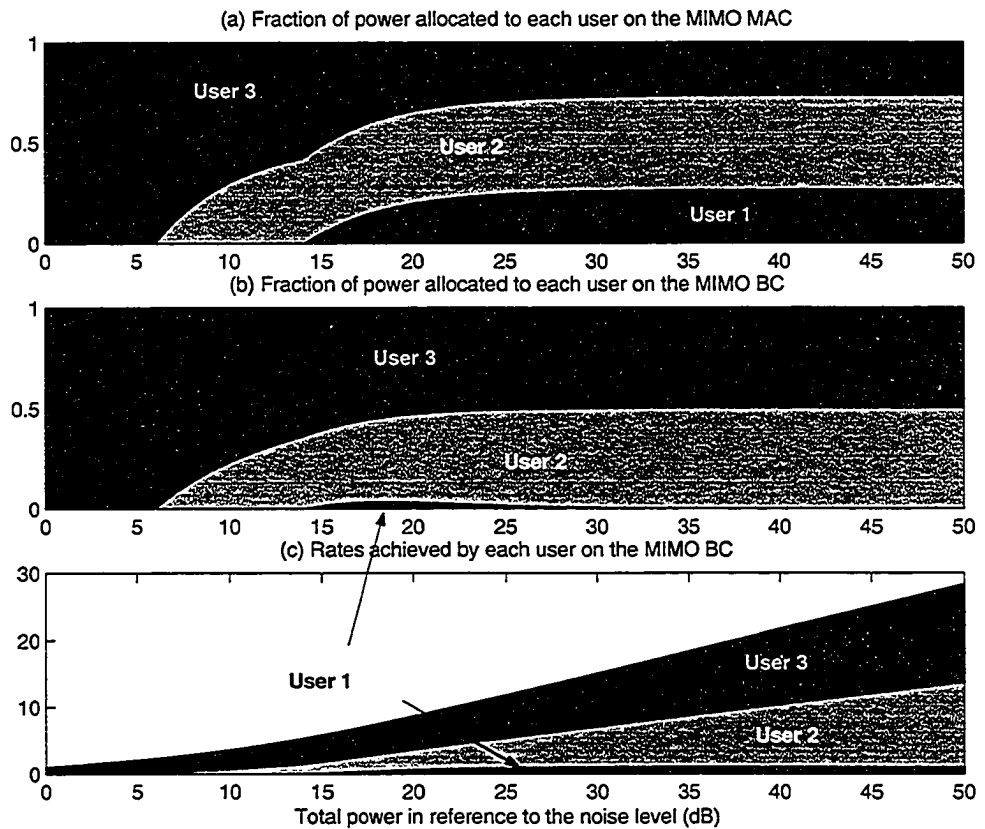


Figure 3-7 (2,1,3) MIMO BC optimal power allocation as a function of the total transmit power in reference to the noise level (a) on the MIMO MAC, (b) on the MIMO BC with encoding order (3,2,1). (c) Users rates on the MIMO BC with encoding order (3,2,1).

several sub-optimal low-complexity N -user scheduling algorithms could provide such a set of N users.

Example 3.5: A given realization of the (3,1,8) MIMO BC is considered. The optimal power allocation on the MIMO MAC, on the MIMO BC with encoding order 8 to 1, and the users rates are shown in Figure 3-8. Only users {1,2,5,6} are allocated a non-vanishing fraction of the total transmit power in the high power region on the MIMO MAC. Since there are 3 base station antennas, after MAC to BC transformations only users {2,5,6} are still allocated a non-vanishing fraction of the total transmit power in the high power region on the MIMO BC. User 1 still achieves a non-zero rate, which becomes asymptotically negligible with respect to the sum-capacity.

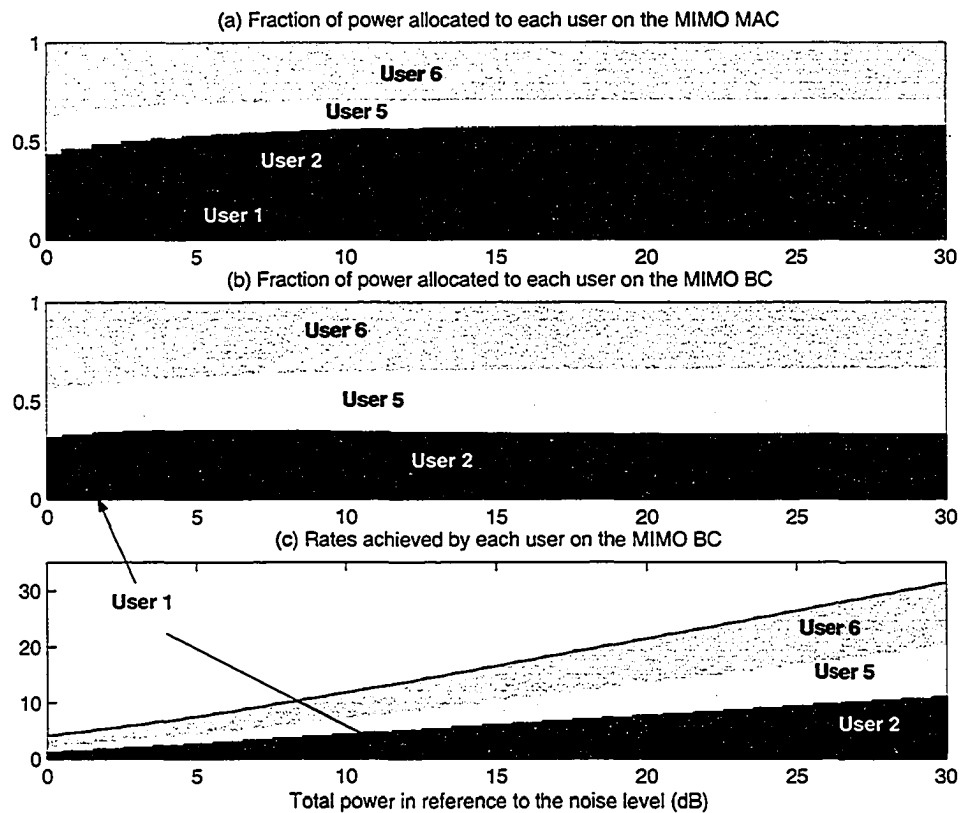


Figure 3-8 (3,1,8) MIMO BC optimal power allocation as a function of the total transmit power in reference to the noise level (a) on the MIMO MAC, (b) on the MIMO BC with encoding order 8 to 1. (c) Users rates on the MIMO BC with encoding order 8 to 1.

3.4.3 The (N,N,K) MIMO BC

In this section we summarize the results proved in Appendix D.4, where we show that only N one-dimensional channels are allocated a non-vanishing fraction of the total transmit power on the MIMO BC when the total transmit power goes to infinity. These N one-dimensional channels all belong to the same user, which is the user that is encoded first by dirty-paper coding. Thus we proved that asymptotically in the high power region, only one user is allocated a non-vanishing fraction of the total transmit power, as long as that user is allocated a non-vanishing fraction of the total transmit power on the dual MIMO MAC and its MAC covariance matrix is full rank asymptotically. The latter two assumptions can always be satisfied as long as at least one user has a full-rank channel matrix, which occurs almost surely in a rich scattering environment. Let $\lim_{P \rightarrow \infty} \text{tr}(\mathbf{P}_K) = \alpha_K P$, where $\alpha_K \neq 0$ is a constant, and \mathbf{P}_k is the optimal transmit covariance matrix of user k on the dual MIMO MAC. We prove in Appendix D.4 that:

$$\lim_{P \rightarrow \infty} \frac{1}{P} \boldsymbol{\Sigma}_K = \frac{1}{N} \mathbf{I}_N, \quad (3.50)$$

$$\lim_{P \rightarrow \infty} \frac{1}{P} \text{tr}(\boldsymbol{\Sigma}_1) = 0, \quad (3.51)$$

$$\lim_{P \rightarrow \infty} \frac{1}{P} \text{tr}(\boldsymbol{\Sigma}_j) = 0 \text{ for } j = 2, \dots, K-1. \quad (3.52)$$

We note that the dual sum-power MIMO MAC solution to the sum-capacity problem in the high power region is largely affected after the MAC to BC transformations. Even though several users could be allocated a non-vanishing fraction of the total transmit power on the MIMO MAC, only one will be allocated a non-vanishing fraction of the total transmit power on the MIMO BC. However, one must be careful in concluding that transmitting to only one user is sufficient to achieve the sum-capacity. We can only say that the ratio of the rate achieved by user K to the sum-capacity tends to one as the total transmit power goes to infinity, but the convergence is slow due to the logarithmic growth of the sum-capacity with the power, and the rates achieved by the other users are still needed to fill the gap with the sum-capacity. Moreover, simulations show that the asymptotic result only occurs at very large values of the total transmit power. Simulations show that as the power is large and increases, but when it is still below the threshold where only one user is allocated power on all its N eigenmodes, then several one-dimensional channels are allocated power such that this power increases with the total transmit power until it reaches the threshold, and these one-dimensional channels belong to more than one user.

Example 3.6: A given realization of the (4,4,4) MIMO BC is considered. Figure 3-9 shows the optimal power allocation on the MIMO MAC, and on the MIMO BC with encoding order 4 to 1, as well as the users rates, as a function of the total transmit power in reference to the noise level. All four users are allocated a non-vanishing fraction of the total transmit power on the MIMO MAC, but after MAC to BC transformations only user 4 will be allocated a non-vanishing fraction of the total transmit power in the high power region. We notice that at 150 dB, the rates of users 2 and 3, which remain constant, are not negligible compared to the sum-capacity. They will only become negligible at much higher values of the total transmit power. We can take a closer look at the power allocation by observing the eigenvalues of the optimal covariance matrices. The eigenvalues of the optimal covariance matrices on the MIMO MAC, normalized to the total transmit power, are shown in Figure 3-10. We

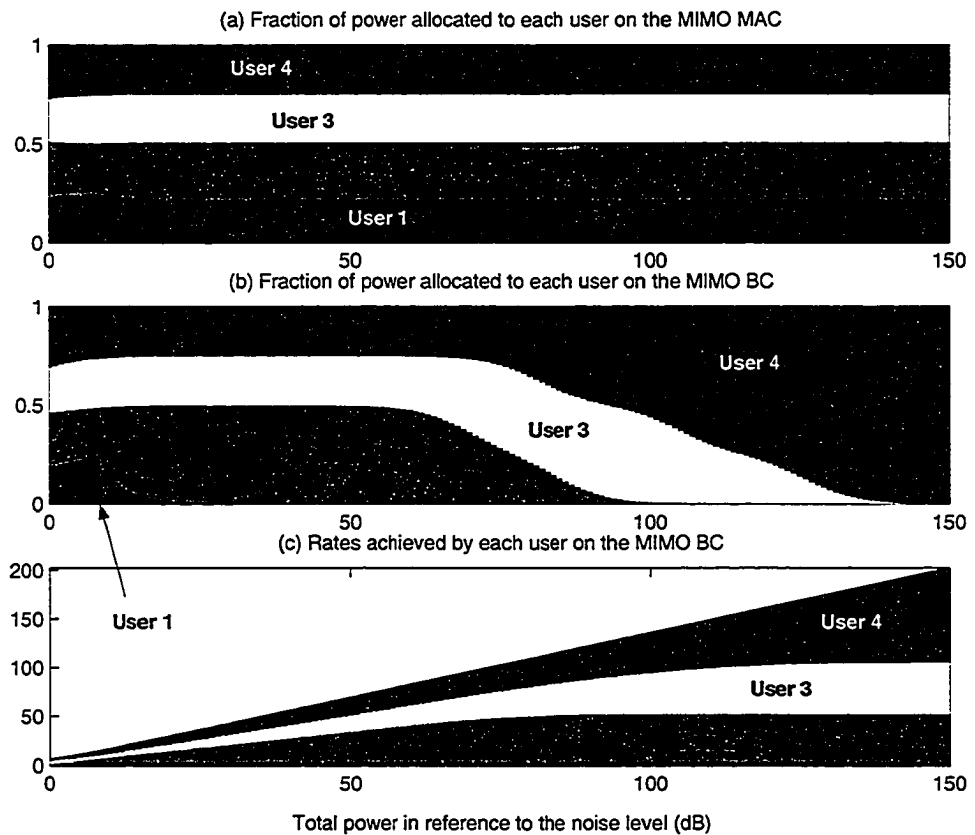


Figure 3-9 (4,4,4) MIMO BC optimal power allocation as a function of the total transmit power in reference to the noise level (a) on the MIMO MAC, (b) on the MIMO BC with encoding order 4 to 1. (c) Users rates on the MIMO BC with encoding order 4 to 1.

notice that in the high power region, users {1,3,4} are allocated a significant fraction of the power on one eigenmode, whereas user 2 is allocated power on two eigenmodes. Thus five one-dimensional channels are allocated a non-vanishing fraction of the total transmit power with four transmit antennas. After MAC to BC transformations with the encoding order 4 to 1, we observe in Figure 3-11 that the power allocation progressively shifts from users 1, 2 and 3 eigenmodes to all of the fourth user's eigenmodes in the high power region. In the intermediate power region, user 3 is also allocated a large amount of power on two of its eigenmodes. On the MIMO MAC, all users are in fact allocated power on all their eigenmodes, but most of these only receive a very small amount of power that cannot be observed in Figure 3-10. This is consistent with the analysis in Appendix D.4.

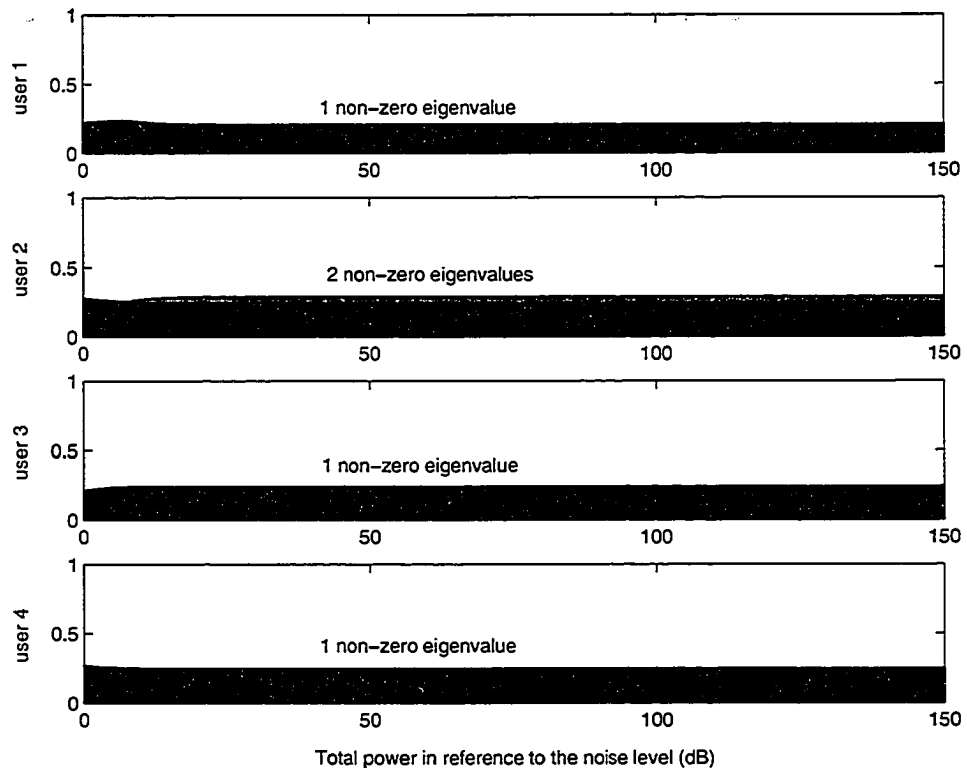


Figure 3-10 Normalized eigenvalues of the optimal MAC covariance matrices as a function of the total power in reference to the noise level on the (4,4,4) MIMO BC.

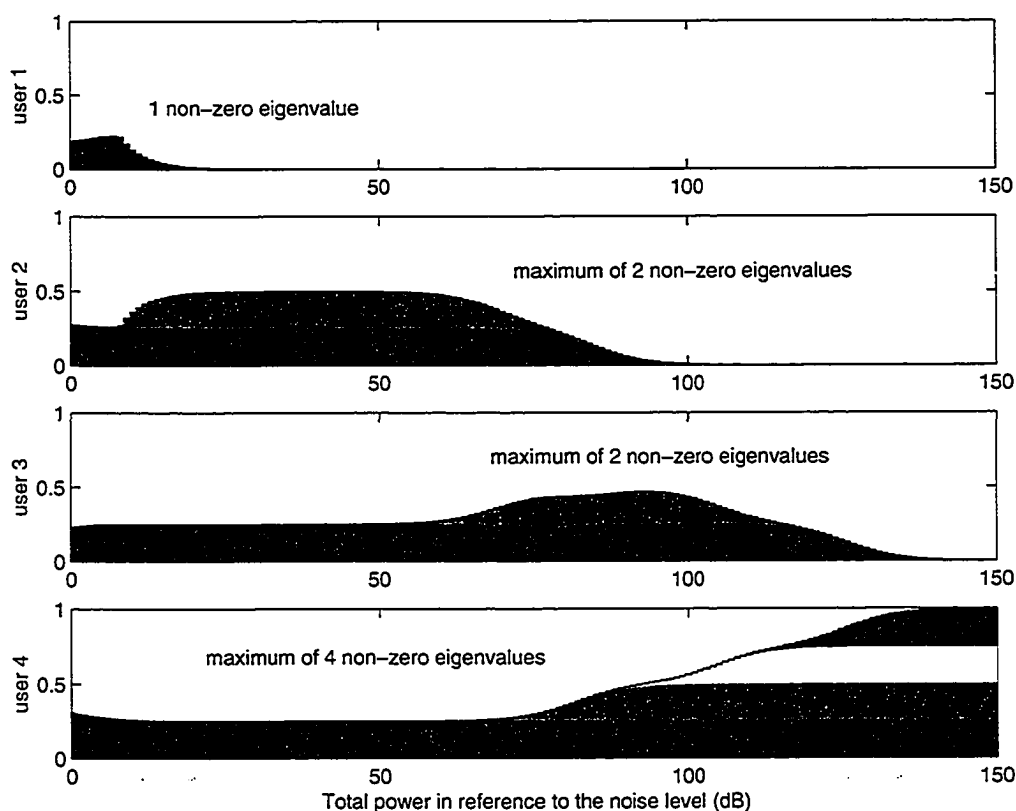


Figure 3-11 Normalized eigenvalues of the optimal BC covariance matrices as a function of the total power in reference to the noise level on the (4,4,4) MIMO BC

3.4.4 The (N, M_k, K) MIMO BC

In general on the (N, M_k, K) MIMO BC, we conjecture that only N one-dimensional channels are allocated a non-vanishing fraction of the total transmit power in the high power region, and these N one-dimensional channels belong to the K' users that are encoded first by dirty-paper coding such that these users are allocated a non-vanishing fraction of the total transmit power on the dual sum-power MIMO MAC and $\sum_{k=K-K'+2}^K M_k \leq N \leq \sum_{k=K-K'+1}^K M_k$.

The underlying idea in the proof of Appendix D.4 is the following. Following (D.80) we define the matrix:

$$\Gamma_j = \frac{1}{P} \sum_{i=j}^K \mathbf{H}_i^* \mathbf{P}_i \mathbf{H}_i. \quad (3.53)$$

We place ourselves in the situation where users K to $j-1$ have already been encoded and the total transmit power is large enough so that they are allocated power on all of their eigenmodes. When

user j is being encoded, if \mathbf{F}_j has full rank N asymptotically in the high power region, then user j and the users that are encoded after that stage will be allocated a vanishing fraction of the total transmit power. Otherwise user j is allocated a non-vanishing fraction of the total transmit power on several of its eigenmodes such that after it is encoded at most N eigenmodes are allocated a non-vanishing fraction of the total transmit power. In order to rigorously prove this claim the analysis should consider not only the trace of the BC covariance matrices but all eigenvalues separately, which renders the analysis a lot more complex. We now illustrate this property with a numerical example.

Example 3.7: We consider a realization of the MIMO BC with 3 transmit antennas and 3 users. User 1 is equipped with two receive antennas, users 2 and 3 each have one receive antenna. We call this channel the $(3, \{2, 1, 1\}, 3)$ MIMO BC, where we explicitly wrote the number of receive antennas of each user. Figure 3-12 shows the normalized eigenvalues of the optimal MAC covariance matrices as a function of the total transmit power in reference to the noise level. In the high power region each user

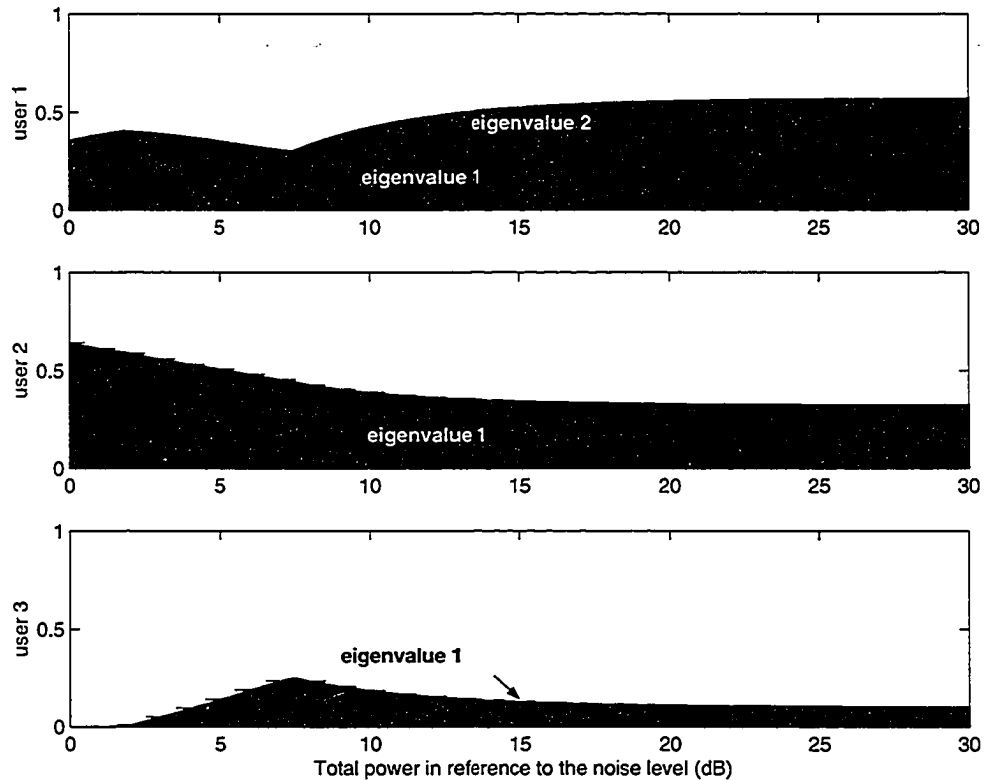


Figure 3-12 Normalized eigenvalues of the optimal MAC covariance matrices as a function of the total power in reference to the noise level on the $(3, \{2, 1, 1\}, 3)$ MIMO BC.

is allocated power on as many one-dimensional channels as their number of receive antennas. The power allocation given by the trace of the MAC covariance matrices is shown in Figure 3-13a. We first consider the encoding order (1,2,3) on the MIMO BC. Figure 3-13b shows the power allocation on the MIMO BC. The detail of the normalized eigenvalues of the BC covariance matrices is shown in Figure 3-14. The rates achieved by the users on the BC are shown in Figure 3-13c. User 3 is no more allocated a non-vanishing fraction of the total transmit power since users 1 and 2 are allocated 3 one-dimensional channels altogether in the high power region. With the encoding order (3,2,1), as shown in Figure 3-15 and Figure 3-16, all three users are allocated a one-dimensional channel each. User 1 is allocated only one-dimensional channel since it is encoded last and two one-dimensional channels have already been allocated to users 3 and 2 before user 1 is encoded.

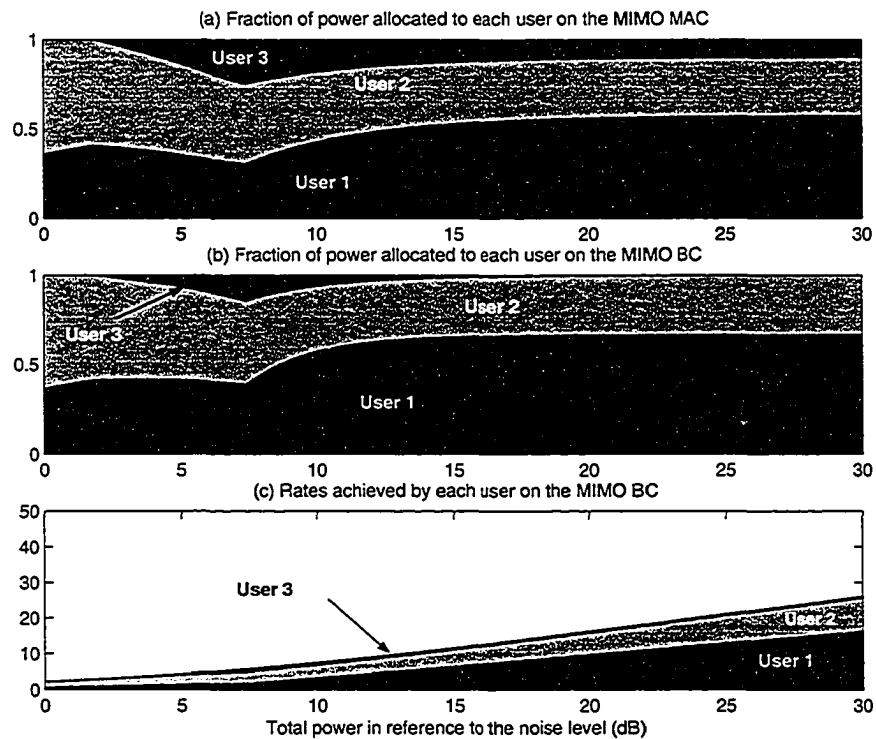


Figure 3-13 (3, {2,1,1}, 3) MIMO BC optimal power allocation as a function of the total transmit power in reference to the noise level (a) on the MIMO MAC, (b) on the MIMO BC with encoding order 1 to 3. (c) Users rates on the MIMO BC with encoding order 1 to 3.

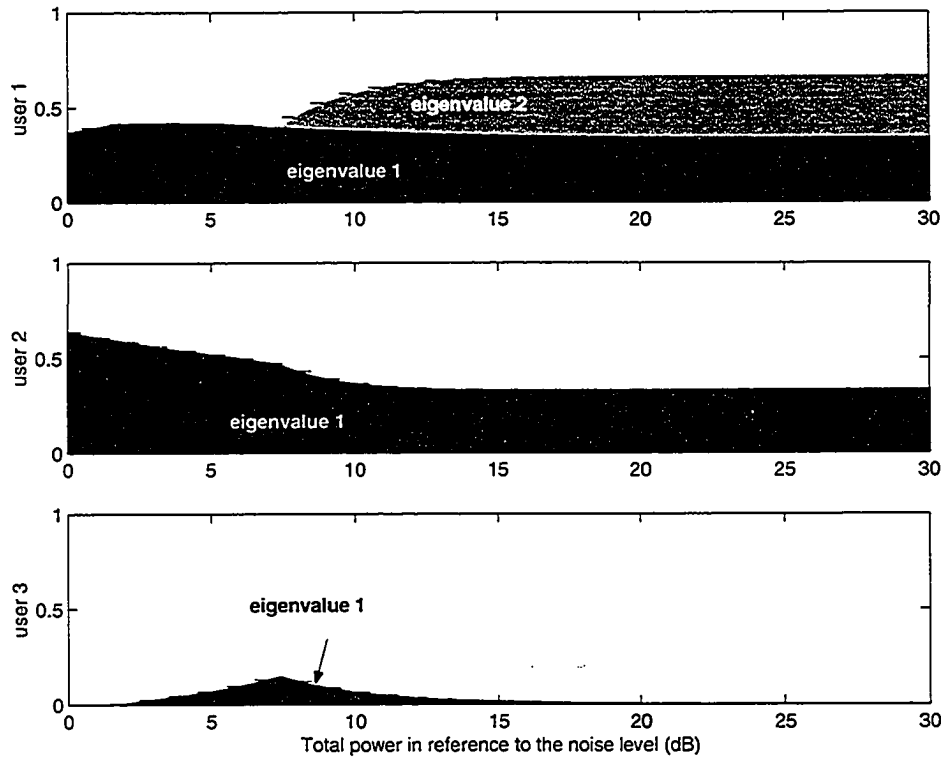


Figure 3-14 Normalized eigenvalues of the optimal BC covariance matrices as a function of the total power in reference to the noise level on the $(3, \{2, 1, 1\}, 3)$ MIMO BC with the encoding order 1 to 3.

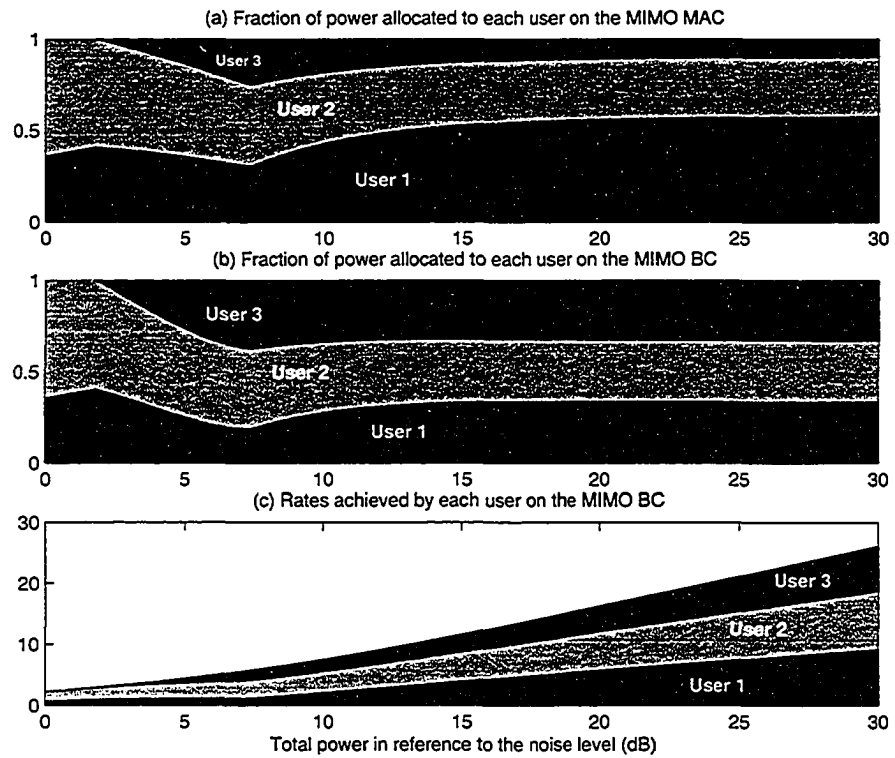


Figure 3-15 $(3, \{2, 1, 1\}, 3)$ MIMO BC optimal power allocation as a function of the total transmit power in reference to the noise level (a) on the MIMO MAC, (b) on the MIMO BC with encoding order 3 to 1. (c) Users rates on the MIMO BC with encoding order 3 to 1.

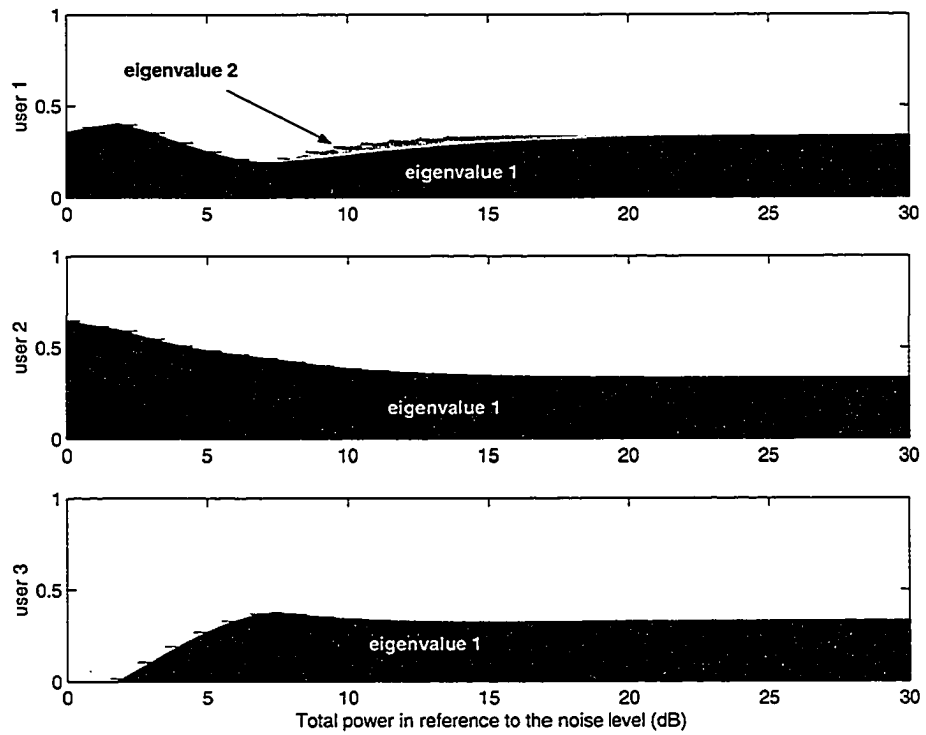


Figure 3-16 Normalized eigenvalues of the optimal BC covariance matrices as a function of the total power in reference to the noise level on the $(3, \{2, 1, 1\}, 3)$ MIMO BC with the encoding order 3 to 1.

3.5 Summary and Conclusions

We have studied the sum-capacity of the (N, M_t, K) MIMO BC and the properties of the optimal power allocation and transmit covariance matrices in the high power region. Our conclusions are summarized in the following points.

- On the sum-power MIMO MAC dual of the $(2, 1, K)$ MIMO BC: the optimal number of active users is at least equal to two in the high power region depending on the channel realization. For a given channel realization, the optimal number of active users can be a non-monotonic function of the total transmit power.
- We gave a complete geometrical characterization of the sum-power MIMO MAC dual of the $(2, 1, 3)$ MIMO BC.
- On the $(N, 1, K)$ MIMO BC, after MAC to BC transformations given a decoding/encoding order: only N users are allocated a non-vanishing fraction of the total transmit power, where these N users are the ones that are encoded first on the BC and decoded last on the MAC. In other words, beyond some power threshold, all the additional power put into the channel is allocated to N users only.
- On the $(N, 1, N)$ MIMO BC in the high power region, the optimal BC covariance matrices remove all the interference remaining after dirty-paper coding. Thus the channel is completely diagonalized. This operation is performed by a QR decomposition of the channel matrix. A closed-form first-order approximation of the asymptotic sum-capacity is deduced from that property.
- On the $(N, 1, K)$ MIMO BC the asymptotically optimal power allocation is uniform among the N users that are allocated a non-vanishing fraction of the total transmit power.
- On the (N, N, K) MIMO BC, by appropriately choosing the encoding order such that the user that is encoded first is allocated a non-vanishing fraction of the total transmit power on

the dual sum-power MIMO MAC and its channel matrix has full rank, then this user will be allocated all the total transmit power asymptotically (in the sense that the ratio of its allocated power to the total transmit power goes to one).

- On the (N, M_k, K) MIMO BC asymptotically N one-dimensional channels will be allocated a non-vanishing fraction of the total transmit power, and these dimensions belong to the users that are encoded first.
- The users that are allocated a vanishing fraction of the total transmit power are nevertheless allocated non-zero power and non-zero rates, although their sum-rate becomes an asymptotically small fraction of the sum-capacity at high values of the total transmit power.
- Studying the optimal number of active users only from the dual sum-power MIMO MAC formulation can be misleading on drawing conclusions for the MIMO BC.

4 Scheduling Algorithms and Linear Processing

4.1 Introduction

In the context of packet-data cellular systems, scheduling algorithms allow to take advantage of multiuser diversity to increase the throughput by scheduling transmission to users when their channel conditions are favourable. With multiple transmit antennas we now want to schedule transmission to several users simultaneously. The design of scheduling algorithms is dependent on several factors. The main ones we will be dealing with in this chapter are the availability of complete or partial CQI and CSIT, the type of transmission scheme adopted whether it is optimal dirty-paper coding or some sub-optimal scheme, and the computational complexity involved in choosing the users to be scheduled in any given time slot. The problem of the fairness in terms of average throughput achieved by each user is addressed in section 4.4.

4.2 Channel Model

We now consider a channel where the channel matrices are kept constant in any given time slot, but change randomly from slot to slot. Thus in contrast to Chapter III, we now consider the (N, M, K) fading MIMO BC. The analysis developed in Chapter III applies to any given time slot as long as we consider throughput maximization. The channel model for proportionally-fair scheduling schemes will be defined in section 4.4.2.

4.3 Throughput Maximization Scheduling Algorithms

4.3.1 Scheduling with Dirty-Paper Coding on the $(N, 1, K)$ MIMO BC

4.3.1.1 Definition

Let us first concentrate on throughput maximization without consideration of fairness among the users. If we let all users have the same fading statistics, then fairness is inherently provided in the sense that all users will achieve the same average rate and delay with any transmission scheme and scheduling algorithm, when the average is taken over all fading states. With dirty-paper coding, maximizing the throughput means achieving the sum-capacity. In this case, solving the sum-capacity optimization problem with the power constraint equal to the available transmit power gives the optimal set of users and the optimal power allocation for each channel realization. In this section, we focus on scheduling algorithms that approach the sum-capacity with the additional constraint that the number of users in any given time slot be limited. We consider this constraint for several reasons.

- Complexity: by limiting the number of active users, the complexity of encoding and decoding is reduced when dirty-paper coding is used.
- Portability to other transmission schemes: studying scheduling algorithms with dirty-paper coding provides an upper bound on the achievable throughput with sub-optimal transmission schemes. Bad scheduling algorithms with dirty-paper coding will also be bad with sub-optimal transmission schemes.

The choice of the maximum number of active users is determined by the spatial multiplexing gain that one wants to achieve, given the number of base station transmit antennas, and the number of receive antennas at each mobile user's equipment. Since dirty-paper coding allows to achieve the same growth rate as receiver cooperation and the maximum achievable spatial multiplexing gain is limited by the minimum of the number of transmit and receive antennas on MIMO channels, transmitting to no more users than the number of transmit antennas should be sufficient to achieve the maximum spatial multiplexing gain when the number of users is large enough. Moreover, from the discussion in Chapter III, we know that this choice of N active users also allows to approach the sum-capacity in the high power region. The intermediary power region is not that well understood. Therefore we mostly resort to simulations to understand this region. These results motivate the choice of scheduling N users at a time even when each user is equipped with N receive antennas. This motivation comes from two facts. Firstly, the asymptotic optimality of allocating only a non-vanishing fraction of the total transmit power to only one user occurs only at very large values of the total transmit power. Secondly, in the intermediary power region we saw that several one-dimensional channels are allocated a large fraction of the total transmit power, and these channels belong to different users.

We define the N -user near-optimality of a scheduling algorithm by its capability of selecting a set of users such that the sum-capacity of the channel restricted to this set of users is close to the sum-capacity of the original channel. Thus, it is possible to approach the sum-capacity of the original channel by using such a scheduling algorithm with dirty-paper coding. However, if a scheduling algorithm is not N -user near-optimal, then it is not possible to closely approach the sum-capacity whether or not optimal dirty-paper coding is used. By lack of a better criterion, whether or not a scheduling algorithm is N -user near-optimal is determined visually by simulations relatively to the sum-capacity curve. We see from this definition that the choice of the scheduling algorithm is a crucial step in the design of a communication system and it can deteriorate the achievable throughput even if a good signalling and coding scheme is used for

transmission. The scheduling algorithm must obviously also be matched to the type of scheme chosen for transmission.

We now illustrate our choice with simulations. We define the best L -user sub-channel as the sub-channel with at most L users that has the largest sum-capacity for a given channel realization. Thus this channel provides the largest achievable spectral efficiency by constraining the number of active users to be at most L . We refer to the scheduling algorithm that selects the L users of the best L -user sub-channel as the Best L -user Scheduling algorithm. Figure 4-1 shows the average spectral efficiency achieved with the Best L -user Scheduling algorithm and dirty-paper coding as a function of the number of transmit antennas N over 1000 channel realizations of the $(N,1,10)$ fading MIMO BC. The results for the $(N,N,10)$ fading MIMO BC are shown in Figure 4-2, where the number of transmit antennas and the number of receive antennas per user are equal and grow simultaneously. We see from these simulations that constraining the number of active users to be $M \geq N$ incurs only a marginal loss in spectral efficiency. The loss in spectral efficiency when $M < N$ becomes more pronounced as N increases. This loss is particularly high if the users are equipped with a single receive antenna since the maximum spatial multiplexing gain cannot be achieved, whereas when the users have N receive antennas the

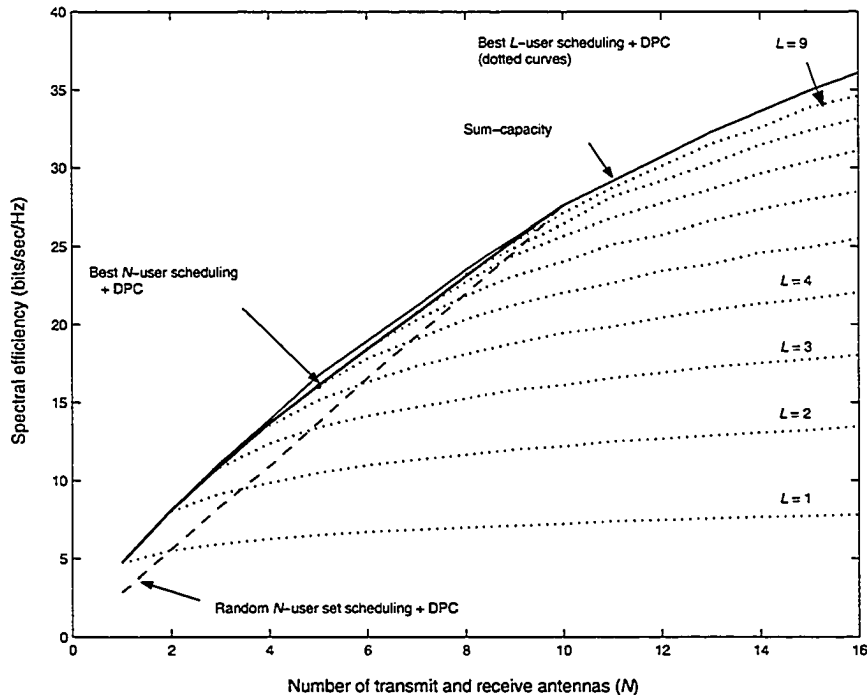


Figure 4-1 Average spectral efficiency of the best L -user sub-channel as a function of the number of transmit antennas N . The total number of users is $K = 10$, each user is equipped with a single receive antenna. The total power in reference to the noise level is 10 dB.

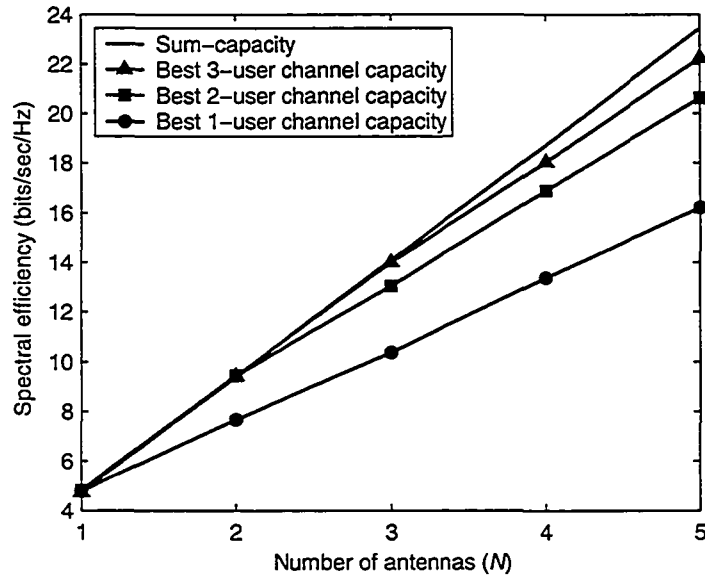


Figure 4-2 Average spectral efficiency of the best L -user sub-channel as a function of the number of antennas N . The total number of users is $K = 10$, each user is equipped with N receive antennas. The total power in reference to the noise level is 10 dB.

loss is due to not achieving the spatial multiplexing gain in the optimal way as given by the sum-capacity optimization solution.

Figure 4-1 also shows the spectral efficiency achieved by choosing a random set of N users for each channel realization. We call this Random N -user Scheduling algorithm. This shows that optimizing the choice of the N users is necessary since a non-negligible portion of the maximum spectral efficiency can be lost by not optimizing the N -user set.

4.3.1.2 Low-Complexity N -User Scheduling Algorithms

We now discuss low-complexity sub-optimal N -user scheduling algorithms for the $(N,1,K)$ fading MIMO BC. A scheduling algorithm based on determining the best N -user set incurs a large computational complexity as the number of users and the number of transmit antennas become large. It requires to look at each subset of N users among K and to perform the sum-capacity calculation for each subset. The number of subsets is C_N^K .

One could think of choosing the N -user set that maximizes the sum-capacity in the high power region. The analysis from Chapter III tells us that if we put the constraint of transmitting to only N users simultaneously the asymptotic sum-capacity is given at the first order by (3.35). We can now find a rule to determine the N -user set that maximizes the asymptotic sum-capacity. Let

us rewrite (3.35) using explicitly the QR decomposition of the channel matrix for a given N -user set:

$$\mathbf{H} = \mathbf{R}\mathbf{Q}. \quad (4.1)$$

Where the positive diagonal elements of the upper triangular matrix \mathbf{R} are given by r_{11}, \dots, r_{NN} .

Hence the asymptotic sum-capacity is given by:

$$\lim_{P \rightarrow \infty} C_{sum}^{BC} = N \log P - N \log N + N \log \left(1 + \frac{1}{P} \sum_{n=1}^N \frac{1}{r_{nn}^2} \right) + \log \left(\prod_{n=1}^N r_{nn}^2 \right). \quad (4.2)$$

For a fixed N and channel matrix, as P goes to infinity, the difference in asymptotic sum-capacity between two different N -user sets is dominated by the last term in the sum. This term is equal to $\log \det \mathbf{H}\mathbf{H}^*$. Thus the best N -user set according to the asymptotic sum-capacity is obtained by maximizing the determinant of the $N \times N$ matrix $\mathbf{H}\mathbf{H}^*$. We call this scheduling algorithm Determinant Scheduling.

There are two drawbacks to this approach:

- It is still computationally expensive since it involves computing the determinant of all $N \times N$ channel matrices among all possible C_N^K such matrices.
- There is no guarantee that the best N -user set in the high power region will be the best N -user set in the intermediate power region given a power constraint, which is of primary interest to us. A counter-example is given in Example 3.3 where users 2 and 3 are optimal in the high power region but users 1 and 2 are optimal below $P = 3.87$.

We now propose a simple scheduling algorithm applicable with perfect channel knowledge at the transmitter whose complexity is proportional to $KN - N(N-1)/2$. We will refer to this scheduling algorithm as the Successive Projections Scheduling algorithm. We motivate our approach using the Determinant Scheduling algorithm. Hadamard's determinant inequality tells us that the determinant of a matrix is maximized when it is diagonal and the diagonal elements are large. Therefore we seek users such that the associated $N \times N$ channel matrix multiplied by its transpose conjugate is close to diagonal and the diagonal elements are large. We assumed that the channel matrix is written in such a way that each row represents the channel vector of one user. In terms of channel matrix, we equivalently seek users such that their channel vectors are close to orthogonal and have large norms.

The first user is arbitrarily chosen to be the one with the largest channel vector norm. At step k , we will choose the k -th user based on the previously selected $k-1$ users. Let

$S_{k-1} = \{u_1, \dots, u_{k-1}\}$ be the set of indices of the previously selected $k-1$ users. Let $\mathbf{H}_{S_{k-1}}$ be the matrix whose rows are the channel vectors of the previously selected $k-1$ users. We want to choose the users jointly in such a way that their cross-interference is small and that all selected users have favourable channel conditions, which means their channel vectors have large norms. The k -th user is selected according to:

$$u_k = \arg \max_{1 \leq i \leq K, i \notin S_{k-1}} \left[\min_{(\alpha_1, \dots, \alpha_{k-1}) \in \mathbb{C}^{k-1}} \left\| \sum_{j \in S_{k-1}} \alpha_j \mathbf{h}_j - \mathbf{h}_i \right\|^2 \right]. \quad (4.3)$$

where the vector $\alpha = (\alpha_1, \dots, \alpha_{k-1}) \in \mathbb{C}^{k-1}$ is used to form all possible linear combinations of the channel vectors of the $k-1$ users selected by the algorithm after step $k-1$. This can be shown to be equivalent to the maximization (see Appendix E):

$$u_k = \arg \max_{1 \leq i \leq K, i \notin S_{k-1}} \left\| \mathbf{h}_i \left[\mathbf{H}_{S_{k-1}}^* (\mathbf{H}_{S_{k-1}} \mathbf{H}_{S_{k-1}}^*)^{-1} \mathbf{H}_{S_{k-1}} - \mathbf{I}_N \right] \right\|^2. \quad (4.4)$$

The algorithm stops when N users have been selected. The matrix inversion is always possible by construction since we are choosing users successively in such a way that their channel vectors are as much linearly independent as possible at each stage. At step k , the algorithm requires computing the argument of the maximization for $K - k + 1$ channel vectors. When $K \geq N$, the total number of times the argument needs to be calculated is $KN - N(N-1)/2$. It is always larger than $N(N+1)/2$, which is achieved when $K = N$, although in this case it is not useful to perform the calculations since there is only one set with N users. However, contrary to the previous scheduling algorithms, no additional computation of the sum-capacity is required and the complexity is much smaller than C_N^K for most values of K and N . This algorithm is likely to selecting a good subset of users in the sense that the mutual interference among these users should be low, and users with relatively large channel gains should be selected. This scheduling algorithm is not matched to any particular transmission scheme and its general properties and its low computational complexity make it an attractive solution. Once the N users have been selected, the sum-rate achievable with dirty-paper coding is completely determined. If we are interested in individual user rates then we need to choose some encoding order, which will give us the achievable rate vector.

Straightforward modifications to the Successive Projections algorithm can be devised. For example it is possible to schedule L users at a time where $L \leq N$. Another modification with a K -fold increase in complexity is to choose a better user set by performing the algorithm K times, each time starting the algorithm with a different choice for the first selected user. Then the K

obtained user sets can be compared with some criterion such as their sum-capacity or their achievable spectral efficiency with some particular transmission scheme other than dirty-paper coding. Another adaptation would be to select one or several users with a high priority in terms of quality of service and then find the remaining users that are most compatible for simultaneous transmission with these high priority users.

4.3.1.3 Relation to Receive Antenna Selection Algorithms on the Single-User MIMO Channel

The problem of scheduling N users at a time for throughput maximization is somewhat similar to the problem of receive antenna selection for capacity maximization in single-user MIMO systems. The algorithms developed for this purpose, for example in [56], are applicable for maximum throughput scheduling, and they perform well. One of the possible goals of receive antenna selection algorithms is to minimize the difference between the capacity of the channel and the capacity of the reduced-channel after a subset of the receive antennas has been selected. This is a similar problem to minimizing the difference between the sum-capacity of the MIMO BC and the sum-capacity of the reduced-channel after a subset of users has been selected. The difference between the two problems is the absence of receiver cooperation on the MIMO BC. However, the authors in [56] treated the problem in the asymptotic regime where the total transmit power goes to infinity. We know that in this situation the open-loop $(N,N,1)$ MIMO capacity asymptotically approaches the sum-capacity of the $(N,1,N)$ MIMO BC. Hence receive antenna selection algorithms should be good in terms of N -user near-optimal scheduling in the high power region.

4.3.1.4 Simulation Results

We first observe the accuracy of the approximation of the sum-capacity by the open-loop single-user MIMO capacity as a function of the total transmit power. We also observe the first-order QR-based approximation provided in Appendix D. Figure 4-3 shows the difference between the average closed-loop cooperative $(4,4,1)$ capacity, which provides an upper bound on the sum-capacity of the $(4,1,4)$ MIMO BC, and the sum-capacity and its different approximations as a function of the total transmit power in reference to the noise level. We see that in the high power region the difference between all approximations and the sum-capacity goes to zero. However in the intermediate power region none of the approximations succeed in staying close to the sum-capacity. The high power approximation of Appendix D is shown as the QR closed-loop capacity obtained in (D.74).

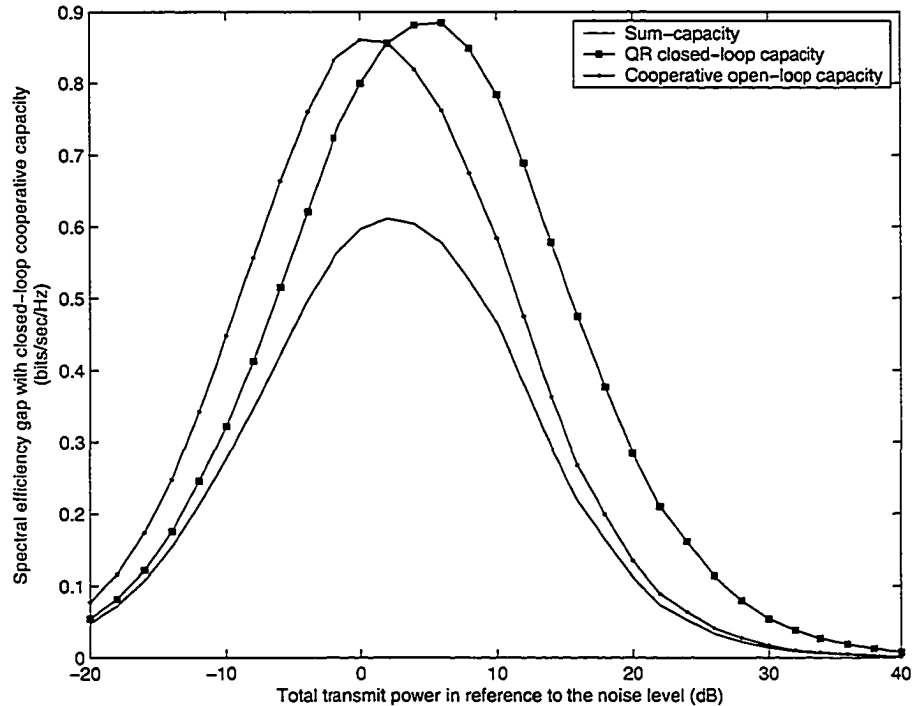


Figure 4-3 Approximations of the sum-capacity as a function of the total power in reference to the noise level on the (4,1,4) MIMO BC.

We now observe the quality of N -user scheduling algorithms as a function of the total transmit power for N transmit antennas and K users equipped with a single receive antenna. The scheduling algorithms that we consider are the following:

- Random N -user Scheduling
- N -user Determinant Scheduling
- Single-User Rates (SUR- N) Scheduling, which is defined as the choice of the N users that have the largest open-loop single-user channel capacities. On the $(N,1,K)$ MIMO BC this is equivalent to choosing the N users with the largest channel vector norms.
- Condition Number Scheduling, which is applicable with complete CSIT, where the base station chooses the N users that minimize the condition number of the channel matrix between the base station and these N users. The condition number of the matrix is the ratio of the largest to the smallest singular value.
- SUR- $(N+1)$ Scheduling algorithm followed by the Best N -user Scheduling algorithm on the reduced channel with $N+1$ users. This choice provides a complexity reduction and a trade-off between SUR- N and the Best N -user Scheduling algorithm applied directly on the $(N,1,K)$ MIMO BC.

- Successive Projections scheduling
- Gorokhov's Algorithm I scheduling [56], or receive antenna selection with the goal of incremental loss minimization.
- Gorokhov's Algorithm II scheduling [56], or receive antenna selection with incremental selection.
- Gorokhov's Algorithm III scheduling [56], or receive antenna selection with decremental selection.
- Best N -user Scheduling

Gorokhov's algorithms are summarized in Appendix F. Gorokhov's Algorithms I and II take the transmit power level into account. Thus we expect that these algorithms can provide better performance in the intermediate power region and not only in the high power region. Incremental selection or decremental selection can also be used to schedule a user in the presence of already scheduled users.

Simulation results reported in Figure 4-4 for the (2,1,6) MIMO BC show that optimizing the choice of the N users is important. This figure shows the difference between the sum-capacity and the spectral efficiency achieved by scheduling N -users with several scheduling algorithms. Random N -user Scheduling loses more than 1 bit/sec/Hz to the sum-capacity and to the Best N -user Scheduling algorithm in the high power region. Condition Number Scheduling ignores the

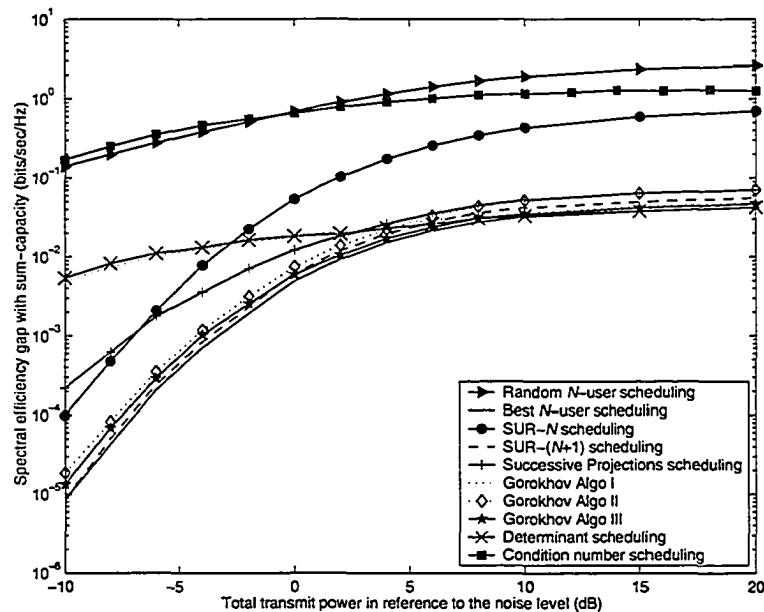


Figure 4-4 Spectral efficiency loss of N -user scheduling algorithms with respect to the sum-capacity on the (2,1,6) MIMO BC.

spatial structure of the channel matrix and is thus not able to closely approach the maximum spectral efficiency obtained with Best N -user Scheduling. It is unable to choose users with individually good channel condition. The Determinant Scheduling algorithm performs well in the high power region as predicted by the analysis in Chapter III. However, it performs poorly in the lower power region. In the low power region, the scheduling algorithm should be able to select the user with the largest channel vector norm in the N -user set in order to approach the sum-capacity. The SUR- N Scheduling algorithm chooses the N users separately so it achieves intermediate performance between the Best N -user Scheduling and the Random N -user Scheduling algorithms. The Successive Projections Scheduling algorithm provides improvement versus SUR- N Scheduling except in the very low power region, but the difference is very small (on the order of 0.0001 bit/sec/Hz). However, it is outperformed in all power regions by other low-complexity scheduling algorithms, especially in the low to medium power regions. Gorokhov's Algorithm I provides good performance in the high power region but performs poorly in the low to medium power regions. Both the Successive Projections Scheduling algorithm and Gorokhov's Algorithm I do not incorporate the effect of power in their procedure so they do not perform well at low to medium power. Gorokhov's Algorithms I and III perform the best in the high power region among the low-complexity scheduling algorithms. Their performance is almost matched to Determinant Scheduling but with a much lower complexity. But Gorokhov's Algorithm II provides good performance in the whole range of power. Gorokhov's Algorithm III outperforms algorithm II in the whole range of power, as predicted by the authors of [56]. Interestingly SUR- $(N+1)$ Scheduling algorithm followed by the Best N -user Scheduling algorithm on the reduced channel with $N+1$ users provides good performance in the whole power region. Thus, it is likely that the best N -user set be such that the N users are among the $N+1$ users with the best individual channel conditions. However, this conclusion might not be true when the total number of users becomes large.

We also notice that the difference between the sum-capacity and the sum-capacity achieved with any of all the N -user scheduling algorithms used with dirty-paper coding converges to an asymptote. Thus the power spectral efficiency loss becomes constant in the high power region and any N -user scheduling algorithm can be used to achieve the maximum spatial multiplexing gain and lose only a vanishing fraction of the sum-capacity asymptotically. Nevertheless we are primarily interested in the medium to high power region where the MIMO capacity gains become apparent and in this region the spectral efficiency difference is not negligible especially as the number of users is much larger than the number of transmit antennas.

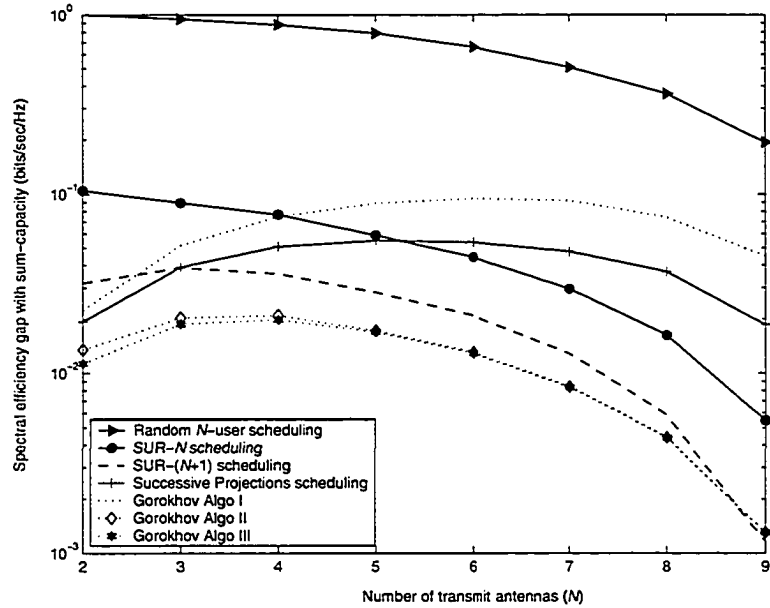


Figure 4-5 Spectral efficiency loss of N -user scheduling algorithms with respect to the sum-capacity on the $(N,1,10)$ MIMO BC. The total power in reference to the noise level is 0 dB.

Figure 4-5 shows the spectral efficiency loss of N -user scheduling algorithms on the $(N,1,10)$ MIMO BC as a function of the number of transmit antennas. Only the reduced-complexity scheduling algorithms are shown. Gorokhov's Algorithms II and III again perform best at all values of the number of transmit antennas. We observe a degradation of SUR- $(N+1)$ Scheduling at $N=2$ with 10 users compared to Figure 4-4.

Since the difference between the sum-capacity and the spectral efficiency achieved with N -user scheduling algorithms can be very small, we also observe the ratio of the spectral efficiency achieved with several N -user scheduling algorithms to the sum-capacity on the $(4,1,K)$ MIMO BC as a function of the number of users K . The results are shown in Figure 4-6. With 15 users, Random N -user Scheduling only achieves 75% of the sum-capacity. Scheduling algorithms that choose users independently of one another, like SUR- N Scheduling and SUR- $(N+1)$ Scheduling, allow to achieve more than 90% of the sum-capacity, but Gorokhov's algorithms and Successive Projections Scheduling perform better.

4.3.2 Scheduling with Linear Processing Schemes on the $(N,1,K)$ MIMO BC

4.3.2.1 Introduction

The previous discussion assumed that dirty-paper coding is used. Practical implementation of dirty-paper coding is still in its infancy. If we consider some sub-optimal

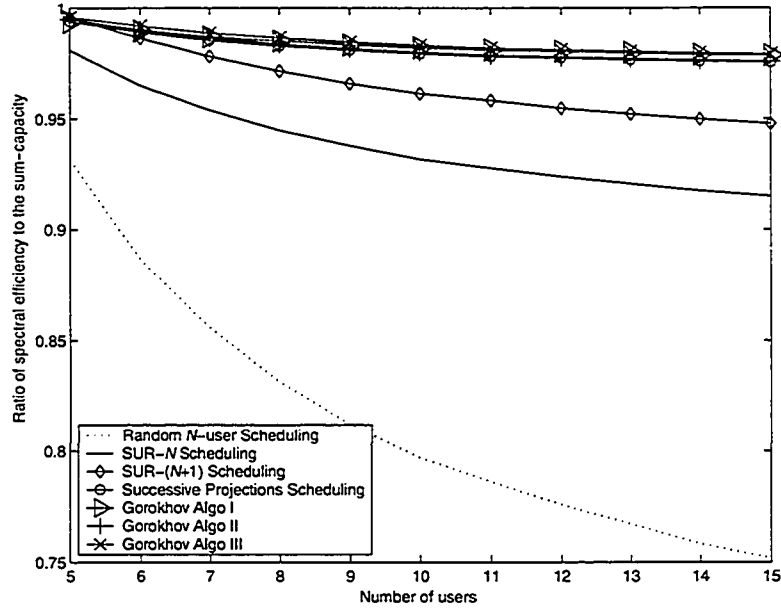


Figure 4-6 Ratio of spectral efficiency of N -user scheduling algorithms to the sum-capacity on the $(4,1,K)$ MIMO BC. The total power in reference to the noise level is 10 dB.

transmission scheme, the scheduling algorithm must also be matched to this particular transmission scheme in order to take advantage of its structure. On the other hand, as shown in the previous section, selecting a user set such that the sum-capacity of the channel restricted to this user set is far from the sum-capacity of the original channel will obviously incur a loss in spectral efficiency with any sub-optimal transmission scheme. In this section we study specific sub-optimal transmission schemes and scheduling algorithms. We consider schemes that involve linear filtering and single-user coding.

4.3.2.2 Scheduling with Complete CQI and CSIT

We consider linear processing at the transmitter in the form of ZFB by pseudo-inversion of the channel matrix followed by waterfilling power allocation as described in [5]. It results in the diagonalization of the channel matrix at the expense of a power penalty. The power penalty becomes more severe as the channel matrix becomes close to singular.

We briefly summarize the signal model for ZFB. At the transmitter, the signal vector is multiplied by the Moore-Penrose pseudo-inverse \mathbf{H}^\dagger of the channel matrix of size $N \times N$. This channel matrix is composed of the channel vectors of the N users that have been selected by the scheduling algorithm. The received signal vector is:

$$\mathbf{y} = \mathbf{H}\mathbf{H}^\dagger \mathbf{x} + \mathbf{n}. \quad (4.5)$$

Applying the analysis in [5] for zero-forcing transmitter processing, the transmit power constraint becomes:

$$P = \text{tr} \left[(\mathbf{H}\mathbf{H}^*)^{-1} \mathbf{S}_x \right] = \sum_{n=1}^N \frac{\pi_n^2}{b_n}. \quad (4.6)$$

$1/b_n$ is the (n,n) element of $(\mathbf{H}\mathbf{H}^*)^{-1}$, and π_n^2 are such that $E[\mathbf{x}\mathbf{x}^*] = \text{diag}(\pi_1^2, \dots, \pi_N^2)$. Let $1/v_n$ is the (n,n) element of $(\mathbf{H}\mathbf{H}^*)^{-1}$, and π_n^2 are such that $E[\mathbf{x}\mathbf{x}^*] = \text{diag}(\pi_1^2, \dots, \pi_N^2)$. Let

$a_n = \pi_n^2/b_n$, $n=1, \dots, N$. The maximization of the mutual information is a conventional waterfilling problem:

$$R_{\text{ZFB}} = \max_{a_n, n=1, \dots, N} \sum_{n=1}^N \log(1 + b_n a_n) \quad (4.7)$$

$$\text{Subject to } \sum_{n=1}^N a_n = P \text{ and } a_n \geq 0, n=1, \dots, N.$$

With the constraints imposed by the structure of the specific spatial multiplexing scheme chosen, our goal is to achieve the maximum achievable sum-rate by optimizing the choice of the scheduled users. We could choose to schedule the users according to the best N -user set in terms of sum-capacity. Although this scheduling algorithm is matched to dirty-paper coding it might not be the best for ZFB. In [57] we proposed a scheduling algorithm matched to ZFB. We refer to it as the Determinant Scheduling algorithm. This scheduling algorithm was introduced in Section 4.3.1.2 and it was motivated by the high power asymptotic approximation of the sum-capacity of the $(N,1,N)$ MIMO BC. The base station chooses the N active users that maximize the determinant of the product of the channel matrix between the base station and the N users by its conjugate transpose. Determinant Scheduling is also motivated by an upper bound to the sum-rate achieved by ZFB with waterfilling power allocation at high SNR with N transmit antennas and N users. We assume that all users experience the same AWGN variance $\sigma_k^2 = 1$, $k=1 \dots K$. If it was not the case we could apply some scaling to the channel vectors and obtain the same model. The upper bound can be directly deduced from the analysis in [5] and Hadamard's determinant inequality [13]:

$$R_{\text{ZFB}} \leq \frac{N}{2} \log \left(\frac{P}{N} + \frac{1}{N} \text{tr} \left[(\mathbf{H}\mathbf{H}^*)^{-1} \right] \right) + \frac{1}{2} \log \det(\mathbf{H}\mathbf{H}^*). \quad (4.8)$$

Determinant Scheduling involves computing the determinants of $N \times N$ matrices of all subsets of N users among K . This search becomes rapidly prohibitive for a large number of users and even a moderate number of transmit antennas. An alternative is to use the Successive Projections Scheduling algorithm or receive antenna selection algorithms. Due to their interference-avoidance properties, these scheduling algorithms can also be used with ZFB to choose the users jointly and

they should provide a good set of users. Simulation results are provided in Section 4.3.2.4. Better performance could be obtained with MMSE beamforming rather than ZFB. However, zero-forcing and MMSE become equivalent criterion in the high power region, thus the performance degradation observed with ZFB would still be present in the high power region.

4.3.2.3 Scheduling with Partial CQI and no CSIT

When the base station cannot obtain the exact value of the fading coefficients for the channels of all users, we consider a system where the users feedback partial channel state information to the base station. In order to achieve spatial multiplexing, we adopt an interference avoidance strategy that compensates for the unfeasibility of linear processing and dirty-paper coding at the transmitter without complete CSIT. Since each user has a single receive antenna, spatial multiuser detection techniques based on array processing cannot be used to separate the interfering signals from the signal of interest. We assume the users cannot perform successive decoding [13], which we motivate by the fact that a simple analysis on the (2,1,2) MIMO BC would show almost no improvement by using successive decoding.

We now describe the signal model assumed in this section. The base station selects N users for transmission based on some scheduling algorithm. All antennas simultaneously transmit independent data streams, each of which is directed to a particular user. The total transmit power is independent of the number of transmit antennas and it is uniformly distributed among them. When transmit antenna j is assigned to user j , the signal received by user j at time t is:

$$y_j(t) = \sqrt{\frac{P}{N}} \sum_{n=1}^N h_{jn} s_n(t) + w_j(t). \quad (4.9)$$

Only the N active users chosen by the scheduler are accounted for in (4.9). The signal s_n intended for user n is sent from antenna n . It has unit average energy. The AWGN w_j has variance σ_j^2 .

Without interference cancellation at the receiver, when the signal transmitted to user j is sent from antenna n , the signals transmitted from the other antennas create interference to user j . The signal to interference plus noise ratio $\text{SINR}_n^{(j)}$ is expressed as the ratio of the desired signal power to the sum of the interference and noise power:

$$\text{SINR}_n^{(j)} = \frac{\frac{P}{N} |h_{jn}|^2}{\sigma_j^2 + \frac{P}{N} \sum_{i=1, i \neq n}^N |h_{ji}|^2}. \quad (4.10)$$

The first scheduling algorithm we consider is referred to as Scheduling Algorithm A. Each user j estimates its $\text{SINR}_n^{(j)}$ for each transmit antenna n and sends the value $\max_{1 \leq n \leq N} \{\text{SINR}_n^{(j)}\}$ and the

corresponding antenna index to the base station. Note that uniform power allocation across the transmit antennas is necessary to allow the users to estimate their $SINR_n^{(j)}$. The base station then chooses the best N users that maximize the SINR for each transmit antenna. The scheduling algorithm can be illustrated as an iterative search through a matrix \mathbf{R} of size $K \times N$ that contains the achievable rates for each user and for each transmit antenna. Let the (j, n) element of \mathbf{R} be

$$r_{j,n} = \log\left(1 + SINR_n^{(j)}\right), \quad (4.11)$$

which is the maximum achievable rate for user j if its signal is sent from antenna n . Scheduling Algorithm A first chooses the user with the maximum rate in the first column, which corresponds to transmit antenna one. The scheduler then chooses the user that maximizes the rate in the second column and so on until all transmit antennas are assigned to a user. This simple feedback strategy allows to evaluate the performance of a scheme based only on the knowledge of the SINR of each user, which would be sufficient on single-antenna multiuser channels.

Scheme A will refer to the system using Scheduling Algorithm A, where each active user makes no attempt at suppressing the interference from the $N-1$ interfering transmit antennas. Thus the MIMO channel can be seen as N parallel AWGN channels, each with its own SINR. Since we have assumed independent fading among transmit antennas and mobile users, the SINR on these parallel channels are i.i.d. random variables. Let R_n be the data rate of user n whose signal is sent from antenna n . We have renumbered the active users according to which transmit antenna they have been assigned. For each of these channels, the maximum supported rate in a given block is:

$$R_n \leq \log\left(1 + SINR_n^{(n)}\right), 1 \leq n \leq N. \quad (4.12)$$

The sum-rate is upper bounded by the sum of the maximum rates supported by each user:

$$R = \sum_{n=1}^N R_n \leq \sum_{n=1}^N \log\left(1 + SINR_n^{(n)}\right). \quad (4.13)$$

In the high power region or as the number of transmit antennas increases for a fixed number of users, Scheme A becomes interference-limited. Thus it is unable to take advantage of the spatial degrees of freedom if the number of users is fixed and the number of transmit antennas increases.

The second scheduling algorithm we consider is referred to as Scheduling Algorithm B, which is an adaptive version of Scheduling Algorithm A. The base station can now choose any subset of the transmit antennas in order to transmit to fewer users simultaneously with fewer transmit antennas in the same way as Scheme A. The maximization is performed among users for each antenna subset and then among all antenna subsets for all sizes of antenna subsets from 1 to N . This strategy requires more feedback from the mobile users than Scheme A. Scheme B will refer to the system using Scheduling Algorithm B. Scheme B can adapt its active user set size to the amount of interference, thus the throughput will keep increasing with the SNR. As a result of the adaptive nature of Scheme B, in the high SNR region only one transmit antenna will be used to transmit to only one user at a time in a selection diversity manner where the best antenna/user pair is selected. The adaptive nature of Scheme B is illustrated in Figure 4-7 and Figure 4-8. The histogram of the number of active users (equivalently the number of transmit antennas effectively used) is shown as a function of the SNR and as a function of the total number of users. As the number of users increases, multiuser diversity allows to use more transmit antennas by choosing a better active user set, thus the throughput increases.

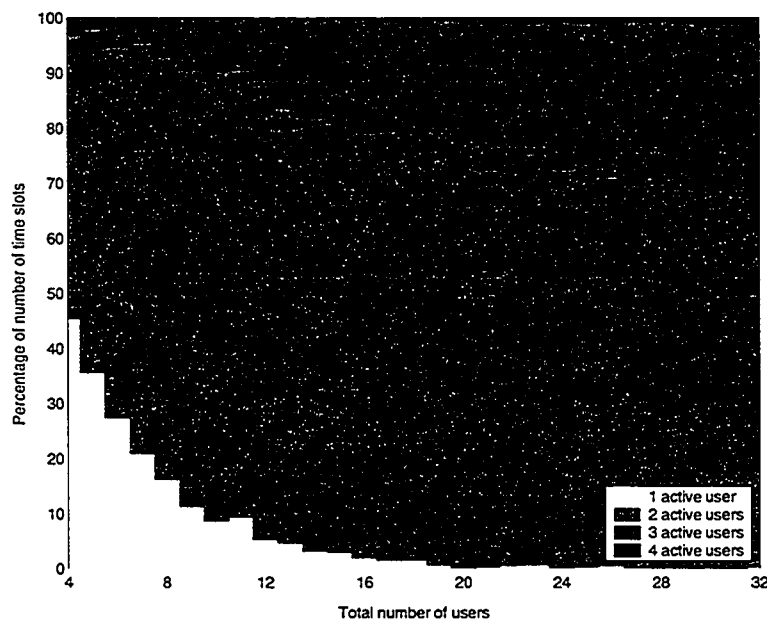


Figure 4-7 Cumulative bar plot of the number of active users for Scheme B. The total power in reference to the noise level is 10 dB. The number of transmit antennas is $N = 4$. 1000 channel realizations.

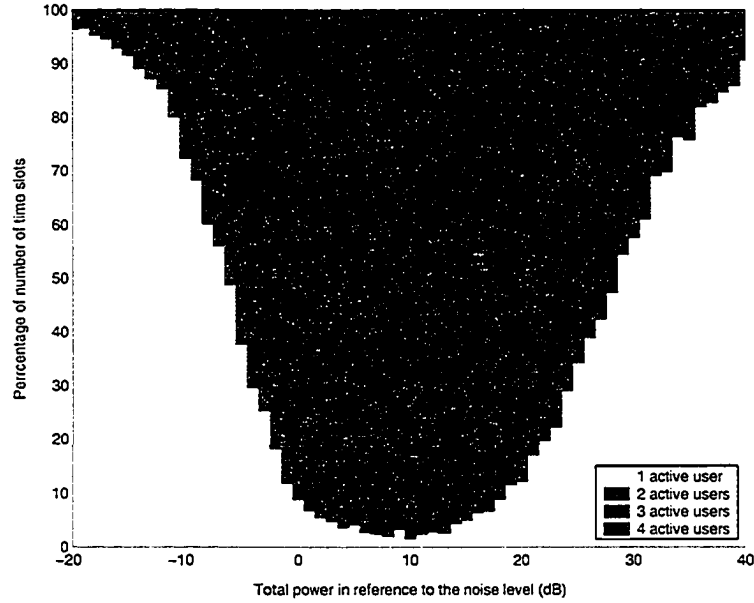


Figure 4-8 Cumulative bar plot of the number of active users for Scheme B. The total number of users is $K = 16$. The number of transmit antennas is $N = 4$. 1000 channel realizations.

4.3.2.4 Simulation Results

Figure 4-9 shows the average of the maximum sum-rate as a function of the number of users for the discussed transmission schemes and scheduling algorithms. The total power in reference to the noise level is 10 dB. The number of transmit antennas is $N = 2$. The AWGN level is assumed to have the same variance of one for all users. We observe that ZFB and Determinant Scheduling algorithm, Successive Projections Scheduling algorithm, and Gorokhov's Algorithm I, achieve a spectral efficiency with approximately the same growth rate as the sum-capacity curve. Thus, these scheduling algorithms can take advantage of multiuser diversity to select a user set that reduces the power penalty due to zero-forcing channel inversion when $N = 2$. In this case, this solution is much less complex than optimal dirty-paper coding. If the transmitter only has partial CQI with the type of feedback described in section 4.3.2.3 we observe a large loss in spectral efficiency. Nevertheless as the number of users increases, Scheme A and Scheme B take advantage of multiuser diversity to achieve a throughput larger than the best spectral efficiency achievable by transmitting to a single user at a time with complete CQI and CSIT using transmitter MRC beamforming, which achieves the single-user closed-loop MISO channel capacity.

Figure 4-10 shows the average of the maximum sum-rate as a function of the total power in reference to the noise level. The number of transmit antennas is $N = 2$. The total number of users is $K = 10$. The AWGN level is assumed to have the same variance of one for all users. We observe that the sum-capacity slope, which represents the spatial multiplexing gain of MIMO systems, is only achieved with complete CSIT. We also see that with a fixed number of users, Scheme A becomes interference-limited as the total transmit power increases. We will see that the same effect appears as the number of transmit antennas increases. In this case, Scheme B allows to achieve approximately the same spectral efficiency as the best single-user closed-loop capacity, although it only uses partial CQI at the transmitter.

Figure 4-11 shows the average of the maximum sum-rate as a function of the number of transmit antennas. The total power in reference to the noise level is 10 dB. The AWGN level is assumed to be the same for all users with a variance of one. The total number of users is $K = 10$. ZFB takes advantage of MIMO spatial multiplexing gain when the number of transmit antennas is small, but it does not allow to take advantage of the MIMO spatial multiplexing gain when the number of transmit antennas is large. Lattice reduction techniques applied at the transmitter side [58][59][60] are required to overcome this problem but this is beyond the scope of this thesis. Partial CQI alone does not allow to achieve spatial multiplexing gain with Schemes A and B, and the interference limitation is apparent as the number of antennas becomes large.

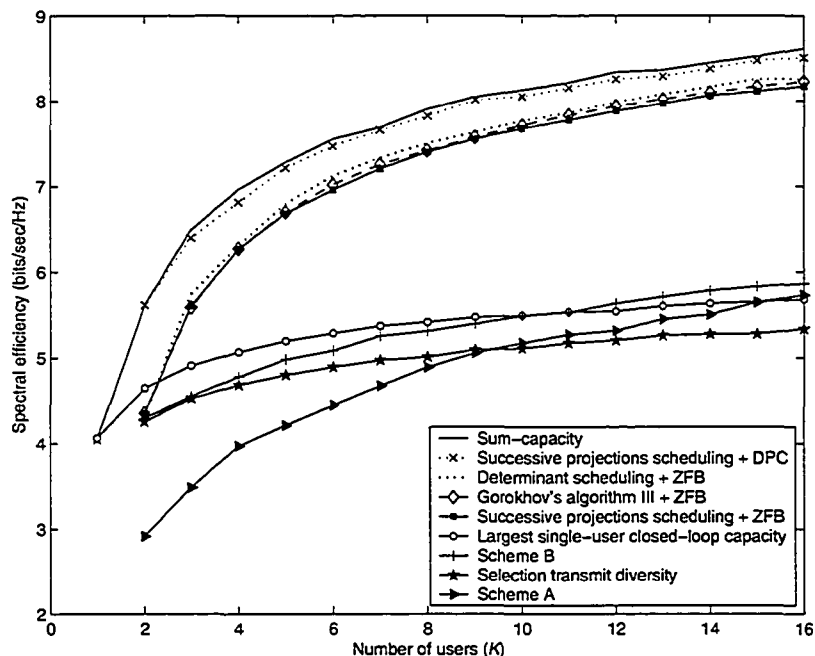


Figure 4-9 Average spectral efficiency as a function of the total number of users K . The number of transmit antennas is $N = 2$. The total power in reference to the noise level is 10 dB.

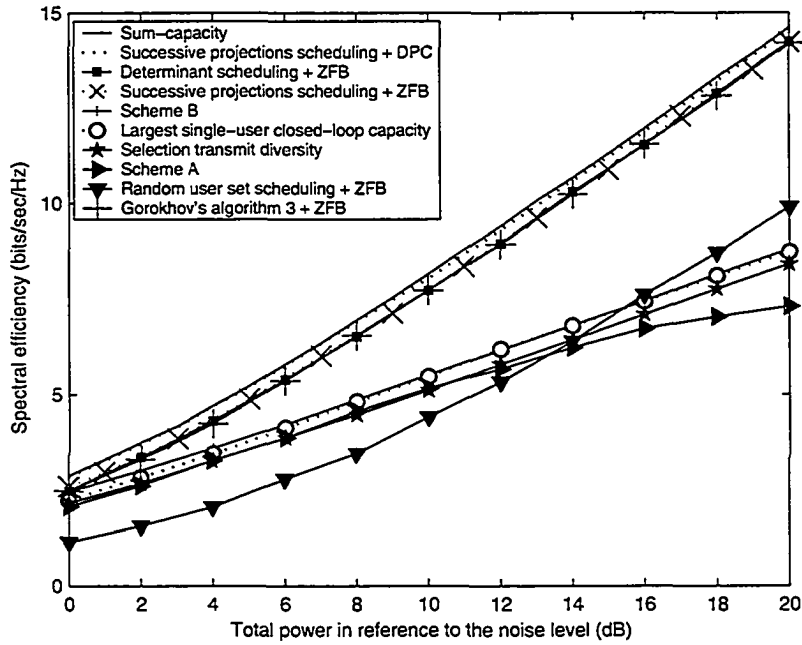


Figure 4-10 Average spectral efficiency as a function of the total power in reference to the noise level. The total number of users is $K = 10$. The number of transmit antennas is $N = 2$.

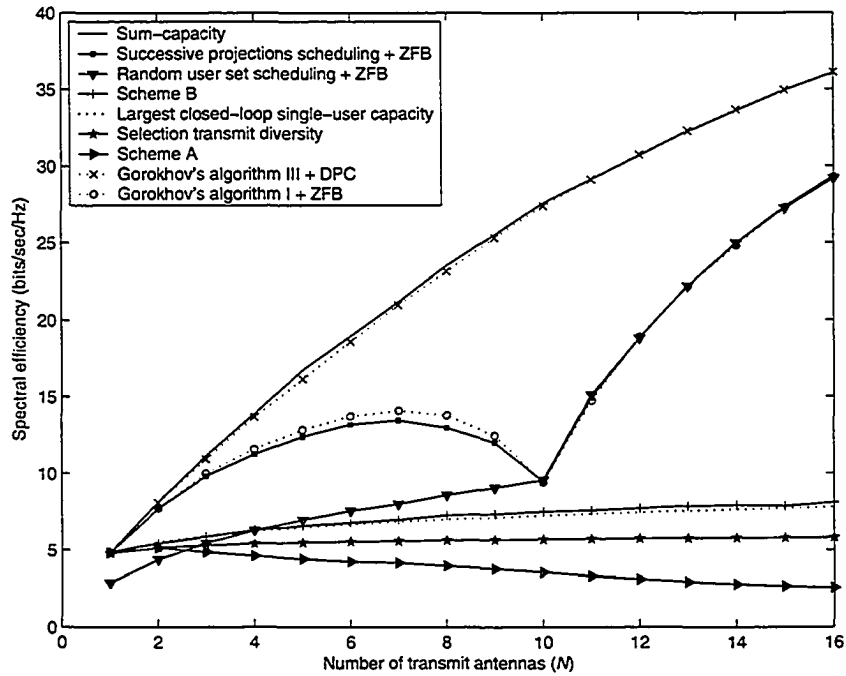


Figure 4-11 Average spectral efficiency as a function of the number of transmit antennas. The total number of users is $K = 10$. The total power in reference to the noise level is 10 dB.

Similar solutions have simultaneously been proposed for interference avoidance in the case of partial CQI and CSIT. In [61] the authors proposed Distributed-Multi-Antenna-Scheduling (DMAS) but they limited their solution to two transmit antennas. They also proposed a solution to improve the transmitter power allocation. In [62][63] very similar solutions were proposed. These schemes can be viewed as an instance of opportunistic beamforming. Scheme A forms N beams with beamforming vectors of the form $[0 \dots 1 \dots 0]$ with only one non-zero element. Put together in a multiplexing matrix they form a permutation of the identity matrix. Even though the beams are not changed with time, the users that fall within a beam are served in an opportunistic manner. The original opportunistic beamforming scheme served only one user at a time [24] and a proposal for spatial multiplexing was mentioned in the appendix. It was later extended to spatial multiplexing in [46] where the authors also conducted an analysis of the growth rate of the maximum sum-rate achievable with that scheme. They proved that the maximum sum-rate scales as $N \log \log K$ when the users are equipped with a single receive antenna. They also proved that linear increase in capacity with the number of transmit antennas can be obtained provided that the number of transmit antennas N does not grow faster than $O(\log K)$. As long as the channel changes independently from one time slot to the next, opportunistic beamforming with spatial multiplexing is exactly equivalent to Scheme A. Thus this analysis of the growth rate applies to Scheme A and it confirms our simulation results. In channels where the channel vectors are constant or change very slowly, time-varying opportunistic beamforming allows to create the illusion of multiuser diversity by arbitrarily creating channel variations, which is not a possibility with Scheme A.

In Figure 4-11, we showed the performance of ZFB with Gorokhov's Algorithm I used for scheduling. In Figure 4-12, we show the spectral efficiency loss of scheduling algorithms used with ZFB in comparison to the optimal scheduling algorithm that performs the exhaustive search for the set of N users that maximize the sum-rate with ZFB. We see that in contrast to the dirty-paper coding capacity performance of these algorithms, if they are used with a sub-optimal transmission scheme their ranking in terms of performance loss can be reversed. With ZFB, Gorokhov's Algorithm I outperforms both Algorithms II and III, which is the opposite to the result obtained in Figure 4-4.

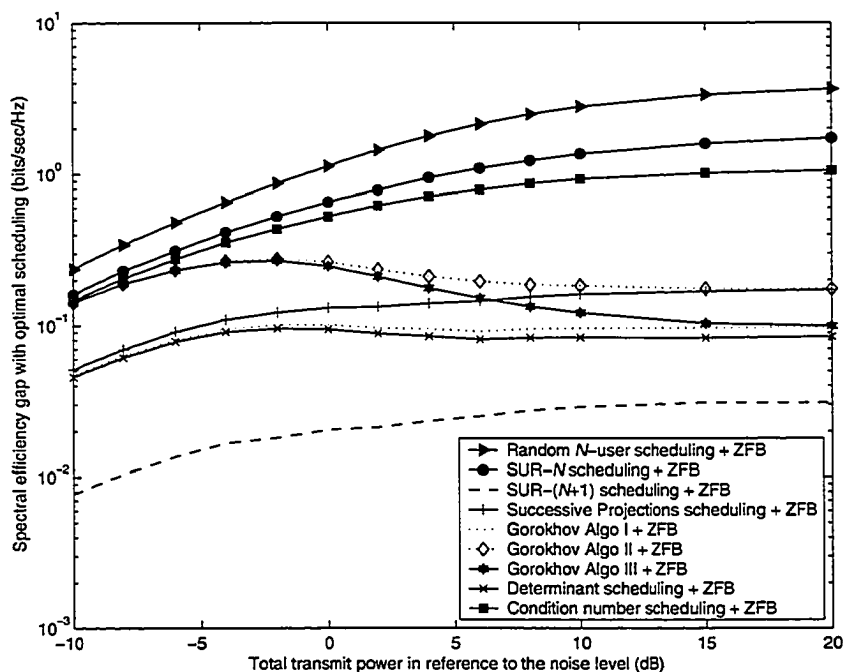


Figure 4-12 Spectral efficiency loss of N -user scheduling algorithms with respect to the exhaustive search on the $(2,1,6)$ MIMO BC with zero-forcing beamforming at the transmitter.

4.3.3 Scheduling with Linear Processing Schemes on the (N,M,K) MIMO BC

4.3.3.1 Introduction

We consider the MIMO broadcast channel where the transmitter and the receivers are equipped with multiple antennas. We propose a new scheme using linear processing at the transmitter and at the receivers to jointly diagonalize the channel so that two users can receive data simultaneously. It is applicable when the users are equipped with any numbers of antennas, and it is able to take advantage of all the spatial degrees of freedom as long as the overall number of all receive antennas is greater than or equal to the number of transmit antennas. The proposed strategy achieves a large portion of the two-user sum-capacity when the base station has two transmit antennas. We provide an asymptotic analysis and simulation results to illustrate our analysis.

4.3.3.2 Previously Proposed Schemes

4.3.3.2.1 Joint-Orthogonalization Schemes

Group zero-forcing, an extension of ZFB for the case of users with multiple receive antennas was proposed in [33]. This scheme has the advantage of enabling simultaneous transmission to several users but it constrains the total number of receive antennas not to be larger than the number of transmit antennas. Thus if users are equipped with the same number of antennas as used by the base station, only one user can receive data at a time. This fact inherently limits the maximum achievable sum-rate. Other recent schemes also have limits on the number of antennas or the number of users [30][31][32][64]. Some works focused on maximizing a lower bound on the product of the SINR of the users, others on maximizing the throughput or minimizing the bit error probability. Iterative solutions or closed-form solutions were sought to find the transmit and receive filters. A summary of the constraints on the number of antennas and on the number of active users for several spatial multiplexing schemes is shown in Table 4-1. Our proposed schemes are also included in this table. When users are equipped with multiple receive antennas, it is possible to transmit several layers consisting of independent codewords to the same user. The number of layers sent to user k is denoted as L_k in the subsequent sections. The number of simultaneously active users is K_a .

Zero-forcing dirty-paper coding [5]	$M_k = M = 1 \forall k, K_a M = K_a \leq N, L_k = 1$
Transmitter zero-forcing beamforming [5]	$M_k = M = 1 \forall k, K_a M = K_a \leq N, L_k = 1$
Scheme A [57]	$M_k = M = 1 \forall k, K_a M = K_a \leq N, 1 \leq L_k \leq N$
Scheme B [57]	$M_k = M = 1 \forall k, K_a M = K_a \leq N, 1 \leq L_k \leq N$
Wong et. al. [30]	$\sum_{i=1}^{K_a} M_i \leq N, L_k \leq M_k$
Antenna-assisted round-robin and beamforming [62]	$M_k = M \forall k, M \geq N, \sum_{i=1}^{K_a} L_i \leq N$
Group zero-forcing beamforming [33]	$M_k = M \forall k, K_a M \leq N$
JLTR-SM [65]	$K_a \leq 2$
Receive zero-forcing beamforming (R-SM) [34]	$M_k \geq N \forall k, L_k \geq 1$
Wong et. al. [66]	$M_k \geq L_k + 1 \forall k, \sum_{i=1}^{K_a} L_i \leq N$
Wong et. al. [31]	$M_k \geq L_k + 1 \forall k, \sum_{i=1}^{K_a} L_i \leq N$
Choi et. al. [32]	$N \geq \max_{1 \leq k \leq K_a} \sum_{i=1, i \neq k}^{K_a} M_i$
Choi et. al. [67]	$\sum_{i=1}^{K_a} M_i \leq N + M_k - 1$
Coordinated Beamforming [35]	$\sum_{i=1}^{K_a} L_i \leq N, 1 \leq L_i \leq N$

Table 4-1 Constraints on the number of transmit and receive antennas and on the number of simultaneously active users of several spatial multiplexing schemes.

4.3.3.2.2 Coordinated Beamforming

A more recent scheme called Coordinated Beamforming is applicable with any number of antennas and users [35]. A brief summary of Coordinated Beamforming follows. In contrast to previously proposed solutions, Coordinated Beamforming overcomes the constraint on the number of receive antennas by incorporating the receive filters in the channels experienced by each user before performing the optimization of the transmit filters. The authors therefore proposed an iterative solution for computing the transmit and receive filters, and claimed that it converges in general. The constraint now applies on the total number of independent layers transmitted instead of being on the total number of receive antennas.

The signal received by user k is

$$\mathbf{x}_k = \sum_{i=1}^{K_a} \mathbf{H}_k \mathbf{F}_i \mathbf{d}_i + \mathbf{n}_k. \quad (4.14)$$

\mathbf{F}_i is the $N \times L_i$ transmit filter for user i , \mathbf{d}_i is the $L_i \times 1$ data vector of user i , \mathbf{n}_k is the $M_k \times 1$ noise vector. Let \mathbf{G}_k be the $M_k \times L_k$ receive filter of user k . After applying this filter user k sees the vector:

$$\hat{\mathbf{d}}_k = \mathbf{G}_k^* \mathbf{H}_k \mathbf{F}_k \mathbf{d}_k + \mathbf{G}_k^* \mathbf{H}_k \sum_{i=1}^{K_a} \mathbf{F}_i \mathbf{d}_i + \mathbf{G}_k^* \mathbf{n}_k. \quad (4.15)$$

Let

$$\bar{\mathbf{H}}_k = \mathbf{G}_k^* \mathbf{H}_k. \quad (4.16)$$

Define

$$\tilde{\tilde{\mathbf{H}}}_k = [\bar{\mathbf{H}}_1^T \quad \dots \quad \bar{\mathbf{H}}_{k-1}^T \quad \bar{\mathbf{H}}_{k+1}^T \quad \dots \quad \bar{\mathbf{H}}_{K_s}^T]^T. \quad (4.17)$$

The size of that matrix is $(\sum_{i \neq k} L_i) \times N$. The transmitter matrix of user k is chosen in such a way that user k does not create interference at the output of the receivers of the other users with a zero-forcing strategy. Hence the matrix \mathbf{F}_k is chosen to lie in the null space of $\tilde{\tilde{\mathbf{H}}}_k$. It is obtained for a fixed set of receive filters by applying the SVD to the matrix $\mathbf{H}_k \tilde{\tilde{\mathbf{V}}}_k^{(0)}$ where $\tilde{\tilde{\mathbf{V}}}_k^{(0)}$ is an orthogonal basis for the null space of $\tilde{\tilde{\mathbf{H}}}_k$. Letting $\mathbf{V}_j^{(1)}$ be the matrix composed of the first L_k right singular vectors of $\mathbf{H}_k \tilde{\tilde{\mathbf{V}}}_k^{(0)}$, the transmit filter for user k is given by

$$\mathbf{F}_k = \tilde{\tilde{\mathbf{V}}}_k^{(0)} \mathbf{V}_j^{(1)}. \quad (4.18)$$

The iterative procedure to obtain the transmit and receive filters starts by assuming a set of receive filters, then proceeds by calculating the set of zero-forcing transmit filters, and continues by updating the set of receive filters using the first L_k left singular vectors of $\mathbf{H}_k \tilde{\tilde{\mathbf{V}}}_k^{(0)}$ and so on until a convergence criterion is reached. The authors in [35] used a threshold to compare to the magnitude of the largest off-diagonal coefficient of the equivalent channel seen by each user given by $\mathbf{G}_k^* \mathbf{H}_k \mathbf{F}_k$. They claimed that convergence is reached with a high probability. Once the channel is orthogonalized, the power is allocated at the transmitter with a waterfilling strategy to maximize the sum-rate. We point out that by allocating all the layers to only one user, Coordinated Beamforming performs the SVD of the channel matrix of that user and transmits according to the closed-loop MIMO capacity achieving strategy [4].

4.3.3.2.3 Receiver Processing Only

Here we use only linear processing at the receivers as proposed in [34] in order for several users to share the spatial channels. We propose to further optimize the power and rate allocation at the transmitter to increase the achievable throughput. We will refer to this scheme as receiver spatial multiplexing (R-SM).

At the receiver of user k , the received vector is multiplied by the Moore-Penrose pseudo-inverse \mathbf{H}_k^\dagger of the channel matrix. The signal seen by user k after pseudo-inversion is:

$$\mathbf{z}_k = \mathbf{u} + \mathbf{H}_k^\dagger \mathbf{n}_k. \quad (4.19)$$

The noise after pseudo-inversion is $\mathbf{w}_k = \mathbf{H}_k^\dagger \mathbf{n}_k$ and its covariance matrix is $E[\mathbf{w}_k \mathbf{w}_k^*] = \sigma_k^2 \mathbf{H}_k^\dagger \mathbf{H}_k^*$. The noise power on row n of the processed received vector is given by $\sigma_k^2 / b_{k,n}$ where $1/b_{k,n}$ is the (n,n) element of $\mathbf{H}_k^\dagger \mathbf{H}_k^*$.

We thus have a set of N parallel degraded broadcast channels with K users and a total power constraint P . The sum-capacity solution was obtained in [17] by transmitting to the user with the highest SNR on each channel with waterfilling power allocation across the channels. The maximum sum-rate is:

$$R_{R-SM} = \max_{a_n^2, n=1, \dots, N} \sum_{n=1}^N \log_2 \left(1 + a_n \max_{1 \leq k \leq K} (b_{k,n} / \sigma_k^2) \right) \quad (4.20)$$

Subject to $\sum_{n=1}^N a_n = P$ and $a_n \geq 0, n = 1, \dots, N$.

The power allocated to the user with the highest SNR on channel n is a_n .

4.3.3.3 Joint-Linear Transmit and Receive Spatial Multiplexing

4.3.3.3.1 Two-User Channel

We first consider the two-user MIMO broadcast channel. We assume that $M_1 + M_2 \geq N$. If this was not the case we could just choose not to use some of the transmit antennas. We perform the Generalized Singular Value Decomposition (GSVD) [68][69] of the two channel matrices as:

$$\begin{aligned} \mathbf{H}_1 &= \mathbf{U}_1 \mathbf{\Omega}_1 \mathbf{X}^* \\ \mathbf{H}_2 &= \mathbf{U}_2 \mathbf{\Omega}_2 \mathbf{X}^* \end{aligned} \quad (4.21)$$

$$\mathbf{\Omega}_1^* \mathbf{\Omega}_1 + \mathbf{\Omega}_2^* \mathbf{\Omega}_2 = \mathbf{I}_N. \quad (4.22)$$

\mathbf{U}_k is a unitary matrix of size $M_k \times M_k$. $\mathbf{\Omega}_k$ is a matrix of size $M_k \times N$ of the form $[\mathbf{A}_k \ \mathbf{0}]^T$, if $M_k \geq N$, or $[\mathbf{A}_k \ \mathbf{0}]$, if $M_k \leq N$, and \mathbf{A}_k is a diagonal matrix of size $M_k \times M_k$ with non-negative elements. \mathbf{X} is a non-singular $N \times N$ matrix. The GSVD is applicable to two matrices with a common dimension. In our case, the number of transmit antennas is the common dimension of the channel matrices of two users. As a particular case, the GSVD of two square matrices, when one of the two matrices (e.g. \mathbf{H}_2) is non-singular, is equivalent to the SVD of $\mathbf{H}_1 \mathbf{H}_2^{-1}$. The GSVD is summarized in Appendix G. By construction of the GSVD [68][69]:

$$\mathbf{X} = \tilde{\mathbf{R}} \mathbf{V}. \quad (4.23)$$

\mathbf{V} is a unitary matrix and $\tilde{\mathbf{R}}$ is the upper left $q \times q$ block of the upper triangular matrix \mathbf{R} in the

QR decomposition of the stacked channel matrix $\mathbf{H} = [\mathbf{H}_1^T \quad \mathbf{H}_2^T]^T$, and $q = \text{rank}(\mathbf{H})$.

Joint transmitter processing is performed by ZFB using the inverse of the matrix \mathbf{X}^* . The vector \mathbf{u} of modulated symbols is processed at the transmitter as:

$$\mathbf{s} = (\mathbf{X}^*)^{-1} \mathbf{u}. \quad (4.24)$$

The signals received by users 1 and 2 are:

$$\begin{aligned} \mathbf{y}_1 &= \mathbf{H}_1 \mathbf{s} + \mathbf{n}_1 = \mathbf{U}_1 \mathbf{\Omega}_1 \mathbf{X}^* (\mathbf{X}^*)^{-1} \mathbf{u} + \mathbf{n}_1 \\ \mathbf{y}_2 &= \mathbf{H}_2 \mathbf{s} + \mathbf{n}_2 = \mathbf{U}_2 \mathbf{\Omega}_2 \mathbf{X}^* (\mathbf{X}^*)^{-1} \mathbf{u} + \mathbf{n}_2. \end{aligned} \quad (4.25)$$

The vectors \mathbf{n}_1 and \mathbf{n}_2 contain the AWGN samples with variances σ_1^2 and σ_2^2 respectively. The received signals are processed respectively by \mathbf{U}_1^* and \mathbf{U}_2^* at the receivers of users 1 and 2 to give:

$$\begin{aligned} \mathbf{z}_1 &= \mathbf{\Omega}_1 \mathbf{u} + \mathbf{U}_1^* \mathbf{n}_1 \\ \mathbf{z}_2 &= \mathbf{\Omega}_2 \mathbf{u} + \mathbf{U}_2^* \mathbf{n}_2. \end{aligned} \quad (4.26)$$

The effective channel matrix is now diagonal for each user, and the channel gains are related through (4.22). We obtained N parallel non-interfering degraded Gaussian broadcast channels. Each of these channels corresponds to a column in the matrices $\mathbf{\Omega}_1$ and $\mathbf{\Omega}_2$. The mutual information is maximized by transmitting to the user with the highest SINR on each of the parallel channels, and performing power and rate allocation by waterfilling across the parallel channels [17].

We choose to send independent data streams on each channel corresponding to the columns of the matrices $\mathbf{\Omega}_1$ and $\mathbf{\Omega}_2$ with powers π_1^2, \dots, π_N^2 . The covariance matrix of the signal vector \mathbf{u} is

$$E[\mathbf{u}\mathbf{u}^*] = \text{diag}(\pi_1^2, \dots, \pi_N^2). \quad (4.27)$$

Applying the analysis in [5] for zero-forcing transmitter processing, the transmit power constraint becomes:

$$P = \text{tr}[(\mathbf{X}^* \mathbf{X})^{-1} \mathbf{S}_{uu}] = \sum_{n=1}^N \frac{\pi_n^2}{b_n}. \quad (4.28)$$

$1/b_n$ is the (n, n) element of $(\mathbf{X}^* \mathbf{X})^{-1}$. Let $a_n = \pi_n^2 / b_n$, $n = 1 \dots N$. Let $\mathbf{\Omega}_i = \text{diag}(\omega_{i1}, \dots, \omega_{iN})$, $i = 1, 2$ so $\omega_{1n}^2 + \omega_{2n}^2 = 1$ for $n = 1 \dots N$. The maximization of the mutual information is a conventional waterfilling problem [48]:

$$R_{JLTR-SM} = \max_{a_n, n=1, \dots, N} \sum_{n=1}^N \log \left(1 + b_n a_n \max \left\{ \frac{\omega_{1n}^2}{\sigma_1^2}, \frac{\omega_{2n}^2}{\sigma_2^2} \right\} \right) \quad (4.29)$$

$$\text{Subject to } \sum_{n=1}^N a_n = P \text{ and } a_n \geq 0, n=1, \dots, N.$$

In the case where $M_1 = M_2 = 1$ this scheme only allows to transmit one data stream to each of the two users and no receiver processing is required. If $N = 2$ and $K = 2$ with $M_1 = M_2 = 1$, JLTR-SM is equivalent to ZFB at the transmitter proposed in [5]. If $N > 2$ or $K > 2$ with $M_1 = M_2 = 1$ JLTR-SM fails to exploit all the spatial dimensions of the MIMO channel. However, as long as there are at least two users in a sector and $M_1 + M_2 \geq N$ this scheme can exploit all the spatial dimensions of the MIMO channel.

We note that the main difference between Coordinated Beamforming and JLTR-SM is that Coordinated Beamforming can accommodate more than two users in a given time slot, where user k uses L_k dimensions such that $\sum_{k=1}^{K_a} L_k \leq N$, where K_a is the number of active users in a time slot. The second difference is that orthogonal channels are created with Coordinated Beamforming, thus each user sees no interference from all other users, whereas JLTR-SM created parallel channels and power allocation is necessary to ensure that no interference is created among users on any of the parallel channels.

4.3.3.2 Asymptotic analysis of the sum-rate

We derive lower and upper bounds on the maximum achievable throughput when the users experience the same noise level at each receive antenna and when $M_1 = M_2 = N$. We assume that the AWGN variance is equal to 1 at each receive antenna. We assume that the total power is larger than some threshold so that all channels are allocated power in (4.29).

Using $1/2 \leq \max(\omega_{1n}^2, \omega_{2n}^2) \leq 1, n=1, \dots, N$, we get:

$$N \left[-\log 2N + \frac{1}{N} \sum_{n=1}^N \log b_n + \log \left(P + 2 \sum_{n=1}^N \frac{1}{b_n} \right) \right] \leq R_{JLTR-SM} \quad (4.30)$$

$$N \left[-\log N + \frac{1}{N} \sum_{n=1}^N \log b_n + \log \left(P + \sum_{n=1}^N \frac{1}{b_n} \right) \right] \geq R_{JLTR-SM}. \quad (4.31)$$

The sum-rate $\bar{R}_{JLTR-SM}$ averaged over the small-scale Rayleigh fading can be approximated by $\mathcal{C} \log(\rho P + \alpha)$ in the high power regime as N approaches infinity, where α is some constant. \mathcal{C} and ρ are constants known as the growth rate and the scaling factor, respectively [45]. The

growth rate is N bits/sec/Hz for each 3 dB increase of the total power P , which proves that this scheme is able to exploit all the available spatial dimensions of the multiuser MIMO channel.

From (4.30) and (4.31) we see that the growth rate is N and the scaling factors for the lower and upper bounds are:

$$\rho_{LB} = \exp \left[\log \left(\frac{1}{2N} \right) + \frac{1}{N} \sum_{n=1}^N \log b_n \right] \geq \left(2 \sum_{n=1}^N \frac{1}{b_n} \right)^{-1} \quad (4.32)$$

$$\rho_{UB} = \exp \left[\log \left(\frac{1}{N} \right) + \frac{1}{N} \sum_{n=1}^N \log b_n \right] \geq \left(\sum_{n=1}^N \frac{1}{b_n} \right)^{-1}. \quad (4.33)$$

We used the inequality between the arithmetic and geometric means [7]:

$$\frac{1}{n} \sum_{i=1}^n x_i \geq \left(\prod_{i=1}^n x_i \right)^{1/n}. \quad (4.34)$$

A result from [45] applied for $M_1 = M_2 = M$ is:

$$\text{tr} \left[(\mathbf{H}^* \mathbf{H})^{-1} \right] \xrightarrow[\substack{N, M \rightarrow \infty \\ 2M/N = \beta \geq 1}]{} \frac{1}{\beta - 1}. \quad (4.35)$$

By definition we know that:

$$\sum_{n=1}^N \frac{1}{b_n} = \text{tr} \left[(\mathbf{X}^* \mathbf{X})^{-1} \right] = \text{tr} \left[(\mathbf{H}^* \mathbf{H})^{-1} \right]. \quad (4.36)$$

Since $M = N$ by hypothesis, then asymptotically:

$$\lim_{N \rightarrow \infty} \rho_{LB} \geq 1/2 \quad (4.37)$$

$$\lim_{N \rightarrow \infty} \rho_{UB} \geq 1. \quad (4.38)$$

This is to be compared to the scaling factor of the SNR in the closed-loop MIMO channel capacity in the high power regime as N grows large. From [70] we know that the (t, r) MIMO channel waterfilling capacity in the high power regime in the limit where (t, r) approach infinity such that $\min(t, r)/\max(t, r) \rightarrow \beta \leq 1$ is:

$$\frac{C_{WF}}{\min(t, r)} \rightarrow \log \left(P + \frac{1}{1 - \beta} \right) + \frac{1 - \beta}{\beta} \log \left(\frac{1}{1 - \beta} \right) - 1. \quad (4.39)$$

Thus for the cooperative upper bound, which gives the capacity of the $(N, 2N)$ MIMO channel, the scaling factor is $\rho_{coop} = 1$. This is obviously an upper bound on the scaling factor ρ_{UB} of our scheme.

Thus the scaling factor of the SNR, asymptotically in the high power regime as N increases when $K = 2$, is:

$$1/2 \leq \rho_{\bar{r}} \leq 1. \quad (4.40)$$

Note that when $N \geq 2M$ the matrices Ω_1 and Ω_2 only have zeros and ones on their main diagonal so the upper bound (9) is achieved, but the previous analysis does not hold since $N/(2M) \geq 1$.

4.3.3.4 Throughput Maximization and Spatial Multiplexing Gain

We consider packet-data access cellular systems. In the case where more than two users are in the queue to receive data from the base station in a given sector, a scheduler is needed in order to choose the users that will be served in a given time slot. With JLTR-SM, the scheduler needs to choose a two-user set. The throughput maximization strategy involves choosing the two users that maximize the sum-rate defined by (4.29). Multiuser diversity can thus be exploited provided that the users experience independent fading [18]. In order to account for differences in the SINR levels among users we need some criterion that takes into account the fairness in the data rate provided to the users. This issue is addressed in section 4.4.

In the following simulations we evaluate the average sum-rate achieved by several schemes over 1000 independent realizations of the channel matrices. Each realization can be seen as a different time slot, in which some users are scheduled. This assumption is valid as long as the duration of a time slot is small compared to the coherence time of the channel. We assume that capacity-achieving codes are used so the maximum rates of (4.20) and (4.29) are achieved on each time slot. We further assume that $\sigma_k^2 = 1$, $k = 1, \dots, K$.

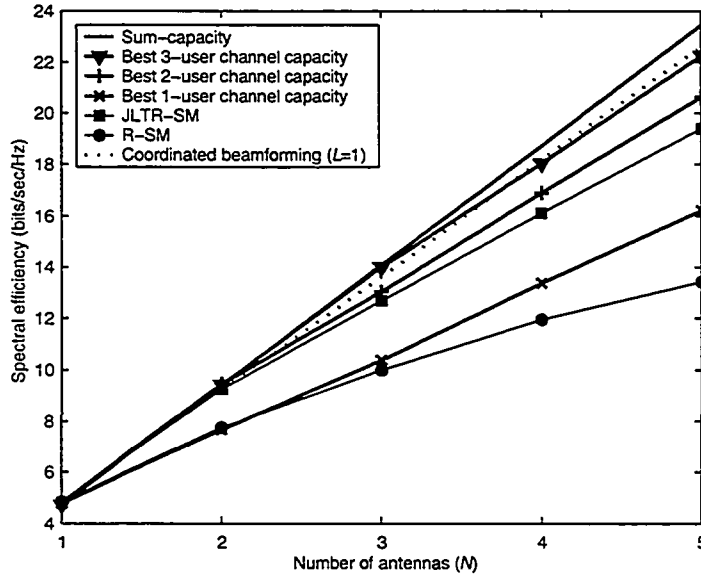


Figure 4-13 Average spectral efficiency on the $(N,N,10)$ BC as a function of the number of antennas N . The total transmit power in reference to the noise level is 10 dB.

Figure 4-13 shows the average spectral efficiency as a function of the number of antennas N at the base station and at each mobile receiver. We saw that on the (N,N,K) BC, constraining the number of active users to be at most N incurs only a marginal loss in spectral efficiency, but constraining the number of users to be strictly less than N incurs an observable loss in spectral efficiency. Thus the spectral efficiency achieved with JLTR-SM can only hope to approach the sum-capacity when $N=2$. On the other hand, although R-SM allows to transmit to N users simultaneously and to take advantage of multiuser diversity, it is unable to achieve a spectral efficiency larger than the single-user closed-loop capacity.

We compared our scheme with the recently proposed Coordinated Beamforming [35]. This strategy is able to transmit as many independent streams as the number of transmit antennas. L_k streams are transmitted to each user. We set $L_k = 1$ for each of the N scheduled users. The scheduler chooses the N users that maximize the sum-rate on any given time slot. Waterfilling power allocation is performed at the transmitter. Coordinated Beamforming is able to achieve almost the same slope as the sum-capacity. Transmitting only one stream to each user in fact approaches the optimal strategy achievable with dirty-paper coding in the intermediary power region.

Figure 4-14 shows the average spectral efficiency as a function of the total power in reference to the noise level. The numbers of transmit antennas and receive antennas for the two mobile users are the same. With only two users, JLTR-SM is able to follow the same behaviour as the sum-capacity. So does Coordinated Beamforming. It is applied with $L_1 = L_2 = 1$ when $N = 2$, $L_1 = 1$ and $L_2 = 2$ when $N = 3$, and $L_1 = L_2 = 2$ when $N = 4$. Both schemes outperform the strategies involving transmitting to a single-user. They also achieve a larger spectral efficiency than obtained using receiver processing only.

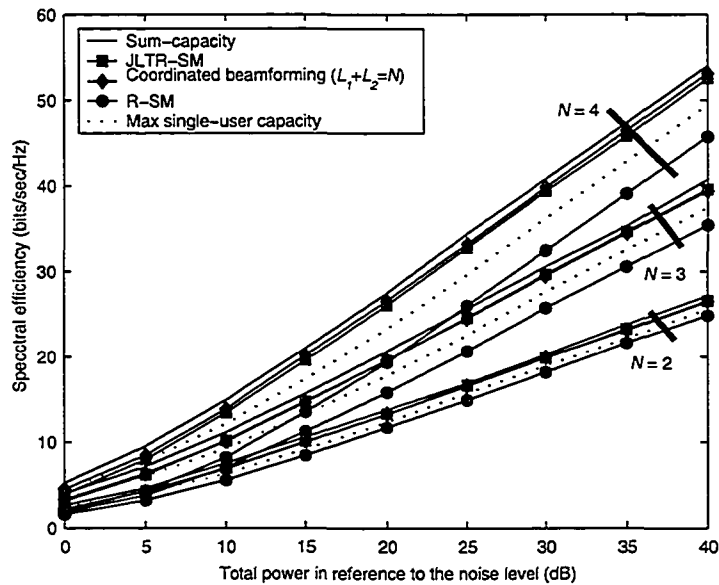


Figure 4-14 Average spectral efficiency on the $(N,N,2)$ BC as a function of the total transmit power in reference to the noise level.

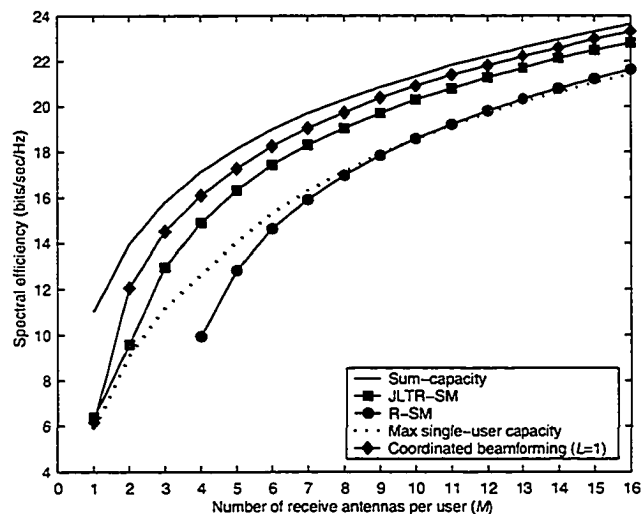


Figure 4-15 Average spectral efficiency on the $(4, M, 4)$ BC as a function of the number of receive antennas M per user. The total power in reference to the noise level is 10 dB.

Figure 4-15 shows the average spectral efficiency as a function of the number of receive antennas per user with a fixed number of transmit antennas and a fixed number of users. We set $L_1 = L_2 = 1$ for Coordinated Beamforming. By transmitting to four users simultaneously, Coordinated Beamforming outperforms JLTR-SM, which is constrained to transmitting to two users only.

Figure 4-16 shows the average spectral efficiency as a function of the total power in reference to the noise level when the total number of receive antennas is equal to the number of transmit antennas. Both JLTR-SM and Coordinated Beamforming with $L_1 = L_2 = 2$ achieve the same slope as the sum-capacity even though each user is equipped with only 2 receive antennas. Linear spatial multiplexing schemes of Table 4.1 with the constraint that $M_k \geq L_k + 1$ and $\sum_{k=1}^{K_u} L_k \leq N$ cannot achieve this spatial multiplexing gain. However Coordinated Beamforming outperforms JLTR-SM in all cases.

In summary, JLTR-SM incurs a power loss by zero-forcing joint-orthogonalization of the channels between the two users, whereas Coordinated Beamforming attempts to orthogonalize the layers sent to possibly more than two users. However Coordinated Beamforming offers more degrees of freedom in the allocation of the number of layers to different users, so it can take better advantage of multiuser diversity in order to mitigate the power loss due to zero-forcing.

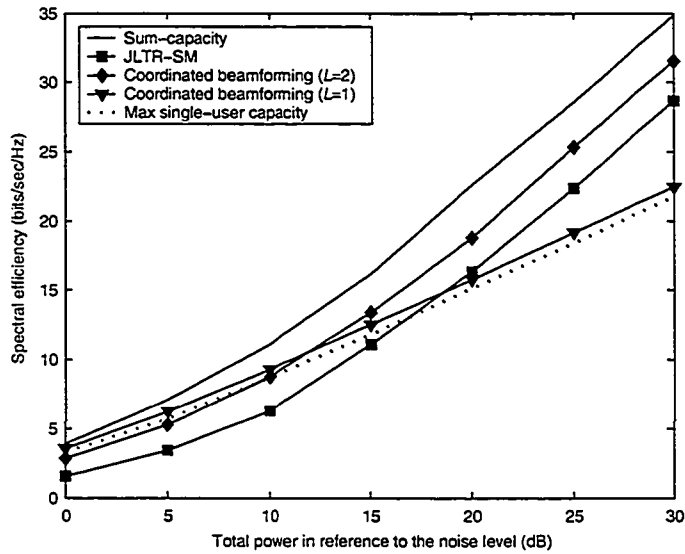


Figure 4-16 Average spectral efficiency on the (4,2,2) BC as a function of the total power in reference to the noise level.

4.4 Proportionally-Fair Scheduling Algorithm

4.4.1 Introduction and Definition

Scheduling algorithms that emphasize throughput maximization often result in some users being denied service because they experience bad channel conditions for a long time. This is particularly true for users that are located far from the base station. The unpredictability of the fading process in the long term renders the scheduling problem difficult. Contrary to maximum throughput with capacity-achieving codes where an optimal solution was found for each fading state independently, scheduling algorithms that provide fairness among users in terms of throughput must continually adapt their strategy based on the knowledge of the fading statistics and on the prediction of the fading states on at most a few subsequent time slots. We do not concern ourselves with channel prediction but we assume as before that the scheduler knows the next fading state, and that capacity-achieving codes can be used such that the decision made by the scheduler can always be achieved without error. Our goal is to show simple but important consequences of using multiple antennas with proportionally-fair scheduling algorithms.

In order to provide fairness among users in terms of throughput, we adopt the proportionally fair criterion described in [33], which is an extension of the proportionally fair criterion to the case of simultaneous transmission to several users. The priority weight for the k -th user is defined as $\mu_k = 1/\bar{R}_k$ where \bar{R}_k is the average throughput received by user k over a

window of past time slots. The choice of the user set in the proportionally fair sense is achieved by maximizing the weighted sum-rate criterion:

$$\max \sum_{k=1}^K \mu_k R_k, \quad (4.41)$$

where the maximum is over all rate vectors (R_1, \dots, R_K) achievable with a given transmission scheme in a given time slot. The authors in [33] proposed a numerical optimization procedure to achieve the maximum weighted sum-rate and to select a rate vector that achieves the maximum weighted sum-rate at a corner point in the dirty-paper coding region, although it is not uniquely determined. With this algorithm, more than N users can be scheduled at a time and dirty-paper coding must be used. If a linear spatial multiplexing scheme is used then this criterion is used to jointly select N users.

The average throughput at time t for user k is computed as:

$$\bar{R}_k(t) = \delta \bar{R}_k(t-1) + (1-\delta) R_k(t) \text{ if user } k \text{ is active,} \quad (4.42)$$

$$\bar{R}_k(t) = \delta \bar{R}_k(t-1) \text{ otherwise,} \quad (4.43)$$

with a forgetting factor δ . The forgetting factor is related to a sliding window over which averaging of the past throughput and the current throughput of user k is done. If we let t_c denote the length of the window in slots, then

$$\delta = 1 - \frac{1}{t_c} \quad (4.44)$$

and (4.42) becomes

$$\bar{R}_k(t) = \frac{1}{t_c} \left[(t_c - 1) \bar{R}_k(t-1) + R_k(t) \right] \quad (4.45)$$

We assume that a time slot is long enough so that capacity-achieving codes can be used, so that every packet can be decoded without an error after its first transmission.

4.4.2 Channel Model

The channel model is slightly modified in the following way to take into account shadow fading and path loss. We adopted the guidelines for the evaluation of radio transmission technologies for IMT-2000 [71]. The path loss model for the vehicular test environment in urban and suburban areas is:

$$L = 40 \left(1 - 4 \times 10^{-3} \Delta h_b \right) \log_{10} R - 18 \log_{10} \Delta h_b + 21 \log_{10} f + 80, \quad (4.46)$$

where R is the distance in kilometres between the base station and the mobile station, f is the carrier frequency of 2000 MHz, and $\Delta h_b = 15$ is the base station antenna height in meters,

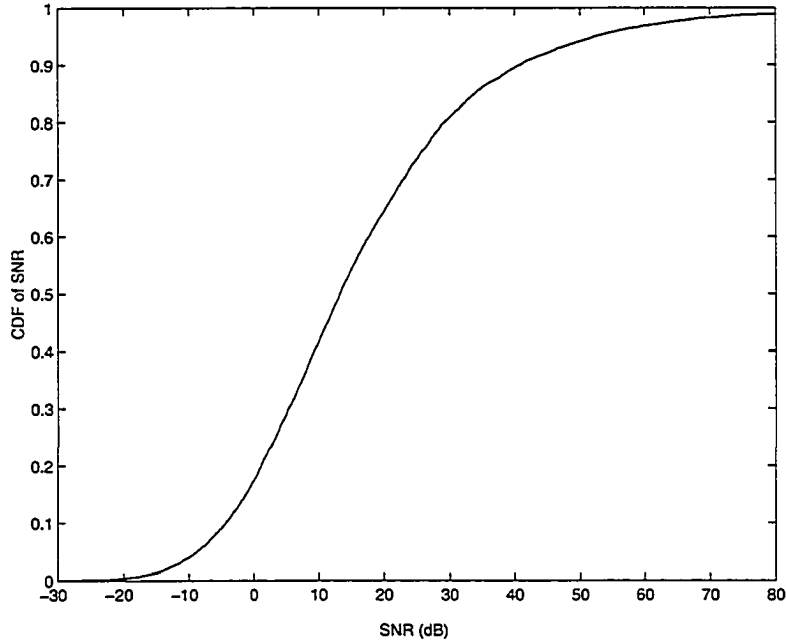


Figure 4-17 CDF of average SNR with path loss and shadow fading.

measured from the average rooftop level. The mean SNR 1 km away from the base station is set to zero. The log-normal shadow fading around the mean path loss in the logarithmic scale is modelled by a Gaussian random variable S with zero mean and standard deviation of 10 dB. The positions of the users in the cell are simulated by generating R as a uniform random variable in the interval $[0, 1]$.

The narrowband channel is assumed to remain constant during a time slot, and to change randomly from slot to slot. The channel between the base station and user k is described by a vector $\mathbf{h}_k = \beta_k \tilde{\mathbf{h}}_k$ of size M_k by N . Path loss and shadow fading as defined above are described by β_k . The elements of $\tilde{\mathbf{h}}_k$ represent small-scale fading and they are modeled as i.i.d. complex Gaussian random variables with zero mean and unit variance. The average SNR is defined as follows. The coefficients β_k are assumed to remain constant during several time slots. The time during which the coefficients β_k remain constant is assumed to be long enough to observe a large number of states of the small-scale fading process $\tilde{\mathbf{h}}_k$, and short enough in comparison with the delay requirements of the application targeted by the mobile user. The average SNR of user k during these time slots is defined as:

$$\rho_k = \beta_k^2 / \sigma^2, \quad (4.47)$$

where σ^2 is the variance of the AWGN at each receive antenna, and we assume it is the same for

all users. The distribution of the SNR averaged over small-scale Rayleigh fading is shown in Figure 4-17. The coefficients β_k then change randomly in the next time slot for every user, as if they were instantaneously and randomly changing location in the cell sector served by the base station.

4.4.3 Scheduling Algorithms for Linear Spatial Multiplexing Schemes

Given two users in a given time slot, given a channel partition and a power allocation, JLTR-SM is used to transmit to these two users simultaneously. In general if we are not interested only in throughput maximization, user 1 will be allocated N_1 channels with indices in the set S_1 and user 2 will be allocated N_2 channels with indices in the set S_2 . The two sets will not have common elements, and $N_1 + N_2 = N$. The two users will thus achieve rates R_1 and R_2 :

$$\begin{aligned} R_1 &= \sum_{n \in S_1} \log \left(1 + b_n a_n \frac{\omega_{1n}^2}{\sigma_1^2} \right) \\ R_2 &= \sum_{n \in S_2} \log \left(1 + b_n a_n \frac{\omega_{2n}^2}{\sigma_2^2} \right). \end{aligned} \quad (4.48)$$

The power allocation a_1, \dots, a_N is performed according to a weighted sum-rate maximization criterion with weights μ_1 and μ_2 :

$$\max_{a_n, 1 \leq n \leq N} \mu_1 R_1 + \mu_2 R_2 \quad (4.49)$$

$$\text{Subject to } \sum_{n=1}^N a_n = P \text{ and } a_n \geq 0, n = 1, \dots, N.$$

We consider five different transmission schemes:

- Single-user: given a single user in a given time slot, single-user transmission involves transmitting with capacity achieving codes such that the achieved rate is equal to the user's closed-loop MIMO channel capacity.
- JLTR-SM: given two users in a given time slot, given a channel partition and a power allocation, JLTR-SM is used to transmit to these two users simultaneously with the rates given by (4.48).
- Equipartition JLTR-SM (EP-JLTR-SM): With this equipartition variation of JLTR-SM, given two users in a given time slot, each user is allocated its $N/2$ strongest channels, or its M_k non-zero channels if $M_k < N/2$, according to (4.22). We choose to split the power equally between the two users. Each of the two users then performs waterfilling power

allocation and rate adaptation on its allocated channels. Thus the rates R_1 and R_2 are completely determined given a two-user set.

- Coordinated Beamforming: orthogonal channels are created, thus each user sees no interference from all other users, whereas JLTR-SM created parallel channels. Thus only power allocation is needed with Coordinated Beamforming, but no partition of the channels. In this paper $L_k = 1$ for each of the $K_a = N$ active users unless otherwise specified.
- Equipartition Coordinated Beamforming (EP-CB): given N users in a given time slot with $L_k = 1$ for each user, the power is uniformly allocated among the users, and the rate vector is completely determined.

We next describe the three types of scheduling algorithms considered in this section.

Single-User Weighted-Rates Scheduling algorithm (SUWR- K_a):

The SUWR- K_a Scheduling algorithm selects the K_a active users with the largest weighted rates R_k / \bar{R}_k , where R_k is the closed-loop capacity of users k . SUWR- K_a was proposed in [33]. One disadvantage of this strategy is that the active users are not jointly chosen so their achievable rates with a given transmission scheme and $K_a - 1$ other active users might be quite different than their individual closed-loop capacities. When this scheduling algorithm is used with JLTR-SM or with Coordinated Beamforming, we perform further maximization of the weighted sum-rate of (4.41) over all channel partitions and power allocations for JLTR-SM, or over all power allocations for Coordinated Beamforming. No such optimization is needed with Equipartition JLTR-SM and Equipartition Coordinated Beamforming.

Full-search proportionally fair scheduling algorithm (FSPF):

The weighted sum-rate criterion (4.41) is used to select the K_a active users by maximizing $\sum_{k=1}^K \mu_k R_k$ over all rates (R_1, \dots, R_K) jointly achievable with a given transmission scheme. This always involves a search though all sets of K_a users among K , where $K_a = 2$ for JLTR-SM and $K_a = N$ for Coordinated Beamforming. In every user set the weighted sum-rate is further maximized over all channel partitions and power allocations for JLTR-SM, or over all power allocations for Coordinated Beamforming, but no such further maximization is needed with Equipartition JLTR-SM and Equipartition Coordinated Beamforming. Searching over all

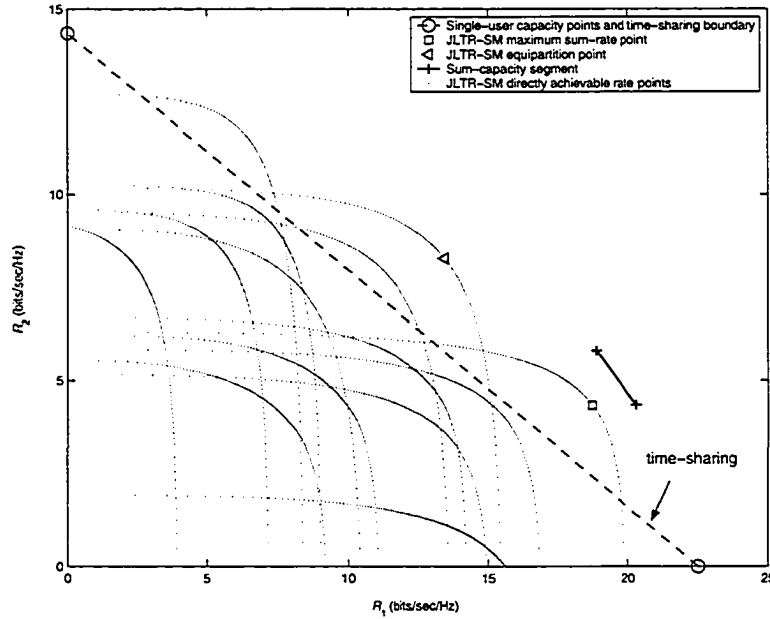


Figure 4-18 Rate region of Coordinated Beamforming and JLTR-SM for one realization of the (4,4,2) MIMO BC.

sets of K_a users among K can incur a large computational complexity.

Round-Robin scheduling algorithm (RR):

For the sake of comparison we consider Round-Robin scheduling where N users are scheduled at a time in a cyclic manner among all K users. The FSPF scheduling algorithm is performed among the N scheduled users on each time slot to adjust the rate and power allocation with a given transmission scheme. So transmission is fair in terms of throughput among the N scheduled users on each time slot, but it is not fair from one time slot to the next. However it is fair in terms of delay as every user experiences the same delay.

Achievable rate regions

In order to illustrate the equipartition strategy and the achievable rates with the proposed linear processing schemes on a given channel we show the rate region for one realization of the (4,4,2) MIMO BC in Figure 4-18. We need to restrict ourselves to the 2-user channel in order to visualize the capacity region. Each dotted curve represents the directly achievable rates with JLTR-SM for a given partition of the parallel channels between the two users. Each dot represents a different power allocation between the two users. We did not take the convex hull operation so the rates achievable by time-sharing are not shown. The maximum achievable sum-rate with JLTR-SM is also shown, as well as the maximum rate with equipartition of layers and power

between the two users. Forcing the equipartition of the channels and the power between the two users incurs some loss in spectral efficiency compared to the maximum sum-rate point. However it provides both users with a good fraction of their maximum achievable rates in a fashion that provides more fairness than at the maximum sum-rate. We also see that it provides a sum-rate larger than the maximum single-user achievable rates.

The next example shows one realization of the (2,2,2) MIMO BC. It illustrates the sub-optimality of JLTR-SM and Coordinated Beamforming in some situations. Each user is allocated one layer for both schemes. On the (2,2,2) MIMO BC, both schemes achieve approximately the same performance in terms of maximum sum-rate and rate region boundary. We see in Figure 4-19 that both schemes cannot provide a maximum sum-rate larger than the largest single-user closed-loop capacity and the rate regions of JLTR-SM and Coordinated Beamforming lie below the time-sharing region with single-user transmission. Both schemes could achieve a maximum sum-rate larger than both single-user closed-loop capacities for other realizations of the (2,2,2) MIMO BC.

We only showed one possible assignment of the layers to the active users for Coordinated Beamforming. If all layers were allocated to only one user then the closed-loop capacity for that user would be achievable with Coordinated Beamforming. Thus, by allowing every possible layer allocation between the users, one could always ensure performance at least as good as the best single-user closed-loop capacity, at the price of an increase in complexity. For every possible

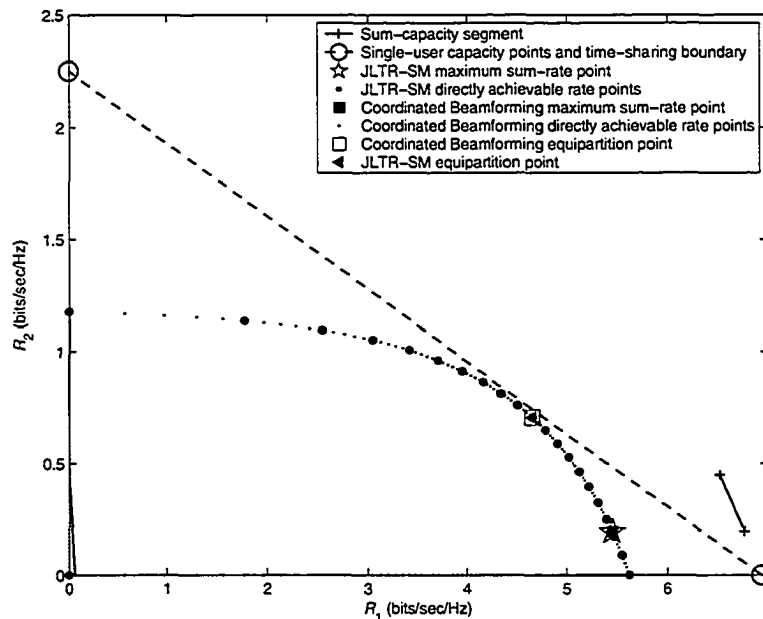


Figure 4-19 Rate region of Coordinated Beamforming and JLTR-SM for one realization of the (2,2,2) MIMO BC.

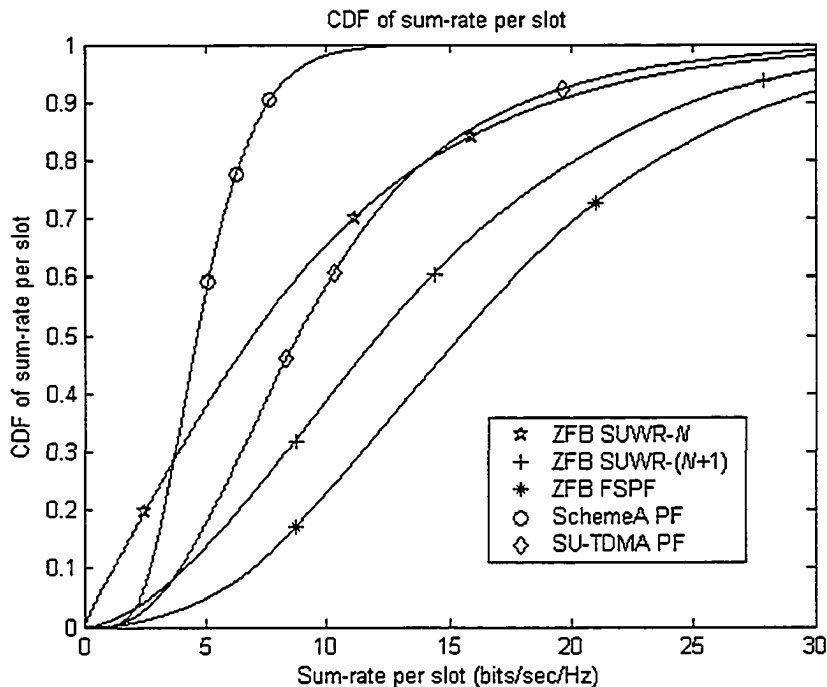


Figure 4-20 CDF of sum-rate per slot on the (2,1,6) MIMO BC. The same legend is used for all simulations for the $(N,1,K)$ MIMO BC in the following three figures.

layer allocation, all transmit and receive filters have to be recomputed for a given set of active users. For JLTR-SM, once the user set is chosen the GSVD gives the transmit and receive filters and the layer allocation is independent of these. However by allocating all the layers to only one user with JLTR-SM we still need to invert the matrix X^* , which incurs a power loss at the transmitter and does not allow to achieve the single-user closed-loop capacity.

4.4.4 Simulation Results

In our simulations, we kept the shadow fading and path loss constant (also defined as the average SNR in (4.47)) for 100 time slots for each user. Then the SNR changes randomly and stays constant for the next 100 time slots. A total of 10^5 time slots are simulated. The forgetting factor is set at $\delta = 0.99$ according to (4.44), so the averaging of past throughput and current throughput is done over a sliding window of length 100 slots. The average user rate is updated according to (4.42) and (4.43). We define the delay experienced by a user as the number of time slots between two consecutive transmissions to that user. We assume that a time slot is long enough so that capacity-achieving codes can be used so that every packet can be decoded without error after its first transmission.

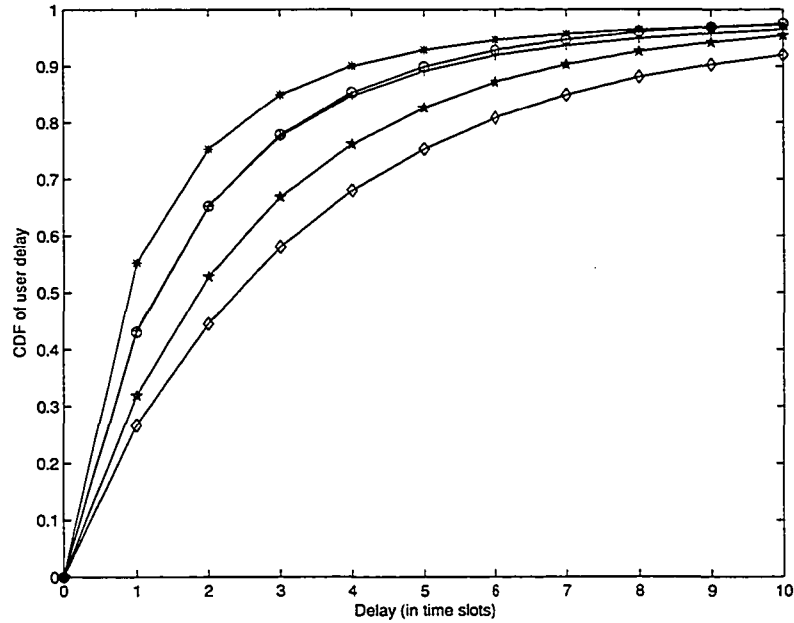


Figure 4-21 CDF of user delay on the (2,1,6) MIMO BC.

We first show simulation results for the (2,1,6) MIMO BC. Scheduling algorithm A can be extended in a straightforward way to perform proportionally fair scheduling. We only need to modify the matrix \mathbf{R} defined in (4.11) to have elements $r_{k,n} = \log(1 + SINR_n^{(k)}) / \bar{R}_k$. Thus in this case the FSPF scheduling algorithm has the same low complexity provided by Scheduling Algorithm A. Figure 4-20 shows the CDF of the sum-rate per slot for several transmission schemes and scheduling algorithms. All scheduling algorithms considered here are based on a proportionally-fair criterion. Zero-forcing beamforming with the FSPF algorithm offers the largest throughput. ZFB with SUWR-($N+1$) Scheduling performs second best, although it already suffers a considerable loss in throughput. ZFB with SUWR- N Scheduling does not beat the single-user TDMA performance. Scheme A provides the smallest throughput but it only relies on partial CQI and no CSIT. Its interference-limited nature does not allow it to achieve high rates. The CDF of the average delay per user is shown in Figure 4-21. Here again ZFB with FSPF scheduling offers the smallest delay per user as well as the steepest CDF, which confirms its proportionally-fair nature. Single-user TDMA yields the largest delay per user since it can only transmit to one user at a time. ZFB and Scheme A take advantage of the multiple antennas to decrease the average delay per user.

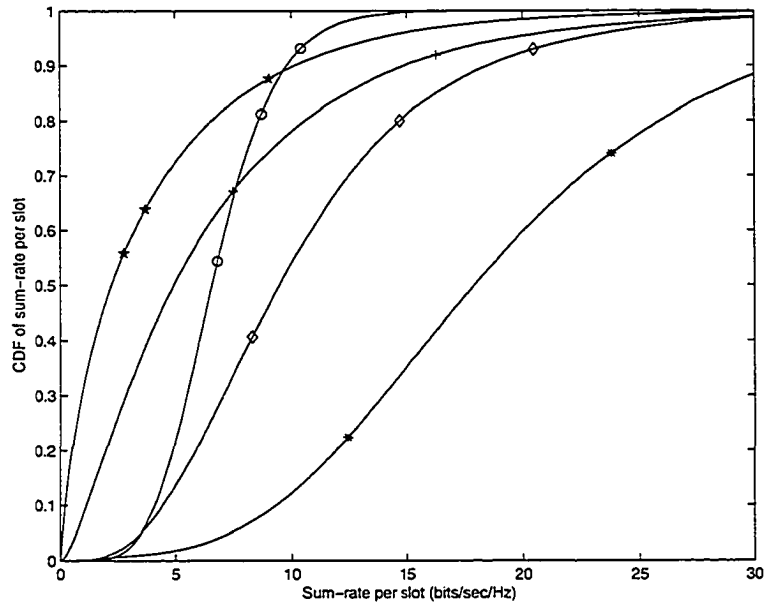


Figure 4-22 CDF of sum-rate per slot on the (2,1,16) MIMO BC.

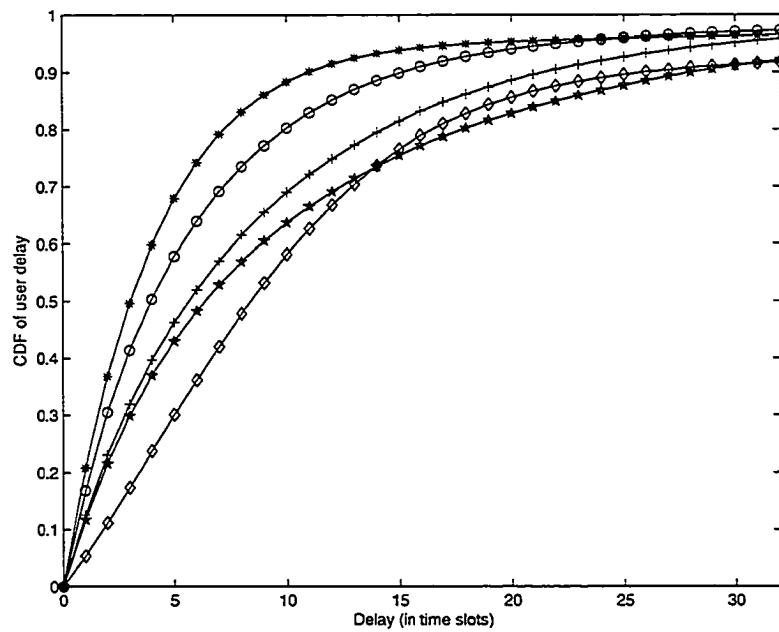


Figure 4-23 CDF of user delay on the (2,1,16) MIMO BC

We now increase the total number of users to 16. The CDF of the sum-rate per slot and the CDF of the average delay per user are shown respectively on Figure 4-22 and Figure 4-23. The relative performances of ZFB with FSPF scheduling, Single-User TDMA and Scheme A remain the same. However we notice the degradation in throughput and delay of ZFB with SUWR- $(N+1)$ and SUWR- N Scheduling. ZFB does not provide a strong enough mechanism to compensate for the disjoint scheduling of the N users in each time slot, whereas ZFB with FSPF schedules N users that jointly offer a large throughput and takes into consideration proportional fairness. FSPF scheduling also has the largest computational complexity. SUWR Scheduling does not appear to be suitable with ZFB when the number of users is large. More efficient low-complexity algorithms based on the proportionally-fair criterion would be needed on the $(N,1,K)$ MIMO BC with ZFB.

We now turn our attention to the case where every user is equipped with multiple receive antennas. We consider the $(4,4,20)$ MIMO BC. Figure 4-24 shows the CDF of the sum-rate per slot, while Figure 4-25 shows the CDF of the user delay, while the legend is given in Figure 4-26. Coordinated Beamforming is such that four users are scheduled in each time slot, and each one of them is allocated one layer. We can easily distinguish four classes of curves. The first class corresponds to Coordinated Beamforming, which provides the largest average throughput. Within this class, the largest average throughput is obtained with SUWR- N Scheduling, followed by Equipartition Coordinated Beamforming with SUWR- N Scheduling. JLTR-SM provides the second set of curves, among which the largest average throughput is provided with FSPF scheduling, followed by SUWR- N Scheduling. JLTR-SM provides a large sum-rate per slot with a higher probability than Coordinated Beamforming. Single-User TDMA provides a considerably lower average throughput than both Coordinated Beamforming and JLTR-SM, although it achieves larger rates with a higher probability. JLTR-SM with Round-Robin scheduling is unable to take advantage of multiuser diversity and thus performs poorly. In terms of user delay, the same classes of curves appear. Due to the fact that four users are scheduled simultaneously with Coordinated Beamforming, it offers the smallest average delay per user. It is however possible that one or more of the four simultaneously scheduled users is allocated a very small or a zero rate after the optimization of the power allocation at the transmitter. However it is apparently less likely to happen with SUWR- N Scheduling since it achieves a smaller delay than with FSPF scheduling. It cannot happen with the Equipartition Coordinated Beamforming since all four users are allocated one-fourth of the total transmit power in this case. The same remark applies for JLTR-SM where FSPF scheduling provides a larger user delay than SUWR- N Scheduling

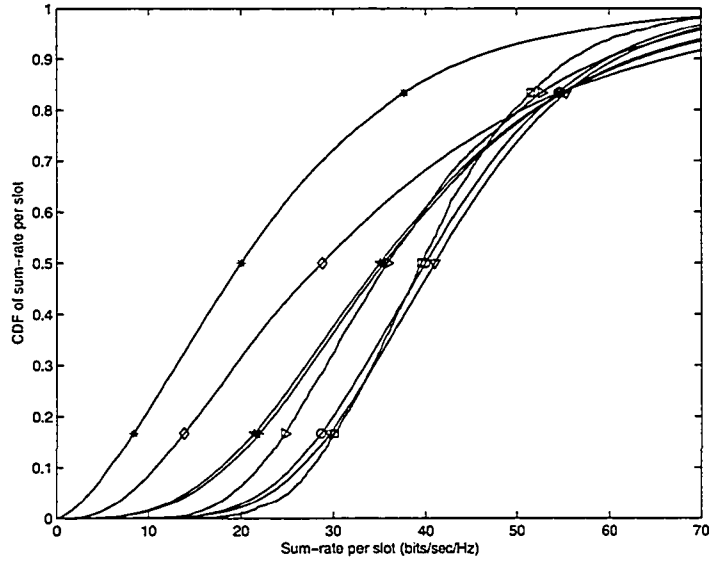


Figure 4-24 CDF of sum-rate per slot on the (4,4,20) MIMO BC.

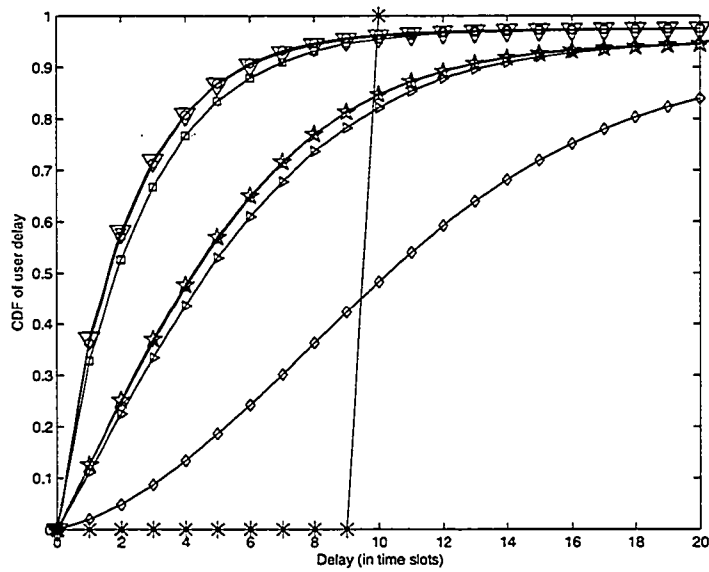


Figure 4-25 CDF of user delay on the (4,4,20) MIMO BC

—▷	JLTRSM FS PF	—□	CB FS PF
—+	JLTRSM SUWR- N	—▽	CB SUWR- N
—*	EP-JLTRSM SUWR- N	—○	EP CB SUWR- N
—*	JLTRSM RR	—◇	SU TDMA PF

Figure 4-26 Legend of simulations for the (N,N,K) MIMO BC.

with or without the Equipartition JLTR-SM. JLTR-SM schedules a maximum of two users simultaneously thus it offers a larger user delay than Coordinated Beamforming, but a smaller user delay than Single-User TDMA. Round-Robin Scheduling offers a constant delay of 10 time slots at the expense of the throughput. The fact that the CDF is not totally vertical comes from boundary effects in the computation of the delay. We also noticed that as the total number of users increases these four classes of curves tend to become more pronounced. On the (N,N,K) MIMO BC, a low-complexity scheduling algorithm such as SUWR- N where the users are chosen separately can perform close to the optimal proportionally-fair scheduling algorithm, although it was not the case when users were equipped with a single receive antenna. This is due to the property of the transmission schemes, such as Coordinated Beamforming and JLTR-SM, that allows to orthogonalize the channels among the scheduled users even though they are chosen separately. We also saw that SUWR- N Scheduling also offers advantages in terms of user delay. Equipartition Coordinated Beamforming and JLTR-SM allowed to achieve approximately the same performance as the optimal power allocation with a further complexity reduction. Thus reduced complexity transmission schemes and scheduling algorithms seem to be more easily accommodated when users are equipped with multiple receive antennas by taking advantage of the properties of the transmit and receive filters that perform joint orthogonalization.

4.5 Summary and Conclusions

In this chapter, we first studied maximum-throughput scheduling algorithms on the $(N,1,K)$ MIMO broadcast channel while allowing the use of dirty-paper coding at the transmitter. We justified our proposals in the high power region of the MIMO broadcast channel, and showed that the problem of scheduling N users at a time is similar to the problem of receive antenna selection with the goals that the capacity of the reduced channel be as close as possible to the capacity of the original channel. We proposed a heuristic low-complexity scheduling algorithm called Successive Projections Scheduling and compared its performance to the optimal N -user scheduling algorithm and to receive antenna selection algorithms proposed in the literature. We then applied these scheduling algorithms to the sub-optimal transmission scheme based on transmitter channel inversion, called zero-forcing beamforming. We showed that differences arise in the relative performance of these scheduling algorithms if a scheme other than dirty-paper coding is used. We also proposed an interference-avoidance transmission scheme applicable with partial CQI at the transmitter and no CSIT. We were able to show that this scheme can achieve spatial multiplexing gain, although it requires that the number of users be very large relative to the number of transmit antennas.

On the (N, M, K) MIMO broadcast channel, we proposed a novel joint transmit and receive linear spatial multiplexing scheme, which is applicable with any number of transmit and receive antennas and allows to jointly transmitting to two users simultaneously. We compared the performance of our scheme with the recently proposed Coordinated Beamforming scheme. Coordinated Beamforming performs approximately the same as JLTR-SM when the transmitter is equipped with two antennas, and it outperforms JLTR-SM when more than two antennas are present at the transmitter. Coordinated Beamforming offers more degrees of freedom in the allocation of layers to the users.

We then conducted some simple simulations to study the effect of using multiple antennas on the performance of proportionally-fair scheduling algorithms. We noticed that the impact of multiple antennas is more pronounced in the delay domain than in the throughput domain. By taking advantage of the spatial multiplexing gain to schedule several users simultaneously in each time slot, we were able to significantly decrease the delay per user in comparison to scheduling one user at a time. The throughput also increases by scheduling several users at a time, as a consequence of the properties of the sum-capacity of the MIMO broadcast channel. We also showed that low-complexity scheduling algorithms benefit from the presence of multiple antennas at the receivers, since the burden of providing a jointly good channel to the simultaneously scheduled users can rest on the transmission scheme rather than on the scheduling algorithm. If users are equipped with a single receive antenna, the considered reduced-complexity scheduling algorithms performed poorly, especially as the total number of users became large. We also proposed to reduce the complexity of the transmission scheme itself by enforcing transmission to a constant number of users with the Equipartition strategy. We only observed a small loss in throughput, as the dynamics of the scheduling algorithm are able to compensate for the equipartition enforcement in the long run. Nevertheless, a more thorough study of the impact of multiple antennas with proportionally-fair scheduling algorithms would be needed as we only conducted simple experiments and we did not consider transmission errors and strategies to cope with them, e.g. ARQ, which would have a great impact.

5 Conclusion

5.1 Summary and Conclusions

This thesis has investigated the problem of enabling high transmission rates on multiuser wireless fading channels with the use of multiple antennas at the transmitter and possibly at the receiver side. Our approach follows the recent trends in the research field, and builds on recent advances in information theory, as well as from the ongoing effort by the industry to provide customers worldwide with increasing transmission rates and quality of service that lead to new paradigms in system design. Our focus has been on packet-data access with scheduling algorithms and rate adaptation.

We began our presentation with background knowledge on multiple antenna channels, multiuser channels, and the state-of-the art in multiuser multiple antenna channels. The earliest attempts at exploiting multiuser diversity along with spatial diversity were first reviewed. It was pointed out that a lot of care must be taken in order not to approach spatial diversity in a way that would impair the benefits provided by multiuser diversity. We illustrated this fact with simple dual antenna systems and pointed out what factors are critical in order to allow multiuser and spatial diversities to benefit from each other, namely the amount of channel state information at the transmitter, and the amount of channel state information carried by the channel quality indicator provided by each user to the base station. We briefly noted that the use of multiple antennas at the receiver alone could benefit from antenna correlations. It was known that correlations can be beneficial among transmit antennas with opportunistic beamforming [24], but to the best of the author's knowledge it has not been mentioned in the case of correlated multiple receive antennas. We concluded the introduction chapter with a discussion of the latest advances in MIMO broadcast channel capacity region and sum-capacity with complete channel state information at the transmitter and at the receivers. We introduced the concept of dirty-paper coding and the duality between the power-constrained MIMO broadcast channel and the dual sum-power constrained MIMO multiple-access channel.

Chapter III was dedicated to the study of the optimal number of active users and the optimal power allocation required to achieve the sum-capacity of the MIMO broadcast channel. Our attention was first focused on the $(2,1,K)$ MIMO broadcast channel. The solution to our problem was studied in the dual multiple-access domain. We were able to analytically characterize the exact number of active users at the sum-capacity for a given channel realization and a given power constraint. Our results show that the optimal number of active users is highly dependent on both the channel matrix structure and the power constraint. We completely

characterized the optimal solution on the (2,1,3) MIMO broadcast channel with a geometric approach. We were able to prove that the number of active users can be a non-monotonic function of the total transmit power for some channel realizations, due to the spatial structure of the interference among the three users served by the transmitter. It was also shown that the optimal number of active users can be larger than the number of transmit antennas in the high power region for some channel realizations, although the maximum spatial multiplexing gain cannot be larger than the number of transmit antennas.

We then turned our attention back to the MIMO broadcast channel by exploiting the MAC to BC transformations of the optimal covariance matrices. The $(N,1,K)$ MIMO broadcast channel with $K \geq N$ was studied first. We provided an asymptotic analysis of the power allocated to each of the active users in the limit where the total transmit power increases to very large values. We were able to prove that only N users are allocated a non-vanishing fraction of the total transmit power in the high power region, and the other active users are only able to achieve a constant rate as the power grows to infinity. As a first-order approximation, the optimal covariance matrices of these N users along with dirty-paper coding completely orthogonalize the channels among themselves. The first-order approximation of the optimal covariance matrices shows that each of the N users beamforming vectors can be obtained by a QR decomposition of the channel matrix between the N transmit antennas and these N users. As a consequence of the waterfilling solution, the optimal power allocation was shown to be uniform among the N users in the high power region. This result is valid for any value of N , although it was only previously known for $N = 2$ and very large values of N . We were able to derive a first-order closed-form approximation to the high power sum-capacity of the $(N,1,K)$ MIMO broadcast channel.

We then studied the high power region asymptotic power allocation on the (N,N,K) MIMO broadcast channel. The MAC to BC transformations of the optimal transmit covariance matrices were the useful tool once more. We were able to prove by a similar argument as the one used for the $(N,1,K)$ MIMO broadcast channel that on the (N,N,K) MIMO broadcast channel only one user is allocated a non-vanishing fraction of the total transmit power as it goes to infinity, and the other users are only able to achieve a constant rate. Extensive numerical examples were provided to illustrate this phenomenon. These examples allowed us to interpret the results and observe the medium power region. It was pointed out that the high power region asymptotic regime only starts to appear at very large values of the total transmit power in a lot of cases, so the medium power region is often of greater interest in realistic environments. In particular, it was observed that if users are equipped with multiple receive antennas, in the medium power region several users will be allocated a large fraction of the total power on one or more of their spatial

dimensions. Finally, we pointed out the specific roles played by dirty-paper coding and spatial processing.

Chapter IV was dedicated to scheduling algorithms. We based our approach on the results obtained in Chapter III with the goal of maximizing the throughput. We concluded that scheduling N users at a time should be a good choice for scheduling, as no more than N users are allocated a non-vanishing fraction of the total transmit power in the high power region. Thus allocating power to no more than N active users should be sufficient to achieve the maximum spatial multiplexing gain offered by the multiple antennas. No fewer than N users are also required for that purpose as the maximum spatial multiplexing gain is determined by the number of transmit antennas provided that there is a large number of users to be served by the base station. Simulation results confirmed our predictions. The goal of scheduling N users at a time was also justified by a complexity argument, as it should be easier to handle simultaneous transmission to a limited number of users. Another argument in favour of scheduling N users at a time came from the envisaged use of sub-optimal transmission schemes whenever dirty-paper coding is not feasible for implementation issues. Sub-optimal linear spatial multiplexing schemes that aim at orthogonalizing the channel impose a constraint on the maximum number of users that can be simultaneously served. This number is limited by the number of base station antennas. Thus N -user scheduling algorithms are required for such schemes, and they must perform well from a capacity point-of-view in order to limit the loss of spectral efficiency. We first focused on the case where the users are equipped with a single receive antenna. The problem of optimal N -user scheduling for maximum throughput with dirty-paper coding was related to the problem of receive antenna selection by a large power argument based on our analysis of Chapter III. We also proposed a heuristic low-complexity N -user scheduling algorithm based on interference-avoidance principles. Simulations showed that recently proposed receive antenna selection algorithms are very efficient and more effective than our proposed low-complexity scheduling algorithm with the use of dirty-paper coding. We also conducted simulations to study the performance of these scheduling algorithms in the medium power region.

We then applied the previous N -user scheduling algorithms for maximum-throughput to sub-optimal linear spatial multiplexing schemes. We observed a change in the relative performance of the scheduling algorithms based on receive antenna selection algorithms. This observation justifies the specific design of N -user scheduling algorithms for a given transmission scheme, as a specific transmission scheme might not exploit the spatial structure the same way a capacity-achieving scheme does. We also proposed an interference-avoidance transmission scheme applicable with only partial channel quality indicator at the base station in the form of a

signal-to-interference and noise ratio feedback from each user. Simulations showed that this scheme can effectively exploit spatial multiplexing provided that the number of users is very large relative to the number of transmit antennas. It was also shown that this scheme is interference-limited in the high power region. We proposed a modified version of this scheme that copes with the interference limitation by adaptively choosing the number of active users, which is not anymore constrained to be equal to the number of transmit antennas on each time slot. We pointed out the relation of our proposed scheme to simultaneous opportunistic beamforming in the case of slow fading channels.

We then shifted our focus to the case where both the base station and the users are equipped with multiple antennas. We first reviewed previously proposed spatial multiplexing schemes and pointed out some of the constraints imposed by these schemes. We then proposed a spatial multiplexing scheme, called Joint Linear Transmit Receive Spatial Multiplexing (JLTR-SM), which is applicable with any number of transmit and receive antennas, and which allows to simultaneously transmit to two users. We proposed an optimized solution with respect to the layer and power allocation. We analytically studied the high power growth rate and scaling factor of the sum-rate provided by this scheme, and we showed that it is able to approach the maximum spatial multiplexing gain in the case of two transmit antennas. We compared our scheme with the simultaneously proposed Coordinated Beamforming algorithm, and found that both schemes perform approximately the same in the case of two transmit antennas, but Coordinated Beamforming outperforms JLTR-SM with more than two transmit antennas, as it is able to transmit to more than two users simultaneously.

We finally provided simple simulations for proportionally-fair scheduling algorithms, with the goal of studying basic impacts of using multiple antennas on throughput and delay when the context is not only to maximize the total throughput. We reviewed the optimal proportionally-fair scheduling algorithm for simultaneous transmission to several users in each time slot, as well as some reduced-complexity scheduling algorithms that choose the scheduled users separately instead of jointly as the optimal solution dictates. We first proposed further complexity reduction of the power and layer allocation based on the observation of the rate region of JLTR-SM and Coordinated Beamforming. Our approach was to provide fairness among the users not only through the scheduling algorithm but also through the specific spatial processing performed at the transmitter. This approach was justified by the complex interaction between the transmission scheme and the dynamics of proportionally-fair scheduling algorithms, through the intuition that complexity-reduction can be achieved by relaxing the optimality of the scheduling algorithm and the power allocation without a significant loss in performance. Simulation results confirmed our

predictions, as reduced-complexity schemes often suffered a small performance loss in either throughput or delay as compared to the high-complexity optimal proportionally-fair scheduling solution. In fact, the complexity reductions often resulted in improved performance in either throughput or delay, illustrating the fuzziness of the concept of optimality without clearly defined quality of service constraints (not considered here as they are out of the scope of this thesis). The only scenario where reduced-complexity scheduling solutions incurred a significant decrease in performance was in the case of single-receive antenna users. In this scenario, the spatial multiplexing schemes considered could only rely on transmit array processing and thus are not powerful enough to cope with the interference caused by scheduling users separately.

5.2 Contributions and Future Work

Our contributions can be briefly summarized as follows. Our analysis of the sum-capacity of the MIMO broadcast channel extended the recent information-theoretic results in this domain. We studied more specifically the optimal power allocation and the optimal number of active users in the high power region. We demonstrated up till now unknown properties of the optimal number of active users and the optimal power allocation in the specific context of the MIMO broadcast channel. In some situations, our analysis allowed us to obtain a closed-form expression for the sum-capacity of the $(N,1,K)$ MIMO broadcast channel, or a closed-form expression of a first-order approximation of the sum-capacity of the $(N,1,N)$ MIMO broadcast channel. We also provided links to other related areas of research, namely receive antenna selection problems. We pointed out the similarities and differences of these problems with our problem. Our study of N -user scheduling algorithms for maximum-throughput provided an original analysis of the problem, and effective solutions were proposed and analyzed with dirty-paper coding and sub-optimal linear spatial multiplexing schemes. An original interference-avoidance scheme was also proposed for the case of partial channel quality indicator feedback to the base station. Simultaneously proposed schemes bear a lot of similarities to our proposed solution, which is not surprising given the fast pace of innovation in the field of multiuser multi-antenna systems. We finally proposed an original spatial multiplexing scheme for multiple receive antenna users that addresses some of the constraints imposed by previously proposed schemes, although a better spatial multiplexing scheme was simultaneously and independently proposed. We nevertheless analyzed the performance of these schemes in the context of proportionally-fair scheduling algorithms with reduced-complexity solutions, and we were able to point out some important characteristics in the interactions of proportionally-fair scheduling, multiple antennas, and reduced-complexity solutions. In conclusion, the work in this thesis should

provide guidelines for the design of systems that aim to exploit multiuser diversity and spatial processing efficiently, as it broadened our understanding of this problem by pointing out some of the fundamental properties of multiuser multiple antenna systems.

This work has been partially published in conferences:

D.J. Mazzaresse and W.A. Krzymień, “High throughput downlink cellular packet data access with multiple antennas and multiuser diversity,” in *Proceedings of the IEEE Semiannual Vehicular Technology Conference (VTC’03-Spring)*, Jeju, Korea, April 22–25, 2003; Vol. 2, pp. 1079–1083.

D.J. Mazzaresse and W.A. Krzymień, “Throughput maximization and optimal number of active users on the two transmit antenna downlink of a cellular system,” In *Proceedings of the IEEE PACRIM Conference*, Victoria, Canada, August 29–30, 2003; Vol. 1, pp. 498 – 501.

D.J. Mazzaresse and W.A. Krzymień, “Linear space-time transmitter and receiver processing and scheduling for the MIMO broadcast channel”, in *Proceedings of the IEEE Semiannual Vehicular Technology Conference (VTC’04-Spring)*, Milan, Italy, May 17 - 19, 2004.

D.J. Mazzaresse and W.A. Krzymień, “Space-Time Linear Processing and Scheduling for the Cellular Downlink,” in *Proceedings of the 13th IST Wireless and Mobile Communications Summit (IST 2004)*, Lyon, France, Vol. 1, pp. 85-90, June 27 – 30, 2004.

D.J. Mazzaresse and W.A. Krzymień, “Design Rules for Efficient Scheduling of Packet Data on Multiple Antenna Downlink,” in *Proceedings of the 14th IST Wireless and Mobile Communications Summit (IST 2005)*, Dresden, Germany, June 19 – 23, 2005.

The work in this thesis obviously opens more questions than it solves, as any scientific work would. Some of the future areas of research that could extend the scope of this work have been identified and are summarized below.

- This thesis mostly assumed the availability of complete channel state information at the transmitter. However it is in general very hard to obtain in multiuser systems with multiple transmit antennas. Solutions that aim at achieving a large throughput with only partial

channel state information feedback are required in order to be applicable in real systems. So far opportunistic beamforming and limited-feedback precoding have been proposed, but none of them allows to closely approach the sum-capacity of the MIMO broadcast channel with complete channel state information.

- This thesis assumed the availability of capacity-achieving codes that were used to provide adaptive coding at the maximum rate without transmission errors. However, in practice at best capacity-approaching codes can be used, and in general they are not used close to the capacity limit but at frame error rates close to 1%. This choice is motivated by the imperfection of channel estimation and prediction. The performance is then further improved by the use of automatic repeat request (ARQ) processes. In particular hybrid ARQ (HARQ) allows for early termination in the transmission of a packet, which is one of the most important enablers of recently standardized packet-data access systems. Designing HARQ with simultaneous transmission to several users with jointly achievable rates appears to be very complex. In particular, what happens after only a few users have achieved a successful transmission and others require a retransmission? Should new users be scheduled along with the users that still require a retransmission? If new users are scheduled, how will it affect the jointly achievable rates for the retransmission? If new users are not scheduled before all retransmissions are successfully decoded or abandoned, then precious resources are wasted. This problem did not arise in single-antenna systems with scheduling algorithm, but it should play an important role in the design and performance of advanced systems with multiple antennas and scheduling algorithms.
- The performance of proportionally-fair scheduling algorithms depends on many parameters. A large number of trade-offs had already been identified in the context of single antenna systems, and more trade-offs appeared with multiple antenna systems. A more complete channel model that includes time variation caused by the mobility of the users, as well as out-of-cell interference, frequency-selectivity, and other real-life characteristics of wireless fading channels would provide more accurate results that could be used to evaluate the gains to be obtained with multiple antennas and the feasibility of specific transmission schemes and scheduling algorithms.

- Some of the more direct questions posed by this thesis are the need for joint proportionally-fair scheduling algorithms with single antenna receivers, the need for practical dirty-paper coding schemes, the need for improved spatial multiplexing schemes with only transmitter side processing with single antenna receivers, and the need for spatial multiplexing schemes with multiple antenna receivers that do not require complete channel state information at both the receiving and transmitting ends.

2 Bibliography

- [1] “One Million Customers Milestone (1992-93)”, History of GSM, http://www.gsmworld.com/about/history/history_page12.shtml.
- [2] “One billion GSM customers worldwide and growing,” Mobile Tech News, 23 March 2004, <http://www.mobiletechnews.com/info/2004/03/23/223226.html>.
- [3] G.J. Foschini and M.J. Gans, “On limits of wireless communications in a fading environment when using multiple antennas,” *Wireless Personal Communications*, Vol. 6, No. 3, pp. 311–335, March 1998.
- [4] I.E. Telatar, “Capacity of multi-antenna Gaussian channels” *European Transactions on Telecommunications*, Vol. 10, No. 6, pp. 585-595, Nov/Dec 1999.
- [5] G. Caire and S. Shamai, “On the achievable throughput of a multiantenna Gaussian broadcast channel,” *IEEE Transactions on Information Theory*, Vol. 49, No. 7, pp. 1691–1706, July 2003.
- [6] S. Vishwanath, N. Jindal and A. Goldsmith, “Duality, achievable rates, and sum-rate capacity of Gaussian MIMO broadcast channels,” *IEEE Transactions on Information Theory*, Vol. 49, No. 10, pp. 2658–2668, October 2003.
- [7] R.A. Horn and C.R. Johnson, *Matrix Analysis*, Cambridge University Press, 1985.
- [8] J.G. Proakis, *Digital Communications*, McGraw-Hill Series in Electrical and Computer Engineering, Third Edition, 1995.
- [9] V. Tarokh, N. Seshadri and A.R. Calderbank, “Space-time codes for high data rate wireless communication: performance criterion and code construction,” *IEEE Transactions on Information Theory*, Vol. 44, No. 2, pp. 744-765, March 1998.
- [10] L. Zheng and D.N.C. Tse, “Diversity and multiplexing: A fundamental tradeoff in multiple antenna channels,” *IEEE Transactions on Information Theory*, Vol. 49, No. 3, pp. 1073–1096, March 2003.
- [11] L. Zheng and D. Tse, “Diversity and freedom: a fundamental tradeoff in multiple antenna channels,” in *Proceedings of IEEE International Symposium on Information Theory (ISIT 2002)*, Lausanne, Switzerland, June 30 – July 5, 2002; p. 476.
- [12] A. Goldsmith, S.A. Jafar, N. Jindal and S. Vishwanath, “Capacity limits of MIMO channels,” *IEEE Journal on Selected Areas in Communications*, Vol. 21, No. 5, pp. 684–702, June 2003.
- [13] T.M. Cover and J.A. Thomas, *Elements of Information Theory*, New-York: Wiley, 1991.

- [14] T.L. Marzetta and B.M. Hochwald, "Capacity of a Mobile Multiple-Antenna Communication Link in Rayleigh Flat Fading," *IEEE Transactions on Information Theory*, Vol. 45, No. 1, pp. 139–157, January 1999.
- [15] E. Biglieri, J. Proakis, and S. Shamai, "Fading channels: information-theoretic and communications aspects." *IEEE Transactions on Information Theory*, Vol. 44, No. 6, pp. 2619–2692, October 1998.
- [16] B. M. Hochwald, T. L. Marzetta, and V. Tarokh, "Multiple-antenna channel hardening and its implications for rate feedback and scheduling," *IEEE Transactions on Information Theory*, Vol. 50, No. 9, pp. 1893 -1909, September 2004.
- [17] D.N.C. Tse, "Optimal power allocation over parallel Gaussian broadcast channels," in *Proceedings of IEEE International Symposium on Information Theory (ISIT 1997)*, Ulm, Germany, June 29–July 4, 1997; p. 27.
- [18] Knopp, R.; Humblet, P.A, "Information capacity and power control in single-cell multiuser communications," in *Proceedings of IEEE International Conference on Communications (ICC 1995)*, Seattle, WA, Vol. 1, pp. 331 – 335, June 18 – 22, 1995.
- [19] TIA/EIA/IS-856. cdma2000 High Speed Packet Data Air Interface Specification. Telecommunications Industry Association, Arlington, VA, November 2000.
- [20] TIA/EIA/IS-2000.2. Physical layer standard for cdma2000 spread spectrum systems – Release C. Telecommunications Industry Association, Arlington, VA, May 2002.
- [21] D. J. Love and R. W. Heath, "Limited feedback precoding for spatial multiplexing systems," in *Proceedings of the IEEE Global Telecommunications Conference (Globecom 2003)*, San Francisco, CA, December 1–5, 2003, Vol. 4, pp. 1857 – 1861.
- [22] D. J. Love, R. W. Heath, W. Santipach and M. L. Honig, "What is the value of limited feedback for MIMO channels?," *IEEE Communications Magazine*, Vol. 42, No. 10 , pp. 54 – 59, October 2004.
- [23] A.G. Kogiantis, N. Joshi and O. Sunay, "On transmit diversity and scheduling in wireless packet data," in *Proceedings of IEEE International Conference on Communications (ICC 2001)*, Helsinki, Finland, June 11-14, 2001; Vol. 8, pp. 2433 – 2437.
- [24] P. Viswanath, D.N.C.Tse and R. Laroia, "Opportunistic beamforming using dumb antennas," *IEEE Transactions on Information Theory*, Vol. 48, No. 6, pp. 1277 – 1294, June 2002.
- [25] W. Rhee, W. Yu and J.M. Cioffi, "Utilizing multiuser diversity for multiple antenna systems," in *Proceedings of IEEE Wireless Communications and Networking Conference (WCNC 2000)*, Chicago, IL, September 23-28, 2000; Vol. 1, pp. 420-425.

- [26] P. Viswanath and D.N.C. Tse, "Sum capacity of the multiple antenna Gaussian broadcast channel," in *Proceedings of IEEE International Symposium on Information Theory (ISIT 2002)*, Lausanne, Switzerland, June 30 – July 5, 2002; p. 497.
- [27] W. Yu and J.M. Cioffi, "Sum capacity of a Gaussian vector broadcast channel," in *Proceedings of IEEE International Symposium on Information Theory (ISIT 2002)*, Lausanne, Switzerland, June 30 – July 5, 2002; p. 498.
- [28] W. Yu and J.M. Cioffi, "Sum capacity of Gaussian vector broadcast channels", *IEEE Transactions on Information Theory*, Vol. 50, No. 9, September 2004.
- [29] P.W. Baier, M. Meurer, T. Weber and H. Troger, "Joint transmission (JT), an alternative rationale for the downlink of time division CDMA using multi-element transmit antennas," in *Proceedings of sixth IEEE International Symposium on Spread Spectrum Techniques and Applications (ISSSTA 2000)*, Parsippany, NJ, September 6-8, 2000; Vol. 1, pp. 1-5.
- [30] K. K.Wong, R. D. Murch, and K. B. Letaief, "Performance enhancement of multiuser MIMO wireless communications systems," *IEEE Transactions on Communications*, vol. 50, no. 12, pp. 1960–1970, December 2002.
- [31] K. K. Wong, R. D. Murch, and K. B. Letaief, "A joint channel diagonalization for multiuser MIMO antenna systems," *IEEE Transactions on Wireless Communications*, vol. 2, pp. 773–786, July 2003.
- [32] L.-U. Choi and R.D. Murch, "A transmit preprocessing technique for multiuser MIMO systems using a decomposition approach," *IEEE Transactions on Wireless Communications*, vol. 3, no. 1, pp. 20 - 24, January 2004.
- [33] H. Viswanathan, S. Venkatesan and H. Huang, "Downlink capacity evaluation of cellular networks with known-interference cancellation," *IEEE Journal on Selected Areas in Communications*, Vol. 21, No. 5, pp. 802–811, June 2003.
- [34] R.W. Heath, M. Airy and A.J. Paulraj, "Multiuser diversity for MIMO wireless systems with linear receivers," in *Proceedings of Asilomar Conference on Signals, Systems, and Computers*, Pacific Grove, California, November 2001; pp. 1194–1199.
- [35] B. Farhang-Boroujeny, Q. Spencer and L. Swindlehurst, "Layering techniques for space-time communication in multi-user networks," in *Proceedings IEEE Semiannual Vehicular Technology Conference (VTC'03-Fall)*, Orlando, FL, October 6 - 9, 2003, Vol. 2, pp. 1339-1343.
- [36] H. Weingarten, Y. Steinberg and S. Shamai, "The capacity region of the Gaussian MIMO broadcast channel," in *Proceedings of IEEE International Symposium on Information Theory (ISIT 2004)*, Chicago, USA, June 27 – July 2, 2004, p. 174.

- [37] M. Costa, "Writing on dirty paper," *IEEE Transactions on Information Theory*, Vol. 29, No. 3; pp. 439–441, May 1983.
- [38] R. Zamir, S. Shamai and U. Erez, "Nested linear/lattice codes for structured multiterminal binning," *IEEE Transactions on Information Theory*, Vol. 48, No. 6, pp.1250-1276, June 2002.
- [39] W. Yu and J.M. Cioffi, "Trellis precoding for the broadcast channel," in *Proceedings of the IEEE Global Telecommunications Conference (Globecom 2001)*, November 25–29, 2001, Vol. 2; pp. 1344–1348.
- [40] M. Tomlinson, "New automatic equalizer employing modulo arithmetic," *Electronic Letters*, Vol. 7, pp. 138-139, March 1971.
- [41] M. Miyakawa and H. Harashima, "A method of code conversion for a digital communication channel with intersymbol interference," *Transactions of the Institute of Electronic Communications Engineering of Japan*, Vol. 52-A, pp. 272-273, June 1969.
- [42] S. Ten Brink and U. Erez, "A close-to-capacity dirty paper coding scheme," in *Proceedings of IEEE International Symposium on Information Theory (ISIT 2004)*, Chicago, USA, June 27 – July 2, 2004, p. 533.
- [43] N. Jindal, S. Vishwanath and A. Goldsmith, "On the duality of Gaussian multiple-access and broadcast channels," *IEEE Transactions on Information Theory*, Vol. 50, No. 5, pp. 768-783, May 2004.
- [44] S. Vishwanath, W. Rhee, N. Jindal, S. Jafar and A. Goldsmith, "Sum power iterative waterfilling for Gaussian vector broadcast channels," in *Proceedings of IEEE International Symposium on Information Theory (ISIT 2003)*, Yokohama, Japan, June 29 – July 4, 2003, p. 467.
- [45] B. Hochwald and S. Vishwanath, "Space-time multiple access: linear growth in the sum-rate," In *Proceeding of the 40th Allerton Conference*, University of Illinois at U-C, Monticello, IL, October 2–4, 2002.
- [46] M. Sharif and B. Hassibi, "On the capacity of MIMO broadcast channel with partial side information," in *Proceedings of Asilomar Conference on Signals, Systems, and Computers*, Pacific Grove, California, 9-12 November 2003; pp. 958–962.
- [47] S. Boyd and L. Vandenberghe, *Convex Optimization*, Cambridge University Press, 2004.
- [48] R.G. Gallager, *Information Theory and Reliable Communication*; Wiley: New York, 1968.

- [49] W. Yu, "Spatial multiplex in downlink multiuser multiple-antenna wireless environments," In *Proceedings of the IEEE Global Telecommunications Conference (Globecom 2003)*, San Francisco, USA, December 1–5, 2003; Vol. 4, pp. 1887 – 1891.
- [50] W. Rhee and J.M. Cioffi, "On the capacity of multiuser wireless channels with multiple antennas," *IEEE Transactions on Information Theory*, Vol. 49, No. 10, pp. 2580-2595, October 2003.
- [51] X. Zhang and S.-Y. Kung, "Capacity analysis for parallel and sequential MIMO equalizers," *IEEE Transactions on Signal Processing*, Vol. 51, No. 11, pp. 2989–3002, November 2003.
- [52] S.T. Chung, A. Lozano and H.C. Huang, "Approaching eigenmode BLAST channel capacity using V-BLAST with rate and power feedback," in *Proceedings of the IEEE Semiannual Vehicular Technology Conference (VTC'01-Fall)*, Atlantic City, NJ, October 7–11, 2001; Vol. 2, pp. 915 – 919.
- [53] M.K. Varanasi and T. Guess, "Optimum decision feedback multiuser equalization with successive decoding achieves the total capacity of the Gaussian multiple-access channel," in *Proceedings of Asilomar Conference on Signals, Systems, and Computers*, 1998; pp. 1405–1409.
- [54] R.S. Blum and J.H. Winters, "On optimum MIMO with antenna selection," *IEEE Communications Letters*, Vol. 6, No. 8, pp. 322-324, August 2002.
- [55] M. Webb, M. Beach and A. Nix, "Capacity limits of MIMO channels with co-channel interference," in *Proceedings of the IEEE Semiannual Vehicular Technology Conference (VTC'04-Spring)*, Milan, Italy, May 17 - 19, 2004.
- [56] A. Gorokhov, D. Gore and A. Paulraj, "Receive antenna selection for MIMO flat-fading channels: theory and algorithms," *IEEE Transactions on Information Theory*, Vol. 49, No. 10, pp. 2687–2697, October 2003.
- [57] D.J. Mazzarese and W.A. Krzymień, "High throughput downlink cellular packet data access with multiple antennas and multiuser diversity," in *Proceedings of the IEEE Semiannual Vehicular Technology Conference (VTC'03-Spring)*, Jeju, Korea, April 22–25, 2003; Vol. 2, pp. 1079–1083.
- [58] H. Yao and G.W. Wornell, "Lattice-reduction-aided detectors for MIMO communication systems," in *Proceedings of the IEEE Global Telecommunications Conference (Globecom 2002)*, November 17–21, 2002, Vol. 1; pp. 424–428.
- [59] R.F.H. Fischer and C.A. Windpassinger, "Improved MIMO precoding for decentralized receivers resembling concepts from lattice reduction," in *Proceedings of the IEEE Global*

- Telecommunications Conference (Globecom 2003)*, San Francisco, CA, December 1–5, 2003; Vol. 4, pp. 1852 - 1856.
- [60] C. Windpassinger, R. F. H. Fischer, T. Vencel, and J. B. Huber, "Precoding in Multiantenna and Multiuser Communications," *IEEE Transactions on Wireless Communications*, Vol. 3, No. 4, pp. 1305 – 1316, July 2004.
- [61] A. Kogiantis and L. Ozarow, "Downlink best-effort packet data with multiple antennas," in *Proceedings of IEEE International Conference on Communications (ICC 2003)*, Anchorage, AK, May 11 – 15, 2003, Vol. 1, pp. 715 – 719.
- [62] O.S. Shin and K.B. Lee, "Packet scheduling for MIMO cellular systems," In *Proceedings of the IEEE Semiannual Vehicular Technology Conference (VTC'03-Spring)*, Jeju, Korea, April 22–25, 2003; Vol. 3, pp. 1694 – 1698.
- [63] D. Aktas and H. El Gamal, "Multiuser scheduling for multiple antenna systems," In *Proceedings of the IEEE PACRIM Conference*, Victoria, Canada, August 29–30, 2003; Vol.1, pp. 502 - 505.
- [64] Q. H. Spencer, A. L. Swindlehurst and M. Haardt, "Zero-forcing methods for downlink spatial multiplexing in multiuser MIMO channels," *IEEE Transactions on Signal Processing*, Vol. 52, No. 2, pp. 461 – 471, February 2004.
- [65] D.J. Mazzarese and W.A. Krzymień, "Linear space-time transmitter and receiver processing and scheduling for the MIMO broadcast channel", in *Proceedings of the IEEE Semiannual Vehicular Technology Conference (VTC'04-Spring)*, Milan, Italy, May 17 - 19, 2004.
- [66] K.K. Wong, R.D. Murch and K.B. Letaief, "MIMO antenna system for frequency selective fading channels," in *Proceedings of the IEEE International Symposium on Personal, Indoor and Mobile Radio Communications (PIMRC 2000)*, London, UK, 18-21 September 2000, pp. 1500-1504.
- [67] R.L.-U. Choi, M.T. Ivrlac, R.D. Murch and J.A. Nossek, "Joint transmit and receive multi-user MIMO decomposition approach for the downlink of multi-user MIMO systems," in *Proceedings IEEE Semiannual Vehicular Technology Conference (VTC'03-Fall)*, Orlando, FL, October 6 - 9, 2003, Vol. 2, pp. 409-413.
- [68] C.F. Van Loan, "Generalizing the singular value decomposition," *SIAM Journal on Numerical Analysis*, 13:76-83, 1976.
- [69] C.C. Paige and M.S. Saunders, "Towards a generalized singular value decomposition," *SIAM Journal on Numerical Analysis*, 18:398-405, 1981.

- [70] A. Grant, "Rayleigh fading multi-antenna channels," *EURASIP Journal on Applied Signal Processing*, Vol. 2002, No. 3, pp. 316-329, March 2002.
- [71] "Guidelines for evaluation of radio transmission technologies for IMT-2000," Recommendation ITU-R M.1225, 1997.

Appendix A: Classical Waterfilling

In this appendix we give a summary of the optimization problem commonly called waterfilling. Its early development was prompted by the problem of power allocation on the frequency-selective channel leading to the maximization of the mutual information [48]. This is a case of convex optimization that can be solved using Lagrange multipliers [47]. The problem is formulated as follows:

$$C = \max_{x_n \geq 0, n=1, \dots, N} \sum_{n=1}^N \log(1 + x_n \alpha_n) \quad (\text{A.1})$$

$$\text{Subject to } \sum_{n=1}^N x_n = P \text{ and } x_n \geq 0, n=1, \dots, N, \quad (\text{A.2})$$

where $\sigma_n^2 = 1/\alpha_n$ is the variance of the AWGN on channel number n .

We can determine x_n for $n=1, \dots, N$ from the equivalent problem:

$$\text{Minimize } -\sum_{n=1}^N \log(\sigma_n^2 + x_n) \quad (\text{A.3})$$

$$\text{Subject to } \sum_{n=1}^N x_n = P \text{ and } x_n \geq 0, n=1, \dots, N.$$

We introduce the Lagrange multipliers $\lambda \in \mathbb{R}^N$ for the inequality constraints and the multiplier ν for the equality constraint. The KKT optimality conditions are [47]:

$$\begin{cases} \sum_{n=1}^N x_n = P, x_n \geq 0, & n=1, \dots, N \\ \lambda_n \geq 0, & n=1, \dots, N \\ \frac{-1}{\sigma_n^2 + x_n} - \lambda_n + \nu = 0, & n=1, \dots, N \\ \lambda_n x_n = 0, & n=1, \dots, N \end{cases} \quad (\text{A.4})$$

Solving this system leads to the waterfilling solution:

$$x_n = \begin{cases} \frac{1}{\nu} - \sigma_n^2, & \nu < \frac{1}{\sigma_n^2} \\ 0, & \nu \geq \frac{1}{\sigma_n^2} \end{cases} \quad (\text{A.5})$$

Where ν is determined by

$$\sum_{n=1}^N \max\left(0, \frac{1}{\nu} - \sigma_n^2\right) = P. \quad (\text{A.6})$$

The particular solution in the high power region is that all channels are allocated power such that:

$$\sum_{n=1}^N \left(\frac{1}{v} - \sigma_n^2 \right) = P. \quad (\text{A.7})$$

So
$$\frac{1}{v} = \frac{P}{N} + \frac{1}{N} \sum_{n=1}^N \sigma_n^2. \quad (\text{A.8})$$

So
$$x_n = \frac{P}{N} + \frac{1}{N} \sum_{i=1}^N (\sigma_i^2 - \sigma_n^2), \quad n = 1, \dots, N. \quad (\text{A.9})$$

So
$$C = \sum_{n=1}^N \log \left(\frac{P}{N} \frac{1}{\sigma_n^2} + \frac{1}{N} \sum_{i=1}^N \frac{\sigma_i^2}{\sigma_n^2} \right). \quad (\text{A.10})$$

Appendix B: Closed-Form Expression of the Sum-Capacity on the (2,1, K_a) MIMO BC

The expression given in (3.20) is proved here. We start from the expression of the sum-capacity by considering only the K_a active users:

$$C = \log \left(1 + \sum_{i=1}^K p_i \|h_i\|^2 + \frac{1}{2} \mathbf{p}^T \mathbf{M} \mathbf{p} \right) \quad (\text{B.1})$$

We recall the definitions:

$$\mathbf{b} = \left[\|h_1\|^2 \quad \dots \quad \|h_K\|^2 \quad P \right]^T \quad (\text{B.2})$$

$$\Phi = \begin{bmatrix} \mathbf{M} & -\mathbf{I}_K \\ -\mathbf{I}_K^T & 0 \end{bmatrix} \quad (\text{B.3})$$

$$\begin{bmatrix} \mathbf{p}^T & v \end{bmatrix}^T = \begin{bmatrix} \mathbf{p} \\ v \end{bmatrix} = -\Phi^{-1} \mathbf{b} \quad (\text{B.4})$$

The all-ones column vector of length K is defined as \mathbf{I}_K . We express:

$$\begin{bmatrix} \mathbf{p} \\ v \end{bmatrix}^T \mathbf{b} = \begin{bmatrix} \mathbf{p} \\ v \end{bmatrix}^T \left[\|h_1\|^2 \quad \dots \quad \|h_K\|^2 \quad P \right]^T = \sum_{i=1}^K p_i \|h_i\|^2 + vP \quad (\text{B.5})$$

So
$$vP = \begin{bmatrix} \mathbf{p} \\ v \end{bmatrix}^T \mathbf{b} - \sum_{i=1}^K p_i \|h_i\|^2 = (-\Phi^{-1} \mathbf{b})^T \mathbf{b} - \sum_{i=1}^K p_i \|h_i\|^2 = -\mathbf{b}^T \Phi^{-1} \mathbf{b} - \sum_{i=1}^K p_i \|h_i\|^2 \quad (\text{B.6})$$

Moreover
$$\mathbf{b} = - \begin{bmatrix} \mathbf{M} & -\mathbf{I}_K \\ -\mathbf{I}_K^T & 0 \end{bmatrix} \begin{bmatrix} \mathbf{p} \\ v \end{bmatrix} = - \begin{bmatrix} \mathbf{M} \mathbf{p} - v \mathbf{I}_K \\ -\sum_{i=1}^K p_i \end{bmatrix} = - \begin{bmatrix} \mathbf{M} \mathbf{p} - v \mathbf{I}_K \\ -P \end{bmatrix} \quad (\text{B.7})$$

Thus
$$\mathbf{b} = -\Phi \begin{bmatrix} \mathbf{p} \\ v \end{bmatrix} = - \begin{bmatrix} \mathbf{M} & -\mathbf{I}_K \\ -\mathbf{I}_K^T & 0 \end{bmatrix} \begin{bmatrix} \mathbf{p} \\ v \end{bmatrix} = - \begin{bmatrix} \mathbf{M} \mathbf{p} - v \mathbf{I}_K \\ -\sum_{i=1}^K p_i \end{bmatrix} = - \begin{bmatrix} \mathbf{M} \mathbf{p} - v \mathbf{I}_K \\ -P \end{bmatrix} \quad (\text{B.8})$$

$$\mathbf{b}^T \Phi^{-1} \mathbf{b} = \mathbf{b}^T (\Phi^{-1} \mathbf{b}) = \begin{bmatrix} \mathbf{M} \mathbf{p} - v \mathbf{I}_K \\ -P \end{bmatrix}^T \begin{bmatrix} \mathbf{p}^T & v \end{bmatrix}^T = \begin{bmatrix} \mathbf{p}^T & v \end{bmatrix} \begin{bmatrix} \mathbf{M} \mathbf{p} - v \mathbf{I}_K \\ -P \end{bmatrix} = \mathbf{p}^T \mathbf{M} \mathbf{p} - vP - vP \quad (\text{B.9})$$

$$\mathbf{b}^T \Phi^{-1} \mathbf{b} = \mathbf{p}^T \mathbf{M} \mathbf{p} - 2vP = \mathbf{p}^T \mathbf{M} \mathbf{p} - 2 \left(-\mathbf{b}^T \Phi^{-1} \mathbf{b} - \sum_{i=1}^K p_i \|h_i\|^2 \right) \quad (\text{B.10})$$

And
$$-\frac{1}{2} \mathbf{b}^T \Phi^{-1} \mathbf{b} = \frac{1}{2} \mathbf{p}^T \mathbf{M} \mathbf{p} + \sum_{i=1}^K p_i \|h_i\|^2 \quad (\text{B.11})$$

Thus
$$C = \log \left(1 + \sum_{i=1}^K p_i \|h_i\|^2 + \frac{1}{2} \mathbf{p}^T \mathbf{M} \mathbf{p} \right) = \log \left(1 - \frac{1}{2} \mathbf{b}^T \Phi^{-1} \mathbf{b} \right) \quad (\text{B.12})$$

Appendix C: Geometric Interpretation of Power Allocation on the (2,1,3) MIMO BC

C.1 Definitions

We can define unambiguously the angle θ between two non-zero vectors \mathbf{x} and \mathbf{y} in \mathbb{C}^n by [7]:

$$\cos \theta = \frac{|\langle \mathbf{y}, \mathbf{x} \rangle|}{\langle \mathbf{x}, \mathbf{x} \rangle^{1/2} \langle \mathbf{y}, \mathbf{y} \rangle^{1/2}}, \quad 0 \leq \theta \leq \frac{\pi}{2}. \quad (\text{C.1})$$

Thus we define the angle θ_{mn} for $1 \leq m, n \leq 3$ such that

$$M_{mn} = \|\mathbf{h}_m\|^2 \|\mathbf{h}_n\|^2 (1 - \cos^2 \theta_{mn}) = \|\mathbf{h}_m\|^2 \|\mathbf{h}_n\|^2 \sin^2 \theta_{mn}. \quad (\text{C.2})$$

Without loss of generality, we assume in the rest of this appendix that

$$\begin{aligned} 0 < \|\mathbf{h}_1\| &\leq \|\mathbf{h}_2\| \\ 0 < \|\mathbf{h}_1\| &\leq \|\mathbf{h}_3\| \end{aligned} \quad (\text{C.3})$$

Define the angles $\tilde{\theta}_{12}$ and $\tilde{\theta}_{13}$ unambiguously on $[0, \pi/2]$ such that

$$\sin(\tilde{\theta}_{12}) = \sqrt{\frac{\|\mathbf{h}_1\|^2}{\|\mathbf{h}_3\|^2}} \sin(\theta_{12}) \quad (\text{C.4})$$

$$\sin(\tilde{\theta}_{13}) = \sqrt{\frac{\|\mathbf{h}_1\|^2}{\|\mathbf{h}_2\|^2}} \sin(\theta_{13}) \quad (\text{C.5})$$

On the (2,1,3) MIMO BC we have:

$$\Phi = \begin{bmatrix} 0 & M_{12} & M_{13} & -1 \\ M_{12} & 0 & M_{23} & -1 \\ M_{13} & M_{23} & 0 & -1 \\ -1 & -1 & -1 & 0 \end{bmatrix} \quad (\text{C.6})$$

We can then express the following determinants:

$$\det \Phi = \det \Phi_{4,1} - \det \Phi_{4,2} + \det \Phi_{4,3} \quad (\text{C.7})$$

$$\det \Phi_{4,1} = M_{23} (M_{23} - M_{12} - M_{13}) \quad (\text{C.8})$$

$$\det \Phi_{4,2} = -M_{13} (M_{13} - M_{12} - M_{23}) \quad (\text{C.9})$$

$$\det \Phi_{4,3} = M_{12} (M_{12} - M_{13} - M_{23}) \quad (\text{C.10})$$

$$\text{Thus } \det \Phi = (M_{12} - M_{13} - M_{23})^2 - 4M_{13}M_{23}. \quad (\text{C.11})$$

If all users are allocated power at the sum-capacity with total transmit power P , the power allocation is expressed by (3.14). We rewrite it as:

$$\begin{aligned}
P_1 &= \frac{M_{23}(M_{23} - M_{12} - M_{13})}{\det \Phi} P + \frac{\sum_{k=1}^3 (-1)^k \|h_k\|^2 \det \Phi_{k,1}}{\det \Phi} \\
P_2 &= \frac{M_{13}(M_{13} - M_{12} - M_{23})}{\det \Phi} P - \frac{\sum_{k=1}^3 (-1)^k \|h_k\|^2 \det \Phi_{k,2}}{\det \Phi} \\
P_3 &= \frac{M_{12}(M_{12} - M_{13} - M_{23})}{\det \Phi} P + \frac{\sum_{k=1}^3 (-1)^k \|h_k\|^2 \det \Phi_{k,3}}{\det \Phi}
\end{aligned} \tag{C.12}$$

We have seen that we can rewrite these inequalities as a system of inequalities on P as in (3.16), (3.17), (3.18). If this system of inequalities is not feasible then all 3 users are never allocated power simultaneously on the (2,1,3) MIMO BC. Thus at most 2 users are active simultaneously. We know that on the (2,1,2) MIMO BC one user is active in the low power region and then both users become active when the total transmit power is increased [5]. Therefore it is not possible that the 3 users be active in turns at some point when increasing the total transmit power without being simultaneously active. Thus if the system of inequalities on P is not feasible then one of the 3 users is never allocated any power. In this appendix we characterize the situations where the system of inequalities on P is feasible.

C.2 High Power Threshold Condition

For this condition to hold, all the factors of P in (C.12) must be positive. Note that since $M_{ij} \geq 0, \forall (i, j)$, it is impossible that two of the three terms $M_{23} - M_{12} - M_{13}$, $M_{13} - M_{12} - M_{23}$ and $M_{12} - M_{13} - M_{23}$ be positive simultaneously. Thus this condition never holds when $\det \Phi > 0$. Consequently we need:

$$\begin{cases} \det \Phi < 0 \\ M_{23} - M_{12} - M_{13} < 0 \\ M_{13} - M_{12} - M_{23} < 0 \\ M_{12} - M_{13} - M_{23} < 0 \end{cases} \tag{C.13}$$

Or equivalently

$$\begin{cases} M_{23}(M_{23} - M_{12} - M_{13}) + M_{13}(M_{13} - M_{12} - M_{23}) + M_{12}(M_{12} - M_{13} - M_{23}) < 0 \\ M_{23} - M_{12} - M_{13} < 0 \\ M_{13} - M_{12} - M_{23} < 0 \\ M_{12} - M_{13} - M_{23} < 0 \end{cases} \tag{C.14}$$

Or equivalently

$$\begin{cases} M_{23} < M_{12} + M_{13} \\ M_{13} < M_{12} + M_{23} \\ M_{12} < M_{13} + M_{23} \end{cases} \quad (\text{C.15})$$

Using (42):

$$\begin{cases} \|h_2\|^2 \|h_3\|^2 \sin^2 \theta_{23} < \|h_1\|^2 \|h_2\|^2 \sin^2 \theta_{12} + \|h_1\|^2 \|h_3\|^2 \sin^2 \theta_{13} \\ \|h_1\|^2 \|h_3\|^2 \sin^2 \theta_{13} < \|h_1\|^2 \|h_2\|^2 \sin^2 \theta_{12} + \|h_2\|^2 \|h_3\|^2 \sin^2 \theta_{23} \\ \|h_1\|^2 \|h_2\|^2 \sin^2 \theta_{12} < \|h_1\|^2 \|h_3\|^2 \sin^2 \theta_{13} + \|h_2\|^2 \|h_3\|^2 \sin^2 \theta_{23} \end{cases} \quad (\text{C.16})$$

Dividing by $\|h_2\|^2 \|h_3\|^2$ we obtain the necessary and sufficient condition for the existence of a high power threshold above which all users are allocated power at the sum-capacity of the (2,1,3) MIMO BC when $0 < \|h_1\| \leq \|h_2\|$ and $0 < \|h_1\| \leq \|h_3\|$:

$$\begin{cases} \sin^2 \theta_{23} < \sin^2 \tilde{\theta}_{12} + \sin^2 \tilde{\theta}_{13} \\ \sin^2 \tilde{\theta}_{13} < \sin^2 \tilde{\theta}_{12} + \sin^2 \theta_{23} \\ \sin^2 \tilde{\theta}_{12} < \sin^2 \tilde{\theta}_{13} + \sin^2 \theta_{23} \end{cases} \quad (\text{C.17})$$

As a particular case, when the channel vectors are real, the angles θ_{ij} represent the true angles between the channel vectors in the Euclidean plane. If we further assume that $0 < \|h_1\| = \|h_2\| \leq \|h_3\|$ then $\tilde{\theta}_{13} = \theta_{13}$ and the condition becomes:

$$\frac{|\sin^2 \theta_{23} - \sin^2 \theta_{13}|}{\sin^2 \theta_{12}} < \frac{\|h_1\|^2}{\|h_3\|^2} < \frac{\sin^2 \theta_{13} + \sin^2 \theta_{23}}{\sin^2 \theta_{12}}. \quad (\text{C.18})$$

Note that the angles between the channel vectors in the real case are not independent. In fact, only four possibilities exist for the relationship between these angles:

$$\begin{aligned} (a) \quad & \theta_{12} = \theta_{13} + \theta_{23} \\ (b) \quad & \theta_{13} = \theta_{12} + \theta_{23} \\ (c) \quad & \theta_{23} = \theta_{12} + \theta_{13} \\ (d) \quad & \theta_{12} + \theta_{13} + \theta_{23} = \pi \end{aligned} \quad (\text{C.19})$$

For example it is easy to prove that if $0 < \|h_1\| = \|h_2\| = \|h_3\|$ then (C.18) can only be true if $\theta_{12} + \theta_{13} + \theta_{23} = \pi$, or in other words if the sum of any two angles is larger than $\pi/2$.

C.3 Non-Monotonicity Condition

Without loss of generality, we assume that users 1 and 2 are active in the high power region, but not user 3. We want to characterize the situations when user 3 is active in some finite interval of power values. From (C.12) we formulate the conditions such that $p_i \geq 0, i=1,2$ in the

high power region, and $p_3 \geq 0$ when P is less than some positive value. We want a system that looks like:

$$\begin{cases} p_1 > \psi_1 \\ p_2 > \psi_2 \\ p_3 < \psi_3 \end{cases} \quad (\text{C.20})$$

With

$$\begin{cases} \psi_3 > 0 \\ \psi_3 > \psi_1 \\ \psi_3 > \psi_2 \end{cases} \quad (\text{C.21})$$

Where

$$\begin{aligned} \psi_1 &= \frac{(\|h_3\|^2 - \|h_2\|^2)(M_{13} - M_{12}) + M_{23}(\|h_1\|^2 - \|h_2\|^2) + M_{23}(\|h_1\|^2 - \|h_3\|^2)}{M_{23}(M_{23} - M_{12} - M_{13})} \\ \psi_2 &= \frac{(\|h_3\|^2 - \|h_1\|^2)(M_{23} - M_{12}) + M_{13}(\|h_2\|^2 - \|h_1\|^2) + M_{13}(\|h_2\|^2 - \|h_3\|^2)}{M_{13}(M_{13} - M_{12} - M_{23})} \\ \psi_3 &= \frac{(\|h_1\|^2 - \|h_2\|^2)(M_{13} - M_{23}) + M_{12}(\|h_3\|^2 - \|h_1\|^2) + M_{12}(\|h_3\|^2 - \|h_2\|^2)}{M_{12}(M_{12} - M_{13} - M_{23})} \end{aligned} \quad (\text{C.22})$$

To satisfy (C.20) we need:

$$\begin{aligned} \frac{\det \Phi_{4,1}}{\det \Phi} &> 0 \\ \frac{\det \Phi_{4,2}}{\det \Phi} &< 0 \\ \frac{\det \Phi_{4,3}}{\det \Phi} &< 0 \end{aligned} \quad (\text{C.23})$$

Thus we need either

$$\begin{cases} \det \Phi > 0 \\ \det \Phi_{4,1} > 0 \\ \det \Phi_{4,2} < 0 \\ \det \Phi_{4,3} < 0 \end{cases} \quad (\text{C.24})$$

Or

$$\begin{cases} \det \Phi < 0 \\ \det \Phi_{4,1} < 0 \\ \det \Phi_{4,2} > 0 \\ \det \Phi_{4,3} > 0 \end{cases} \quad (\text{C.25})$$

Using (C.8) and (C.9), we see that the second and third inequalities in (C.24) are not feasible simultaneously since the terms $M_{23} - M_{12} - M_{13}$ and $M_{13} - M_{12} - M_{23}$ cannot be positive simultaneously. Thus we need $\det \Phi < 0$. In this case we can show that:

$$\psi_3 - \psi_1 = \frac{\det \Phi \left[\left(\|h_3\|^2 - \|h_2\|^2 \right) M_{12} + \left(\|h_2\|^2 - \|h_1\|^2 \right) M_{23} \right]}{\det \Phi_{4,1} \det \Phi_{4,3}} \quad (\text{C.26})$$

$$\psi_3 - \psi_2 = \frac{\det \Phi \left[\left(\|h_3\|^2 - \|h_1\|^2 \right) M_{12} + \left(\|h_1\|^2 - \|h_2\|^2 \right) M_{13} \right]}{-\det \Phi_{4,2} \det \Phi_{4,3}} \quad (\text{C.27})$$

And

$$\psi_3 = \frac{\sum_{k=1}^3 (-1)^k \|h_k\|^2 \det \Phi_{k,3}}{\det \Phi_{4,3}} = \frac{2\psi_3 - (\psi_1 + \psi_2)}{\det \Phi_{4,3}} \quad (\text{C.28})$$

The first inequality in (C.21) is true whenever the second and third inequalities are true due to (C.28) and $\det \Phi_{4,3} > 0$ from (C.25). Thus we can reduce (C.21) to:

$$\begin{cases} \psi_3 > \psi_1 \\ \psi_3 > \psi_2 \end{cases} \quad (\text{C.29})$$

We can rewrite (C.25) and (C.29) using (C.8), (C.9), (C.10), (C.11), (C.26) and (C.27) as

$$\begin{cases} (M_{12} - M_{13} - M_{23})^2 < 4M_{13}M_{23} \\ M_{23} - M_{13} < M_{12} \\ M_{13} - M_{23} < M_{12} \\ M_{13} + M_{23} < M_{12} \\ 0 < \left(\|h_3\|^2 - \|h_2\|^2 \right) M_{12} + \left(\|h_2\|^2 - \|h_1\|^2 \right) M_{23} \\ 0 < \left(\|h_3\|^2 - \|h_1\|^2 \right) M_{12} + \left(\|h_1\|^2 - \|h_2\|^2 \right) M_{13} \end{cases} \quad (\text{C.30})$$

We note that the second and third inequalities are true whenever the fourth inequality is true since $M_{ij} \geq 0, \forall (i, j)$. At this point we notice that if $\|h_3\| \leq \|h_2\|$ and $\|h_3\| \leq \|h_1\|$ then either the fifth or sixth inequality in (C.30) cannot be true. Thus user 3 cannot have the smallest channel vector norm. We can now use (C.3) without loss of generality. We then divide all remaining inequalities by $\|h_2\|^2 \|h_3\|^2$ to obtain:

$$\begin{cases} \left(\sin^2 \bar{\theta}_{12} - \sin^2 \bar{\theta}_{13} - \sin^2 \theta_{23} \right)^2 < 4 \sin^2 \bar{\theta}_{13} \sin^2 \theta_{23} \\ \sin^2 \bar{\theta}_{13} + \sin^2 \theta_{23} < \sin^2 \bar{\theta}_{12} \\ \left(\|h_2\|^2 - \|h_3\|^2 \right) \sin^2 \bar{\theta}_{12} < \left(\|h_2\|^2 - \|h_1\|^2 \right) \sin^2 \theta_{23} \\ \left(\|h_1\|^2 - \|h_3\|^2 \right) \sin^2 \bar{\theta}_{12} < \left(\|h_1\|^2 - \|h_2\|^2 \right) \sin^2 \bar{\theta}_{13} \end{cases} \quad (\text{C.31})$$

Or equivalently

$$\begin{cases} \sin^2 \tilde{\theta}_{13} + \sin^2 \theta_{23} < \sin^2 \tilde{\theta}_{12} < (\sin \tilde{\theta}_{13} + \sin \theta_{23})^2 \\ (\|\mathbf{h}_2\|^2 - \|\mathbf{h}_3\|^2) \sin^2 \tilde{\theta}_{12} < (\|\mathbf{h}_2\|^2 - \|\mathbf{h}_1\|^2) \sin^2 \theta_{23} \\ (\|\mathbf{h}_1\|^2 - \|\mathbf{h}_3\|^2) \sin^2 \tilde{\theta}_{12} < (\|\mathbf{h}_1\|^2 - \|\mathbf{h}_2\|^2) \sin^2 \tilde{\theta}_{13} \end{cases} \quad (\text{C.32})$$

Note that a necessary condition is

$$\sin^2 \tilde{\theta}_{13} + \sin^2 \theta_{23} < 1 \text{ with } \tilde{\theta}_{13}, \theta_{23} \in [0 \ \pi/2]. \quad (\text{C.33})$$

Or equivalently

$$0 \leq \tilde{\theta}_{13} + \theta_{23} < \pi/2 \text{ with } \tilde{\theta}_{13}, \theta_{23} \in [0 \ \pi/2]. \quad (\text{C.34})$$

Another necessary condition is that $\|\mathbf{h}_1\| = \|\mathbf{h}_2\| = \|\mathbf{h}_3\|$ be false.

In the case of real channel vectors and $0 < \|\mathbf{h}_1\| = \|\mathbf{h}_2\| < \|\mathbf{h}_3\|$, the necessary and sufficient condition becomes

$$\begin{cases} \frac{\sin^2 \theta_{13} + \sin^2 \theta_{23}}{\sin^2 \theta_{12}} < \frac{\|\mathbf{h}_1\|^2}{\|\mathbf{h}_3\|^2} < \left(\frac{\sin \theta_{13} + \sin \theta_{23}}{\sin \theta_{12}} \right)^2 \\ \theta_{12} = \theta_{13} + \theta_{23} < \pi/2 \end{cases} \quad (\text{C.35})$$

Appendix D: Asymptotically Optimal Power Allocation on the MIMO BC in the High Power Region

D.1 Goal and Summary

This section presents the proofs of the asymptotically optimal power allocation on the MIMO BC in the high power region. The optimality refers to achieving the sum-capacity. The proofs are given separately for the $(N,1,K)$ MIMO BC and for the (N,N,K) MIMO BC. Our goal is to characterize the number of one-dimensional channels that are allocated a non-vanishing fraction of the total transmit power in the limit where the total transmit power goes to infinity. In the particular case of the $(N,1,K)$ MIMO BC this reduces to studying the asymptotically optimal number of active users. We prove that the number of one-dimensional channels that are allocated a non-vanishing fraction of the total transmit power is equal to N on the $(N,1,K)$ MIMO BC and also to N on the (N,N,K) MIMO BC.

Moreover on the $(N,1,K)$ MIMO BC, we prove the orthogonality of the optimal covariance matrix of user j on the BC with the channel matrices of the users that are allocated an asymptotically non-vanishing fraction of the total transmit power on the MIMO BC and that are encoded prior to user j using dirty-paper coding, where user j is itself allocated an asymptotically non-vanishing fraction of the total transmit power on the MIMO BC. This result implies that on the $(N,1,K)$ MIMO BC, in the high power region, the combined action of dirty-paper coding and of the asymptotically optimal BC covariance matrices completely diagonalizes the channel among the N users that are allocated an asymptotically non-vanishing fraction of the total transmit power. We can consequently derive a closed-form expression of the asymptotic sum-capacity of the $(N,1,N)$ MIMO BC in the high power region.

On the (N,N,K) MIMO BC, we prove that in the high power region, only one user is allocated a non-vanishing fraction of the total transmit power, as long as its channel matrix is full rank. Other users are allocated either a non-zero but vanishing fraction of the total transmit power, or no power if they are allocated no power on the dual sum-power MIMO MAC. In general on the (N,M,K) MIMO BC, we conjecture that only N one-dimensional channels are allocated a non-vanishing fraction of the total transmit power in the high power region, and these N one-dimensional channels belong to the K' users that are encoded first by dirty-paper coding

such that these users are allocated a non-vanishing fraction of the total transmit power on the dual sum-power MIMO MAC and $\sum_{k=K-K'+2}^K M_k \leq N \leq \sum_{k=K-K'+1}^K M_k$.

D.2 Definitions and Notation

Background

This section summarizes the MAC to BC transformations introduced in [6]. We consider the same encoding and decoding orders as in [6] and we use the MAC to BC transformations to obtain the optimal covariance matrices on the MIMO BC in order to achieve the sum-capacity and the same rate vector as on the dual MIMO MAC. On the MIMO MAC, the decoding order is the following: user 1 is decoded first, user 2 is decoded second, and so on until user K is decoded last. The same rate vector is achieved on the MIMO BC using the covariance matrices obtained with the MAC to BC transformations when user 1 is encoded last, user 2 is encoded second to last, and so on with user K being encoded first.

The channel matrix of user j is \mathbf{H}_j of size $M_j \times N$. The optimal covariance matrix of size $M_k \times M_k$ of user j on the MIMO MAC is \mathbf{P}_j . It does not depend on the decoding order chosen on the MAC. The rate achieved by user j on the MAC is:

$$R_j^{MAC} = \log \frac{\left| \mathbf{I}_N + \sum_{i=j}^K (\mathbf{H}_i^* \mathbf{P}_i \mathbf{H}_i) \right|}{\left| \mathbf{I}_N + \sum_{i=j+1}^K (\mathbf{H}_i^* \mathbf{P}_i \mathbf{H}_i) \right|}. \quad (\text{D.1})$$

The MAC to BC transformations give the optimal covariance matrices for the MIMO BC such that each user achieves the same rate as on the dual MIMO MAC. The optimal covariance matrix of size $N \times N$ of user j on the MIMO BC with the given encoding order is [6]:

$$\boldsymbol{\Sigma}_j = \mathbf{B}_j^{-1/2} \overline{\mathbf{A}_j^{1/2} \mathbf{P}_j \mathbf{A}_j^{1/2}} \mathbf{B}_j^{-1/2}, \quad (\text{D.2})$$

where $\overline{\mathbf{A}_j^{1/2} \mathbf{P}_j \mathbf{A}_j^{1/2}}$ is the covariance matrix on the flipped channel that achieves the same rate as the covariance matrix $\mathbf{A}_j^{1/2} \mathbf{P}_j \mathbf{A}_j^{1/2}$ on the effective channel $\mathbf{B}_j^{-1/2} \mathbf{H}_j^* \mathbf{A}_j^{-1/2}$, where the flipped channel is defined as $(\mathbf{B}_j^{-1/2} \mathbf{H}_j^* \mathbf{A}_j^{-1/2})^*$. \mathbf{A}_j and \mathbf{B}_j , which represent the interference experienced by user j on the BC and on the MAC respectively, are defined as follows:

$$\mathbf{A}_j = \mathbf{I}_{M_j} + \mathbf{H}_j \left(\sum_{i=1}^{j-1} \boldsymbol{\Sigma}_i \right) \mathbf{H}_j^*. \quad (\text{D.3})$$

$$\mathbf{B}_j = \mathbf{I}_N + \sum_{i=j+1}^K \mathbf{H}_i^* \mathbf{P}_i \mathbf{H}_i. \quad (\text{D.4})$$

The BC covariance matrices can be expressed explicitly as:

$$\boldsymbol{\Sigma}_j = \mathbf{B}_j^{-1/2} \mathbf{F}_j \mathbf{G}_j^* \mathbf{A}_j^{1/2} \mathbf{P}_j \mathbf{A}_j^{1/2} \mathbf{G}_j \mathbf{F}_j^* \mathbf{B}_j^{-1/2}. \quad (\text{D.5})$$

Using the SVD of the effective channel:

$$\mathbf{B}_j^{-1/2} \mathbf{H}_j^* \mathbf{A}_j^{-1/2} = \mathbf{F}_j \mathbf{A}_j \mathbf{G}_j^*. \quad (\text{D.6})$$

The left hand-side of (D.6) is the effective channel and the right hand-side is its singular value decomposition. \mathbf{F}_j and \mathbf{G}_j are unitary matrices, and \mathbf{A}_j is a square diagonal matrix of size $\max(N, M_j)$.

The rate achieved by user j on the BC is:

$$R_j^{BC} = \log \frac{\left| \mathbf{I}_{M_j} + \sum_{i=1}^j (\mathbf{H}_i \boldsymbol{\Sigma}_i \mathbf{H}_i^*) \right|}{\left| \mathbf{I}_{M_j} + \sum_{i=1}^{j-1} (\mathbf{H}_i \boldsymbol{\Sigma}_i \mathbf{H}_i^*) \right|}. \quad (\text{D.7})$$

Definitions and Notation

We introduce new definitions and notations that will allow us to prove our claims. Let $p_i = \text{tr}(\mathbf{P}_i)$ be the power allocated to user i at the sum-capacity of the dual MIMO MAC. It is a function of the total transmit power P . Let $r_i = p_i/P$ represent the fraction of the total power allocated to user i on the dual sum-power MIMO MAC.

For the sake of simplicity, we choose to eliminate from the channel the users that are not allocated power in the high power region on the MIMO MAC. Obviously from the MAC to BC transformations we see that they would not be allocated any power on the MIMO BC either. Thus we do not need to consider them in our analysis. We consider only the users that are allocated some power in the high power region of the MIMO MAC thus $\lim_{P \rightarrow \infty} r_i > 0$ for all $i = 1, \dots, K$. Hence the new channel we consider is the (N, M_k, K) MIMO BC where all users are asymptotically active on the MIMO MAC. In other words, $p_i \neq 0$ for all $i = 1, \dots, K$ as the total transmit power P tends to infinity.

More specifically, assume that user i is allocated a non-vanishing fraction of the total transmit power on g_i eigenmodes. Let $\lambda_1(\mathbf{P}_i) \geq \dots \geq \lambda_{M_i}(\mathbf{P}_i)$ be the ordered eigenvalues of \mathbf{P}_i .

Thus g_i is the number of eigenvalues whose ratio to the total transmit power P does not vanish to 0 as the total transmit power P increases to infinity. Let

$$\lambda_m(\mathbf{P}_i) = l_{i,m} P, \quad (\text{D.8})$$

such that:

$$\lim_{P \rightarrow \infty} l_{i,m} > 0, \quad m = 1, \dots, g_i \quad (\text{D.9})$$

$$\lim_{P \rightarrow \infty} l_{i,m} = 0, \quad m = g_i + 1, \dots, M_i. \quad (\text{D.10})$$

Thus
$$\lim_{P \rightarrow \infty} \frac{\lambda_m(\mathbf{P}_i)}{P} = 0, \quad \forall m = g_i + 1, \dots, M_i. \quad (\text{D.11})$$

As a consequence $\lim_{P \rightarrow \infty} r_i = \lim_{P \rightarrow \infty} \sum_{m=1}^{g_i} l_{i,m}$. Let the eigenvalue decomposition of \mathbf{P}_i be:

$$\mathbf{P}_i = \mathcal{U}_i \mathbf{\Pi}_i \mathcal{U}_i^*, \quad (\text{D.12})$$

where $\mathbf{\Pi}_i = \text{diag}(\lambda_1(\mathbf{P}_i), \dots, \lambda_{M_i}(\mathbf{P}_i))$ and \mathcal{U}_i is a square unitary matrix of size $M_i \times M_i$. Let $\mathbf{u}_{i,m}$ be the m -th column of \mathcal{U}_i . Thus:

$$\mathbf{P}_i = \sum_{m=1}^{M_i} \mathbf{u}_{i,m} \lambda_m(\mathbf{P}_i) \mathbf{u}_{i,m}^*. \quad (\text{D.13})$$

D.3 Proof for the $(N,1,K)$ MIMO BC

Problem Statement

In this section we prove that only N users are allocated a non-vanishing fraction of the total transmit power on the MIMO BC when the total transmit power goes to infinity, provided that $K \geq N$. If $K < N$ then obviously all the K users will be allocated a non-vanishing fraction of the total transmit power in the high power region. This can be deduced from the following proof in a straightforward manner so we do not explicitly treat this case. In order to prove this statement, we show that:

$$\lim_{P \rightarrow \infty} \frac{\text{tr}(\boldsymbol{\Sigma}_j)}{P} = 0 \quad \text{if } j \leq K - N. \quad (\text{D.14})$$

$$\exists \varepsilon > 0 \quad \text{such that } \lim_{P \rightarrow \infty} \frac{\text{tr}(\boldsymbol{\Sigma}_j)}{P} > \varepsilon \quad \text{if } j > K - N. \quad (\text{D.15})$$

Optimal BC Covariance Matrices

In the particular case where $M_k = 1$ for all $k = 1, \dots, K$ the optimal covariance matrices on the MIMO BC obtained from the MAC to BC transformations can be expressed in a more

compact way. This expression was already used in the particular case of uniform power allocation on the dual MAC in [45]. We derive it here for a general MAC power allocation. We prove that

$$\Sigma_j = P_j \frac{\mathbf{B}_j^{-1} \mathbf{H}_j^* \mathbf{H}_j \mathbf{B}_j^{-1}}{\mathbf{H}_j \mathbf{B}_j^{-1} \mathbf{H}_j^*} \mathbf{A}_j. \quad (\text{D.16})$$

The SVD (D.6) in this case is not full-rank, thus one has to be careful in deriving the optimal covariance matrix on the flipped channel \mathbf{H}^* , and subsequently the MAC to BC transformation formulas. Here we specifically derive the MAC to BC transformations for the $(N,1,K)$ MIMO BC.

We first prove that if P is the power allocation on a given channel \mathbf{H} of size $N \times 1$, then the covariance matrix that achieves the same rate on the flipped channel is:

$$\mathbf{Q} = \mathbf{F} \begin{pmatrix} P & & & \\ & 0 & & \\ & & \ddots & \\ & & & 0 \end{pmatrix} \mathbf{F}^*. \quad (\text{D.17})$$

\mathbf{F} is the unitary $N \times N$ matrix in the SVD of \mathbf{H} given by $\mathbf{H} = \mathbf{F} \mathbf{A} \mathbf{G}^*$. \mathbf{A} is a $N \times 1$ vector, and $\mathbf{G} = \mathbf{1}$. Moreover $\mathbf{A} = [\|\mathbf{H}\| \ \mathbf{0} \ \dots \ \mathbf{0}]^T$.

To see this consider the channel capacity of the original single transmit antenna channel with transmit power constraint P :

$$C = \log \left| \mathbf{I}_N + \mathbf{H} \mathbf{P} \mathbf{H}^* \right| = \log \left(1 + P \|\mathbf{H}\|^2 \right). \quad (\text{D.18})$$

The channel capacity of the flipped channel \mathbf{H}^* with transmit covariance matrix \mathbf{Q} of size $N \times N$ such that $\text{tr}(\mathbf{Q}) = P$ is:

$$C_{\text{flipped}} = \log \left(1 + \mathbf{H}^* \mathbf{Q} \mathbf{H} \right). \quad (\text{D.19})$$

Using the SVD of \mathbf{H} we obtain:

$$\begin{aligned} C_{\text{flipped}} &= \log \left(1 + \mathbf{G} \mathbf{A}^* \mathbf{F}^* \mathbf{Q} \mathbf{F} \mathbf{A} \mathbf{G}^* \right) \\ &= \log \left(1 + \mathbf{A}^* \mathbf{F}^* \mathbf{Q} \mathbf{F} \mathbf{A} \right) \\ &= \log \left(1 + \mathbf{A}^* \mathbf{U} \mathbf{A} \right) \end{aligned} \quad (\text{D.20})$$

$\mathbf{U} = \mathbf{F}^* \mathbf{Q} \mathbf{F}$ so $\mathbf{Q} = \mathbf{F} \mathbf{U} \mathbf{F}^*$. Hence $C = \log \left(1 + \|\mathbf{H}\|^2 u_1 \right)$ where $\mathbf{U} = \text{diag}(u_1 \ \dots \ u_N)$ is required to maximize the mutual information, thus to achieve the capacity (this follows from Hadamard's determinant inequality as shown in [4]). Moreover $\text{tr}(\mathbf{Q}) = \text{tr}(\mathbf{U}) = P$ and obviously $u_1 = P$ thus $u_i = 0, \forall i = 2, \dots, N$. Thus the optimal transmit covariance matrix on the flipped channel is:

$$\mathbf{Q} = \mathbf{F} \begin{pmatrix} P & & & \\ & 0 & & \\ & & \ddots & \\ & & & 0 \end{pmatrix} \mathbf{F}^*. \quad (\text{D.21})$$

We now apply this result to the effective channel $\mathbf{B}_j^{-1/2} \mathbf{H}_j^* \mathbf{A}_j^{-1/2}$ of size $N \times 1$ where the power allocation is given by $\mathbf{A}_j^{1/2} \mathbf{P}_j \mathbf{A}_j^{1/2}$, which is a scalar for the $(N, 1, K)$ MIMO BC. Thus we have:

$$\overline{\mathbf{A}_j^{1/2} \mathbf{P}_j \mathbf{A}_j^{1/2}} = \mathbf{F} \begin{pmatrix} \mathbf{A}_j^{1/2} \mathbf{P}_j \mathbf{A}_j^{1/2} & & & \\ & 0 & & \\ & & \ddots & \\ & & & 0 \end{pmatrix} \mathbf{F}^*, \quad (\text{D.22})$$

where $\mathbf{B}_j^{-1/2} \mathbf{H}_j^* \mathbf{A}_j^{-1/2} = \mathbf{F} \mathbf{A} \mathbf{G}^*$. Thus $\mathbf{F} \mathbf{A} = \mathbf{B}_j^{-1/2} \mathbf{H}_j^* \mathbf{A}_j^{-1/2}$ since $\mathbf{G} = 1$. Using (D.2):

$$\boldsymbol{\Sigma}_j = \mathbf{B}_j^{-1/2} \mathbf{F} \begin{pmatrix} \mathbf{A}_j^{1/2} \mathbf{P}_j \mathbf{A}_j^{1/2} & & & \\ & 0 & & \\ & & \ddots & \\ & & & 0 \end{pmatrix} \mathbf{F}^* \mathbf{B}_j^{-1/2}. \quad (\text{D.23})$$

Moreover notice that:

$$\mathbf{A} \mathbf{A}^* = \begin{pmatrix} \|\mathbf{B}_j^{-1/2} \mathbf{H}_j^* \mathbf{A}_j^{-1/2}\|^2 & & & \\ & 0 & & \\ & & \ddots & \\ & & & 0 \end{pmatrix}. \quad (\text{D.24})$$

Thus
$$\boldsymbol{\Sigma}_j = \frac{\mathbf{A}_j^{1/2} \mathbf{P}_j \mathbf{A}_j^{1/2}}{\|\mathbf{B}_j^{-1/2} \mathbf{H}_j^* \mathbf{A}_j^{-1/2}\|} \mathbf{B}_j^{-1/2} \mathbf{F} \mathbf{A} \mathbf{A}^* \mathbf{F}^* \mathbf{B}_j^{-1/2}. \quad (\text{D.25})$$

So
$$\boldsymbol{\Sigma}_j = \frac{\mathbf{A}_j^{1/2} \mathbf{P}_j \mathbf{A}_j^{1/2}}{\|\mathbf{B}_j^{-1/2} \mathbf{H}_j^* \mathbf{A}_j^{-1/2}\|} \mathbf{B}_j^{-1/2} (\mathbf{B}_j^{-1/2} \mathbf{H}_j^* \mathbf{A}_j^{-1/2}) (\mathbf{B}_j^{-1/2} \mathbf{H}_j^* \mathbf{A}_j^{-1/2})^* \mathbf{B}_j^{-1/2}. \quad (\text{D.26})$$

And
$$\boldsymbol{\Sigma}_j = (\mathbf{A}_j^{1/2} \mathbf{P}_j \mathbf{A}_j^{1/2}) \frac{\mathbf{A}_j^{-1} \mathbf{B}_j^{-1/2} \mathbf{B}_j^{-1/2} \mathbf{H}_j^* \mathbf{H}_j \mathbf{B}_j^{-1/2} \mathbf{B}_j^{-1/2}}{\mathbf{A}_j^{-1/2} \mathbf{H}_j \mathbf{B}_j^{-1/2} \mathbf{B}_j^{-1/2} \mathbf{H}_j^* \mathbf{A}_j^{-1/2}}. \quad (\text{D.27})$$

Finally
$$\boldsymbol{\Sigma}_j = \mathbf{P}_j \frac{\mathbf{B}_j^{-1} \mathbf{H}_j^* \mathbf{H}_j \mathbf{B}_j^{-1}}{\mathbf{H}_j \mathbf{B}_j^{-1} \mathbf{H}_j^*} \mathbf{A}_j. \quad (\text{D.28})$$

Proof by Induction

$\text{Tr}(\boldsymbol{\Sigma}_j)$ is the power allocated to user j at the sum-capacity on the MIMO BC with the same rate vector as on the dual sum-power MIMO MAC. We study the asymptotic behavior of

$\text{tr}(\Sigma_j)$ as P increases given the encoding order K to 1 for dirty-paper coding on the MIMO BC for the active users. Note that with single-antenna users A_j and P_j are scalar, with $P_j = p_j$. We can see that:

$$\text{tr}(\Sigma_j) = P_j A_j \frac{\text{tr}(\mathbf{B}_j^{-1} \mathbf{H}_j^* \mathbf{H}_j \mathbf{B}_j^{-1})}{\mathbf{H}_j \mathbf{B}_j^{-1} \mathbf{H}_j^*} = r_j P A_j \frac{\mathbf{H}_j \mathbf{B}_j^{-2} \mathbf{H}_j^*}{\mathbf{H}_j \mathbf{B}_j^{-1} \mathbf{H}_j^*}. \quad (\text{D.29})$$

And that

$$\mathbf{B}_j = \mathbf{I}_N + \sum_{i=j+1}^K \mathbf{H}_i^* P_i \mathbf{H}_i = \mathbf{I}_N + P \sum_{i=j+1}^K r_i \mathbf{H}_i^* \mathbf{H}_i. \quad (\text{D.30})$$

Consider the eigenvalue decomposition:

$$\sum_{i=j+1}^K r_i \mathbf{H}_i^* \mathbf{H}_i = \mathbf{U}_j \mathbf{D}_j \mathbf{U}_j^*. \quad (\text{D.31})$$

Where \mathbf{U}_j is an $N \times N$ unitary matrix, and \mathbf{D}_j is a square $N \times N$ diagonal matrix. Since $r_j > 0$ for every $j = 1, \dots, K$ and $\text{rank}(\mathbf{H}_i^* \mathbf{H}_i) = 1$, we can conclude that \mathbf{D}_j is full rank N almost surely when $K - j \geq N$, otherwise its rank is $K - j$ almost surely at all values of the total transmit power in the high power region, in particular as the total transmit power goes to infinity. Let

$$\mathbf{D}_j = \text{diag}(d_{j,1} \quad \dots \quad d_{j,K-j} \quad 0 \quad \dots \quad 0). \quad (\text{D.32})$$

Thus

$$\lim_{P \rightarrow \infty} d_{j,i} > 0, \quad \forall i = 1, \dots, K - j. \quad (\text{D.33})$$

Then

$$\mathbf{B}_j^{-1} = (\mathbf{I}_N + P \mathbf{U}_j \mathbf{D}_j \mathbf{U}_j^*)^{-1} = \mathbf{U}_j (\mathbf{I}_N + P \mathbf{D}_j)^{-1} \mathbf{U}_j^*. \quad (\text{D.34})$$

And

$$\text{tr}(\Sigma_j) = r_j P A_j \frac{\mathbf{H}_j \mathbf{U}_j (\mathbf{I}_N + P \mathbf{D}_j)^{-2} \mathbf{U}_j^* \mathbf{H}_j^*}{\mathbf{H}_j \mathbf{U}_j (\mathbf{I}_N + P \mathbf{D}_j)^{-1} \mathbf{U}_j^* \mathbf{H}_j^*}. \quad (\text{D.35})$$

Consider the $1 \times N$ vector $\mathbf{H}_j \mathbf{U}_j$ with elements $(\mathbf{H}_j \mathbf{U}_j)_n$ for $n = 1, \dots, N$. We then express:

$$\frac{\text{tr}(\Sigma_j)}{P} = r_j A_j \frac{\sum_{n=1}^{\text{rank}(\mathbf{D}_j)} \frac{|(\mathbf{H}_j \mathbf{U}_j)_n|^2}{(1 + P d_{j,n})^2} + \sum_{n=\text{rank}(\mathbf{D}_j)+1}^N |(\mathbf{H}_j \mathbf{U}_j)_n|^2}{\sum_{n=1}^{\text{rank}(\mathbf{D}_j)} \frac{|(\mathbf{H}_j \mathbf{U}_j)_n|^2}{1 + P d_{j,n}} + \sum_{n=\text{rank}(\mathbf{D}_j)+1}^N |(\mathbf{H}_j \mathbf{U}_j)_n|^2}. \quad (\text{D.36})$$

So

$$\frac{\text{tr}(\Sigma_j)}{P} = \begin{cases} r_j A_j \frac{\sum_{n=1}^N \frac{|(H_j U_j)_n|^2}{(1 + P d_{j,n})^2}}{\sum_{n=1}^N \frac{|(H_j U_j)_n|^2}{1 + P d_{j,n}}} & \text{if } j \leq K - N \\ r_j A_j \frac{\sum_{n=1}^{K-j} \frac{|(H_j U_j)_n|^2}{(1 + P d_{j,n})^2} + \sum_{n=K-j+1}^N |(H_j U_j)_n|^2}{\sum_{n=1}^{K-j} \frac{|(H_j U_j)_n|^2}{1 + P d_{j,n}} + \sum_{n=K-j+1}^N |(H_j U_j)_n|^2} & \text{if } j > K - N \end{cases} \quad (\text{D.37})$$

With

$$A_j = \begin{cases} 1 + H_j \left(\sum_{i=1}^{j-1} \Sigma_i \right) H_j^* & \text{if } j \leq K - N \\ 1 + H_j \left(\sum_{i=1}^{K-N} \Sigma_i \right) H_j^* + H_j \left(\sum_{i=K-N+1}^{j-1} \Sigma_i \right) H_j^* & \text{if } j > K - N \end{cases} \quad (\text{D.38})$$

We prove the statements of (D.14) and (D.15) by induction.

Induction Proof Part 1: Proof for User $j = 1$

$$\frac{\text{tr}(\Sigma_1)}{P} = \begin{cases} r_1 \frac{\sum_{n=1}^N \frac{|(H_1 U_1)_n|^2}{(1 + P d_{1,n})^2}}{\sum_{n=1}^N \frac{|(H_1 U_1)_n|^2}{1 + P d_{1,n}}} & \text{if } N+1 \leq K \\ r_1 \frac{\sum_{n=1}^{K-1} \frac{|(H_1 U_1)_n|^2}{(1 + P d_{1,n})^2} + \sum_{n=K}^N |(H_1 U_1)_n|^2}{\sum_{n=1}^{K-1} \frac{|(H_1 U_1)_n|^2}{1 + P d_{1,n}} + \sum_{n=K}^N |(H_1 U_1)_n|^2} & \text{if } N+1 > K \end{cases} \quad (\text{D.39})$$

Note that $(H_j U_j)_n \neq 0$ almost surely, because there is no relation between H_j and U_j since U_j comes from the SVD of $\sum_{i=j+1}^K r_i H_i^* H_i$.

$$\text{Hence} \quad \lim_{P \rightarrow \infty} \frac{\text{tr}(\Sigma_1)}{P} = \begin{cases} 0 & \text{if } N+1 \leq K \\ \lim_{P \rightarrow \infty} r_1 > 0 & \text{if } N+1 > K \end{cases} \quad (\text{D.40})$$

Thus we see that if $K \geq N+1$, the fraction of the total power allocated to user 1 asymptotically in

the high power region is zero, even if $\lim_{P \rightarrow \infty} r_1 > 0$. On the other hand, if $K \leq N$ then user 1 is allocated an asymptotically non-zero fraction of the total transmit power.

If $N+1 > K$ then the proof continues directly in part 3 of the proof. Otherwise if $N+1 \leq K$ the proof continues in part 2.

Induction Proof Part 2: Proof for User $j \leq K - N$

Induction hypothesis for all i such that $1 \leq i < j$:

$$\lim_{P \rightarrow \infty} \frac{\text{tr}(\Sigma_i)}{P} = 0 \text{ for } i \leq K - N \text{ and } \forall i = 1, \dots, j-1. \quad (\text{D.41})$$

We have proved it for $i=1$ in the previous section when $N+1 \leq K$.

Let $1 < j \leq K - N$ then D_j is full rank almost surely and thus:

$$\frac{\text{tr}(\Sigma_j)}{P} \underset{P \rightarrow \infty}{\sim} r_j \frac{A_j}{P} \frac{\sum_{n=1}^N \frac{|(\mathbf{H}_j \mathbf{U}_j)_n|^2}{d_{j,n}^2}}{\sum_{n=1}^N \frac{|(\mathbf{H}_j \mathbf{U}_j)_n|^2}{d_{j,n}}}. \quad (\text{D.42})$$

Moreover

$$\begin{aligned} A_j &= 1 + \mathbf{H}_j \left(\sum_{i=1}^{j-1} \Sigma_i \right) \mathbf{H}_j^* \\ &= \text{tr} \left(1 + \mathbf{H}_j \left(\sum_{i=1}^{j-1} \Sigma_i \right) \mathbf{H}_j^* \right) \\ &= 1 + \sum_{i=1}^{j-1} \text{tr}(\mathbf{H}_j \Sigma_i \mathbf{H}_j^*) \\ &= 1 + \sum_{i=1}^{j-1} \text{tr}(\mathbf{H}_j^* \mathbf{H}_j \Sigma_i) \end{aligned} \quad (\text{D.43})$$

From (D.28) we see that $\text{rank}(\Sigma_i) = 1$ for all i , thus $\exists \mathbf{v}_i \in \mathbb{C}^{1 \times N} / \Sigma_i = \mathbf{v}_i^* \mathbf{v}_i$. Thus using the properties of the trace and Cauchy-Schwartz's inequality:

$$\text{tr}(\mathbf{H}_j^* \mathbf{H}_j \Sigma_i) = \text{tr}(\mathbf{v}_i \mathbf{H}_j^* \mathbf{H}_j \mathbf{v}_i^*) = \left| \langle \mathbf{H}_j, \mathbf{v}_i \rangle \right|^2 \leq \|\mathbf{H}_j\|^2 \|\mathbf{v}_i\|^2 = \|\mathbf{H}_j\|^2 \text{tr}(\Sigma_i). \quad (\text{D.44})$$

Thus

$$A_j = 1 + \mathbf{H}_j \left(\sum_{i=1}^{j-1} \Sigma_i \right) \mathbf{H}_j^* \leq 1 + \|\mathbf{H}_j\|^2 \sum_{i=1}^{j-1} \text{tr}(\Sigma_i). \quad (\text{D.45})$$

Using the induction hypothesis (D.41) we conclude that

$$\lim_{P \rightarrow \infty} \frac{A_j}{P} = 0. \quad (\text{D.46})$$

Then from (D.42) we prove that

$$\lim_{P \rightarrow \infty} \frac{\text{tr}(\boldsymbol{\Sigma}_j)}{P} = 0. \quad (\text{D.47})$$

Proof Part 3: Proof for User $j > K - N$

Let $j > K - N$. Starting from (D.37) and using $A_j \geq 1$ we find that:

$$\frac{\text{tr}(\boldsymbol{\Sigma}_j)}{P} \underset{P \rightarrow \infty}{\sim} A_j r_j \geq r_j. \quad (\text{D.48})$$

Using the hypothesis that $\lim_{P \rightarrow \infty} r_i > 0$ we conclude that

$$\lim_{P \rightarrow \infty} \frac{\text{tr}(\boldsymbol{\Sigma}_j)}{P} \geq \lim_{P \rightarrow \infty} r_i > 0 \text{ for } j > K - N. \quad (\text{D.49})$$

We have thus proved that only N users are allocated a non-vanishing fraction of the total transmit power asymptotically in the high power region on the $(N, 1, K)$ MIMO BC when $K \geq N$, and these users have index $j = K - N + 1, \dots, K$ with the specific encoding order that we considered.

Orthogonality Property

We prove for a given $j > K - N$ that:

$$\lim_{P \rightarrow \infty} \mathbf{H}_j \boldsymbol{\Sigma}_i \mathbf{H}_j^* = 0 \text{ for all } i \text{ such that } K - N < i < j. \quad (\text{D.50})$$

And at the same time that
$$\lim_{P \rightarrow \infty} \frac{A_j}{P} = 0. \quad (\text{D.51})$$

This result tells us that asymptotically in the high power region on the $(N, 1, K)$ MIMO BC, the optimal covariance matrix of user $i > K - N$ on the BC becomes orthogonal to the channel matrix of user j for all $j > i$. In other words, the optimal transmit covariance matrix of user $i > K - N$ becomes asymptotically orthogonal to the channel matrices of all others users that are allocated an asymptotically non-vanishing fraction of the total transmit power and that are encoded with dirty-paper coding prior to user i .

The fact that A_j does not grow with P but that it converges to a constant as P increases is intuitively obvious otherwise $\text{tr}(\boldsymbol{\Sigma}_j)$ in (D.48) would increase faster than P , which could contradict the power constraint.

We first need to prove the following lemma:

Lemma: $\forall j = i+1, \dots, K$ and $n > \text{rank}(\mathbf{D}_i)$: $(\mathbf{H}_j \mathbf{U}_i)_n = 0$. (D.52)

The proof is as follows. Recall the SVD (D.31): $\sum_{j=i+1}^K r_j \mathbf{H}_j^* \mathbf{H}_j = \mathbf{U}_i \mathbf{D}_i \mathbf{U}_i^*$.

Thus $\mathbf{D}_i = \sum_{j=i+1}^K r_j \mathbf{U}_i^* \mathbf{H}_j^* \mathbf{H}_j \mathbf{U}_i$, which has rank $\min(K-i, N)$. We express for $j \geq i+1$:

$$\mathbf{H}_j \mathbf{U}_i (\mathbf{I}_N + P \mathbf{D}_i)^{-1} = \begin{bmatrix} \frac{(\mathbf{H}_j \mathbf{U}_i)_1}{1 + P d_{i,1}} & \dots & \frac{(\mathbf{H}_j \mathbf{U}_i)_{\text{rank}(\mathbf{D}_i)}}{1 + P d_{i, \text{rank}(\mathbf{D}_i)}} & (\mathbf{H}_j \mathbf{U}_i)_{\text{rank}(\mathbf{D}_i)+1} & \dots & (\mathbf{H}_j \mathbf{U}_i)_N \end{bmatrix} \quad (\text{D.53})$$

So $\|\mathbf{H}_j \mathbf{U}_i (\mathbf{I}_N + P \mathbf{D}_i)^{-1} \mathbf{U}_i^*\|^2 = \sum_{n=1}^{\text{rank}(\mathbf{D}_i)} \frac{|(\mathbf{H}_j \mathbf{U}_i)_n|^2}{(1 + P d_{i,n})^2} + \sum_{n=\text{rank}(\mathbf{D}_i)+1}^N |(\mathbf{H}_j \mathbf{U}_i)_n|^2$. (D.54)

The second term is equal to zero due to the SVD. We get directly:

$$\sum_{j=i+1}^K r_j (\mathbf{H}_j \mathbf{U}_i)^* (\mathbf{H}_j \mathbf{U}_i) = \mathbf{D}_i = \begin{pmatrix} d_{i,1} & & & & & \\ & \ddots & & & & \\ & & d_{i, \text{rank}(\mathbf{D}_i)} & & & \\ & & & & & \\ & & & & & 0 \end{pmatrix}. \quad (\text{D.55})$$

The diagonal element (n, n) is $d_{i,n} = \sum_{j=1}^K r_j |(\mathbf{H}_j \mathbf{U}_i)_n|^2$, which is equal to 0 if $n > \text{rank}(\mathbf{D}_i)$. Since it is a sum of positive elements and $r_j > 0$ for all j , then all the elements must be equal to 0 if $n > \text{rank}(\mathbf{D}_i)$. Thus $(\mathbf{H}_j \mathbf{U}_i)_n = 0$ for all $j = i+1, \dots, K$ and $n > \text{rank}(\mathbf{D}_i)$. □

Let j and i be given such that $K - N < i < j$. We start by using (D.28) and (D.34) to find:

$$\begin{aligned} \mathbf{H}_j \boldsymbol{\Sigma}_i \mathbf{H}_j^* &= \frac{P_i \mathbf{A}_i}{\mathbf{H}_i \mathbf{B}_i^{-1} \mathbf{H}_i^*} \mathbf{H}_j \mathbf{B}_i^{-1} \mathbf{H}_i^* \mathbf{H}_i \mathbf{B}_i^{-1} \mathbf{H}_j^* \\ &= \frac{P_i \mathbf{A}_i}{\mathbf{H}_i \mathbf{B}_i^{-1} \mathbf{H}_i^*} \left[\mathbf{H}_j \mathbf{U}_i (\mathbf{I}_N + P \mathbf{D}_i)^{-1} \right] \mathbf{U}_i^* \mathbf{H}_i^* \mathbf{H}_i \mathbf{U}_i \left[(\mathbf{I}_N + P \mathbf{D}_i)^{-1} \mathbf{U}_i^* \mathbf{H}_j^* \right] \end{aligned} \quad (\text{D.56})$$

We use (D.52) and $\mathbf{H}_i \mathbf{B}_i^{-1} \mathbf{H}_i^* = \sum_{n=1}^{\text{rank}(\mathbf{D}_i)} \frac{|(\mathbf{H}_i \mathbf{U}_i)_n|^2}{1 + P d_{i,n}} + \sum_{n=\text{rank}(\mathbf{D}_i)+1}^N |(\mathbf{H}_i \mathbf{U}_i)_n|^2$ to get:

$$\begin{aligned} \mathbf{H}_j \mathbf{U}_i (\mathbf{I}_N + P \mathbf{D}_i)^{-1} &= \begin{bmatrix} \frac{(\mathbf{H}_j \mathbf{U}_i)_1}{1 + P d_{i,1}} & \dots & \frac{(\mathbf{H}_j \mathbf{U}_i)_{\text{rank}(\mathbf{D}_i)}}{1 + P d_{i,\text{rank}(\mathbf{D}_i)}} & (\mathbf{H}_j \mathbf{U}_i)_{\text{rank}(\mathbf{D}_i)+1} & \dots & (\mathbf{H}_j \mathbf{U}_i)_N \end{bmatrix} \\ &= \begin{bmatrix} \frac{(\mathbf{H}_j \mathbf{U}_i)_1}{1 + P d_{i,1}} & \dots & \frac{(\mathbf{H}_j \mathbf{U}_i)_{\text{rank}(\mathbf{D}_i)}}{1 + P d_{i,\text{rank}(\mathbf{D}_i)}} & 0 & \dots & 0 \end{bmatrix} \end{aligned} \quad (\text{D.57})$$

And

$$\mathbf{H}_j \boldsymbol{\Sigma}_i \mathbf{H}_j^* \underset{P \rightarrow \infty}{\sim} \frac{r_i P A_i}{\sum_{n=1}^{\text{rank}(\mathbf{D}_i)} \frac{|(\mathbf{H}_i \mathbf{U}_i)_n|^2}{1 + P d_{i,n}} + \sum_{n=\text{rank}(\mathbf{D}_i)+1}^N |(\mathbf{H}_i \mathbf{U}_i)_n|^2} \frac{c}{P^2} \underset{P \rightarrow \infty}{\sim} \frac{1}{P} \frac{c r_i A_i}{\sum_{n=\text{rank}(\mathbf{D}_i)+1}^N |(\mathbf{H}_i \mathbf{U}_i)_n|^2} \quad (\text{D.58})$$

Where c is a constant that does not depend on the power P .

We only need to prove that $\lim_{P \rightarrow \infty} \frac{A_i}{P} = 0$ for $i > K - N$. We now prove this result by induction. We already proved it for $i \leq K - N$ in (D.46). Now let $j > K - N$.

$$\text{Induction hypothesis:} \quad \lim_{P \rightarrow \infty} \frac{A_i}{P} = 0 \text{ for all } i < j. \quad (\text{D.59})$$

We need to prove that $\lim_{P \rightarrow \infty} \frac{A_j}{P} = 0$.

Using the induction hypothesis (D.59) and (D.58):

$$\lim_{P \rightarrow \infty} \mathbf{H}_j \boldsymbol{\Sigma}_i \mathbf{H}_j^* = 0 \text{ for all } K - N < i < j. \quad (\text{D.60})$$

Using $\mathbf{H}_j \boldsymbol{\Sigma}_i \mathbf{H}_j^* \leq \|\mathbf{H}_j\|^2 \text{tr}(\boldsymbol{\Sigma}_i)$ and (D.14):

$$\lim_{P \rightarrow \infty} \mathbf{H}_j \frac{\boldsymbol{\Sigma}_i}{P} \mathbf{H}_j^* = 0 \text{ for all } i \leq K - N. \quad (\text{D.61})$$

Thus

$$\lim_{P \rightarrow \infty} \frac{1}{P} A_j = \lim_{P \rightarrow \infty} \frac{1}{P} \left(1 + \sum_{i=1}^{K-N} \mathbf{H}_j \boldsymbol{\Sigma}_i \mathbf{H}_j^* + \sum_{i=K-N+1}^{j-1} \mathbf{H}_j \boldsymbol{\Sigma}_i \mathbf{H}_j^* \right) = 0. \quad (\text{D.62})$$

Thus we have proved (D.50) and (D.51).

The channel is completely orthogonalized by the joint action of dirty-paper coding and the optimization of the transmit covariance matrices to achieve the sum-capacity of the MIMO BC. To see this, we recall that the rank of the optimal covariance matrix of any user that is allocated non-zero power is equal to one when the users are equipped with a single receive antenna. $\text{rank}(\boldsymbol{\Sigma}_j) = 1$ since $M_j = 1$ so we define $\mathbf{v}_j \in \mathbb{C}^{1 \times N}$ such that $\boldsymbol{\Sigma}_j = \pi_j \mathbf{v}_j^* \mathbf{v}_j$, $\|\mathbf{v}_j\| = 1$, and

we define $\pi_j \geq 0$ such that $\text{tr}(\Sigma_j) = \pi_j$. The vector \mathbf{v}_j^* is the beamforming vector for user j at the transmitter. The orthogonality property can be restated such that for a given $i > K - N$ we have:

$$\lim_{P \rightarrow \infty} \mathbf{H}_j \mathbf{v}_i^* = 0 \text{ for all } j \text{ such that } K - N < i < j.$$

Thus the signal of user i is beamformed at the transmitter orthogonally to the channels of all users that are encoded after it by dirty-paper coding, asymptotically in the high power region.

Asymptotic Sum-Capacity and Power Allocation

Note that if $r_j = 0$ for $j < K - N$ then only N users are allocated a non-vanishing fraction of the total transmit power P asymptotically in the high power region on the MIMO MAC, and the same N users are allocated a non-vanishing fraction of the total transmit power asymptotically on the MIMO BC. These fractions are then the same on the MIMO MAC and on the MIMO BC since in this case $\lim_{P \rightarrow \infty} A_j = 1$, due to the limit (D.48).

Moreover, the rates achieved by each of these N users are asymptotically as a first order approximation, using (D.7) and (D.50):

$$\lim_{P \rightarrow \infty} R_j^{BC} \approx \log \left| \mathbf{I}_{M_j} + \mathbf{H}_j \Sigma_j \mathbf{H}_j^* \right|. \quad (\text{D.63})$$

As a consequence, we can solve for the asymptotic value of the sum-capacity of the $(N, 1, N)$ MIMO BC in the high power region in a simple way as follows.

$$\lim_{P \rightarrow \infty} C_{sum}^{BC} = \sum_{j=1}^N \lim_{P \rightarrow \infty} R_j^{BC} \approx \sum_{j=1}^N \log \left| \mathbf{I}_{M_j} + \mathbf{H}_j \Sigma_j \mathbf{H}_j^* \right|. \quad (\text{D.64})$$

The sum-capacity optimization can be reformulated as:

$$\lim_{P \rightarrow \infty} C_{sum}^{BC} \approx \max_{\substack{\pi_1, \dots, \pi_N \\ \mathbf{v}_1, \dots, \mathbf{v}_N}} \sum_{j=1}^N \log \left(1 + \pi_j \mathbf{H}_j \mathbf{v}_j^* \mathbf{v}_j \mathbf{H}_j^* \right)$$

$$\text{Subject to } \sum_{j=1}^N \pi_j = P \text{ and } \pi_j \geq 0, \quad j = 1, \dots, N.$$

$$\text{And for each } j = 1, \dots, N: \mathbf{H}_i \mathbf{v}_j^* = 0, \quad \forall i > j \text{ and } \|\mathbf{v}_j\| = 1. \quad (\text{D.65})$$

It is obvious that for a given set of $\{\pi_1, \dots, \pi_N\}$ the argument is maximized by individually optimizing each vector \mathbf{v}_j under the orthogonality constraints. Define the matrix $\mathbf{H}_{j+1:N} = [\mathbf{H}_{j+1}^* \quad \dots \quad \mathbf{H}_N^*]^*$ of size $(N - j) \times N$. We need \mathbf{v}_j to belong to the null space of $\mathbf{H}_{j+1:N}$. Consider the SVD $\mathbf{H}_{j+1:N}^* = \mathbf{W}_{j+1} \mathbf{D}_{j+1} \mathbf{V}_{j+1}^*$, where \mathbf{W}_{j+1} is unitary of size $N \times N$, and \mathbf{V}_{j+1}

is unitary of size $(N-j) \times (N-j)$. Thus $\mathbf{H}_{j+1:N}^* \mathbf{H}_{j+1:N} = \mathbf{W}_{j+1} \mathbf{D}_{j+1}^2 \mathbf{W}_{j+1}^*$, with $\mathbf{D}_{j+1}^2 = \text{diag}(0, \dots, 0, d_{j+1}^2, \dots, d_N^2)$. Define $\mathbf{W}_{1:j}$ as the $N \times j$ matrix composed of the first j columns of \mathbf{W}_{j+1} . For any $\mathbf{x} \in \mathbb{C}^{1 \times N}$ that belongs to the null space of $\mathbf{H}_{j+1:N}$ we can define $\boldsymbol{\mu} \in \mathbb{C}^{1 \times j}$ uniquely such that $\mathbf{x}^* = \mathbf{W}_{1:j} \boldsymbol{\mu}^*$.

We can thus find the optimum \mathbf{v}_j as:

$$\mathbf{v}_j = \underset{\mathbf{x} \in \mathbb{C}^{1 \times N}}{\text{argmax}} \left\| \mathbf{H}_j \mathbf{x}^* \right\|^2$$

$$\text{Subject to } \|\mathbf{x}\| = 1 \text{ and } \mathbf{x} \text{ belongs to the null space of } \mathbf{H}_{j+1:N}. \quad (\text{D.66})$$

We rewrite this problem as:

$$\mathbf{v}_j^* = \mathbf{W}_{1:j} \boldsymbol{\mu}_j^*$$

$$\text{Such that } \boldsymbol{\mu}_j = \underset{\boldsymbol{\mu} \in \mathbb{C}^{1 \times j}}{\text{argmax}} \left\| \mathbf{H}_j \mathbf{W}_{1:j} \boldsymbol{\mu}^* \right\|^2$$

$$\text{Subject to } \|\boldsymbol{\mu}\| = 1. \quad (\text{D.67})$$

Invoking Weyl's theorem [7], $\boldsymbol{\mu}_j$ is the eigenvector of $\mathbf{H}_j \mathbf{W}_{1:j}$ associated with the largest eigenvalue. Since $\mathbf{H}_j \mathbf{W}_{1:j}$ is a $1 \times j$ vector it is straightforward to conclude:

$$\boldsymbol{\mu}_j = \frac{\mathbf{H}_j \mathbf{W}_{1:j}}{\|\mathbf{H}_j \mathbf{W}_{1:j}\|}, \quad (\text{D.68})$$

and

$$\mathbf{v}_j^* = \frac{\mathbf{W}_{1:j} \mathbf{W}_{1:j}^* \mathbf{H}_j^*}{\|\mathbf{H}_j \mathbf{W}_{1:j}\|}. \quad (\text{D.69})$$

Consequently

$$\mathbf{H}_j \mathbf{v}_j^* \mathbf{v}_j \mathbf{H}_j^* = \|\mathbf{H}_j \mathbf{W}_{1:j}\|^2. \quad (\text{D.70})$$

Thus (D.65) becomes:

$$\lim_{P \rightarrow \infty} C_{sum}^{BC} \approx \max_{\pi_1, \dots, \pi_N} \sum_{j=1}^N \log \left(1 + \pi_j \|\mathbf{H}_j \mathbf{W}_{1:j}\|^2 \right)$$

$$\text{Subject to } \sum_{j=1}^N \pi_j = P \text{ and } \pi_j \geq 0, j = 1, \dots, N. \quad (\text{D.71})$$

This is a classical waterfilling problem, and in the high power region the solution is given by (refer to Appendix A):

$$\pi_j = \frac{P}{N} + \frac{1}{N} \sum_{n=1}^N \left(\frac{1}{\|\mathbf{H}_n \mathbf{W}_{1:n}\|^2} - \frac{1}{\|\mathbf{H}_j \mathbf{W}_{1:j}\|^2} \right). \quad (\text{D.72})$$

$$\lim_{P \rightarrow \infty} C_{sum}^{BC} \approx \sum_{j=1}^N \log \left(1 + \frac{P}{N} \|\mathbf{H}_j \mathbf{W}_{1:j}\|^2 + \frac{1}{N} \sum_{n=1}^N \left(\frac{\|\mathbf{H}_j \mathbf{W}_{1:j}\|^2}{\|\mathbf{H}_n \mathbf{W}_{1:n}\|^2} - 1 \right) \right). \quad (\text{D.73})$$

Or equivalently $\lim_{P \rightarrow \infty} C_{sum}^{BC} \approx N \log \left(P + \sum_{n=1}^N \frac{1}{\|\mathbf{H}_n \mathbf{W}_{1:n}\|^2} \right) + \sum_{j=1}^N \log \left(\|\mathbf{H}_j \mathbf{W}_{1:j}\|^2 \right) - N \log N.$ (D.74)

We also note from (D.72) that the optimal power allocation in the high power region is asymptotically uniform among the N users, which is valid for all values of N . This result was known for $N=2$ [5] and it could be deduced for large values of N from (D.48) and [45], where the authors proved that uniform power allocation is optimal on the dual MIMO MAC of the $(N,1,N)$ MIMO BC as N becomes large for any P .

The vectors obtained in (D.69) are such that we have performed a QR decomposition [7] of the matrix \mathbf{H} . Let $\mathbf{V} = [\mathbf{v}_1 \ \dots \ \mathbf{v}_N]$. It is obvious from the constraints in (D.65) that $\mathbf{H}\mathbf{V}^*$ is upper triangular. Moreover from (D.69) we see that \mathbf{v}_j belongs to the null space of vectors \mathbf{H}_{j+1} to \mathbf{H}_N and it belongs to the space spanned by \mathbf{H}_j . Thus for any $i < j$, \mathbf{v}_i belongs to the null space of \mathbf{H}_j and \mathbf{v}_j belongs to the image space of \mathbf{H}_j , thus \mathbf{v}_i and \mathbf{v}_j are orthogonal. Since they are also normal, then we can conclude that \mathbf{V} is a unitary matrix, and we effectively obtained a QR decomposition of the channel matrix as $\mathbf{H} = \mathbf{R}\mathbf{V}$, where the unitary matrix is one the right side of the multiplication.

These results on the limit rates and sum-capacity are valid as a first order approximation since our results are asymptotic in the study of the ratio of the optimal covariance matrices to the total transmit power. Thus one must be careful in concluding that the above expressions are tight to the sum-capacity asymptotically in the high power region, but they are not equal to the limit of the sum-capacity. A more detailed discussion can be found in Chapter III.

D.4 Proof for the (N,N,K) MIMO BC

Problem Statement

In this section we prove that only N one-dimensional channels are allocated a non-vanishing fraction of the total transmit power on the MIMO BC when the total transmit power goes to infinity, and these N one-dimensional channels all belong to the same user, the user that is encoded first by dirty-paper coding.

The proof is made of several parts. We make the following two assumptions on the asymptotically optimal power allocation on the dual sum-power MIMO MAC:

1. $\text{rank}(\mathbf{H}_K) = N$
2. $\lim_{P \rightarrow \infty} \text{tr}(\mathbf{P}_K) = \alpha_K^{\text{MAC}} P$ where $\alpha_K^{\text{MAC}} \neq 0$ is a constant

We then prove sequentially in the next section that:

- $\lim_{P \rightarrow \infty} \frac{1}{P} \boldsymbol{\Sigma}_K = \frac{1}{N} \mathbf{I}_N$.
- $\lim_{P \rightarrow \infty} \frac{1}{P} \text{tr}(\boldsymbol{\Sigma}_1) = 0$.
- And by induction: $\lim_{P \rightarrow \infty} \frac{1}{P} \text{tr}(\boldsymbol{\Sigma}_j) = 0$ for $j = 2, \dots, K-1$.

Thus we will have proven that asymptotically in the high power region, only one user is allocated a non-vanishing fraction of the total transmit power, as long as that user is allocated a non-vanishing fraction of the total transmit power on the dual MIMO MAC and its MAC covariance matrix is full rank. This phenomenon occurs beyond the point where the total transmit power reaches some threshold that corresponds to the moment when user K starts being allocated a non-vanishing fraction of the total transmit power on all its N eigenchannels due to the properties of waterfilling.

Proof

Proof Part 1: Asymptotically Optimal Covariance Matrix of User K

The optimal covariance matrix of user K , which is encoded first, is given by (D.5). It can be rewritten as

$$\boldsymbol{\Sigma}_K = \mathbf{F}_K \mathbf{G}_K^* \mathbf{A}_K^{1/2} \mathbf{P}_K \mathbf{A}_K^{1/2} \mathbf{G}_K \mathbf{F}_K^*, \quad (\text{D.75})$$

where

$$\mathbf{A}_K = \mathbf{I}_{M_K} + \mathbf{H}_K \left(\sum_{i=1}^{K-1} \boldsymbol{\Sigma}_i \right) \mathbf{H}_K^*. \quad (\text{D.76})$$

The rate achieved by user K on the MIMO BC is given by (D.7). It can be rewritten as in [6] with $M_K = N$:

$$R_K^{\text{BC}} = \log \left| \mathbf{I}_N + \mathbf{A}_K^{-1} \mathbf{H}_K \boldsymbol{\Sigma}_K \mathbf{H}_K^* \right|. \quad (\text{D.77})$$

Given the constant interference \mathbf{A}_K^{-1} created by users 1 to $K-1$ when their optimal covariance

matrices are fixed, and given that user K does not contribute any interference to users 1 to $K-1$ because it is encoded first by dirty-paper coding, the optimal covariance matrix Σ_K of user K can be found by maximizing R_K^{BC} subject to the power constraint $\text{tr}(\Sigma_K) = \text{tr}(A_K P_K)$ asymptotically in the high power region. Since only semidefinite positive matrices are involved in A_K , we know that $\text{tr}(\Sigma_K) \geq \text{tr}(P_K)$, thus the power constraint grows to infinity as P grows to infinity due to the assumption. The effective channel of user K is $H_K^* A_K^{-1/2}$. Its SVD is $H_K^* A_K^{-1/2} = F_K A_K G_K^*$. From single-user MIMO channel capacity theory we know that uniform power allocation across the N eigenmodes of user K is asymptotically optimal in the high power region so the asymptotically optimal covariance matrix is:

$$\lim_{P \rightarrow \infty} \frac{1}{P} \Sigma_K = G_K \left(\frac{\alpha_K^{BC}}{N} I_N \right) G_K^* = \frac{\alpha_K^{BC}}{N} I_N. \quad (\text{D.78})$$

where α_K^{BC} is a constant such that $\alpha_K^{BC} \geq \alpha_K^{MAC}$. Note that this result only holds if $H_K^* A_K^{-1/2}$ is full rank. We know that $\text{rank}(A_K) = N$ since the second term in (D.3) is only composed of semidefinite positive matrices, and $\text{rank}(H_K) = N$ by assumption. $\text{rank}(H_K) = N$ with probability one on the (N, N, K) MIMO BC when the elements of H_K are i.i.d. complex Gaussian random variables, thus $H_K^* A_K^{-1/2}$ is full rank with high probability.

This result also proves that $\text{rank}(P_K) = N$ since (D.5) induces that $\text{rank}(P_K) = \text{rank}(\Sigma_K) = N$ asymptotically, since all other matrices in (D.5) are full rank. Furthermore, at least one user is allocated a non-vanishing fraction of the total transmit power on the MIMO MAC in the high power region, thus we can set that user to be user K so that $\lim_{P \rightarrow \infty} \text{tr}(P_K) = \alpha_K^{MAC} P$ be true.

Proof Part 2: Initialization

The optimal covariance matrix of user 1 is given by:

$$\Sigma_1 = B_1^{-1/2} F_1 G_1^* P_1 G_1 F_1^* B_1^{-1/2}. \quad (\text{D.79})$$

Consider the eigenvalue decomposition:

$$\frac{1}{P} \sum_{i=2}^K H_i^* P_i H_i = U_1 D_1 U_1^*. \quad (\text{D.80})$$

Where U_j is an $N \times N$ unitary matrix, and D_j is a square $N \times N$ diagonal matrix of rank denoted by $\text{rank}(D_j)$. We have

$$\frac{1}{P} \sum_{i=2}^K \mathbf{H}_i^* \mathbf{P}_i \mathbf{H}_i = \frac{1}{P} \sum_{i=2}^{K-1} \mathbf{H}_i^* \mathbf{P}_i \mathbf{H}_i + \frac{1}{P} \mathbf{H}_K^* \mathbf{P}_K \mathbf{H}_K. \quad (\text{D.81})$$

This matrix is full rank thanks to the assumption that $\text{rank}(\mathbf{P}_K) = N$ and since $\text{rank}(\mathbf{H}_K) = N$ almost surely. Thus $\text{rank}(\mathbf{D}_j) = N$ almost surely. Recalling (D.4) we have:

$$\mathbf{B}_1^{-1} = (\mathbf{I}_N + \mathbf{P} \mathbf{U}_1 \mathbf{D}_1 \mathbf{U}_1^*)^{-1} = \mathbf{U}_1 (\mathbf{I}_N + \mathbf{P} \mathbf{D}_1)^{-1} \mathbf{U}_1^*. \quad (\text{D.82})$$

Let $\mathbf{D}_j = \text{diag}(d_{j,1} \ \dots \ d_{j,N})$ where $d_{j,n} \neq 0$ for all $n=1, \dots, N$ in the high power region.

So

$$(\mathbf{I}_N + \mathbf{P} \mathbf{D}_j)^{-1} = \begin{pmatrix} \frac{1}{1 + \mathbf{P} d_{j,1}} & & \\ & \ddots & \\ & & \frac{1}{1 + \mathbf{P} d_{j,N}} \end{pmatrix}. \quad (\text{D.83})$$

We now study the asymptotic power allocated to user 1 as the transmit power becomes large. Using the properties of the trace, the SVD (D.13) for user 1, and (D.8):

$$\begin{aligned} \text{tr}(\boldsymbol{\Sigma}_1) &= \text{tr}(\mathbf{B}_1^{-1/2} \mathbf{F}_1 \mathbf{G}_1^* \mathbf{P}_1 \mathbf{G}_1 \mathbf{F}_1^* \mathbf{B}_1^{-1/2}) \\ &= \text{tr}(\mathbf{B}_1^{-1} \mathbf{F}_1 \mathbf{G}_1^* \mathbf{P}_1 \mathbf{G}_1 \mathbf{F}_1^*) \\ &= \text{tr}(\mathbf{U}_1 (\mathbf{I}_N + \mathbf{P} \mathbf{D}_1)^{-1} \mathbf{U}_1^* \mathbf{F}_1 \mathbf{G}_1^* \mathbf{P}_1 \mathbf{G}_1 \mathbf{F}_1^*) \\ &= \text{tr} \left((\mathbf{I}_N + \mathbf{P} \mathbf{D}_1)^{-1} (\mathbf{U}_1^* \mathbf{F}_1 \mathbf{G}_1^*) \left(\sum_{m=1}^{M_1} \mathbf{u}_{1,m} \lambda_m(\mathbf{P}_1) \mathbf{u}_{1,m}^* \right) (\mathbf{G}_1 \mathbf{F}_1^* \mathbf{U}_1) \right) \\ &= \mathbf{P} \sum_{m=1}^{M_1} \lambda_m \text{tr} \left((\mathbf{I}_N + \mathbf{P} \mathbf{D}_1)^{-1} (\mathbf{U}_1^* \mathbf{F}_1 \mathbf{G}_1^*) \mathbf{u}_{1,m} \mathbf{u}_{1,m}^* (\mathbf{G}_1 \mathbf{F}_1^* \mathbf{U}_1) \right) \end{aligned} \quad (\text{D.84})$$

The (n, n) term on the diagonal of the matrix $(\mathbf{I}_N + \mathbf{P} \mathbf{D}_1)^{-1} (\mathbf{U}_1^* \mathbf{F}_1 \mathbf{G}_1^*) \mathbf{u}_{1,m} \mathbf{u}_{1,m}^* (\mathbf{G}_1 \mathbf{F}_1^* \mathbf{U}_1)$ is equal to $\frac{c_m}{1 + \mathbf{P} d_{j,n}}$, where c_m does not depend on \mathbf{P} . All the dependence on \mathbf{P} is given explicitly in (D.84),

with the exception of the terms $d_{j,n}$ although we know that they are bounded away from zero in the limit of infinite power. Therefore:

$$\lim_{\mathbf{P} \rightarrow \infty} \frac{1}{\mathbf{P}} \text{tr}(\boldsymbol{\Sigma}_1) = 0. \quad (\text{D.85})$$

An even stronger conclusion can be drawn using the same arguments to show that every element in the matrix $\boldsymbol{\Sigma}_1$ is inversely proportional to \mathbf{P} . Thus we can say that:

$$\lim_{\mathbf{P} \rightarrow \infty} \frac{1}{\mathbf{P}} \boldsymbol{\Sigma}_1 = \mathbf{0}_N. \quad (\text{D.86})$$

Proof Part 3: Induction

We prove that:

$$\lim_{P \rightarrow \infty} \frac{1}{P} \text{tr}(\boldsymbol{\Sigma}_j) = 0 \text{ for } j = 1, \dots, K-1. \quad (\text{D.87})$$

We have just proved it for $j=1$. Set j such that $1 < j \leq K-1$.

Induction hypothesis: we use the strong result

$$\lim_{P \rightarrow \infty} \frac{1}{P} \boldsymbol{\Sigma}_i = \mathbf{0}_N \text{ for } 1 \leq i < j. \quad (\text{D.88})$$

Similarly to the proof for user 1, let:

$$\mathbf{B}_j^{-1} = (\mathbf{I}_N + P\mathbf{U}_j\mathbf{D}_j\mathbf{U}_j^*)^{-1} = \mathbf{U}_j(\mathbf{I}_N + P\mathbf{D}_j)^{-1}\mathbf{U}_j^*. \quad (\text{D.89})$$

$$\frac{1}{P} \sum_{i=j+1}^K \mathbf{H}_i^* \mathbf{P}_i \mathbf{H}_i = \frac{1}{P} \sum_{i=j+1}^{K-1} \mathbf{H}_i^* \mathbf{P}_i \mathbf{H}_i + \frac{1}{P} \mathbf{H}_K^* \mathbf{P}_K \mathbf{H}_K. \quad (\text{D.90})$$

Thus $\text{rank}(\mathbf{D}_j) = N$ almost surely in the high power region.

$$\begin{aligned} \text{tr}(\boldsymbol{\Sigma}_j) &= \text{tr}(\mathbf{B}_j^{-1/2} \mathbf{F}_j \mathbf{G}_j^* \mathbf{A}_j^{1/2} \mathbf{P}_j \mathbf{A}_j^{1/2} \mathbf{G}_j \mathbf{F}_j^* \mathbf{B}_j^{-1/2}) \\ &= \text{tr}(\mathbf{B}_j^{-1} \mathbf{F}_j \mathbf{G}_j^* \mathbf{A}_j^{1/2} \mathbf{P}_j \mathbf{A}_j^{1/2} \mathbf{G}_j \mathbf{F}_j^*) \\ &= \text{tr}(\mathbf{U}_j (\mathbf{I}_N + P\mathbf{D}_j)^{-1} \mathbf{U}_j^* \mathbf{F}_j \mathbf{G}_j^* \mathbf{A}_j^{1/2} \mathbf{P}_j \mathbf{A}_j^{1/2} \mathbf{G}_j \mathbf{F}_j^*) \\ &= \text{tr} \left((\mathbf{I}_N + P\mathbf{D}_j)^{-1} (\mathbf{U}_j^* \mathbf{F}_j \mathbf{G}_j^*) \mathbf{A}_j^{1/2} \left(\sum_{m=1}^{M_j} \mathbf{u}_{j,m} \lambda_m(\mathbf{P}_j) \mathbf{u}_{j,m}^* \right) \mathbf{A}_j^{1/2} (\mathbf{G}_j \mathbf{F}_j^* \mathbf{U}_j) \right) \\ &= P \sum_{m=1}^{M_j} l_{j,m} \text{tr} \left((\mathbf{I}_N + P\mathbf{D}_j)^{-1} (\mathbf{U}_j^* \mathbf{F}_j \mathbf{G}_j^*) \mathbf{A}_j^{1/2} \mathbf{u}_{j,m} \mathbf{u}_{j,m}^* \mathbf{A}_j^{1/2} (\mathbf{G}_j \mathbf{F}_j^* \mathbf{U}_j) \right) \end{aligned} \quad (\text{D.91})$$

Recall (D.3):

$$\mathbf{A}_j = \mathbf{I}_N + \mathbf{H}_j \left(\sum_{i=1}^{j-1} \boldsymbol{\Sigma}_i \right) \mathbf{H}_j^*. \quad (\text{D.92})$$

Using the induction hypothesis (D.88) we see that:

$$\lim_{P \rightarrow \infty} \frac{1}{P} \mathbf{A}_j = \mathbf{0}_N. \quad (\text{D.93})$$

Thus the elements of the matrices $(\mathbf{U}_j^* \mathbf{F}_j \mathbf{G}_j^*) \mathbf{A}_j^{1/2} \mathbf{u}_{j,m} \mathbf{u}_{j,m}^* \mathbf{A}_j^{1/2} (\mathbf{G}_j \mathbf{F}_j^* \mathbf{U}_j)$ cannot increase faster than or as fast as P . Therefore each one of the traces in the sum in (D.91) is inversely proportional to P . We can conclude:

$$\lim_{P \rightarrow \infty} \frac{1}{P} \text{tr}(\boldsymbol{\Sigma}_j) = 0. \quad (\text{D.94})$$

And the strong result is obtained with the same argument by considering each element of the matrix Σ_j :

$$\lim_{P \rightarrow \infty} \frac{1}{P} \Sigma_j = \mathbf{0}_N. \quad (\text{D.95})$$

It is now straightforward to recognize that only user K is allocated an increasing amount of power as the power grows to infinity beyond some threshold. Thus we can conclude from (D.78) that $\alpha_K^{bc} = 1$ so

$$\lim_{P \rightarrow \infty} \frac{I}{P} \Sigma_K = \frac{1}{N} \mathbf{I}_N$$

Appendix E: N -user Scheduling Algorithm Optimization

We rewrite (4.3) as

$$u_k = \arg \max_{1 \leq i \leq K, i \in S_{k-1}} \left[\min_{\alpha \in \mathbb{C}^{k-1}} \left\| \alpha H_{S_{k-1}} - h_i \right\|^2 \right]. \quad (\text{E.1})$$

The inner minimization leads to

$$\begin{aligned} \alpha_{\min} &= \arg \min_{\alpha \in \mathbb{C}^{k-1}} \left\| \alpha H_{S_{k-1}} - h_i \right\|^2 \\ \alpha_{\min} &= \arg \min_{\alpha \in \mathbb{C}^{k-1}} \left(\alpha H_{S_{k-1}} H_{S_{k-1}}^* \alpha^* - \alpha H_{S_{k-1}} h_i^* - h_i H_{S_{k-1}}^* \alpha^* - h_i h_i^* \right). \end{aligned} \quad (\text{E.2})$$

We derive the real-valued quadratic argument with respect to α and we find that α_{\min} is the solution to

$$2 H_{S_{k-1}} H_{S_{k-1}}^* \alpha^* - 2 H_{S_{k-1}} h_i^* = 0. \quad (\text{E.3})$$

By construction $H_{S_{k-1}} H_{S_{k-1}}^*$ is square of size $k-1$ by $k-1$ and full-rank if there are at least $k-1$ linearly independent channel vectors, thus

$$\alpha_{\min} = h_i H_{S_{k-1}}^* \left(H_{S_{k-1}} H_{S_{k-1}}^* \right)^{-1}, \quad (\text{E.4})$$

and

$$\min_{\alpha \in \mathbb{C}^{k-1}} \left\| \alpha H_{S_{k-1}} - h_i \right\|^2 = \left\| h_i H_{S_{k-1}}^* \left(H_{S_{k-1}} H_{S_{k-1}}^* \right)^{-1} H_{S_{k-1}} - h_i \right\|^2. \quad (\text{E.5})$$

Then (E.1) reduces to (4.4):

$$u_k = \arg \max_{1 \leq i \leq K, i \in S_{k-1}} \left\| h_i \left[H_{S_{k-1}}^* \left(H_{S_{k-1}} H_{S_{k-1}}^* \right)^{-1} H_{S_{k-1}} - I_N \right] \right\|^2. \quad (\text{E.6})$$

Appendix F: Gorokhov's Receive Antenna Selection Algorithms

In this appendix we give a summary of the receive antenna selection algorithms proposed by Gorokhov et. al. in [56]. The channel model is the following. The transmitter is equipped with N antennas and the receiver is equipped with M antennas. The channel is constant and described by a matrix H of size $M \times N$. The signal-to-noise ratio per receive antenna is defined as E_s / N_o . Given a set $r = \{r_1, \dots, r_N\}$ of receive antennas, the matrix composed of the rows corresponding to these receive antennas is denoted as H_r . We denote by $B_\perp(U)$ any orthonormal basis of the orthogonal complement to the row space of matrix U .

Algorithm I: Incremental loss minimization

Define U as an $M \times N$ orthonormal basis of the column space of H . Algorithm I aims at minimizing a certain loss factor between the capacity of the original channel with all M receive antennas and the capacity of the reduced channel with only N receive antennas. An $N \times N$ block \underline{U} of U will be selected as follows:

Set $\underline{U} = U_{l_1}$, where $l_1 = \arg \max_{1 \leq l \leq M} \|U_l\|^2$

For $n = 1$ to $(N - 1)$

Compute $B_\perp(\underline{U})$

Update $\underline{U} = [\underline{U}^T, U_{l_n}^T]^T$, where $l_n = \arg \max_{1 \leq l \leq M} \|U_l B_\perp(\underline{U})\|^2$

End

Algorithm II: Incremental selection

The set of receive antennas indexes is obtained as follows:

Set $A = (E_s / N_o) I_N$ and $r_1 = \arg \max_{1 \leq l \leq M} \|H_l\|^2$

For $n = 1$ to $(N - 1)$

Update $A = A - AH_{r_n}^* (1 + H_{r_n} A H_{r_n}^*)^{-1} H_{r_n} A$

Compute $r_{n+1} = \arg \max_{l \in \{r_1, \dots, r_n\}} H_l A H_l^*$

End

Algorithm III: Decremental selection

The set of receive antennas indexes is obtained as follows:

$$\text{Set } A = \left((E_s / N_o)^{-1} I_N + H^* H \right)^{-1}$$

$$p = \arg \min_{1 \leq i \leq M} H_i A H_i^*$$

$$r = \{1, \dots, p-1, p+1, \dots, M\}$$

For $n=1$ to $(M-N-1)$

$$\text{Update } A = A + A H_p^* (1 - H_p A H_p^*)^{-1} H_p A$$

$$\text{Compute } p = \arg \min_{i \in r} H_i A H_i^*$$

Remove p from the set r

End

Appendix G: The Generalized Singular Value Decomposition

In this appendix we give a summary of the generalized singular value decomposition introduced in [68] and [69]. Given two matrices A and B of size $m \times n$ and $p \times n$ respectively, there exist unitary matrices U_1 and U_2 , block-diagonal matrices D_1 and D_2 , and a non-singular $n \times n$ matrix X such that:

$$A = U_1 D_1 X^* \quad (\text{G.1})$$

$$B = U_2 D_2 X^* \quad (\text{G.2})$$

$$D_1^* D_1 + D_2^* D_2 = I_n. \quad (\text{G.3})$$

We define

$$k = \text{rank} \left(\begin{bmatrix} A \\ B \end{bmatrix} \right). \quad (\text{G.4})$$

We then perform the QR decomposition

$$GR = \begin{bmatrix} A \\ B \end{bmatrix}. \quad (\text{G.5})$$

G is a $(m+p) \times (m+p)$ unitary matrix, and R is a $(m+p) \times n$ such that

$$R = \begin{bmatrix} R_{up} \\ 0_{m+p-k,n} \end{bmatrix}. \quad (\text{G.6})$$

We define Q as the matrix composed of the first k columns of G , and R_{up} is a $k \times k$ upper triangular matrix.

We then perform the CS decomposition on the matrix Q . Define Q_1 and Q_2 with size $m \times k$ and $p \times k$ respectively as

$$Q = \begin{bmatrix} Q_1 \\ Q_2 \end{bmatrix}. \quad (\text{G.7})$$

If $m = k$, $p = k$

We compute the SVD

$$Q_1 = U_1 C W^*. \quad (\text{G.8})$$

C is a diagonal matrix of size $k \times k$. We define

$$\bar{Q}_2 = Q_2 W. \quad (G.9)$$

We then normalize each column of \bar{Q}_2 to obtain the $p \times p$ matrix U_2 and we construct the matrix

$$S = U_2^* \bar{Q}_2. \quad (G.10)$$

We obtain the matrices

$$D_1 = \begin{bmatrix} C \\ \theta_{m-k,k} \end{bmatrix} \quad (G.11)$$

$$D_2 = \begin{bmatrix} S \\ \theta_{p-k,k} \end{bmatrix}. \quad (G.12)$$

Finally

$$\begin{bmatrix} U_1^* & \theta \\ \theta & U_2^* \end{bmatrix} \begin{bmatrix} Q_1 \\ Q_2 \end{bmatrix} W = \begin{bmatrix} C \\ \theta_{m-k,k} \\ S \\ \theta_{p-k,k} \end{bmatrix}. \quad (G.13)$$

C and S are nonnegative diagonal matrices satisfying

$$C^2 + S^2 = I_k. \quad (G.14)$$

To complete the GSVD we define the matrix

$$X^* = U_2^* R_{up}. \quad (G.15)$$

We have obtained

$$A = U_1 D_1 X^* \quad (G.16)$$

$$B = U_2 D_2 X^* \quad (G.17)$$

$$D_1^2 + D_2^2 = I_k. \quad (G.18)$$

The situations where m , p and k are not equal are obtained similarly by adapting the block matrices by incorporating zero and identity blocks when necessary, as described in [68][69].